DISSOLVED INORGANIC CARBON CYCLING IN THE OFFSHORE AMAZON RIVER PLUME AND THE WESTERN TROPICAL NORTH ATLANTIC OCEAN

by

SARAH R. COOLEY

(Under the Direction of Patricia L. Yager)

ABSTRACT

The Amazon River discharges low-salinity, low-carbon water into the western tropical North Atlantic (WTNA), where the resultant plume stretches thousands of kilometers offshore and creates a sink for atmospheric carbon dioxide (CO_2). The presence of a carbon sink in tropical oceans is noteworthy because tropical waters typically release CO_2 to the atmosphere; the relative contributions of physical mixing and biological production must be understood, however, before the potential for changes in the magnitude of the sink can be determined. Biological production and subsequent export is the only process in tropical waters that can lead to a long-term sequestration of atmospheric carbon. This dissertation combines observational data and modeling studies to quantify the major inorganic carbon fluxes through the WTNA, so that the Amazon plume-related carbon sink can be understood mechanistically. I first distinguish between physical and biological effects on CO_2 in the offshore plume using observational data, and find that biological drawdown is greatest in association with diazotroph-containing diatoms. Then I determine the relative importance of seasonality in plume supply or processing on the offshore plume-related atmospheric carbon sink, and conclude that although supply of inorganic carbon to the Amazon plume does vary through the year, offshore biological processing year-

round has the greatest capacity to alter the magnitude of the sink, although its impact may vary depending on meteorological control. Finally, I examine the role of mixing at the edge of the plume, to understand the ultimate fate of the plume-related deficit in inorganic carbon. Vertical mixing is too small to completely eliminate plume-related inorganic carbon deficits, and horizontal advection and mixing must occur to bring plume water to nonplume conditions in the observed lifetime of the plume. As a result, the Amazon River plume-associated deficit may reduce WTNA inorganic carbon efflux beyond the borders of its low-salinity plume.

INDEX WORDS: Ocean carbon cycle, CO_2, atmospheric CO_2 sink, Amazon River, Tropical Atlantic Ocean

DISSOLVED INORGANIC CARBON CYCLING IN THE OFFSHORE AMAZON RIVER PLUME AND THE WESTERN TROPICAL NORTH ATLANTIC OCEAN

by

SARAH R. COOLEY

B.S., Haverford College, 1999

A Dissertation Submitted to the Graduate Faculty of The University of Georgia in Partial Fulfillment of the Requirements for the Degree

DOCTOR OF PHILOSOPHY

ATHENS, GEORGIA

2006

DISSOLVED INORGANIC CARBON CYCLING IN THE OFFSHORE AMAZON RIVER PLUME AND THE WESTERN TROPICAL NORTH ATLANTIC OCEAN

by

SARAH R. COOLEY

Major Professor: Patricia L. Yager

Committee: Brian J. Binder
Adrian B. Burd
Wei-Jun Cai
Victoria Coles

Electronic Version Approved:

Maureen Grasso
Dean of the Graduate School
The University of Georgia
August 2006

ACKNOWLEDGEMENTS

Salary support was provided to S.R.C. by the University of Georgia Presidential Graduate Fellowship, the NASA Earth System Science Fellowship, and the University of Georgia Department of Marine Science. This research was supported by the Office of Science (BER), U.S. Department of Energy, grant no. DE-FG02-02ER63472, NOAA Office of Global Programs grant NA16GP2689, and by faculty research support from the University of Georgia to Patricia Yager.

TABLE OF CONTENTS

Page

LIST OF TABLES

Page

LIST OF FIGURES

Page

CHAPTER 1

INTRODUCTION

Study context

Exchange of carbon dioxide (CO_2) between the large oceanic and atmospheric reservoirs was still poorly understood when data collected during the 1957-1958 International Geophysical Year showed that atmospheric CO_2 was rising faster than previously anticipated (Keeling 1960). Subsequent calculations showed that the ocean could not absorb CO_2 fast enough to keep pace with rising atmospheric levels (Revelle and Suess 1957; Bolin and Eriksson 1959). Roger Revelle noted that by adding CO_2 to the atmosphere, "human beings are carrying on a large-scale geophysical experiment of a kind that could not have happened in the past, nor be reproduced in the future" (Revelle and Suess 1957). Contemporary carbon cycle studies attempt to determine the consequences and mechanisms involved in this "experiment" to understand the Earth system and the consequences of ongoing anthropogenic perturbation.

Climatology- and tracer-based estimates of the average recent global air-sea CO_2 flux suggest that at an approximate rate of 2 Pg C yr^{-1}, ocean uptake is now 29-33% of the magnitude of anthropogenic carbon emissions (6-7 Pg C yr^{-1}, Feely et al. 2001; Takahashi et al. 1997; Siegenthaler and Sarmiento 1993; Quay et al. 1992). Global flux estimates are frequently based on the disequilibrium between atmospheric and surface oceanic CO_2 values, which primarily drives oceanic uptake of atmospheric CO_2 (Feely et al. 2001; Takahashi et al. 2002; Karl et al. 2001). However, interpolating spatially and temporally limited oceanic CO_2 observations to obtain global air-sea fluxes adds up to 75% error (Takahashi et al. 1997). Ideally, this error

could be reduced by directly measuring oceanic CO_2 values at all seasons in more locations. Since such sampling density is unlikely, more mechanistic or process-oriented approaches are needed to link ocean CO_2 concentrations to data with better coverage, such as that from satellite images or continuously measured underway datasets.

Global air-sea CO_2 flux estimates frequently do not include contributions of coastal margins, where observations are few or carbon system dynamics are complex (Figure 1.1). However, coastal oceans and estuaries represent 5-7% of the Earth's surface and are responsible for as much as 10% of worldwide primary production (Turner and Adger 1996; Ver et al. 1999). At the same time, the organic carbon produced supplies respiration in both coastal margins and oceans (Bauer and Druffel 1998), but the status of coastal margins as a net global carbon source or sink due to net heterotrophy or autotrophy is a matter of current debate (Frankignoulle and Borges 2001; Thomas et al. 2004a; Cai and Dai 2004; Thomas et al. 2004b; Borges et al. 2005). Recent work emphasizes the importance of ecosystem variations in setting regional balances between CO_2 emission or uptake (Borges et al. 2005). Observational studies that quantify carbon fluxes through near-shore environments are needed to improve our understanding of coastal influences on the global carbon flux.

The western tropical North Atlantic Ocean (WTNA) is an area whose participation in global inorganic carbon cycling is not completely understood. The offshore region is subject to coastal influences via the Amazon River outflow. The Amazon is the largest river in the world, delivering 16% of global riverine transport to the ocean (Oltman 1968). The resultant plume of high-chlorophyll river water stretches hundreds of kilometers offshore in ocean pigment satellite images (Hochman et al. 1994; Muller-Karger et al. 1988; Muller-Karger et al. 1995, Figure 1.2). Plume water can also be identified *in situ* by its low salinity, low levels of dissolved CO_2 and

carbonate species, and high concentrations of organic and inorganic nutrients (Lentz and Limeburner 1995; DeMaster et al. 1996; Ternon et al. 2000; DeMaster and Aller 2001). The plume's chemical environment is strongly influenced by processes that occur in the river mainstem or on the continental shelf, tightly linking the South American continent with the offshore Atlantic Ocean.

The size, low CO_2, and high pigment concentrations of the plume imply that it could represent a vast seasonally appearing sink for atmospheric carbon whose uptake is enhanced by biological activity (Ternon et al. 2000; Körtzinger 2003). Low-latitude oceans are typically atmospheric CO_2 sources because primary production in the tropics is outpaced by solubility-driven degassing (Figure 1.1, and Sarmiento et al. 1995; Takahashi 1989). The low CO_2 values in the Amazon plume initially set the direction of air-sea flux into the plume (see 5-10N, 50W, Figure 1.1). Then, when the plume supplies nutrients to the WTNA, the biological pump exports inorganic carbon to the deeper WTNA, lowering surface pCO_2 further (Volk and Hoffert 1985; Sarmiento et al. 1995; Sarmiento and Orr 1991). Quantifying the fluxes associated with the WTNA carbon sink requires an interdisciplinary perspective; ocean chemistry in this dynamic region cannot be examined independently from biological, atmospheric, physical, and geological influences. The resulting mechanistic understanding of WTNA carbon cycling will improve predictions of future regional behavior and may help constrain carbon cycles of other low-latitude coastal zones influenced by large rivers.

The carbonate system

Solution chemistry

CO_2 complexes with water upon dissolution to form carbonic acid, a weak multiprotic acid that quickly reaches chemical equilibrium in a series of dissociation reactions dependent on pH and temperature:

$$CO_2(g) \leftrightarrow CO_2(aq) \quad (1)$$

$$CO_2(aq) + H_2O \leftrightarrow H_2CO_3 \quad (2)$$

$$H_2CO_3 \leftrightarrow H^+ + HCO_3^- \quad (3)$$

$$HCO_3^- \leftrightarrow H^+ + CO_3^{2-} \quad (4)$$

Concentrations of these ions cannot be directly measured, but they can be calculated using other measured parameters of the carbonate system. The sum of all carbonate species in solution (H_2CO_3, HCO_3^-, CO_3^{2-} and $CO_{2(aq)}$) is frequently referred to as dissolved inorganic carbon (DIC) or total inorganic carbon. DIC is measured by coulometric titration of seawater. Dissolved CO_2 values in seawater can also be reported as partial pressures. Henry's law relates the partial pressure of a gas such as CO_2 to its quantity in solution:

$$[CO_2^*] = k_H(pCO_2) \quad (5)$$

where k_H is the Henry's law constant, which varies with salinity, pressure, and temperature (Libes 1992; Weiss 1974). $[CO_2^*]$ represents the total quantity of $CO_{2(aq)}$ and H_2CO_3, and pCO_2 is the partial pressure of CO_2. pCO_2 can be measured with a seawater-air equilibrator and an infrared detector. The total excess base in seawater that balances the charge of dissolved positive ions is known as total alkalinity (TA), which is composed mostly of ions from the carbonate system:

$$TA = [HCO_3^-] + 2[CO_3^{2-}] + [B(OH)_4^-] + [OH^-] + [HPO_4^{2-}] + 2[PO_4^{3-}] \quad (6)$$

$$[SiO(OH)_3^-] + [NH_3] + [HS^-] + \ldots - [H^+] - [HSO_4^-] - [HF] - [H_3PO_4] - \ldots$$

where the ellipses represent minor acid/base species whose concentrations are low enough that they may be neglected (DOE 1997). TA is also pH and temperature dependent, and it is measured by potentiometric titration of seawater. All the carbon species (DIC, pCO_2, or TA) can be calculated using the dissociation constants for the equilibrium reactions (1-4) and any two measured carbonate system parameters (any combination of pH, DIC, TA, or pCO_2). In this study, we measured DIC, TA, and pCO_2, and calculated pCO_2 if measurements were not available.

Inorganic carbon distributions in the ocean

Ocean DIC values increase with depth in all basins, where CO_2 is highly soluble due to deep ocean low temperatures and high pressures (Chester 1990; Lundberg 1994; Weiss 1974). The "solubility pump" moves inorganic carbon to the deep ocean when atmospheric CO_2 dissolves into poleward-moving (cooling) surface water, which then sinks into the deep ocean containing high CO_2. At the same time, the two-part "biological pump" exports additional carbon to deep water (Volk and Hoffert 1985). Respiration of sinking organic matter from the euphotic zone releases DIC in the deep ocean ("soft tissue pump", Volk and Hoffert 1985). Furthermore, some plankton form calcite shells that remove additional carbonate from surface waters. When these organisms sink, the calcite dissolves, releasing carbonate into the deep ocean ("carbonate pump", Volk and Hoffert 1985; Libes 1992). The solubility pump establishes a surface-to-deep DIC gradient that is greatly magnified by the biological pump. In the absence

of anthropogenic CO_2 perturbations, these oceanic processes set atmospheric CO_2 (Volk and Hoffert 1985; Sarmiento and Orr 1991).

Atmosphere-ocean connections

Air-sea CO_2 exchange varies regionally due to changes in physical, chemical, and biological conditions. The CO_2 flux across the air-sea interface (F) depends on the general equation (Wanninkhof and McGillis 1999):

$$F = K \cdot s \cdot (pCO_{2\,sea} - pCO_{2\,atm}) \qquad (7)$$

where K is the gas transfer velocity (also called "piston velocity") and s is gas solubility. Gas transfer velocity increases non-linearly with windspeed (Wanninkhof and McGillis 1999, and references therein), while gas solubility decreases with temperature and salinity, and increases with pressure (Weiss 1974). Biological activity or pH changes can influence pCO_{2sea}, which then alters the overall air-sea CO_2 flux.

Precipitation and evaporation influence CO_2 values in surface waters, changing both DIC and TA. Precipitation delivers low-carbon fresh water to the surface mixed layer, diluting inorganic carbon, nutrients, salts, and organic matter. Evaporation removes water vapor, concentrating dissolved constituents. In ocean studies, precipitation and evaporation effects are neutralized by normalizing DIC and TA to a fixed average oceanic salinity (e.g., Friis et al. 2003, and references therein). However, this approach causes misleading results if river-ocean mixing is occurring, such as in the WTNA, because the riverine zero-salinity endmember usually has nonzero DIC and TA (Friis et al. 2003; Robbins 2001). Instead, a mixing model approach is required that accounts for the systematic addition of both freshwater and carbon to the system.

Estuarine Mixing

River and ocean mixing can be quantified by plotting dissolved constituents against each other along the mixing gradient. Dissolved constituents that are neither consumed nor formed during mixing, known as conservative tracers (e.g., salinity), usually appear in plots as the independent variable. If the dependent variable is a nonconservative tracer (a constituent produced/consumed along the mixing gradient, e.g., nitrate), the resulting mixing curve will indicate addition processes if the mixing line curves upwards, and removal if the mixing line curves downwards. These curves are described by the relationship: (Chester 1990; Boyle et al. 1974)

$$\frac{dQ_c}{dS} = -Q_w (S - S_r) \frac{d^2 C}{dS^2} \qquad (16)$$

where Q_w is the flux of the river water, Q_c is the flux of the dissolved component being measured, S_r is the salinity of the river end-member, S is the salinity at the point in question, and C is the concentration of the component at that point. This treatment is fairly straightforward for nutrients and trace metals that travel exclusively in the dissolved phase, but becomes more involved when addition and removal processes include atmospheric exchange, as for dissolved gases like carbon dioxide. More complex models incorporating air-water gas transfer are needed to include the influence of the atmospheric reservoir steadily along the two-endmember (river-ocean) mixing curve.

Amazon River basin processes

The Amazon River drains the largest single watershed in the world, covering 6 million km^2, including 1100 major tributaries. Terrestrial processes occurring far upland in the Amazon watershed supply most of the river's fresh water and dissolved constituents, closely connecting

the continent to the open ocean. The river lies in a classic river basin, where highlands border a vast central plain that leads to extensive floodplains. Surrounding the basin are the Guiana Highlands to the north, the Andean Cordillera to the west, and the Brazilian Highlands to the south (Figure 1.3). Tributaries drain Andean regions (Rios Solimões, Madeira), weathered lowland terrain (Rio Negro), or shield (highland) areas (Rios Trombetas, Xingú, Tapajós, Devol and Hedges 2001). The floodplains along the river mainstem, or várzea, contain heavily vegetated lowlands and small lakes, which undergo periodic flooding (Melack and Forsberg 2001).

Sources of water to the Amazon mainstem fall into four categories: white water, clear water, black water, and várzea drainage. White-water rivers such as the Rio Madeira drain Andean areas and contain high loads of suspended sediments, nutrients, and ions (Devol and Hedges 2001). Andean white-water tributaries are the primary source of alkalinity to the mainstem and early river plume, raising pH and adding low levels of dissolved organic carbon (DOC) to the mainstem (Degens et al. 1991). DOC can be respired and raise DIC levels in the river. Clear-water rivers drain weathered highland areas, carrying small loads of suspended sediments and DOC to the mainstem (Devol and Hedges 2001). Black-water rivers such as the Rio Negro are dark brown due to high concentrations of dissolved organic matter. These rivers do not contribute carbonate alkalinity or sediments to the mainstem (Degens et al. 1991), because they drain central basin forest areas whose soils are already highly weathered (Devol and Hedges 2001; McClain and Elsenbeer 2001). Precipitation in the Andes provides more alkalinity and higher pH to the Amazon mainstem; rainfall in the highlands lowers pH and total alkalinity but adds DOC. Várzea regions process nutrients and organic matter in mainstem water and host high rates of both respiration and production. When várzea waters rejoin the mainstem after a flood,

they contribute newly produced, labile DOC and broken-down, previously refractory DOC (Richey et al. 1990; Melack and Forsberg 2001).

Timing of tributary contributions depends on movement of local rainfall maxima, which roughly follow the meridional movement of solar heating (Marengo et al. 2001). Rainfall is also influenced by oceanic moisture supply and by local changes in convection and atmospheric stability (Marengo and Nobre 2001; Fu et al. 2001). In boreal winter, a thermally driven low-pressure system over the South American continent between 20 and 30˚S displaces the intertropical convergence zone (ITCZ) far south, while a high-pressure zone dominates the tropical North Atlantic. A strong northeasterly flow consequently develops, bringing moisture and heat from the tropical North Atlantic to the southern Amazon basin (Figure 1.4, Marengo et al. 2001; Brown et al. 1989). Consequently, maximum precipitation in the western and southern Amazon region occurs from November to January (Marengo and Nobre 2001; Curtis and Hastenrath 1999; Grimm 2003; Marengo et al. 2001), driving the boreal winter peak in Amazon mainstem alkalinity. From June – August, thermal heating of South America is at a minimum, and the ITCZ shifts northward to near 5˚N over the continent (Brown et al. 1989). This arrangement permits an east-southeasterly cross-equatorial flow during boreal summer (Brown et al. 1989; Marengo and Nobre 2001; Curtis and Hastenrath 1999), moving heat and moisture to the Amazon basin from the equatorial and tropical South Atlantic (Figure 1.4, Curtis and Hastenrath 1999). The northern Amazon region experiences highest rainfall from May to July (Marengo et al. 2001; Curtis and Hastenrath 1999; Grimm 2003; Marengo and Nobre 2001), driving the boreal summer drop in mainstem alkalinity. Tributaries draining the Brazilian Highlands contribute to the Amazon mainstem in boreal spring and cause the initial spring decline in TA (Devol and Hedges 2001).

Global-scale multi-year cycles such as the El Niño/Southern Oscillation (ENSO) and the North Atlantic Oscillation (NAO) influence western tropical Atlantic sea surface temperature (SST), Amazon basin precipitation, and river discharge through atmospheric connections (Fu et al. 2001; Grimm 2003; Marengo and Nobre 2001; Visbeck et al. 2001; Richey et al. 1989). In general, "El Niño events" (Southern Oscillation negative phases) precede periods of low Amazon flow, and watershed-scale drought. "La Niña events" (Southern Oscillation positive phases) lead to higher Amazon precipitation and discharge (Marengo et al. 2001; Richey et al. 1989; Grimm 2003). For example, El Niño causes atmospheric circulation changes, such as weaker continental convection and reduced Hadley flow, that diminish tropical Atlantic trade winds (Wang 2005), which move less moisture to the Amazon basin (Marengo et al. 2001; Marengo and Nobre 2001). NAO's effects on the Amazon River are not as well known, but its largely positive index for the past thirty years may have lowered tropical Atlantic SSTs, thereby reducing moisture transport into the Amazon Basin (Visbeck et al. 2001). Atmospheric oscillations are not solely responsible for all of the interannual streamflow variability observed; local and basin-scale precipitation influences such as natural insolation and convection variations are also partially responsible (Richey et al. 1989; Marengo and Nobre 2001; Fu et al. 2001; Wang 2002). For example, the Amazon Basin experienced severe drought in 2005 (rainfall anomaly map, www.cpc.ncep.noaa.gov/products/precip/realtime/SA/annual.cycle.y2005.anom.gif) that may have been related to high WTNA SSTs (e.g., Nobre and Shukla 1996). The cause of 2005's high SSTs has not yet been determined, but suggests that global warming could cause widespread changes in Amazon discharge. Whether discharge variations related to ENSO, NAO, or other sea surface temperature changes alter Amazon River plume chemistry has not

been studied, but connections seem logical given the importance of seasonal precipitation maxima in river alkalinity.

Nutrient concentrations in the mainstem tend to be greater than in the ocean and vary seasonally over small ranges (Table 1.1, Richey et al. 1991), despite the large seasonal variation in Amazon discharge volume (100 x 10^3 m^3 s^{-1} in November, and 250 x 10^3 m^3 s^{-1} in May-June)(Nittrouer and DeMaster 1996). Although Amazon mainstem DIC and TA values are 3-4 times lower than those of the WTNA (Table 1.1), river pCO_2 exceeds atmospheric pCO_2 because the lower mainstem pH (Devol et al. 1987; Devol and Hedges 2001) partitions 80-90% of the riverine DIC load in bicarbonate, and the remainder in hydrated gaseous CO_2 (Degens et al. 1991; Devol and Hedges 2001).

Primary production is not always light limited in the floodplains as it is in the turbid Amazon mainstem, and the várzea host high rates of both primary production and respiration. Values for pCO_2 in the várzea can be quite high as a result (up to 44,000 μatm, Richey et al. 2002). The floodplains are net autotrophic, supporting area-integrated net primary production of 2 Tg C y^{-1} (Melack and Forsberg 2001). When the várzea flood, organic carbon released to the mainstem supports half the *in situ* oxidation there (Richey et al. 1990; Melack and Forsberg 2001). Respiration of DOM from upland and várzea regions dominates production in the river mainstem, regenerating nutrients and releasing about 14 Tg C y^{-1} by air-water exchange (Devol et al. 1987).

Early Plume/Continental Shelf Oceanic processes

The magnitude of Amazon discharge causes estuarine processes to occur on the continental shelf instead of within the river mouth (Nittrouer and DeMaster 1996). Strong tidal

mixing on the inner continental shelf is believed to break down vertical density stratification, preventing an estuarine return flow of saline water from developing along the river bottom (Nittrouer and DeMaster 1996; Geyer et al. 1996). Once river water moves seaward of the very shallow (10-15 m) frontal zone, it remains a coherent, brackish surface plume atop the North Brazil Current (NBC)-origin ocean water separated by a strong pycnocline (Geyer et al. 1996; Lentz and Limeburner 1995). Turbulent vertical mixing across this boundary is somewhat restricted (Sprintall and Tomczak 1992; Pailler et al. 1999), causing plume processes to depend mostly on the river-set composition of the plume rather than on properties of ocean water below the plume.

Riverine nutrients and dissolved organic matter support primary production in the offshore plume (DeMaster and Pope 1996; DeMaster and Aller 2001; DeMaster et al. 1996; Richey et al. 1991). In general, river water contributes nutrients, sediments, and DOC to the ocean, and dilutes DIC, TA and salinity (Table 1.1). When river and ocean water mix, pH changes release additional phosphate from ferric hydroxide complexes (Chase and Sayles 1980; DeMaster and Aller 2001; Fox 1989; Richey et al. 1991), and pCO_2 drops following a shift in carbonate equilibria (Körtzinger 2003). DIC and TA values near the river mouth and in the early plume are not well quantified (river values in Table 1.1 were measured 1600 km upstream at Obidos, Richey et al. 1991), but DIC in November 1991 outside the river mouth was 363 μmol L^{-1} (Druffel et al. 2005). Presumably, TA at the mouth should also be low, because only highland tributaries join the mainstem after Obidos and they do not add TA.

Although riverine nutrients are abundant in the early plume, near-shore primary production in areas less than 20m deep is initially light-limited by high suspended sediment loads (Nittrouer and DeMaster 1996). Respiration is unhindered, processing river-borne organic

matter and releasing nutrients throughout the plume. Primary production resumes on the shelf after turbidity drops below about 10 mg L^{-1} (DeMaster et al. 1996), which occurs quickly; 95 % of the sediment load settles out by salinity 3 (Edmond et al. 1981), located about 150 km from the river mouth (Geyer et al. 1996). Mean shelf production is 2.0x 10^{11} g C d^{-1} (Smith and DeMaster 1996), but ongoing regeneration re-releases 92-98% of Si, N, and P back into the water column (DeMaster and Pope 1996). Nitrate on the continental shelf limits primary production (DeMaster and Pope 1996) and is removed additionally by organic matter deposition and denitrification (DeMaster and Aller 2001). Nitrogen is limiting in waters leaving the shelf, causing primary production in the offshore plume also to be nitrogen-limited; this increases the likelihood that nitrogen fixation will be important offshore.

Offshore Oceanic Processes and Plume

As the Amazon plume moves offshore, it alters the physical, chemical, and biological characteristics of the normally oligotrophic WTNA, where high volume currents converge (Bub and Brown 1996; Arhan et al. 1998; Bourles et al. 1999a; Bourles et al. 1999b; Stramma and Schott 1999; Metcalf and Stalcup 1967; Mamayev 1975) and mix water masses from the northern and southern tropics, subtropical gyres, and poles (Figure 1.5). The southernmost, wind-driven portion of the geostrophic equatorial current system flows westward across the Atlantic Ocean near 10˚S as the South Equatorial Current (SEC) (Johns et al. 1998; Bourles et al. 1999b), which splits into northward- and southward-flowing segments when it encounters South America. The northern portion supplies the North Brazil Current (NBC), which flows northwestward along the coast of South America. Most of the NBC-associated transport is in the upper 150m of the water column, but transport also occurs down to 300m and varies in strength

seasonally (Johns et al. 1998). The NBC feeds the easterly South Equatorial Under Current (SEUC), the Equatorial Under Current (EUC), the North Equatorial Undercurrent (NEUC), and the North Equatorial Counter Current (NECC) (Johns et al. 1998; Bourles et al. 1999a; Bourles et al. 1999b; Metcalf and Stalcup 1967). By the time the NBC reaches the equator and acquires Amazon water, it transports 32 Sv (Johns et al. 1998). Because the NBC entrains Amazon water and feeds several currents (Bourles et al. 1999a; Metcalf and Stalcup 1967; Bourles et al. 1999b), Amazon plume properties can reach far throughout the Atlantic basin.

Wind and heat changes alter currents seasonally, carrying the Amazon plume to different areas of the WTNA in a coherent mass (Stramma and Schott 1999; Lentz 1995; Marengo and Nobre 2001). In general, the plume turns northward outside the river mouth into the North Atlantic due to the dominance of wind forcing and NBC entrainment over weak, low-latitude Coriolis acceleration (Geyer et al. 1996). From December to February, onshore wind stress is approximately normal to the Brazilian coast, encouraging the Amazon plume entrained in the northwesterly NBC to remain close to the coastline in a long, thin band (Geyer et al. 1996; Nittrouer and DeMaster 1996). At this time, the NECC is weakest (Bourles et al. 1999b, and references therein), so Amazon water primarily reaches the Caribbean rather than the offshore WTNA. During boreal winter and spring, trade winds sometimes shift to a more northerly direction and impede along-shelf northwesterly transport, causing fresh water to build up on the continental shelf (Geyer et al. 1996). Subsequently, east-southeasterly winds carry the plume along the northern Brazilian coastal shelf with the North Brazil Current from June to August; Coriolis acceleration acting on the wind-driven, faster, along-shelf NBC encourages the plume to detach from the coast anticyclonically and retroflect northeast into the WTNA (Nittrouer and DeMaster 1996; Geyer et al. 1996). The late summer plume is very broad (Geyer et al. 1996),

and it exposes a large volume of low carbon, high chlorophyll plume water to sunlight and air-sea gas exchange. The NBC retroflection occurs at 6-8˚N, feeding the NECC's annual peak flow (Bourles et al. 1999b; Brown et al. 1989; Fratantoni and Glickson 2002, and references therein). Drifter tracks and satellite chlorophyll a images trace plume water as far as the east coast of Africa during late summer (Geyer et al. 1996; Muller-Karger et al. 1988). At the same time, rings of NBC water pinch off from the retroflected NBC/NECC flow and drift northwestward into the Caribbean Sea (Bourles et al. 1999b; Fratantoni and Glickson 2002; Johns et al. 1990), maintaining transport of South Atlantic water and Amazon water with high chlorophyll and low carbon northward even during NBC retroflection (Fratantoni and Glickson 2002, and references therein).

While the plume is offshore, it remains atop the ocean water column as a 5-15 m lens of warm, fresh water (Lentz and Limeburner 1995; Pailler et al. 1999). The ocean water below the plume, normally "surface" ocean water when the plume is absent, receives the export flux of OM from the highly productive plume. Organic matter sinking below the surface ocean water into intermediate water across the main pycnocline (σ_t= 26.00, between 100-200m, Bub and Brown 1996; Mamayev 1975) creates the total WTNA export flux, removing inorganic carbon from surface waters to the less frequently ventilated deep ocean. Intermediate watermasses are mixtures of North and South Atlantic Subtropical Water (NASW, SASW), Antarctic Intermediate Water (AAIW), and North Atlantic Deep Water (NADW, Bub and Brown 1996; Sverdrup et al. 1942). Subtropical watermasses tend to ventilate with the atmosphere on the order of a few decades (Doney et al. 1998), whereas NADW and AAIW ventilation times are on the order of centuries. Organic matter exported from the Amazon plume is remineralized throughout the water column into watermasses with a range of ventilation timescales. Therefore,

"export" from the surface ocean/plume does not automatically equal long-term sequestration; rather, it indicates removal of this carbon for at least a few decades, and possibly longer. The dynamics of deep remineralization under future conditions of change are not yet known.

Inorganic carbon supply does not limit primary production in areas free of river influence; low concentrations and supply rates of other nutrients do (Table 1.1). In the absence of the river plume, WTNA DIC, TA, and dissolved oxygen levels are similar to those in other tropical surface oceans, but total inventories of N, P, and Si are lower in the Atlantic than in the Pacific or Indian Oceans (Broecker and Peng 1982). The major source of phosphorus to the WTNA is from the summertime Amazon River flood (Conkright et al. 2000). Plumes of mineral dust from Africa and Europe travel to the WTNA on easterly winds and deposit small amounts of nitrogen, iron, and phosphorus there (Prospero et al. 1996). Model estimates suggest that 10-36 μmol N m^{-2} d^{-1} is deposited between 0-10˚N and 40-60˚W (Prospero et al. 1996). Airborne iron and summertime riverine phosphorus fluxes to the surface WTNA (Prospero et al. 1996; Chen and Siefert 2004) favor the high Fe and P requirements of diazotrophs (Sanudo-Wilhelmy et al. 2001; Capone et al. 1997), which are known to contribute new nitrogen to oligotrophic, tropical oceans at rates comparable to eddy-induced upwelling (Capone et al. 1997; Karl et al. 1997). In the tropical Atlantic, the upwelling flux of new nitrogen ranges from 30-150 μmol N m^{-2} d^{-1} (outside of equatorial upwelling zones, Capone et al. 1997). Although the plume-area-integrated ($2x10^6$ km^2, Körtzinger 2003) fluxes of nitrogen from the atmosphere and upwelling (2.4x107-3.6x108 mol d-1) span the Amazon dissolved nitrogen supply ($2.5x10^8$ mol N d^{-1}, DeMaster and Aller 2001), these processes act over such a large area that primary production per meter is not greatly enhanced. If all nitrogen supplied resulted in carbon fixation with a C:N ratio of 6.6, only 0.06-1 mmol C m^{-2} d^{-1} would be fixed, which is far below typical primary production rates

(2-30 mmol C m^{-2} d^{-1}) in the oligotrophic ocean (Maranon et al. 2003). In the absence of the river plume, the low supply of nutrients to the WTNA implies low primary production rates in the surface ocean.

When the plume brings summertime inorganic and organic nutrients to the WTNA, its associated nutrients support dense plankton populations across the early plume which are visible in satellite chlorophyll *a* images (Muller-Karger et al. 1988; Muller-Karger et al. 1995). Primary production and export may intensify the mixing-induced inorganic carbon sink in the Amazon plume (Ternon et al. 2000; Körtzinger 2003). According to the Redfield paradigm, maximum production of inorganic carbon in this plume water is possible when inorganic nutrients are available in the ideal ratio. Although Amazon waters are nutrient-rich, they are nitrogen-limited in the Redfield definition (TN:TP = 5, Richey et al. 1991), and the upwelling nutrient supply has an NO_3+NH_4: PO_4 ratio of 7.7 (DeMaster and Aller 2001; DeMaster and Pope 1996; Richey et al. 1990; Richey et al. 1991). Both sources are well below the Redfield ratio of 16. Using the available excess river-provided phosphate in the WTNA (Conkright et al. 2000) requires more biologically available inorganic nitrogen, which is likely provided by nitrogen fixation (DeMaster and Aller 2001; Carpenter et al. 1999; Carpenter et al. 2004).

Macroscopic diazotrophs such as *Trichodesmium* spp. and diatoms with diazotrophic endosymbionts such as *Hemiaulus hauckii* with *Richelia intracellularis* are numerous in the WTNA, providing biologically usable nitrogen to the N-limited WTNA community (Capone et al. 1997; Carpenter and Roenneberg 1995; Carpenter et al. 1999; Carpenter et al. 2004). The exact distributions of these organisms relative to Amazon plume conditions are still under study (R. Shipe, pers. comm.), but some trends are apparent. Diatom assemblages containing more estuarine/coastal species (R. Shipe, pers. comm.) are common in the early plume (Milliman and

Boyle 1975) due to high silicate levels and abundant nutrients. Diatoms with diazotrophic symbionts succeed initial diatom assemblages (R. Shipe, pers. comm., Subramaniam et al. *in revision*) as initial nutrient supplies are regenerated from organic matter stocks and nitrogen becomes limiting. Finally, free-living *Trichodesmium* becomes prevalent late in the plume, after diatoms sink or are grazed and dissolved silicate and phosphorus concentrations decrease (Subramaniam et al. *in revision*). Non-diazotrophic phytoplankton are also found in the offshore plume (Subramaniam et al. *in revision*) and these "echo blooms" (Coles et al. 2004) may depend on leakage of fixed nitrogen from *Trichodesmium*.

Scope of Study

Although the Amazon plume is known to create a sink for atmospheric carbon by virtue of spreading low-carbon water over a large region, the mechanisms controlling carbon fluxes through the euphotic WTNA year-round are not yet determined. The following chapters' overriding goals are to determine the relative importance of physical, biological, chemical, and geological processes in establishing and maintaining the Amazon plume carbon sink, and to quantify the movement of inorganic carbon through the surface WTNA so that future basin-wide carbon cycle studies will more accurately include processes relevant to the Amazon plume. Chapter 2 quantifies physical mixing effects and biological effects on WTNA inorganic carbon distributions by comparing plume- and nonplume-influenced conditions in two seasons. We find that diazotrophic primary production, especially that of diatoms with diazotrophic symbionts, can remove additional inorganic carbon and prolong the undersaturation of the plume, perhaps for longer than the duration of the physical plume structure itself. Chapter 3 investigates the role of seasonal variability in carbon supply and processing on plume inorganic carbon distributions.

Although the seasonal ranges of WTNA ocean temperature and windspeed are small, causing little seasonal variability in air-sea CO_2 transfer compared to subtropical locations, seasonal variations in the Amazon River discharge supply seasonally varying low values of TA and DIC to the offshore plume. There, biologically mediated inorganic carbon deficits enhance air-sea CO_2 transfer throughout the year. Without major changes in biological drawdown, the true controllers of Amazon plume CO_2 uptake are meteorological conditions; changes in local climate are most likely to enhance or minimize the sink. Chapter 4 is a modeling study that examines the role of vertical mixing on plume breakdown, and whether vertical fluxes are sufficient to remediate the plume-associated inorganic carbon deficit. Finally, Chapter 5 summarizes the main findings of my research and highlights areas for future research.

References:

Arhan, M., H. Mercier, B. Bourles and Y. Gouriou (1998). Hydrographic sections across the Atlantic at 7 degrees 30N and 4 degrees 30S. *Deep-Sea Research Part I-Oceanographic Research Papers 45*(6): 829-872.

Bauer, J. E. and E. R. M. Druffel (1998). Ocean margins as a significant source of organic matter to the deep ocean. *Nature 392*: 482-485.

Bolin, B. and E. Eriksson (1959). Changes in the Carbon Dioxide Content of the Atmosphere and Sea Due to Fossil Fuel Combustion. *The Atmosphere and the Sea in Motion*. B. Bolin. Rockefeller Institute Press, New York: 130-142.

Borges, A. V., B. Delille and M. Frankignoulle (2005). Budgeting sinks and sources of CO_2 in the coastal ocean: Diversity of ecosystems counts. *Geophysical Research Letters 32*(L14601): doi: 10.1029/2005GL023053.

Bourles, B., Y. Gouriou and R. Chuchla (1999a). On the circulation in the upper layer of the western equatorial Atlantic. *Journal of Geophysical Research-Oceans 104*(C9): 21,151-21,170.

Bourles, B., R. L. Molinari, E. Johns, W. D. Wilson and K. D. Leaman (1999b). Upper layer currents in the western tropical North Atlantic (1989-1991). *Journal of Geophysical Research-Oceans 104*(C1): 1361-1375.

Boyle, E. A., R. Collier, A. T. Dengler, J. M. Edmond, A. C. Ng and R. F. Stallard (1974). On the chemical mass-balance in estuaries. *Geochimica et Cosmochimica Acta 38*: 1719-28.

Broecker, W. S. and T.-H. Peng (1982). *Tracers in the Sea*. Lamont-Doherty Geological Observatory, Columbia University; Eldigio Press, Palisades, New York.

Brown, J., A. Colling, D. Park, J. Phillips, D. Rothery and J. Wright (1989). *Ocean Circulation*. Butterworth-Heinemann, Oxford.

Bub, F. L. and W. S. Brown (1996). Intermediate layer water masses in the western tropical Atlantic ocean. *Journal of Geophysical Research-Oceans 101*(C5): 11903-11922.

Cai, W.-J. and M. Dai (2004). Comment on "Enhanced Open Ocean Storage of CO_2 from Shelf Sea Pumping". *Science 306*: 1477c.

Capone, D. G., J. P. Zehr, H. W. Paerl, B. Bergman and E. J. Carpenter (1997). *Trichodesmium*, a globally significant marine cyanobacterium. *Science 276*: 1221-1229.

Carpenter, E. J., J. P. Montoya, J. Burns, M. R. Mulholland, A. Subramaniam and D. G. Capone (1999). Extensive bloom of a N_2-fixing diatom/cyanobacterial association in the tropical Atlantic Ocean. *Marine Ecology Progress Series 185*: 273-283.

Carpenter, E. J. and T. Roenneberg (1995). The marine planktonic cyanobacteria *Trichodesmium* spp.: photosynthetic rate measurements in the SW Atlantic Ocean. *Marine Ecology Progress Series 118*: 267-273.

Carpenter, E. J., A. Subramaniam and D. G. Capone (2004). Biomass and primary productivity of the cyanobacterium *Trichodesmium* spp. in the tropical N. Atlantic Ocean. *Deep-Sea Resarch I 51*: 173-203.

Chase, E. M. and F. L. Sayles (1980). Phosphorus in suspended sediments of the Amazon River. *Estuarine, Coastal, and Marine Science 11*: 383-391.

Chen, Y. and R. Siefert (2004). Seasonal and spatial distributions and dry deposition fluxes of atmospheric total and labile iron over the tropical and subtropical North Atlantic Ocean. *Journal of Geophysical Research-Atmospheres 109*(D09315): doi:10.1029/2003JD003958.

Chester, R. (1990). *Marine Geochemistry*. Unwin Hyman Ltd., London.

Coles, V. J., C. Wilson and R. R. Hood (2004). Remote sensing of new production fuelled by nitrogen fixation. *Geophysical Research Letters 31*(L06301): doi:10.1029/2003GL019018.

Conkright, M. E., W. W. Gregg and S. Levitus (2000). Seasonal cycle of phosphate in the open ocean. *Deep-Sea Research I 47*: 159-175.

Curtis, S. and S. Hastenrath (1999). Trends of upper-air circulation and water vapour over equatorial South America and adjacent oceans. *International Journal of Climatology 19*: 863-876.

Degens, E. T., S. Kempe and J. E. Richey (1991). Summary: Biogeochemistry of Major World Rivers. *Biogeochemistry of Major World Rivers*. E. T. Degens, S. Kempe and J. E. Richey. John Wiley & Sons, Ltd., New York: 323-348.

DeMaster, D. J. and R. C. Aller (2001). Biogeochemical Processes on the Amazon Shelf: Changes in Dissolved and Particulate Fluxes during River/Ocean Mixing. *The Biogeochemistry of the Amazon Basin*. M. E. McClain, R. L. Victoria and J. E. Richey. Oxford University Press: 328-357.

DeMaster, D. J. and R. H. Pope (1996). Nutrient Dynamics in Amazon Shelf Waters - Results from AMASSEDS. *Continental Shelf Research 16*(3): 263-289.

DeMaster, D. J., W. O. Smith, D. M. Nelson and J. Y. Aller (1996). Biogeochemical processes in Amazon shelf waters: chemical distributions and uptake rates of silicon, carbon and nitrogen. *Continental Shelf Research 16*(5-6): 617-643.

Devol, A. H. and J. I. Hedges (2001). Organic Matter and Nutrients in the Mainstem Amazon River. *The Biogeochemistry of the Amazon Basin*. M. E. McClain, R. L. Victoria and J. E. Richey. Oxford University Press, New York: 275-306.

Devol, A. H., P. D. Quay, J. E. Richey and L. A. Martinelli (1987). The role of gas exchange in the inorganic carbon, oxygen, and ^{222}Rn budgets of the Amazon River. *Limnology and Oceanography 32*(1): 235-248.

DOE (1997). Handbook of methods for the analysis of the various parameters of the carbon dioxide system in sea water. A. G. Dickson and C. Goyet, eds., ORNL/CDIAC-74.

Doney, S. C., J. L. Bullister and R. Wanninkhof (1998). Climatic variability in upper ocean ventilation rates diagnosed using chlorofluorocarbons. *Geophysical Research Letters 25.*: 1399–1402.

Druffel, E. R. M., J. E. Bauer and S. Griffin (2005). Input of particulate organic and dissolved inorganic carbon from the Amazon to the Atlantic Ocean. *Geochemistry Geophysics Geosystems 6*(3): doi: 10.1029/2004GC000842.

Edmond, J. M., E. A. Boyle, B. Grant and R. F. Stallard (1981). The chemical mass balance in the Amazon plume - I. The nutrients. *Deep-Sea Resarch 28A*(11): 1339-1374.

Feely, R. A., C. L. Sabine, T. Takahashi and R. Wanninkhof (2001). Uptake and storage of carbon dioxide in the ocean: the global CO_2 survey. *Oceanography: Special Issue--JGOFS 14*(4): 18-32.

Fox, L. E. (1989). A model for inorganic control of phosphate concentrations in river waters. *Geochimica et Cosmochimica Acta 53*: 417-428.

Frankignoulle, M. and A. V. Borges (2001). European continental shelf as a significant sink for atmospheric carbon dioxide. *Global Biogeochemical Cycles 15*(3): 569-576.

Fratantoni, D. M. and D. A. Glickson (2002). North Brazil Current ring generation and evolution observed with SeaWiFS. *Journal of Physical Oceanography 32*: 1058-1074.

Friis, K., A. Kortzinger and D. W. R. Wallace (2003). The salinity normalization of marine inorganic carbon chemistry data. *Geophysical Research Letters 30*(2): doi: 10.1029/2002GL015898.

Fu, R., R. E. Dickinson, M. Chen and H. Wang (2001). How do tropical sea surface temperatures influence the seasonal distribution of precipitation in the equatorial Atlantic? *Journal of Climate 14*: 4003-4026.

Geyer, W. R., R. C. Beardsley, S. J. Lentz, J. Candela, R. Limeburner, W. E. Johns, B. M. Castro and I. D. Soares (1996). Physical oceanography of the Amazon shelf. *Continental Shelf Research 16*(5-6): 575-616.

Grimm, A. M. (2003). The El Niño Impact on the Summer Monsoon in Brazil: Regional Processes versus Remote Influences. *Journal of Climate 16*: 263-280.

Hochman, H. T., F. E. Muller-Karger and J. J. Walsh (1994). Interpretation of the coastal zone color scanner signature of the Orinoco River plume. *Journal of Geophysical Research-Oceans 99*(C4): 7443-7455.

Johns, W. E., T. N. Lee, R. C. Beardsley, J. Candela, R. Limeburner and B. Castro (1998). Annual cycle and variability of the North Brazil Current. *Journal of Physical Oceanography 28*(1): 103-128.

Johns, W. E., T. N. Lee, F. A. Schott, R. J. Zantopp and R. H. Evans (1990). The North Brazil Current retroflection: Seasonal structure and eddy variability. *Journal of Geophysical Research 95*(C12): 22103-22120.

Karl, D., R. Letelier, L. Tupas, J. Dore, J. Christian and D. Hebel (1997). The role of nitrogen fixation in biogeochemical cycling in the subtropical North Pacific Ocean. *Nature 388*(6642): 533-538.

Karl, D. M., J. E. Dore, R. Lukas, A. F. Michaels, N. R. Bates and A. Knap (2001). Building the long term-picture: The U.S. JGOFS time-series programs. *Oceanography 14*(4): 8-17.

Keeling, C. D. (1960). The concentration and isotopic abundances of carbon dioxide in the atmosphere. *Tellus 12*: 200-203.

Körtzinger, A. (2003). A significant CO_2 sink in the tropical Atlantic Ocean associated with the Amazon River plume. *Geophysical Research Letters 30*(24): 2287-2290.

Lentz, S. J. (1995). Seasonal Variations in the Horizontal Structure of the Amazon Plume Inferred from Historical Hydrographic Data. *Journal of Geophysical Research-Oceans 100*(C2): 2391-2400.

Lentz, S. J. and R. Limeburner (1995). The Amazon River Plume During AMASSEDS - Spatial Characteristics and Salinity Variability. *Journal of Geophysical Research-Oceans 100*(C2): 2355-2375.

Libes, S. M. (1992). *An Introduction to Marine Biogeochemistry*. John Wiley & Sons, Inc., New York.

Lundberg, L. (1994). CO_2 Air-Sea Exchange in the Nordic Seas - an Attempt to Make an Estimate Based on Data. *Oceanologica Acta 17*(2): 159-175.

Mamayev, O. I. (1975). *Temperature-Salinity Analysis of World Ocean Waters*. Elsevier, New York.

Maranon, E., M. J. Behrenfeld, N. González, B. Mouriño and M. V. Zubkov (2003). High variability of primary production in oligotrophic waters of the Atlantic Ocean:

uncoupling from phytoplankton biomass and size structure. *Marine Ecology - Progress Series 257*: 1-11.

Marengo, J. A., B. Liebmann, V. E. Kousky, N. P. Filizola and I. C. Wainer (2001). Onset and End of the Rainy Season in the Brazilian Amazon Basin. *Journal of Climate 14*: 833-852.

Marengo, J. A. and C. A. Nobre (2001). General characteristics and variability of climate in the Amazon basin and its links to the global climate system. *The Biogeochemistry of the Amazon Basin*. C. R. McClain, R. L. Victoria and J. E. Richey. Oxford University Press: 17-41.

McClain, M. E. and H. Elsenbeer (2001). Terrestrial Inputs to Amazon Streams and Internal Biogeochemical Processing. *The Biogeochemistry of the Amazon Basin*. M. E. McClain, R. L. Victoria and J. E. Richey. Oxford University Press, London: 185-208.

Melack, J. M. and B. R. Forsberg (2001). Biogeochemistry of Amazon Floodplain lakes and Associated Wetlands. *The Biogeochemistry of the Amazon Basin*. M. E. McClain, R. L. Victoria and J. E. Richey. Oxford University Press, London: 235-274.

Metcalf, W. G. and M. C. Stalcup (1967). Origin of the Atlantic Equatorial Undercurrent. *Journal of Geophysical Research 72*(20): 4959-4975.

Milliman, J. D. and E. A. Boyle (1975). Biological uptake of dissolved silica in the Amazon River estuary. *Science 189*: 995-997.

Muller-Karger, F. E., C. R. McClain and P. L. Richardson (1988). The dispersal of the Amazon's water. *Nature 333*(56-59).

Muller-Karger, F. E., P. L. Richardson and D. J. McGillicuddy (1995). On the offshore dispersal of the Amazon's plume in the North Atlantic: Comments. *Deep-Sea Research Part I-Oceanographic Research Papers 42*(11-12): 2127-2137.

Nittrouer, C. A. and D. J. DeMaster (1996). The Amazon shelf setting: tropical, energetic, and influenced by a large river. *Continental Shelf Research 16*(5-6): 553-573.

Nobre, P. and J. Shukla (1996). Variations of Sea Surface Temperature, Wind Stress, and Rainfall over the Tropical Atlantic and South America. *Journal of Climate 9*: 2464-2479.

Oltman, R. E. (1968). *Reconnaissance investigations of the discharge and water quality of the Amazon River*. U.S. Geological Survey, Washington, D.C.

Pailler, K., B. Bourles and Y. Gouriou (1999). The barrier layer in the Western Tropical Atlantic Ocean. *Geophysical Research Letters 26*(14): 2069-2072.

Prospero, J. M., K. Barrett, T. Church, F. Dentener, R. A. Duce, J. N. Galloway, H. Levy, II, J. Moody and P. Quinn (1996). Atmospheric deposition of nutrients to the North Atlantic Basin. *Biogeochemistry 35*: 27-73.

Quay, P. D., B. Tilbrook and C. S. Wong (1992). Oceanic Uptake of Fossil Fuel CO_2: Carbon-13 Evidence. *Science 256*: 74-78.

Revelle, R. and H. E. Suess (1957). Carbon dioxide exchange between atmosphere and ocean and the question of an increase of atmospheric CO_2 during the past decades. *Tellus 9*: 18-27.

Richey, J. E., J. I. Hedges, A. H. Devol, P. D. Quay, R. L. Victoria, L. A. Martinelli and B. R. Forsberg (1990). Biogeochemistry of carbon in the Amazon River. *Limnology and Oceanography 35*(2): 352-371.

Richey, J. E., J. M. Melack, A. K. Aufdenkampe, V. M. Ballester and L. L. Hess (2002). Outgassing from Amazonian rivers and wetlands as a large tropical source of atmospheric CO_2. *Nature 416*: 617-620.

Richey, J. E., C. A. Nobre and C. Deser (1989). Amazon River Discharge and Climate Variability: 1903 to 1985. *Science 246*: 101-103.

Richey, J. E., R. L. Victoria, E. Salati and B. R. Forsberg (1991). The Biogeochemistry of a Major River System: The Amazon Case Study. *Biogeochemistry of Major World Rivers*. E. T. Degens, S. Kempe and J. E. Richey. John Wiley & Sons, New York. *42*: 57-74.

Robbins, P. E. (2001). Oceanic carbon transport carried by freshwater divergence: Are salinity normalizations useful? *Journal of Geophysical Research 106*(C12): 30939-30946.

Sanudo-Wilhelmy, S. A., A. B. Kustka, C. J. Gobler, D. A. Hutchins, M. Yang, K. Lwiza, J. Burns, D. G. Capone, J. A. Raven and E. J. Carpenter (2001). Phosphorus limitation of nitrogen fixation by Trichodesmium in the central Atlantic Ocean. *Nature 411*(6833): 66-69.

Sarmiento, J. L., R. Murnane and C. LeQuere (1995). Air-Sea CO_2 Transfer and the Carbon Budget of the North- Atlantic. *Philosophical Transactions of the Royal Society of London Series B-Biological Sciences 348*(1324): 211-219.

Sarmiento, J. L. and J. C. Orr (1991). Three-dimensional simulations of the impact of Southern Ocean nutrient depletion on atmospheric CO_2 and ocean chemistry. *Limnology and Oceanography 36*(8): 1928-1950.

Siegenthaler, U. and J. L. Sarmiento (1993). Atmospheric Carbon-Dioxide and the Ocean. *Nature 365*(6442): 119-125.

Smith, W., O., Jr. and D. J. DeMaster (1996). Phytoplankton biomass and productivity in the Amazon River plume: correlation with seasonal river discharge. *Continental Shelf Research 16*(3): 291-319.

Sprintall, J. and M. Tomczak (1992). Evidence of the Barrier Layer in the Surface Layer of the Tropics. *Journal of Geophysical Research 97*(C5): 7305-7316.

Stramma, L. and F. Schott (1999). The mean flow field of the tropical Atlantic Ocean. *Deep-Sea Research Part Ii-Topical Studies in Oceanography 46*(1-2): 279-303.

Subramaniam, A., E. J. Carpenter, P. L. Yager, S. R. Cooley, R. Del Vecchio, D. Karl, C. Mahaffey, S. A. Sanudo-Wilhelmy, R. Shipe, A. Tovar-Sanchez and D. G. Capone (*in revision*). Amazon River amplifies C and N cycles in the Tropical North Atlantic Ocean.

Sverdrup, H. U., M. W. Johnson and R. H. Fleming (1942). *The Oceans: Their physics, chemistry, and general biology*. Prentice-Hall, Inc., Englewood Cliffs, N.J.

Takahashi, T. (1989). The Carbon Dioxide Puzzle. *Oceanus 32*: 22-29.

Takahashi, T., R. A. Feely, R. F. Weiss, R. H. Wanninkhof, D. W. Chipman, S. C. Sutherland and T. T. Takahashi (1997). Global air-sea flux of CO_2: An estimate based on measurements of sea-air pCO_2 difference. *Proceedings of the National Academy of Sciences of the United States of America 94*(16): 8292-8299.

Takahashi, T., S. C. Sutherland, C. Sweeney, A. Poisson, N. Metzl, B. Tilbrook, N. R. Bates, R. Wanninkhof, R. A. Feely, C. L. Sabine, J. Olafsson and Y. Nojiri (2002). Global sea-air CO_2 flux based on climatological surface ocean pCO_2, and seasonal biological and temperature effects. *Deep-Sea Resarch II 49*: 1601-1622.

Ternon, J. F., C. Oudot, A. Dessier and D. Diverres (2000). A seasonal tropical sink for atmospheric CO_2 in the Atlantic Ocean: the role of the Amazon River discharge. *Marine Chemistry 68*: 183-201.

Thomas, H., Y. Bozec, K. Elkalay and H. J. W. de Baar (2004a). Enhanced open ocean storage of CO_2 from shelf-sea pumping. *Science 304*: 1005-1008.

Thomas, H., Y. Bozec, K. Elkalay and H. J. W. de Baar (2004b). Response to Comment on "Enhanced Open Ocean Storage of CO_2 from Shelf Sea Pumping". *Science 306*: 1477d.

Turner, R. K. and W. N. Adger (1996). Coastal zone resources assessment guidelines. Land-Ocean Interactions in the Coastal Zone Core Project of the IGBP. Den Berg, Texel, The Netherlands, Netherlands Institute of Sea Research: 101 pp.

Ver, L. M. B., F. T. Mackenzie and A. Lerman (1999). Carbon cycle in the coastal zone: effects of global perturbations and change in the past three centuries. *Chemical Geology 159*: 283-304.

Visbeck, M. H., J. W. Hurrell, L. Polvani and H. M. Cullen (2001). The North Atlantic Oscillation: Past, present and future. *Proceedings of the National Academy of Sciences of the United States of America 98*(23): 12876-12877.

Volk, T. and M. I. Hoffert (1985). Ocean carbon pumps: analysis of relative strengths and efficiencies in ocean driven CO_2 changes. *The carbon cycle and atmospheric CO_2: natural variations, Archean to present*. E. T. Sundquist and W. S. Broecker. American Geophysical Union, Washington, D.C. *32*: 99-110.

Wang, C. (2002). Atmospheric Circulation Cells Associated with ENSO and Atlantic Climate Variability. The Hadley Circulation: Past, Present, and Future, International Pacific Research Center, Honolulu, HI.

Wang, C. (2005). ENSO, Atlantic climate variability, and the Walker and Hadley circulations. *The Hadley Circulation: Present, Past and Future*. H. F. Diaz and R. S. Bradley. Kluwer Academic Publishers, The Netherlands: 173–202.

Wanninkhof, R. and W. R. McGillis (1999). A cubic relationship between air-sea CO_2 exchange and wind speed. *Geophysical Research Letters 26*(13): 1889-1892.

Weiss, R. F. (1974). Carbon dioxide in water and seawater: The solubility of a nonideal gas. *Marine Chemistry 2*: 203-215.

Table 1.1: Mean values of dissolved material in Amazon River and WTNA

	River Concentration/Value		Ocean concentration/Value	
Nitrate/Nitrite	10-16	(DeMaster and Pope 1996; Devol and Hedges 2001; Edmond et al. 1981)	1	(80m, DeMaster and Pope 1996)
Ammonium	0-2	(DeMaster and Pope 1996; Lesack 1993; Richey et al. 1991)	0.16	(80m, DeMaster and Pope 1996)
Phosphate	0.5-0.7	(DeMaster and Pope 1996; Devol and Hedges 2001; Edmond et al. 1981; Richey et al. 1991)	0.15-0.24	(80m, DeMaster and Pope 1996; surface, Conkright et al. 2000)
Silicate	120-144	(DeMaster and Pope 1996; Edmond et al. 1981; Edmond et al. 1985; Key et al. 1985; DeMaster et al. 1983; Milliman and Boyle 1975; Nittrouer and DeMaster 1986)	1-3	(80m, DeMaster and Pope 1996; DeMaster and Aller 2001)
Suspended Sediments*	50-200	(Nittrouer and DeMaster 1986)	N/A	
DOC	330	(Devol and Hedges 2001)	80	(DeMaster and Aller 2001)
DIC	485-667	(Richey et al. 1991)	2000-2100	(surface, DeMaster and Aller 2001; Ternon et al. 2000)
TA	400-600	(Devol and Hedges 2001)	2300	(surface, Ternon et al. 2000)
pH	6.2-7.2	(Devol and Hedges 2001; Devol et al. 1987)	7.9-8.2	(surface, WOCE data from CDIAC[†])
pCO_2*	2500-5000	(Devol and Hedges 2001)	350	(surface, Ternon et al. 2000, WOCE data from CDIAC)

*All measurements are in µmol/L except for sediments (mg L^{-1}) and pCO_2 (µatm). River concentrations listed represent the values available from farthest downstream.

[†] Carbon Dioxide Information Analysis Center, http://cdiac.ornl.gov.

Figure 1.1: Mean annual global air-sea flux for 1995, adapted from Takahashi et al. 2002. Note the dearth of flux estimates in coastal zones (circled).

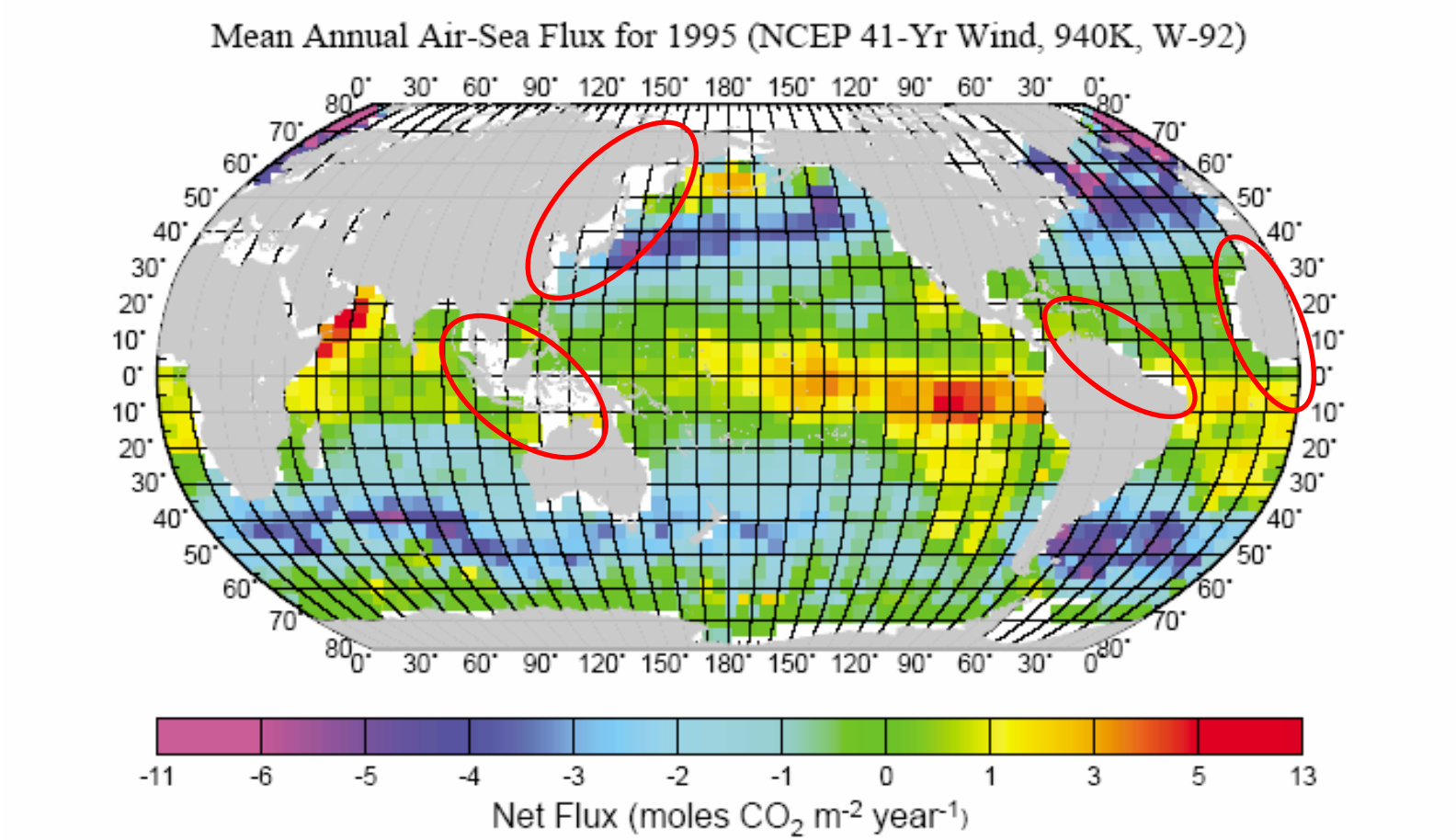

Figure 1.2: False-color satellite image of WTNA chlorophyll a in July 2001, provided by the SeaWiFS Project, NASA/Goddard Space Flight Center and ORBIMAGE (http://seawifs.gsfc.nasa.gov/cgi/level3.pl)

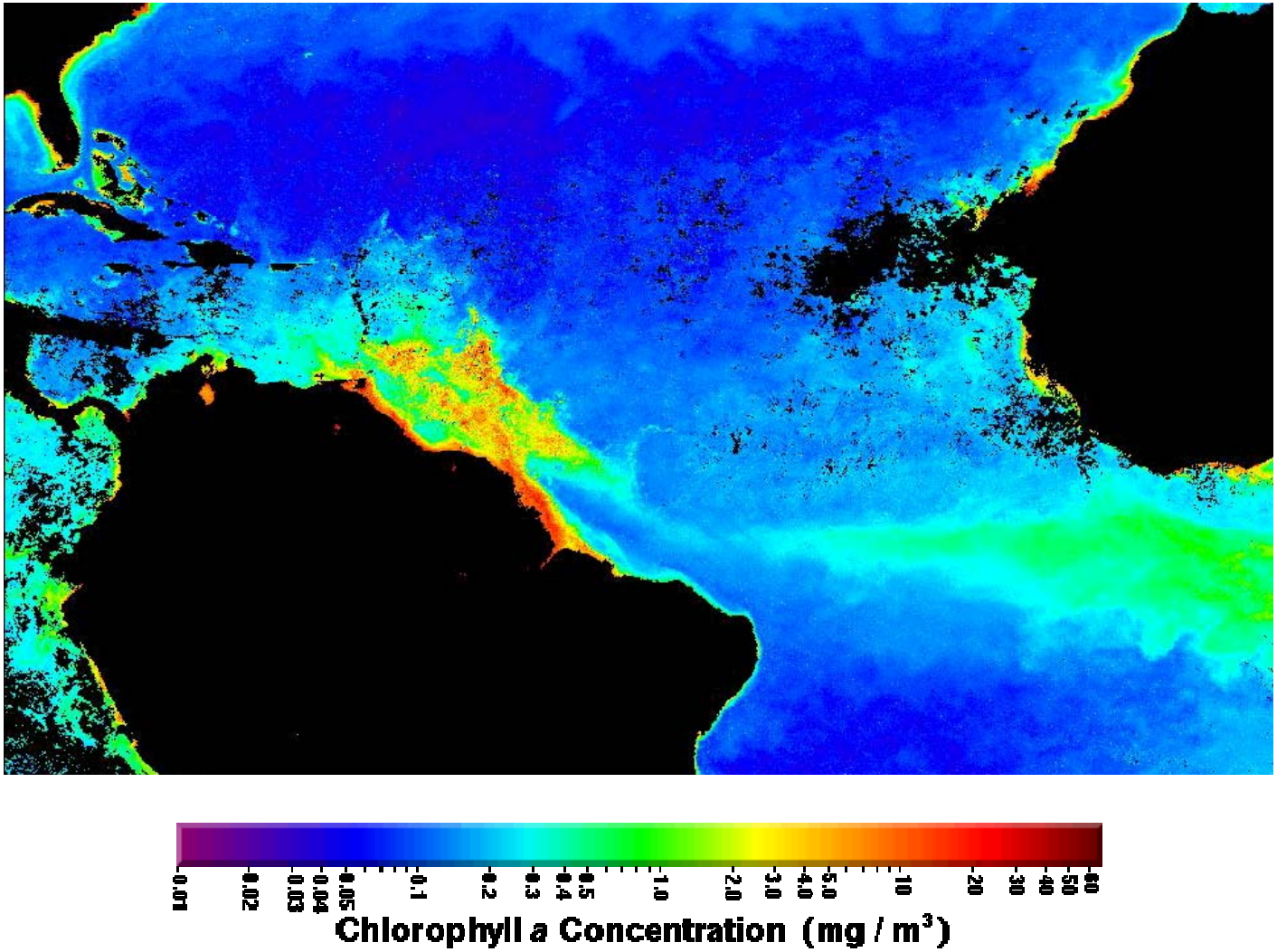

Figure 1.3: Amazon River tributary map with inset aerial photo of the river mouth, adapted from http://www.mbarron.net/Amazon/bigmap.htm (September 22, 2005)

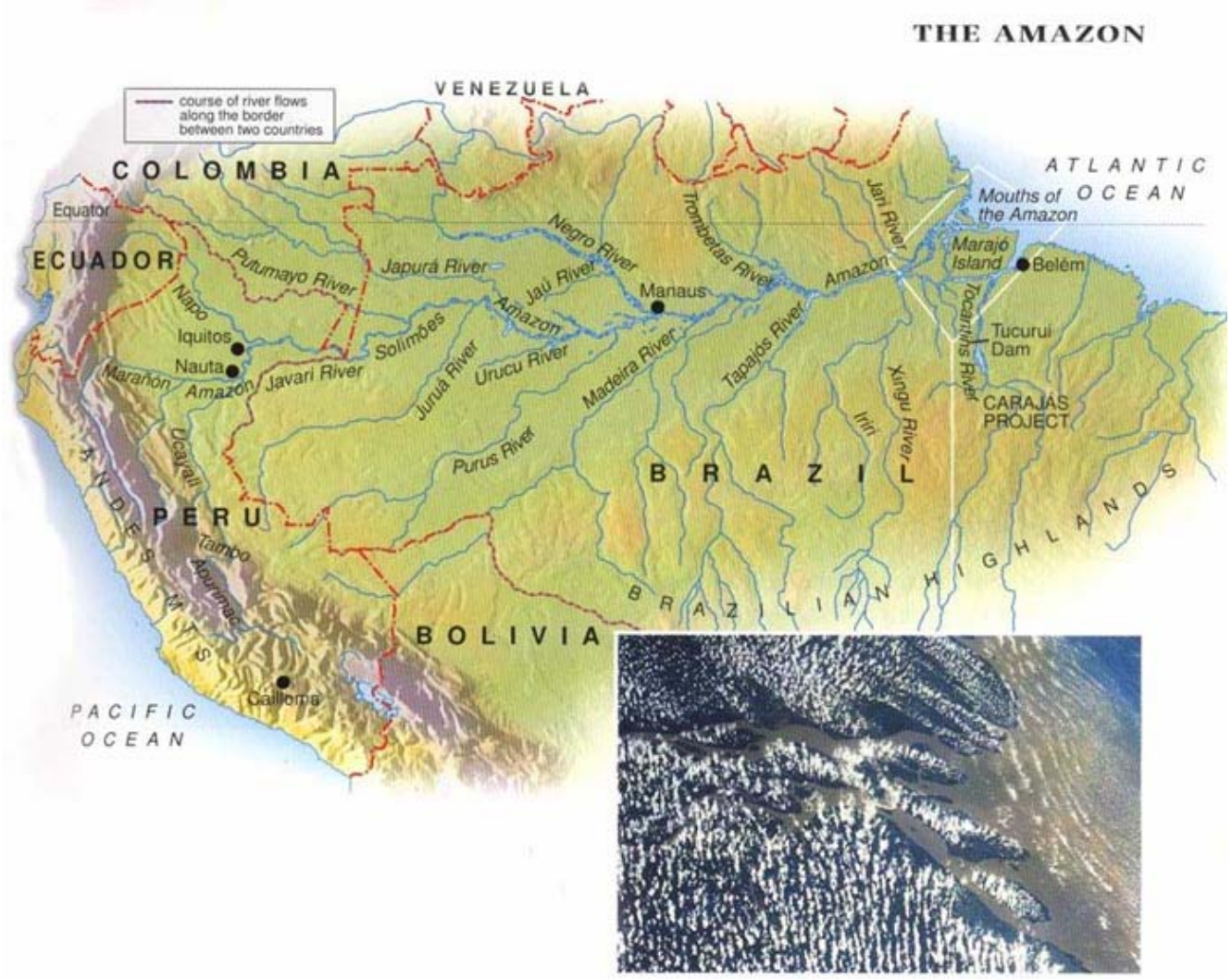

Figure 1.4: Map showing summer (dashed line) and winter (solid line) positions of the Intertropical Convergence Zone (ITCZ) adapted from http://www.newmediastudio.org/DataDiscovery/Hurr_ED_Center/Stages_of_Hurricane_Dev/ITCZ/ITCZ_fig02.jpg. Regions of high pressure ("H"), low pressure ("L"), and the direction of moisture transport into the Amazon River basin (thick arrows) have been added.

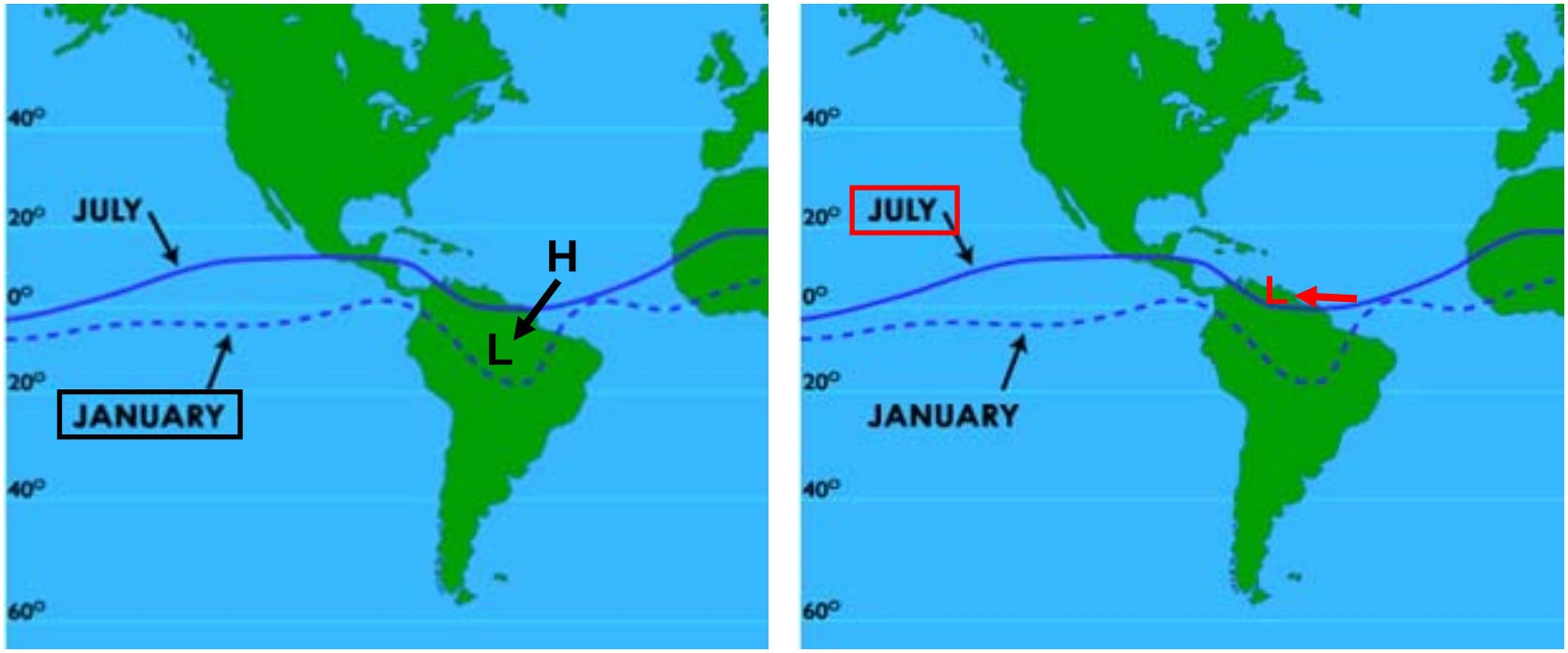

Figure 1.5: Upper water column currents in the Western Tropical Atlantic that are in communication with the North Brazil Current (NBC; see text for other abbreviations). Dashed arrows indicate undercurrents.

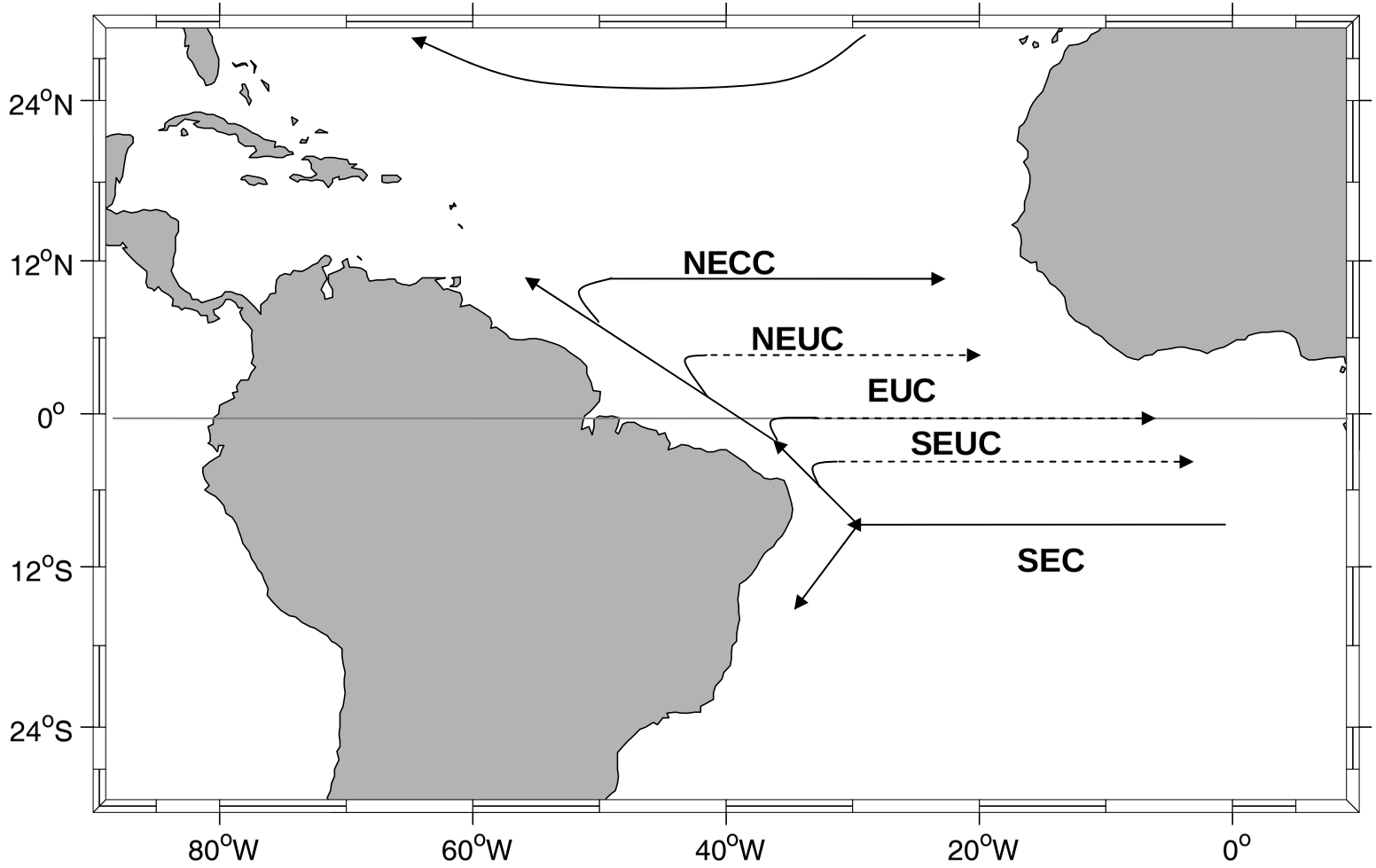

CHAPTER 2

PHYSICAL AND BIOLOGICAL CONTRIBUTIONS TO THE WESTERN TROPICAL NORTH ATLANTIC OCEAN CARBON SINK FORMED BY THE AMAZON RIVER PLUME[1]

[1] S. R. Cooley, P. L. Yager. Accepted by *Journal of Geophysical Research – Oceans*. Reprinted here with permission of publisher (5/23/06).

Abstract

Dissolved inorganic carbon (DIC) and total alkalinity (TA) were measured in the upper 1000 m of the western tropical North Atlantic Ocean (WTNA; study area 3-15 °N, 40-59 °W) in January-February and July-August 2001. Values of DIC and TA in surface samples (0-10 m) influenced by the Amazon River plume were up to 400 μmol C kg^{-1} (20%) lower than oceanic surface samples. In this region, physical dilution by river water dominates DIC and TA inventories, driving CO_2 partial pressure (pCO_2) well below atmospheric levels. Nevertheless, DIC values at most plume-influenced stations were 10-90 μmol C kg^{-1} below levels expected from conservative mixing of seawater with low-salinity, low-CO_2 Amazon River water. In this otherwise oligotrophic region, the diazotrophs *Trichodesmium spp*. and *Richelia intracellularis* were often abundant, supporting a link between increased carbon drawdown and nitrogen fixation in the outer plume. Net community production in the plume must surpass the fluxes of inorganic carbon from below and air-sea CO_2 replacement to leave biologically mediated DIC deficits, which is possible under observed conditions. Biological activity lowers plume pCO_2 30-120 μatm below the conservative mixing line, and contributes to a CO_2 deficit in the northern WTNA that outlasts the plume's physical structure.

Introduction:

The Amazon River discharge creates a 5-10 m deep plume of low-salinity, low-inorganic carbon water atop the western tropical North Atlantic (WTNA, Nittrouer and DeMaster 1986; Lentz and Limeburner 1995; Ternon et al. 2000), forming a sink for atmospheric carbon covering approximately two million square kilometers (Körtzinger 2003). Tropical Atlantic seawater normally releases CO_2 to the atmosphere (0.15 Pg C yr^{-1}, Takahashi et al. 2002) because solubility-driven degassing exceeds biological production in lower latitudes (Goyet et al. 1998; Lee et al. 1997; Takahashi et al. 1997; Takahashi et al. 2002; Sarmiento et al. 1995). In contrast, the Amazon carbon sink removes an estimated 0.014 ± 0.005 Pg C yr^{-1} (0.001 Pmol C yr^{-1}, Körtzinger 2003) from the atmosphere. Plume CO_2 uptake averages 1.35 mmol C m^{-2} d^{-1}, compared to the tropical Atlantic average loss of 1.84 mmol C m^{-2} d^{-1} (Körtzinger 2003). Since the Amazon River's discharge and biogeochemistry are apt to vary with changing climate, understanding the present and future WTNA carbon sink requires quantifying mechanistic controls on regional carbon fluxes.

Rivers and ocean margins supply the ocean with organic carbon (Bauer et al. 1995), fueling heterotrophy near the coast. Coastal regions become autotrophic when inorganic nutrients are abundant from upwelling or runoff (Mackenzie et al. 1998). The Amazon River delivers high concentrations of both nutrients and organic matter to the WTNA (Smith and DeMaster 1996; DeMaster et al. 1996; Ternon et al. 2000; Körtzinger 2003). Simultaneously, the river fosters primary production on the continental shelf (DeMaster and Pope 1996) and promotes CO_2 release via photooxidation or respiration of terrestrial organic matter in the WTNA (Aller et al. 1996; DeMaster and Aller 2001; Smith and DeMaster 1996; Benner et al. 1995; Del Vecchio and Subramaniam 2004). The balance between oceanic heterotrophy and

autotrophy, influenced by community structure (Serret et al. 2001), determines the magnitude and direction of the air-sea CO_2 flux (del Giorgio et al. 1997; Duarte and Agustí 1998; Williams 1998; Geider 1997; Williams and Bowers 1999; Duarte et al. 2001). Frequent diazotroph blooms in the WTNA may foster CO_2 drawdown directly or by fertilizing other autotrophs with biologically available nitrogen (Capone et al. 1997; Carpenter et al. 1999). The resulting plume photosynthesis:respiration balance will then intensify or weaken the CO_2 sink created by the discharge of undersaturated river water. Quantifying total dissolved inorganic carbon (DIC) in seawater constrains biological variables, such as the magnitudes of net community production and organic carbon export (Bender et al. 1987; Yager et al. 1995; Sweeney et al. 2000), but accounting for biological processes in the Amazon plume carbon sink depends first on distinguishing them from physical mixing effects in the WTNA.

We collected vertical profiles of discrete DIC and TA samples in winter and summer 2001 with the NSF Biocomplexity MANTRA/PIRANA Project, which examined influences on WTNA diazotrophs. Our study took place between previously studied on-shelf and offshore plume-influenced areas (Ternon et al. 2000; Körtzinger 2003). Winter samples from this region were not influenced by the plume, whereas summer samples included both plume- and non-plume-influenced regions. In this paper, we test the null hypothesis that physical processes solely influence WTNA inorganic carbon distributions. If physical mixing is insufficient to explain observed variation, we hypothesize that the residual is due to biological processes. We present measured DIC and TA (1-500 m) with calculated surface CO_2 partial pressure (pCO_2). We then use a mechanistic approach to quantify significant variations in DIC not explained by physical processes, and we compare our findings to previous work in the WTNA.

Methods:

Sampling

The winter dataset was collected during daily stations aboard the *R/V Seward Johnson I* throughout the first Atlantic MANTRA/PIRANA cruise (MP1; January 19 – February 22, 2001), within 5-14 ˚N, 40-59 ˚W (Figure 2.1a). The summer dataset was collected during the second Atlantic MANTRA/PIRANA cruise (MP3; July 9-August 19, 2001) aboard the *R/V Knorr*, within 3-15 ˚N, 42-57 ˚W (Figure 2.1b).

During both cruises, water samples were collected from discrete depths using Niskin bottles between 1 and 1000 m, with occasional deep (up to 4000 m) casts to compare with historical datasets. DIC and TA samples were collected according to established protocols (DOE 1997). Winter samples were analyzed aboard ship within 1 week of sampling for DIC and TA. Summer samples were kept cool aboard ship until they were returned to Georgia, where they were stored in the dark at 4 ˚C until processing. Seawater collected and stored following this protocol was stable for DIC and TA analysis for at least 4 years (P.L. Yager, unpublished data). Summer samples were analyzed within 2-3 months of collection.

Sample Analysis

DIC

Dissolved inorganic carbon measurements were performed on a SOMMA system (Single Operator Multiparameter Metabolic Analyzer, Johnson et al. 1993) connected to a CO_2 coulometer (UIC, Inc. Model 5011). Samples were analyzed following standard protocols (Johnson et al. 1993; DOE 1997; Bates et al. 1996). Sample conductivity was measured with a Sea-Bird conductivity cell (SBE-4) plumbed into the SOMMA gas-driven delivery system.

Salinity (practical salinity scale, unitless) was calculated based on cell calibration to IAPSO salinity standards.

Primary system calibration was based on analysis of pure (99.995%) CO_2 gas and Certified Reference Materials (CRMs; supplied by A.G. Dickson, Scripps Institute of Oceanography). DIC measurements were corrected to daily standards. Instrument precision for the winter dataset, based on analysis of replicate standards (DOE 1997), was ±0.559 µmol C kg SW^{-1}, and precision based on replicate samples was ±0.832 µmol C kg SW^{-1}. Precisions for the summer dataset were ±0.401 µmol C kg SW^{-1} and ±0.601 µmol C kg SW^{-1}, respectively.

TA

Total alkalinity was measured using a programmable open-cell potentiometric titration system (Dickson et al. 2003; Bates et al. 1996). Winter samples analyzed aboard ship were dispensed with a 100 mL volumetric pipette; sample temperature was measured while filling, and sample mass was calculated (Millero and Poisson 1981). Summer samples analyzed on shore were weighed using an electronic balance accurate to within 0.06 g (0.05% of typical sample mass) with a precision of ± 0.2 mg. Samples were titrated with small additions of 0.1 N HCl in 0.7 M NaCl and total alkalinity was determined with a modified Gran calculation (Dickson et al. 2003; Goyet et al. 1998; Bates et al. 1996; DOE 1997; Millero et al. 1993).

CRMs were used as primary alkalinity standards to back-calculate titration acid concentration. This forced the absolute accuracy of samples to CRM standards. Instrument precision for the winter dataset based on replicate standards (DOE 1997) was ±1.74 µmol kg SW^{-1}, while precision based on duplicate samples was ±2.97 µmol kg SW^{-1}. For the summer dataset, precisions were ±2.16 µmol kg SW^{-1}, and ±2.45 µmol kg SW^{-1}, respectively.

Data Analysis

pCO_2 calculations

Measurements of underway seawater CO_2 partial pressure were unavailable for these cruises, so partial pressure (pCO_2) at *in situ* temperature (pCO_2(SST)) or at 28 °C (pCO_2(28)) was calculated from discrete, near-surface DIC and TA data using the computer program CO2SYS (Lewis and Wallace 1998), which uses Weiss (1974) solubility. Calculating pCO_2 at 28 °C permitted comparing the inorganic carbon inventory between seasons, isolating changes from seasonal temperature effects. The operator-chosen constants used in CO2SYS calculations were: carbonate dissociation constants of Mehrbach *et al.* (1973), refit by Dickson and Millero (1987, valid for salinities 20-40) and the KSO_4 dissociation constants from Dickson (1990). Recalculation of pCO_2 at different temperatures and *in situ* salinity using CO2SYS was within 3% of the empirically based Takahashi *et al.* method (1993, data not shown).

Plume definition

The Amazon plume near the north Brazilian shelf is a 5-10 m thick layer of low-salinity water separated from underlying oceanic water by a sharp, 5 m halocline (Lentz and Limeburner 1995, and references therein), which creates a shallow surface mixed layer (Pailler et al. 1999). Because plume waters cannot be identified by geographic characteristics, plume-influenced stations in our summer 2001 dataset were identified by their low surface salinities (<35) and shallow haloclines (<10 m, Lentz and Limeburner 1995; Lentz 1995; Geyer 1991). Because of the extremely shallow SML depths at plume stations, we usually collected samples at only one depth in the SML. Therefore, the "surface" and "SML" data groupings used herein are nearly

equivalent. Nonplume surface waters in the WTNA, with no distinctive salinity or density features in the upper 80 m (Lentz and Limeburner 1995, and GEOSECS and WOCE data: details below), have salinities near 36 throughout the entire SML.

Statistics

Mean values are reported with standard errors throughout this paper, unless otherwise noted; SML characteristics were compared using Welch's approximate t-test after F-tests detected significant differences between statistic variances (Sokal and Rohlf 2000). The critical value used in all statistical tests was α=0.05.

Regressions against salinity were used to describe conservative mixing between plume and ocean water. Since both salinity and the inorganic carbon system are subject to natural variation and/or measurement error, Model II regression statistics were used throughout the analysis (reduced major axis, Sokal and Rohlf 2000). Model II statistics are recalculated here for 0-15 m data from the ETAMBOT 1, 2 and SABORD cruises originally published by Ternon and co-workers (2000, data obtained online: details below).

Supplementary data

Air-sea CO_2 gradients (ΔpCO_2; $pCO_2 - pCO_{2atm}$) were determined using calculated *in situ* surface pCO_2 (pCO_2) and the average atmospheric pCO_2 (pCO_{2atm}) for each cruise at Ragged Point, Barbados (NOAA CMDL; www.cmdl.noaa.gov/infodata). "Winter" (Jan.-Feb.) and "summer" (Jul.-Aug.) pCO_{2atm} averaged 371.9 ± 0.6 µatm and 369.3 ± 1.0 µatm, respectively.

Air-sea CO_2 fluxes were calculated using ΔpCO_2, solubility (Weiss 1974), and piston velocity from the long term wind formulation of Wanninkhof (1992) at an average windspeed of 8 m s^{-1} (generalized from our data; see below).

Average surface mixed layer (SML) depths were calculated from CTD profiles at each station using a density gradient criterion ($\Delta\sigma_t/\Delta z$ = 0.01, Brainerd and Gregg 1995). Diazotrophic organism counts, nutrient measurements, and underway data were provided by MANTRA/PIRANA project collaborators (see Acknowledgments). Inorganic carbon data from the ETAMBOT 1, 2, and SABORD cruises (Ternon et al. 2000) were obtained from the IFREMER FTP site (www.ifremer.fr/sismer). CO_2 fugacity (fCO_2, nearly equal to pCO_2 in seawater) from the Meteor 55 cruise (Körtzinger 2003) were kindly provided by the author. NOAA NCEP NCAR reanalysis data (Kalnay et al. 1996) were from the IRI-LDEO Climate Data Library (http://ingrid.ldeo.columbia.edu). GEOSECS and WOCE inorganic carbon data were obtained for comparison from IRI-LDEO (GEOSECS) or the Carbon Dioxide Information Analysis Center (http://cdiac.esd.ornl.gov/, WOCE).

PWP mixed layer model for the non-plume WTNA

Daily mixed layer depths and average SML inorganic carbon inventory changes for the winter and summer non-plume-influenced WTNA were simulated using the Price-Weller-Pinkel mixed layer model for Matlab (Price et al. 1986)(available at http://www.po.gso.uri.edu/rafos/research/pwp/)[2]. The summer non-plume-influenced WTNA was further divided into two groups: those stations south of the plume structure, with oversaturated pCO_2 (stations 33, 35, 36, 38) and those northeast of the plume structure, with undersaturated pCO_2 (stations 17, 19, 21). In each run, the model was initialized with a depth

[2] See chapter 4 for an extended application of the PWP model in the WTNA.

profile of mean temperature, salinity, DIC, and TA for that station group from CTD data and interpolated bottle data. Background vertical eddy diffusivity was set at 1 x 10^{-5} m^2 s^{-1} (Ledwell et al. 1993). Underway windspeed, relative humidity, short wave radiation, barometric pressure, and precipitation were unavailable for the winter cruise, so we forced the winter model with daily heat, fresh water, and momentum fluxes for the WTNA from the NCEP-NCAR reanalysis (Kalnay et al. 1996). Short wave radiation was unavailable for 2001 from NCEP-NCAR, so we used 2002 data. Heat fluxes driving the summer model runs were calculated following Gill (Christian 2005; Gill 1982), using hourly mean underway windspeed, SST, air temperature, relative humidity, barometric pressure, precipitation, and short wave radiation. Wind stress was calculated following Yelland and Taylor (1996). Mixed layer inorganic carbon inventory changes were estimated by treating DIC as a passive tracer that is affected by vertical flux and net evaporation/precipitation (Sabine et al. 2004) but not by air-sea transfer or biology. Equations describing DIC mixing in the model were therefore based on corresponding equations for salt. The rates of change in mixed layer inventories were calculated between initial and final SML values over the 31- or 32-day cruise interval modeled (($C_{initial} - C_{final}$)/(model duration; for both winter and summer). To estimate the impact of precipitation and evaporation on modeled SML DIC inventories, the three model runs were also performed with zero freshwater influence on DIC. The salinity budget was still influenced by freshwater to permit proper development of the modeled mixed layer. Modeled SML carbon inventory changes from the zero-freshwater runs represent only the vertical carbon flux, whereas DIC SML inventory changes calculated from the full runs represent the vertical carbon flux plus evaporation/precipitation-induced inventory changes.

Plume physical influences

Plume mixed layer dynamics were not evaluated with the PWP vertical mixing model, because the plume's existence depends on horizontal mixing between low-salinity, low-carbon river water and surface WTNA water (Lentz and Limeburner 1995). In general, strong density stratification between the plume and underlying ocean water attenuates vertical mixing (Pailler et al. 1999; Sprintall and Tomczak 1992) and forces a shallow mixed layer[3], and background vertical diffusion may not weaken (Ferry and Reverdin 2004). During the plume's approximately 80-day transit from the Amazon mouth to the locations sampled (Hellweger and Gordon 2002, and references therein), only gas exchange, the net effects of evaporation and precipitation, and horizontal mixing influence DIC. Plume water is therefore treated in this analysis as an isolated, vertically homogenous watermass atop the WTNA; its one-dimensional carbon budget is influenced by surface processes only, including gas exchange and export, with no acquisition of inorganic carbon via vertical mixing from below.

Mixing Model

Building on the approaches of Ternon et al. (2000) and Körtzinger (2003), we used a simple conservative mixing model to calculate the proportions of Amazon plume water and seawater in a given plume sample. We assumed that the effects of precipitation and evaporation on the carbon and freshwater mass balances were small compared to the river (Lentz 1995; Lentz and Limeburner 1995) over a 10 m-deep plume (see Section 3.5). Additional variations in DIC not attributable to mixing were then ascribed to biology. For each discrete SML sample collected, we solved the following system of equations for the proportions of river (r) and seawater (s) present:

[3] See chapter 4 for an exploration of this assumption.

$$S_r * r + S_s * s = S_{obs} \qquad (1)$$

$$r + s = 1 \qquad (2)$$

S_r, S_s and S_{obs} are salinities for the river endmember, the seawater endmember, and the observed sample, respectively.

Assuming that alkalinity was conservative, the alkalinity of the river endmember was then calculated from each sample alkalinity (A_{obs}) and the oceanic alkalinity endmember (A_s), using *r* and *s* from above:

$$A_r = \frac{A_{obs} - A_s * s}{r} \qquad (3)$$

Because the Amazon River mainstem DIC load is ~0% carbonate, 82% bicarbonate, and 18% dissolved CO_2 gas (Richey et al. 1991; Devol and Hedges 2001), the river DIC endmember (DIC_r) in our model was calculated to be :

$$DIC_r = \frac{A_r}{0.82} \qquad (4)$$

The expected inorganic carbon value for that sample (DIC_{ex}) was then calculated using *r*, *s*, and river (DIC_r) and seawater (DIC_s) endmembers:

$$DIC_{ex} = DIC_r * r + DIC_s * s \qquad (5)$$

DIC_{ex}, A_{obs}, and *in situ* nutrient concentrations were then used to calculate the pCO_2 expected (pCO_{2ex}) from conservative mixing using CO2SYS. Nonconservative variations in DIC attributed to biology (ΔDIC_{BIO}) were the differences between expected and observed DIC values:

$$\Delta DIC_{BIO} = DIC_{ex} - DIC_{obs} \qquad (6)$$

Positive ΔDIC_{BIO} values correspond to inorganic carbon deficits, implying that production exceeds respiration and the system is net autotrophic. Negative values indicate inorganic carbon surpluses, suggesting that respiration exceeds production, and the system is net heterotrophic.[4]

Errors in derived quantities were estimated using a Monte Carlo-type error analysis (see Yager et al. 1995).

Model Endmembers

Surface mixed layer DIC, TA, and salinity were averaged for the four southeastern summer nonplume stations to provide seawater endmember values and their standard deviations (A_s = 2369.4 ± 5.9, S_s=36.0 ± 0.1, DIC_s=2024.5 ± 6.8, n=12). These stations (33, 35, 36, 38) were located in the North Brazil Current (NBC), the watermass that entrains the Amazon plume (Bourles et al. 1999; Johns et al. 1998). River salinity (S_r) was assumed to equal 0 ± 0, as 0 psu salinity water has been documented outside of the river mouth (Lentz 1995; Lentz and Limeburner 1995; Geyer et al. 1996; Edmond et al. 1981). The mixing line slope implied by this model was calculated using solved mean A_r, A_s, S_r, and S_s (or DIC_r, DIC_s, S_r, and S_s) and a Monte Carlo-type analysis (see Yager et al. 1995) that kept track of error propagation.

Results:

Observational

DIC and TA values in the Amazon plume-influenced upper WTNA were up to 400 μmol kg^{-1} lower than oceanic (nonplume) values (Table 2.1; Figure 2.2A). Surface pCO_2 at *in situ* temperatures (pCO_2(SST)) was also about 50 μatm lower in the plume; the difference between plume and nonplume surface pCO_2 was enhanced when temperature differences were reconciled

[4] See Discussion for an examination of the assumptions required by this method.

(Table 2.1; pCO_2(28°C)). This significant inorganic carbon reduction was always associated with low-density plume water atop the water column (σ_t = 17 – 23; Figure 2.2B). At nonplume stations, average surface mixed layer (SML) DIC, TA, salinity, SML depth, and pCO_2(28) were statistically indistinguishable between seasons (Table 2.3).

Over the salinity range sampled, DIC and TA were linearly correlated to salinity (Table 2.2, Figure 2.3A). The relationship between plume TA and salinity was not significantly different from that of previously published data from the ETAMBOT/SABORD projects (Fall 1995 and Spring 1996, Ternon et al. 2000, Table 2.2). In addition, the residuals around the TA-salinity regression line are much smaller on the whole than the residuals around the DIC-salinity regression (Figure 2.3B).

During the winter cruise, sea surface temperature (SST) and sea surface salinity (SSS) ranged between 20.9 – 26.6 °C and 35.2 – 36.3, respectively (Figure 2.4a, b). Mixed layer depths ranged between 47 and 133 m (Figure 2.4c). Due to an equipment malfunction, underway windspeed was not archived for this cruise; windspeeds shown are from station logfiles, and range between 7-15 m s^{-1} (Figure 2.4.1d). During the summer cruise, SST ranged between 25.8 – 30.0°C and SSS ranged between 26.4 – 36.7 (Figure 2.4.2e, f). Lower SSS and higher SST were indicative of the Amazon plume (Figure 2.4.2, Table 2.1). Summer mixed layer depths ranged between 2 - 103 m (Figure 2.4.2g). Summer windspeed ranged between 0 and 12 m s^{-1} (Figure 2.4.2h). Shallow MLDs in summer (<15 m) were always associated with SSS below 35.

Air-sea CO_2 gradients

Air-sea CO_2 gradients in summer 2001 varied over a larger range (ΔpCO_2 = -135 to +30 µatm) than in winter (ΔpCO_2 = -48 to +10 µatm; Figure 2.5). Stations most undersaturated with

respect to the atmosphere (negative ΔpCO_2; stations 23 and 27) were far from the river mouth, in the middle of the observed salinity range. The most oversaturated stations (positive ΔpCO_2; summer stations 33, 35, 36, 38) were outside plume-influenced waters. The only oversaturated station within plume water (station 43) was close to the river mouth and on the continental shelf. Station 43 was unusual in that, although salinity, DIC, and TA were characteristic of plume water, they were vertically homogenous throughout the 80 m water depth; no surface mixed layer was evident. Outside the plume, the small significant difference observed between winter and summer mean pCO_2(SST) was partly attributable to seasonal changes in SST (Table 2.3). Winter pCO_2(SST) was undersaturated due to cool temperatures, but summer nonplume pCO_2(SST) was not uniformly oversaturated due to warm temperatures. Summer nonplume stations fell into two groups: stations whose pCO_2(SST) was greater than the atmospheric value (33, 35, 36, and 38, south of the plume; Fig. 2.5b), and those whose pCO_2(SST) was less than atmospheric pCO_2 (15, 17, 19, and 21, north and east of the plume; Fig 2.5b, stations labeled on 2.1b). The difference between the two summer groups' pCO_2(SST) was unrelated to temperature (Table 2.3), as the difference remained when temperature changes were reconciled. The overall mean non-plume pCO_2(SST) undersaturation (Table 2.1) resulted from grouping cooler, undersaturated winter stations with the two types of warmer summer stations.

Air-sea fluxes

The mean flux at plume stations (ΔpCO_2 = -61.0 ± 8.3 µatm, salinity = 31.6 ± 0.4, SST = 28.8 ± 0.1 °C, windspeed 8 m s^{-1}) was 9.7 ± 1.3 mmol C m^{-2} d^{-1} into the water. The air-sea fluxes at summer nonplume stations were quite different from the plume: south of the plume (ΔpCO_2 = 19.3 ± 4.4 µatm, salinity = 36.0 ± 0.06, SST = 27.4 ± 0.2 °C, windspeed = 8 m s^{-1}), CO_2 was

released to the atmosphere (mean flux = 3.0 ± 0.7 mmol C m^{-2} d^{-1}); north of the plume (ΔpCO_2 = -10.3 ± 0.7 µatm, salinity = 35.9 ± 0.09, SST = 27.6 ± 0.1 °C, windspeed = 8 m s^{-1}), the average CO_2 flux was 1.6 ± 0.1 mmol C m^{-2} d^{-1} into the water, 6x lower than the rate for the plume. The average calculated air-sea CO_2 flux for winter nonplume stations (ΔpCO_2 = -16.7 ± 2.8 µatm, salinity = 36.0 ± 0.05, SST = 25.9 ± 0.1 °C, windspeed = 8 m s^{-1}) was 2.6 ± 0.4 mmol C m^{-2} d^{-1} into the water, only slightly greater than the northern summer non-plume stations. In the winter, observed windspeeds were generally greater than 8 m s^{-1} (7-15 m s^{-1}), so the in situ flux could be somewhat greater than estimated here (the effect would be amplified if we had applied the Wanninkhof and McGillis, 1999, long term formulation for the gas transfer velocity instead of Wanninkhof, 1992, since the two formulations diverge above 8 m s^{-1}), whereas observed summer winds (1-12 m s^{-1}) could generate slightly lower fluxes than estimated here.

PWP mixed layer model

Winter SML depths from the PWP mixed layer model (Table 2.4) agreed favorably with SML depth observations. In winter, salinity increased in the SML at a rate of 0.003 d^{-1} (or ~0.01% d^{-1}). Carbon increased at a somewhat faster rate (0.36 µmol kg^{-1} d^{-1} or ~0.02% d^{-1}) because of the stronger vertical gradient in DIC. Integrating over the modeled mixed layer depth, the change in the integrated mixed layer salt inventory (storage) is 2.8 mg salt m^{-2} s^{-1} and the change in the mixed layer carbon inventory is 27 mmol C m^{-2} d^{-1}. Excluding the freshwater influence on winter SML DIC, the change in the carbon inventory was only 16 mmol C m^{-2} d^{-1}; net winter evaporation therefore concentrates SML DIC to cause the additional 11 mmol C m^{-2} d^{-1} increase (Table 2.4). The model predicted shallower mixed layers under late summer conditions than we observed at either group of summer nonplume stations. Calculated summer

mixed layer depths were 15.0 ± 0.5 and 14.4 ± 0.4 (southern and northern groups respectively), significantly shallower than the mean observed nonplume mixed layer depths of 54.3 ± 8.1 and 76.0 ± 10.6 m. Modeled summer mixed layer salinity decreased at a rate of 0.0005 – 0.0009 d^{-1}, and mixed-layer DIC decreased 0.01 – 0.03 μmol kg^{-1} d^{-1}. When integrated over the modeled mixed layer depth, the mixed layer salt inventory lost 0.1 – 0.2 mg m^{-2} s^{-1}, and the mixed layer DIC inventory lost 0.22 – 0.53 mmol m^{-2} d^{-1}. Excluding freshwater effects in summer, the SML DIC inventory increased 0.4 – 0.6 mmol C m^{-2} d^{-1} (southern and northern stations, respectively), so net precipitation decreased DIC inventories by 0.92 – 0.83 mmol C m^{-2} d^{-1}. A preliminary yearlong PWP model run forced with daily NCEP-NCAR data (results not shown) indicates that our observations were at the start of annual WTNA autumn mixed layer shoaling, when mixed layer depths oscillate rapidly.

Plume physical influences

The average air-sea CO_2 flux into the plume (9.7 ± 1.3 mmol C m^{-2} d^{-1}) causes a DIC increase of 1.0 μmol C kg^{-1} d^{-1} in a 10 m plume. At the same time, late summer net precipitation (E-P = -1.4 ± 1.3 mm d^{-1}, calculated from the summer 2001 underway data) dilutes dissolved species and lowers DIC. Adding 1.4 mm d^{-1} or 1.4 L m^{-2} d^{-1} water to a 10 m mixed layer with DIC = 2100 μmol C kg^{-1} will lower DIC values by 0.3 μmol C kg^{-1} d^{-1} [5]. Adding this much precipitation to the plume at the river mouth where DIC = 308.8 μmol kg^{-1} (see note below) will lower DIC by 0.03 μmol kg^{-1} d^{-1}. Assuming a linear change between the two values gives a mean precipitation-driven DIC change throughout the plume of 0.17 μmol kg^{-1} d^{-1}. During the plume's approximately 80-day transit from the Amazon mouth to the locations sampled

[5] Assume mixed layer DIC before rain = 2100 μmol kg^{-1}. Volume of a 10m ML = 10,000 L. Assume rain adds no DIC. $C_1V_1 = C_2V_2$; 2100 μmol kg^{-1} * 10,000 L = C_2 μmol kg^{-1} * 10,001.4 L; C_2 = 1999.72 μmol kg^{-1}. Decrease in DIC due to precipitation = 0.3 μmol kg^{-1}.

(Hellweger and Gordon 2002, and references therein), mean air-sea transfer can therefore increase plume DIC by 80 μmol C kg^{-1} and net precipitation can decrease DIC by approximately 13.6 μmol C kg^{-1}. In total (66 μmol C kg^{-1}), these physical processes contribute up to only 3.8% of the DIC acquired by a water parcel between the river (DIC_r = 308.8 μmol kg^{-1}, see below) and the offshore ocean (DIC_s = 2024.5 μmol kg^{-1}).

Mixing Model

The percent riverwater present at plume stations (%R = $r/(r+s)$) ranged between 3 and 22%. Stations with lower salinity and a higher proportional contribution of riverwater were not necessarily closer to the river mouth. Mixing model solutions for non-plume SML samples consistently returned small values for the riverwater proportion (r). The mean A_r endmember for plume samples was 253.3 ± 9.5 μmol kg^{-1} (n=25), making the mean DIC_r = 308.8 ± 11.6 μmol kg^{-1} (n=25, Table 2.2).

Variations in DIC unexplained by the mixing model (ΔDIC_{BIO}) were up to 93 μmol C kg^{-1} at mid-range salinities (Figure 2.6). Plume summer stations generally had significantly positive ΔDIC_{BIO}, whereas only station 43 had a significantly negative ΔDIC_{BIO}. As well as having oversaturated pCO_2 and a homogenous water column, station 43 was located on the 80 m continental shelf and CDOM levels were especially high. Of the 17 plume stations with positive ΔDIC_{BIO}, the diazotrophic cyanobacteria *Trichodesmium* spp. was especially prevalent at 7 stations; diatoms (*Hemiaulus hauckii*) containing the diazotrophic endosymbiont *Richelia intracellularis* were especially abundant at 3 stations (sampled multiple times as part of a time series); and large quantities of both *Trichodesmium* and *Richelia* were found at 3 stations (Figure 2.6). Although there was no bottle-to-bottle correlation between ΔDIC_{BIO} and algal biomass at

discrete depths, a significant positive correlation was found between ΔDIC_{BIO} in the plume and the integrated *Richelia* biomass at a given station ($r = 0.707$; $n = 29$, $p < 0.001$). The six samples with the greatest deviation from expected DIC values (ΔDIC_{BIO} = 60-95 μmol C kg^{-1}) were associated with large blooms of *Richelia*; other plume stations with either *Trichodesmium* or no prevailing diazotroph population showed smaller deviations between 10-40 μmol C kg^{-1}. If all production occurs in a 10 m-deep plume and ΔDIC_{BIO} represents a homogeneous DIC deficit at a plume station, then the depth-integrated biological DIC deficit in the plume (excluding station 43) would range between 0.1 and 0.9 mol C m^{-2}, with an average of 0.4 ± 0.06 mol C m^{-2} (n= 24).

Expected pCO_2 from mixing model results

In nearly all cases, the pCO_2 expected from conservative mixing, pCO_{2exp}, was higher than the pCO_2 calculated from observed DIC and TA (pCO_{2obs}, equal to pCO_2(SST)) at plume stations (Figure 2.7). Conservative mixing is expected to drive pCO_2 below atmospheric pCO_2 consistently at salinities less than 33 (Figure 2.7). The pCO_{2obs} at plume stations was routinely about 30 μatm lower than pCO_{2exp}. At plume stations such as 23 and 27, where large numbers of *Hemiaulus/Richelia* were observed, in situ biological activity appears to intensify the sink by lowering pCO_2 60-120 μatm below expected levels.

Discussion:

Nonplume WTNA

In the absence of the Amazon River plume, modest seasonal changes in WTNA meteorology (Figure 2.4) drive changes in modeled mixed layer depths and mixed layer

inventories (Table 2.4). Winter winds and net evaporation promote mixed-layer deepening and increases of salt and DIC. The late-summer drop in wind, followed by increased fall precipitation (see Figure 3c in Yoo and Carton 1990) promotes mixed-layer shoaling and a small mixed-layer decrease in salinity and DIC. The large sensitivity of WTNA mixed layers to the freshwater balance differs from the familiar convectively driven North Atlantic model, in which winter cooling and high winds promote deep mixing until summer's warm temperatures and calmer conditions stratify the water column (e.g., Hansell and Carlson 2001; Michaels et al. 1994, and references therein).

Although our PWP model results for SML DIC predict an increase in winter and a decrease in summer, observed mixed-layer WTNA DIC and TA values outside the plume vary little between seasons (these data, GEOSECS, WOCE, and ETAMBOT/ SABORD data). Invoking seasonally varying air-sea gas transfer to balance the carbon budget is insufficient to explain the observed lack of seasonal DIC change. At winter and summer southern nonplume stations, the favored direction of air-sea gas transfer enhances the SML carbon inventory change (Tables 2.3, 2.4, Figure 2.8). Only north of the plume in summer does air-sea exchange oppose the net change in SML carbon inventory (Table 2.4, Figure 2.8). In short, the favored direction of air-sea carbon transfer often drives the system further from steady state.

Estimating the vertical fluxes, by removing the effects of precipitation and evaporation on modeled SML DIC, highlights the strong influence of the freshwater balance on regional carbon inventories, but still does not help balance the budget. In summer, the vertical flux is very small, and precipitation-driven changes cause the observed loss in SML carbon. In contrast, the winter vertical flux is large and accounts for over half the SML carbon inventory increase (Figure 2.8). To maintain the small seasonal differences we observed in the WTNA non-plume,

predicted carbon inventory changes must be offset by additional seasonally varying processes such as plume-ocean mixing, horizontal advection, or export.

Summer northern WTNA nonplume stations are in position to receive retroflected plume water, which is characterized by low pCO_2 and salinity. Although the small difference between SML salinities north and south of the plume is not statistically significant (data not shown), the significant, temperature-independent difference between the groups' pCO_2(SST)(Table 2.3) suggests that northern stations contain a small amount of plume water. If only vertical processes replaces carbon, the pCO_2 undersaturation at these stations will take a long time to be replaced, because both the vertical carbon flux (+0.61 mmol C m^{-2} d^{-1}) and air-sea gas transfer (+1.6 mmol C m^{-2} d^{-1}) into the SML are quite small.

A three-dimensional salinity budget at the nearby PIRATA array (4-15ºN, 38ºW) indicates that advection varies seasonally in the tropical Atlantic and can significantly affect the SML values of dissolved constituents (Foltz et al. 2004). In February, advection at the 8ºN, 38ºW buoy contributes -1 mg m^{-2} s^{-1} salt to the total accumulation of +2 ± 1.5 mg m^{-2} s^{-1} (Foltz et al. 2004). If similar horizontal advection were applied to our vertically modeled salinity increase (+2.8 mg m^{-2} s^{-1}), the net WTNA salinity increase would be 1.8 mg m^{-2} s^{-1} , which agrees with the net increase of Foltz et al. (2004). Later, advection and precipitation at the PIRATA mooring site increase, removing accumulated salt (Foltz et al. 2004) and, presumably, DIC.

While mixing, air-sea gas exchange, and advection physically alter SML DIC values in the non-plume WTNA, low levels of biological activity may also remove some of the predicted winter and northern summer DIC accumulation, and intensify the predicted southern summer nonplume DIC loss. Observed primary production rates in the oligotrophic Atlantic Ocean are 2 - 30 mmol C m^{-2} d^{-1} (Maranon et al. 2003), with higher rates in the WTNA during

Richelia/Hemiaulus blooms (100 mmol C m^{-2} d^{-1}, Carpenter et al. 1999, although these large blooms tend to occur in fresher waters) which could remove significant amounts of DIC (see below and Subramaniam et al. *in revision*). If 10% of primary production is exported (Broecker 1974), 0.2-10 mmol C m^{-2} d^{-1} of the expected DIC accumulation (accounting for 15- >100% of the summer northern total and 0.1-38% of the winter total) can be removed biologically. In comparison, biological production in the winter 2001 Eastern Equatorial Pacific removed 17% of SML DIC in a system dominated by air-sea gas exchange and upwelling (Sabine et al. 2004). In the absence of the river plume, the WTNA inorganic carbon budget therefore appears to be most affected by physical influences on the water column, but uncertainties in removal terms underscore the importance of better understanding the timing and magnitude of both advection and export in the WTNA carbon cycle.

Plume – influenced WTNA

In the plume-influenced WTNA, low-salinity, low-carbon Amazon water remains atop the water column in a coherent lens and alters physical conditions in the SML. A strong pycnocline separating plume and ocean water hampers vertical mixing (Pailler et al. 1999; Sprintall and Tomczak 1992), forces a shallow mixed layer, and necessarily attenuates the upward carbon flux[6]. Together, air-sea CO_2 transfer and net precipitation (Figure 2.8) only add 3.8% of the observed inorganic carbon increase between the river and the ocean. Without large carbon fluxes into the plume, DIC and TA distributions in the offshore plume therefore reflect primarily conservative mixing (presumably lateral) between river and ocean water (Figure 2.3, Table 2.1, Ternon et al. 2000; Körtzinger 2003). Gas exchange, evaporation, and biology (see

[6] See chapter 4 for an exploration of vertical mixing between the plume and ocean.

below) determine only the smaller residual differences between the conservative mixing line and the observations.

Biological processes influence DIC throughout the plume (Muller-Karger et al. 1988; Longhurst 1993; Muller-Karger et al. 1995; Ternon et al. 2000; Körtzinger 2003; Benner et al. 1995; Richey et al. 1990; DeMaster and Pope 1996; Aller et al. 1996; Devol et al. 1987). Respiration in the early plume supported by river-borne organic matter releases CO_2 (Benner et al. 1995; Richey et al. 1990; DeMaster and Pope 1996; Aller et al. 1996; Devol et al. 1987), creating areas like station 43, whose high pCO_2 and CDOM suggested terrestrial DOM was being respired (Smith and DeMaster 1996; Del Vecchio and Subramaniam 2004; DeMaster and Pope 1996). Further offshore, lower turbidity allows production to exceed respiration (DeMaster et al. 1996), permitting enhancement of the mixing-induced sink by causing additional decreases in pCO_2 (Station 23, Figures 2.5, 2.6, & 2.7, Ternon et al. 2000; Körtzinger 2003). It should be noted that growth of carbonate-forming organisms could alter plume TA nonconservatively, but they were not observed on these cruises (E.J. Carpenter, personal communication). Satellite images show blooms of the coccolithophore *Emiliana huxleyi*, one of the two most common coccolithophore species found in WTNA sediments (Kinkel et al. 2000), were very limited in the WTNA (Iglesias-Rodriguez et al. 2002). Diatoms are expected to outcompete coccolithophores in unstable environments (like the Amazon plume) where silicate, nitrate, and phosphate are more abundant and are not common in the WTNA (Iglesias-Rodriguez et al. 2002).

Quantifying the influence of biology on plume waters

During an algal bloom, production and export remove SML inorganic carbon faster than gas exchange and vertical mixing replace it, decreasing DIC in proportion to net community

production. In this study, typical ΔDIC_{BIO} values were about 20 μmol kg^{-1}, with the highest values found at diazotroph-dominated stations (Figure 2.6). If these near-surface samples reflected conditions throughout the SML, depth-integrated inorganic carbon deficits were approximately 200 mmol C m^{-2}. Steadily exporting 10% of diazotroph-associated primary production (reported rates for Trichodesmium and Richelia-rich communities are 67-93 mmol C m^{-2} d^{-1}, Carpenter et al. 2004; Carpenter et al. 1999) would generate this integrated deficit in 22 to 30 days. Export may occur in even less time; salp swarms observed feeding on diazotroph-rich communities in summer (E.J. Carpenter, personal communication) could periodically increase export. Our results suggest that WTNA carbon sequestration depends on algal community structure (Subramaniam et al. *in revision*).

Using ΔDIC_{BIO} as a direct proxy for export neglects the likelihood that some dissolved and particulate organic material remains in the mixed layer (DOC, POC), and that physical processes such as air-sea exchange start reducing inorganic carbon deficits as soon as they are created. Lacking organic matter data for the 2001 cruises, we assume the WTNA POC pool behaves similarly to that of BATS, where the euphotic zone suspended particle stock is constant (25-35 μg kg^{-1}) between seasons (Bates et al. 1996). We also assume WTNA DOC production is similar to that of the oligotrophic open ocean, comprising 10-20% of net community production (Hansell and Carlson 1998). As a result, ΔDIC_{BIO}- based export estimates could overestimate the downward carbon flux by 10-20%. On the other hand, not including the effects of air-sea replacement and net precipitation in the mixing model may cause ΔDIC_{BIO} to underestimate net community production. Observed deficits (the net result of biological and physical processes) were 20-90 μmol C kg^{-1}, so our biological impact estimates could more than double if physical effects are included (adding up to 56 μmol C kg^{-1} over an 80-day transit). Patchy blooms (e.g.

Carpenter et al., 1999, Subramaniam et al., submitted) remove plume DIC over days to weeks, whereas steady physical processes add DIC over weeks to months. In total, ΔDIC_{BIO}-based numbers likely underestimate biological impacts on the plume carbon cycle because ongoing physical processes likely add more carbon to the deficit than DOC production removes. More information on the timing of biological production and export in the WTNA is required to calculate biological impacts on WTNA DIC precisely. For example, deficits from early-plume bloom/export cycles could be completely replaced by physical processes before the watermass was sampled, causing large underestimates of ΔDIC_{BIO}. Further along the mixing gradient, export could create large DIC deficits that were only partially replaced by physical processes at the time of sampling. In this case, our export estimates would be more accurate. Although the timescale of ΔDIC_{BIO} accumulation is not precisely known, we conclude that enough time elapses during the plume transit to accumulate measurable ΔDIC_{BIO} representative of integrated biological impacts on the plume.

The consistent positive difference between pCO_{2exp} and pCO_{2obs} at plume stations regardless of diazotroph abundance (about 30 μatm; Figure 2.7) supports the hypothesis that inorganic carbon deficits in the outer plume carry the integrated record of biological drawdown over some period of the plume's travel time. The conservative mixing model data, the observed temperature-independent pCO_2 undersaturation at northerly WTNA nonplume stations, and the mixed layer model results suggest that after the plume structure breaks down, a lasting small carbon deficit initiated by physical mixing and enhanced by biological drawdown is distributed over a deep SML. In that situation, both air-sea and vertical carbon fluxes are slow, lengthening the time to replace the carbon deficit. Thus, the Amazon plume causes a portion of the oceanic-

salinity WTNA to take up atmospheric carbon, expanding the area and duration of the plume-related sink and opposing the expected paradigm of CO_2 release from tropical seawater.

Our estimate of ΔDIC_{BIO} relies on some assumptions about river chemistry, because little is known about the carbonate system in the early plume. Previous studies used river DIC and TA measured at Obidos (1400 km upstream) to predict mixing curves for the carbonate system in the offshore plume (Ternon et al. 2000). However, several rivers from low-carbonate watersheds flow into the Amazon between Obidos and the estuary (Devol and Hedges, 2001), and carbonate system equilibria in river water shift upon meeting ocean water (Körtzinger 2003; Lewis and Wallace 1998); therefore, early plume DIC and TA values are likely different from upstream river values. To date, only 1 DIC value (374 μM, November 1991, Druffel et al. 2005) has been published for the zero salinity, early plume water (referred to as "river" water in our mixing model). A single hand sample collected for us in this zone during April 2002 had salinity of zero and TA of 440.71 ± 0.37 (± s.d., n=2; S.R. Cooley, unpublished data). The Druffel et al. (2005) DIC value is closer to our solved DIC_r than the upriver value of DIC_r = 600 used previously (Ternon et al. 2000, and references therein), suggesting that solving for A_r and DIC_r may introduce less error into this model of a poorly characterized system[7]. The 0.82 TA:DIC ratio may indeed change in the near-shore mixing zone, but it is not likely to exceed unity until salinity increases above zero. If we instead used a ratio of 1 (see Ternon et al. 2000), ΔDIC_{BIO} estimates would be about 40% smaller at the lowest-salinity stations (e.g. stations 29, 41, 48, 51), and 10-20% lower for samples with salinities 32-35.

[7] See chapter 3 for an investigation of this issue.

Conclusions

The seasonal appearance of the Amazon plume creates a high-nutrient, low-carbon incubator that is somewhat isolated from the oligotrophic water column beneath. DIC and TA distributions in our samples ($27 < S < 36$) reflect primarily conservative mixing between the ocean and the river, but biologically induced variations in DIC accumulate because of rapid production and slow carbon replacement. Most of the WTNA stations with DIC deficits occurred where high numbers of *Trichodesmium* or *Richelia*/diatom symbioses were found, suggesting that diazotrophic activity is associated with increased carbon drawdown in the Amazon plume. Stations with high *Richelia*/diatom concentrations tended to have greater deficits than other stations. These deficits enhance and prolong the undersaturation of the plume. In the absence of the Amazon River plume, inorganic carbon cycling in the WTNA was dominated by physical processes such as the freshwater balance, air-sea gas exchange, and vertical entrainment, but accounting for two- or three-dimensional processes is required to explain the observed lack of seasonality in the non-plume DIC inventory. Our calculations show that residual DIC deficits both from river dilution and biological activity may endure for many months, and reduce the overall tendency of the WTNA to outgas CO_2.

Acknowledgements

This research was supported by the Office of Science (BER), U.S. Department of Energy, Grant No. DE-FG02-02ER63472, NOAA Office of Global Programs Grant NA16GP2689, and by faculty research support from the University of Georgia to P.L.Y. Financial support was provided to S.R.C. by the University of Georgia Presidential Graduate Fellowship and the NASA Earth System Science Fellowship. A.F. Michaels, D.G. Capone, and E.J. Carpenter graciously invited us into the MANTRA/PIRANA Biocomplexity Project. E.J. Carpenter, D.G. Capone, A.

Subramaniam, and M. Neumann shared data with us and provided excellent sampling access. M. J. Erickson assisted with sampling and offered helpful insight. A. Goodrich assisted with sample analysis. A.B. Burd and V. Coles provided technical assistance and guidance on the Monte Carlo-type model. F. le Hingrat at IFREMER made the ETAMBOT/SABORD datasets available. A. Kortzinger made the Meteor 55 pCO_2 data set available. D. Di Iorio and J. Christian provided helpful commentary regarding the PWP model. The manuscript was greatly improved by the comments of B. Hales, one anonymous reviewer, A. Burd, V. Coles, and J.C. Fisher.

References:

Aller, R. C., N. E. Blair, Q. Xia and P. D. Rude (1996). Remineralization rates, recycling, and storage of carbon in Amazon shelf sediments. *Continental Shelf Research 16*: 753-786.

Bates, N. R., A. F. Michaels and A. H. Knap (1996). Seasonal and interannual variability of oceanic carbon dioxide species at the US JGOFS Bermuda Atlantic Time-series Study (BATS) site. *Deep-Sea Research Part II-Topical Studies in Oceanography 43*(2-3): 347-383.

Bauer, J., C. Reimers, E. Druffel and P. Williams (1995). Isotopic constraints on carbon exchanges between deep ocean sediments and seawater. *Nature 373*: 686-689.

Bender, M., K. Grande, K. Johnson, J. Marra, P. J. L. Williams, J. Sieburth, M. Pilson, C. Langdon, G. Hitchcock, J. Orchardo, C. Hunt, P. Donaghay and K. Heinemann (1987). A comparison of four methods for determining planktonic community production. *Limnology and Oceanography 32*(5): 1085-1098.

Benner, R., S. Opsahl, G. Chin-Leo, J. E. Richey and B. R. Forsberg (1995). Bacterial carbon metabolism in the Amazon River system. *Limnology and Oceanography 40*(7): 1262-1270.

Bourles, B., Y. Gouriou and R. Chuchla (1999). On the circulation in the upper layer of the western equatorial Atlantic. *Journal of Geophysical Research-Oceans 104*(C9): 21,151-21,170.

Brainerd, K. E. and M. C. Gregg (1995). Surface mixed and mixing layer depths. *Deep-Sea Research I 42*(9): 1521-1543.

Broecker, W. S. (1974). *Chemical Oceanography*. Harcourt Brace Jovanovich, New York.

Capone, D. G., J. P. Zehr, H. W. Paerl, B. Bergman and E. J. Carpenter (1997). *Trichodesmium*, a globally significant marine cyanobacterium. *Science 276*: 1221-1229.

Carpenter, E. J., J. P. Montoya, J. Burns, M. R. Mulholland, A. Subramaniam and D. G. Capone (1999). Extensive bloom of a N_2-fixing diatom/cyanobacterial association in the tropical Atlantic Ocean. *Marine Ecology Progress Series 185*: 273-283.

Carpenter, E. J., A. Subramaniam and D. G. Capone (2004). Biomass and primary productivity of the cyanobacterium *Trichodesmium* spp. in the tropical N. Atlantic Ocean. *Deep-Sea Resarch I 51*: 173-203.

Christian, J. R. (2005). Biogeochemical cycling in the oligotrophic ocean: Redfield and non-Redfield models. *Limnology and Oceanography 50*(2): 646-657.

del Giorgio, P. A., J. J. Cole and A. Cimbleris (1997). Respiration rates in bacteria exceed phytoplankton production in unproductive aquatic systems. *Nature 385*: 148-151.

Del Vecchio, R. and A. Subramaniam (2004). Influence of the Amazon River on the surface optical properties of the Western Tropical North Atlantic Ocean. *Journal of Geophysical Research - Oceans 109*(C11): doi:10.1029/2004JC002503.

DeMaster, D. J. and R. C. Aller (2001). Biogeochemical Processes on the Amazon Shelf: Changes in Dissolved and Particulate Fluxes during River/Ocean Mixing. *The Biogeochemistry of the Amazon Basin*. M. E. McClain, R. L. Victoria and J. E. Richey. Oxford University Press: 328-357.

DeMaster, D. J. and R. H. Pope (1996). Nutrient Dynamics in Amazon Shelf Waters - Results from AMASSEDS. *Continental Shelf Research 16*(3): 263-289.

DeMaster, D. J., W. O. Smith, D. M. Nelson and J. Y. Aller (1996). Biogeochemical processes in Amazon shelf waters: chemical distributions and uptake rates of silicon, carbon and nitrogen. *Continental Shelf Research 16*(5-6): 617-643.

Devol, A. H. and J. I. Hedges (2001). Organic Matter and Nutrients in the Mainstem Amazon River. *The Biogeochemistry of the Amazon Basin*. M. E. McClain, R. L. Victoria and J. E. Richey. Oxford University Press, New York: 275-306.

Devol, A. H., P. D. Quay, J. E. Richey and L. A. Martinelli (1987). The role of gas exchange in the inorganic carbon, oxygen, and ^{222}Rn budgets of the Amazon River. *Limnology and Oceanography 32*(1): 235-248.

Dickson, A. G. (1990). Standard potential of the reaction: $AgCl_{(s)} + 1/2\ H_{2(g)} = Ag_{(s)} + HCl_{(aq)}$, and the standard acidity constant of the ion $HSO_4^{(-)}$ in synthetic seawater from 273.15 to 318.15K. *Journal of Chemical Thermodynamics 22*: 113-127.

Dickson, A. G., J. D. Afghan and G. C. Anderson (2003). Reference materials for oceanic CO_2 analysis: a method for the certification of total alkalinity. *Marine Chemistry 80*: 185-197.

Dickson, A. G. and F. J. Millero (1987). A comparison of the equilibrium constants for the dissociation of carbonic acid in seawater media. *Deep-Sea Research Part A-Oceanographic Research Papers 34*(10): 1733-1743.

DOE (1997). Handbook of methods for the analysis of the various parameters of the carbon dioxide system in sea water. A. G. Dickson and C. Goyet, eds., ORNL/CDIAC-74.

Druffel, E. R. M., J. E. Bauer and S. Griffin (2005). Input of particulate organic and dissolved inorganic carbon from the Amazon to the Atlantic Ocean. *Geochemistry Geophysics Geosystems 6*(3): doi: 10.1029/2004GC000842.

Duarte, C. M. and S. Agustí (1998). The CO_2 balance of unproductive aquatic ecosystems. *Science 281*: 234-236.

Duarte, C. M., S. Agusti, J. Aristegui, N. González and R. Anadón (2001). Evidence for a heterotrophic subtropical northeast Atlantic. *Limnology and Oceanography 46*(2): 425-428.

Edmond, J. M., E. A. Boyle, B. Grant and R. F. Stallard (1981). The chemical mass balance in the Amazon plume - I. The nutrients. *Deep-Sea Resarch 28A*(11): 1339-1374.

Ferry, N. and G. Reverdin (2004). Sea surface salinity interannual variability in the western tropical Atlantic: an ocean general circulation model study. *Journal of Geophysical Research 109*(doi: 10.1029/2003JC002122).

Foltz, G. R., S. A. Grodsky, J. A. Carton and M. J. McPhaden (2004). Seasonal salt budget of the northwestern tropical Atlantic Ocean along 38W. *Journal of Geophysical Research 109*: doi:10.1029/2003JC002111.

Geider, R. J. (1997). Photosynthesis or planktonic respiration? *Nature 388*: 132-133.

Geyer, W. R. (1991). The physical oceanography of Amazon outflow. *Oceanography 4*: 8-14.

Geyer, W. R., R. C. Beardsley, S. J. Lentz, J. Candela, R. Limeburner, W. E. Johns, B. M. Castro and I. D. Soares (1996). Physical oceanography of the Amazon shelf. *Continental Shelf Research 16*(5-6): 575-616.

Gill, A. E. (1982). *Atmosphere-Ocean Dynamics*. Academic Press, New York.

Goyet, C., R. Adams and G. Eischeid (1998). Observations of the CO_2 system properties in the tropical Atlantic Ocean. *Marine Chemistry 60*(1-2): 49-61.

Hansell, D. A. and C. A. Carlson (1998). Net community production of dissolved organic carbon. *Global Biogeochemical Cycles 12*(3): 443-453.

Hansell, D. A. and C. A. Carlson (2001). Biogeochemistry of total organic carbon and nitrogen in the Sargasso Sea: control by convective overturn. *Deep-Sea Resarch II 48*: 1649-1667.

Hellweger, F. L. and A. L. Gordon (2002). Tracing Amazon River water into the Caribbean Sea. *Journal of Marine Research 60*(4): 537-549.

Iglesias-Rodriguez, M. D., C. W. Brown, S. C. Doney, J. A. Kleypas, D. Kolber, Z. S. Kolber, P. K. Hayes and P. G. Falkowski (2002). Representing key phytoplankton functional groups in ocean carbon cycle models: Coccolithophorids. *Global Biogeochemical Cycles 16*(4): doi:10.1029/2001GB001454.

Johns, W. E., T. N. Lee, R. C. Beardsley, J. Candela, R. Limeburner and B. Castro (1998). Annual cycle and variability of the North Brazil Current. *Journal of Physical Oceanography 28*(1): 103-128.

Johnson, K. M., K. D. Wills, D. B. Butler, W. K. Johnson and C. S. Wong (1993). Coulometric total carbon-dioxide analysis for marine studies: Maximizing the performance of an automated gas extraction system and coulometric detector. *Marine Chemistry 44*: 167-187.

Kalnay, E., M. Kanamitsu, R. Kistler, W. Collins, D. Deaven, L. Gandin, M. Iredell, S. Saha, G. White, J. Woollen, Y. Zhu, M. Chelliah, W. Ebisuzaki, W. Higgins, J. Janowiak, K. C. Mo, C. Ropelewski, J. Wang, A. Leetmaa, R. Reynolds, R. Jenne and D. Joseph (1996). The NCEP/NCAR 40-Year Reanalysis Project. *Bulletin of the American Meterological Society 77*(3): 437-471.

Kinkel, H., K.-H. Baumann and M. Cepek (2000). Coccolithophores in the equatorial Atlantic Ocean: response to seasonal and Late Quaternary surface water variability. *Marine Micropaleontology 39*: 87-112.

Körtzinger, A. (2003). A significant CO_2 sink in the tropical Atlantic Ocean associated with the Amazon River plume. *Geophysical Research Letters 30*(24): 2287-2290.

Ledwell, J. R., A. J. Watson and C. S. Law (1993). Evidence for slow mixing across the pycnocline from an open-ocean tracer-release experiment. *Nature 364*: 701-703.

Lee, K., F. J. Millero and R. Wanninkhof (1997). The carbon dioxide system in the Atlantic Ocean. *Journal of Geophysical Research 102*(C7): 15,693-15,707.

Lentz, S. J. (1995). Seasonal Variations in the Horizontal Structure of the Amazon Plume Inferred from Historical Hydrographic Data. *Journal of Geophysical Research-Oceans 100*(C2): 2391-2400.

Lentz, S. J. and R. Limeburner (1995). The Amazon River Plume During AMASSEDS - Spatial Characteristics and Salinity Variability. *Journal of Geophysical Research-Oceans 100*(C2): 2355-2375.

Lewis, E. and D. W. R. Wallace (1998). *Program developed for CO2 System Calculations. Version 1.05.* ORNL/CDIAC-105. Carbon Dioxide Information Analysis Center, Oak Ridge National Laboratory, U.S. Department of Energy, Oak Ridge, Tennesee.

Longhurst, A. (1993). Seasonal cooling and blooming in tropical oceans. *Deep-Sea Resarch Part I 40*: 2145-2165.

Mackenzie, F. T., A. Lerman and L. M. B. Ver (1998). Role of the continental margin in the global carbon balance during the past three centuries. *Geology 26*(5): 423-426.

Maranon, E., M. J. Behrenfeld, N. González, B. Mouriño and M. V. Zubkov (2003). High variability of primary production in oligotrophic waters of the Atlantic Ocean: uncoupling from phytoplankton biomass and size structure. *Marine Ecology - Progress Series 257*: 1-11.

Mehrbach, C., C. H. Culberson, J. E. Hawley and R. M. Pytkowicz (1973). Measurement of apparent dissociation constants of carbonic acid in seawater at atmospheric pressure. *Limnology and Oceanography 18*(6): 897-907.

Michaels, A. F., A. H. Knap, R. L. Dow, K. Gundersen, R. J. Johnson, J. Sorensen, A. Close, G. A. Knauer, S. E. Lohrenz, V. A. Asper, M. Tuel and R. Bidigare (1994). Seasonal patterns of ocean biogeochemistry at the US JGOFS Bermuda Atlantic Time-series Study site. *Deep Sea Research Part I 41*: 1013-1038.

Millero, F. J. and A. Poisson (1981). International one-atmosphere equation of state for sea water. *Deep-Sea Resarch 28*: 625-629.

Millero, F. J., J.-Z. Zhang, K. Lee and D. M. Campbell (1993). Titration alkalinity of seawater. *Marine Chemistry 44*: 153-165.

Muller-Karger, F. E., C. R. McClain and P. L. Richardson (1988). The dispersal of the Amazon's water. *Nature 333*(56-59).

Muller-Karger, F. E., P. L. Richardson and D. J. McGillicuddy (1995). On the offshore dispersal of the Amazon's plume in the North Atlantic: Comments. *Deep-Sea Research Part I-Oceanographic Research Papers 42*(11-12): 2127-2137.

Nittrouer, C. A. and D. J. DeMaster (1986). Sedimentary Processes on the Amazon Continental-Shelf - Past, Present and Future-Research. *Continental Shelf Research 6*(1-2): 5-30.

Pailler, K., B. Bourles and Y. Gouriou (1999). The barrier layer in the Western Tropical Atlantic Ocean. *Geophysical Research Letters 26*(14): 2069-2072.

Price, J. F., R. A. Weller and R. Pinkel (1986). Diurnal Cycling: Observations and Models of the Upper Ocean Response to Diurnal Heating, Cooling, and Wind Mixing. *Journal of Geophysical Research 91*: 8411-8427.

Richey, J. E., J. I. Hedges, A. H. Devol, P. D. Quay, R. L. Victoria, L. A. Martinelli and B. R. Forsberg (1990). Biogeochemistry of carbon in the Amazon River. *Limnology and Oceanography 35*(2): 352-371.

Richey, J. E., R. L. Victoria, E. Salati and B. R. Forsberg (1991). The Biogeochemistry of a Major River System: The Amazon Case Study. *Biogeochemistry of Major World Rivers*. E. T. Degens, S. Kempe and J. E. Richey. John Wiley & Sons, New York. *42*: 57-74.

Sabine, C. L., R. A. Feely, G. C. Johnson, P. G. Strutton, M. F. Lamb and K. E. McTaggart (2004). A mixed layer carbon budget for the GasEx-2001 experiment. *Journal of Geophysical Research 109*(C08S05): 10.1029/2002JC001747.

Sarmiento, J. L., R. Murnane and C. LeQuere (1995). Air-Sea CO_2 Transfer and the Carbon Budget of the North- Atlantic. *Philosophical Transactions of the Royal Society of London Series B-Biological Sciences 348*(1324): 211-219.

Serret, P., C. Robinson, E. Fernandez, E. Teira and G. Tilstone (2001). Latitudinal variation of the balance between plankton photosynthesis and respiration in the eastern Atlantic Ocean. *Limnology and Oceanography 46*(7): 1642-1652.

Smith, W., O., Jr. and D. J. DeMaster (1996). Phytoplankton biomass and productivity in the Amazon River plume: correlation with seasonal river discharge. *Continental Shelf Research 16*(3): 291-319.

Sokal, R. R. and F. J. Rohlf (2000). *Biometry: The Principles and Practice of Statistics in Biological Research*. W.H. Freeman and Co., New York.

Sprintall, J. and M. Tomczak (1992). Evidence of the Barrier Layer in the Surface Layer of the Tropics. *Journal of Geophysical Research 97*(C5): 7305-7316.

Subramaniam, A., E. J. Carpenter, P. L. Yager, S. R. Cooley, R. Del Vecchio, D. Karl, C. Mahaffey, S. A. Sanudo-Wilhelmy, R. Shipe, A. Tovar-Sanchez and D. G. Capone (*in revision*). Amazon River amplifies C and N cycles in the Tropical North Atlantic Ocean.

Sweeney, C., D. A. Hansell, C. A. Carlson, L. Codispoti, L. I. Gordon, J. Marra, F. J. Millero, W. O. Smith and T. Takahashi (2000). Biogeochemical regimes, net community production and carbon export in the Ross Sea, Antarctica. *Deep Sea Research Part II 47*(15-16): 3369-3394.

Takahashi, T., R. A. Feely, R. F. Weiss, R. H. Wanninkhof, D. W. Chipman, S. C. Sutherland and T. T. Takahashi (1997). Global air-sea flux of CO_2: An estimate based on measurements of sea-air pCO_2 difference. *Proceedings of the National Academy of Sciences of the United States of America 94*(16): 8292-8299.

Takahashi, T., J. Olafsson, J. G. Goddard, D. Chipman and S. C. Sutherland (1993). Seasonal variation of CO_2 and nutrients in the high-latitude surface oceans: A comparative study. *Global Biogeochemical Cycles 7*(4): 843-878.

Takahashi, T., S. C. Sutherland, C. Sweeney, A. Poisson, N. Metzl, B. Tilbrook, N. R. Bates, R. Wanninkhof, R. A. Feely, C. L. Sabine, J. Olafsson and Y. Nojiri (2002). Global sea-air CO_2 flux based on climatological surface ocean pCO_2, and seasonal biological and temperature effects. *Deep-Sea Resarch II 49*: 1601-1622.

Ternon, J. F., C. Oudot, A. Dessier and D. Diverres (2000). A seasonal tropical sink for atmospheric CO_2 in the Atlantic Ocean: the role of the Amazon River discharge. *Marine Chemistry 68*: 183-201.

Wanninkhof, R. (1992). Relationship between Wind-Speed and Gas-Exchange over the Ocean. *Journal of Geophysical Research-Oceans 97*(C5): 7373-7382.

Weiss, R. F. (1974). Carbon dioxide in water and seawater: The solubility of a nonideal gas. *Marine Chemistry 2*: 203-215.

Williams, P. J. L. (1998). The balance of plankton respiration and photosynthesis in the open oceans. *Nature 394*: 55-57.

Williams, P. J. L. and D. G. Bowers (1999). Regional carbon imbalances in the oceans. *Science 284*: 1735b.

Yager, P. L., D. W. R. Wallace, K. M. Johnson, W. O. J. Smith, P. J. Minnett and J. W. Deming (1995). The Northeast Water Polynya as an atmospheric CO_2 sink: A seasonal rectification hypothesis. *Journal of Geophysical Research 100*(C3): 4389-4398.

Yelland, M. and P. K. Taylor (1996). Wind stress measurements from the open ocean. *Journal of Physical Oceanography 26*(4): 541-558.

Yoo, J.-M. and J. A. Carton (1990). Annual and interannual variation of the freshwater budget in the Tropical Atlantic Ocean and the Caribbean Sea. *Journal of Physical Oceanography 20*: 831-845.

Table 2.1: Mean surface mixed layer (SML) characteristics (±1SE) for winter and summer 2001.

	Nonplume	Plume
Stations	(n=27)	(n=18)
SML depth (m)	78.0 ± 4.4	9.2 ± 1.5
SML samples	(n=123)	(n=25)
DIC (μmol C kg^{-1})	2017.2 ± 1.5	1786.2 ± 15.8
TA (μeq C kg^{-1})	2365.7 ± 1.2	2124.3 ± 19.7
Salinity	36.05 ± 0.02	31.91 ± 0.36
SST (ºC)	26.13 ± 0.08	28.68 ± 0.10
Surface samples	(n=36)	(n=21)
pCO_2(SST) (μatm)	359.5 ± 2.7	308.3 ± 8.3
pCO_2(28°C) (μatm)	383.9 ± 2.5	297.0 ± 8.4

All plume means except pCO_2(SST) were significantly different ($p<0.05$) from nonplume means (Welch's t-test).

Table 2.2: Model II regression statistics (±1SE) for the carbonate system versus salinity.

	DIC			TA		
	r[1]	*slope*	*y-intercept*	*r*	*slope*	*y-intercept*
Plume (n=25)	0.912	44.1 ± 3.8	378.5 ± 120.4	0.983	55.0 ± 2.1	369.7 ± 68.1
ETAMBOT I, II, SABORD[2] *(n=158)*	0.997	49.6 ± 0.3	223.6 ± 9.5	0.998	59.0 ± 0.3	268.4 ± 9.7
Mixing model (n=25)[3]		47.6 ± 0.3	308.8 ± 11.6		58.8 ± 0.3	253.3 ± 9.5
Obidos river endmember[4]			600			600

Slopes and intercepts for plume and ETAMBOT/SABORD groupings were significantly different from nonplume conditions.

[1] *r* = correlation coefficient; all correlations shown were significant at the α=0.05 level.
[2] ETAMBOT 1, 2, and SABORD data (Fall 1995, Spring 1996) from Ternon et al. (2000) were pooled and analyzed using Model II regressions.
[3] Slope implied by mixing-model-generated Y-intercepts and ocean endmembers (see Methods).
[4] Obidos river endmember used by Ternon *et al*. (2000), from Richey *et al*. (1990).

Table 2.3: Breakdown of pCO_2 values (± 1SE) by subgroup for nonplume WTNA samples.

	All (n=36)	Winter (n=26)	Summer (n=10)	Summer southern[5] (n=4)	Summer northern[6] (n=6)
SST	26.3 ± 0.2	**25.9 ± 1.0**[7]	**27.5 ± 0.0**	27.4 ± 0.2	27.6 ± 0.1
pCO_2(SST)	359.5 ± 2.7	**355.2 ± 2.8**	**370.8 ± 5.1**	**388.6 ± 4.4**	**359.0 ± 0.7**
pCO_2(28)	383.9 ± 2.5	386.3 ± 2.6	377.6 ± 5.6	**397.4 ± 3.0**	**364.4 ± 1.9**

[5] Includes stations 33, 35, 36, 38 (Figure 1).
[6] Includes stations 17, 19, 21 (Figure 1).
[7] Bold values indicate a significant difference (winter is compared with summer, summer southern is compared to summer northern).

Table 2.4: Mixed layer model results for the WTNA surface mixed layer (SML; ±1SE) in winter and summer 2001.

	Winter[8]	Summer, southern	Summer, northern
	Jan. 19 – Feb. 22	*Jul.14 – Aug. 15*	
Stations	(n=24)	(n=4)	(n=4)
Observed SML depth (m)	78.5 ± 4.5	54.3 ± 8.1	76.0 ± 10.6
I. Model Output (+ freshwater effects on DIC)			
Duration (days)	31	32	32
Mean SML depth (m)	74.9 ± 0.2	15.0 ± 0.5	14.4 ± 0.4
SML Salinity change[9] (psu d^{-1})	+ 0.003	-0.0009	-0.0005
SML Salinity change (g salt m^{-3} d^{-1})	+ 3.3	-0.9	-0.5
SML Salinity inventory change [10] (mg m^{-2} s^{-1})	+ 2.8	-0.2	-0.1
SML DIC change (µmol kg^{-1} d^{-1})	+ 0.36	-0.034	-0.015
SML DIC inventory change (mmol C m^{-2} d^{-1})	+27	-0.53	-0.22
II. Model Output (- freshwater effects on DIC)[11]			
SML DIC change (µmol kg^{-1} d^{-1})	+0.21	+0.026	+0.041
SML DIC inventory change (mmol C m^{-2} d^{-1})	+16	+0.39	+0.61
Change in SML DIC inventory due to evaporation/precipitation (mmol C m^{-2} d^{-1})[12]	+11	-0.92	-0.83

[8] The winter run was forced with daily NCEP meteorological output, and the summer runs were forced with hourly average underway data (see Methods).
[9] Change in SML value $\Delta C = (C_{final} - C_{initial})/Duration$.
[10] Inventory change = ΔC*(Density)*(Mean SML depth)*. SML salt inventory change (storage) is presented per second to facilitate comparison with the literature (see Discussion).
[11] All other model outputs for II (e.g., MLD, salinity changes) were the same as the results listed for run I above.
[12] The difference between SML DIC inventory changes calculated during the two model runs.

Figure 2.1: Map of a) winter 2001 and b) summer 2001 sea surface salinities (summer station numbers noted) in the western tropical North Atlantic Ocean. The gray line approximately follows the salinity 35 contour of the plume edge, generated using a correlation between K_{490} and salinity (Del Vecchio and Subramaniam 2004) and satellite-derived monthly climatology of K_{490} (February and August), provided by A. Subramaniam.

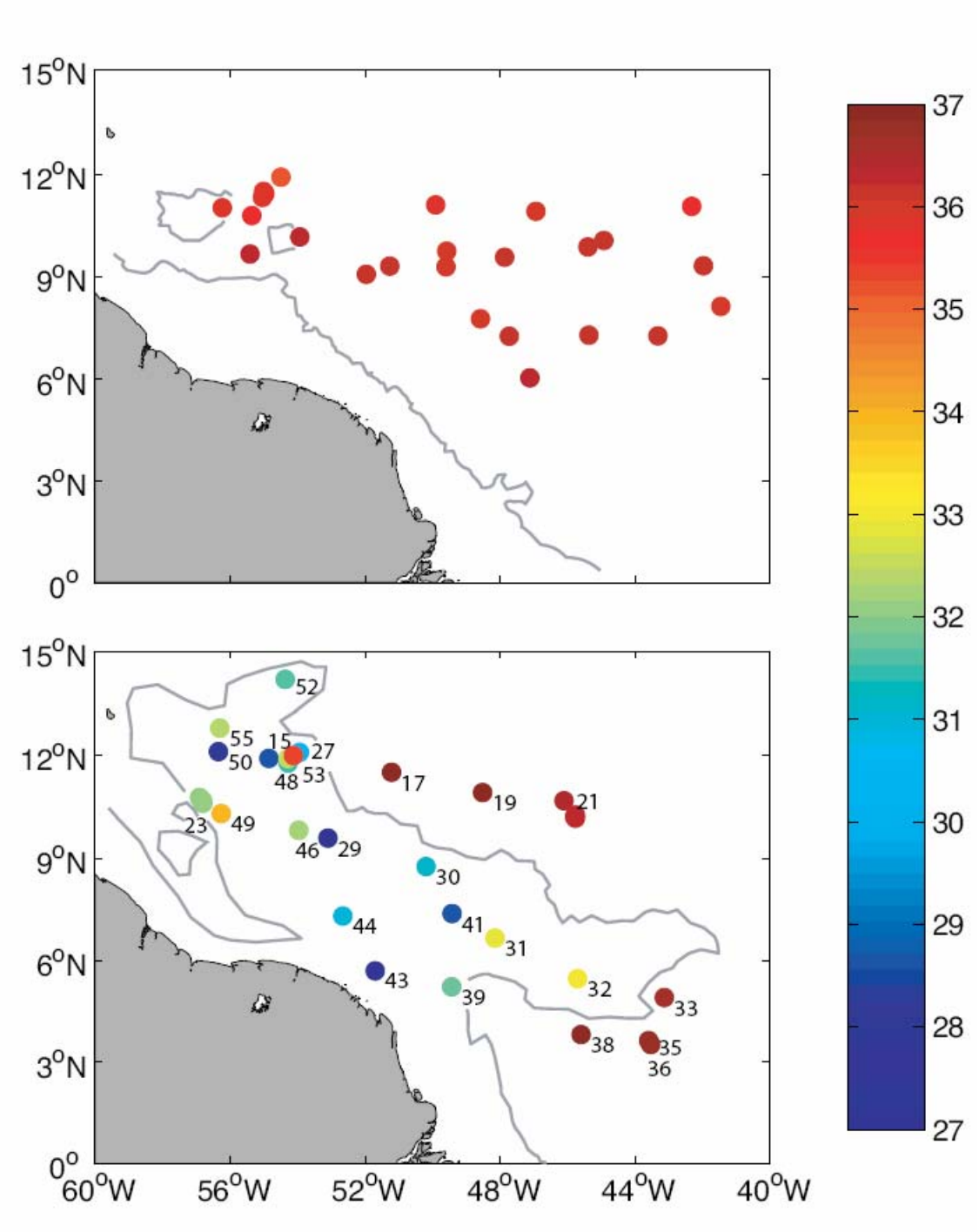

Figure 2.2: Winter (filled gray symbols) and summer 2001 (open black symbols) DIC (Δ) and TA (O) in the WTNA plotted against (a) depth and (b) σ_t. σ_t =27 is approximately 500 m.

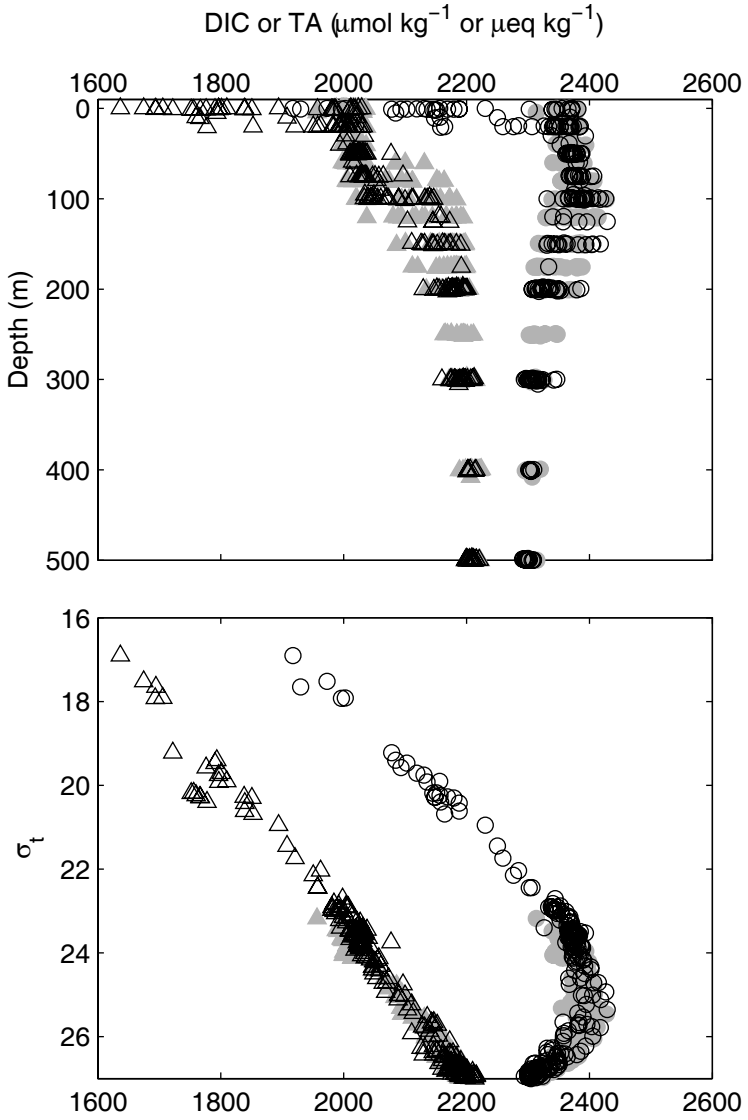

Figure 2.3: a) DIC (Δ) and TA (O) against salinity for summer 2001 (open symbols) and winter 2001 (filled gray symbols). The statistics for the plume-influenced solid regression lines shown are in Table 2.2. Dashed lines indicate mixing lines implied by the mixing model, whose slope and intercept are in Table 2.2. b) Residual of summer and winter DIC and TA around the plume-influenced regressions. The shaded regions above salinity 35 indicate data outside the influence of the plume.

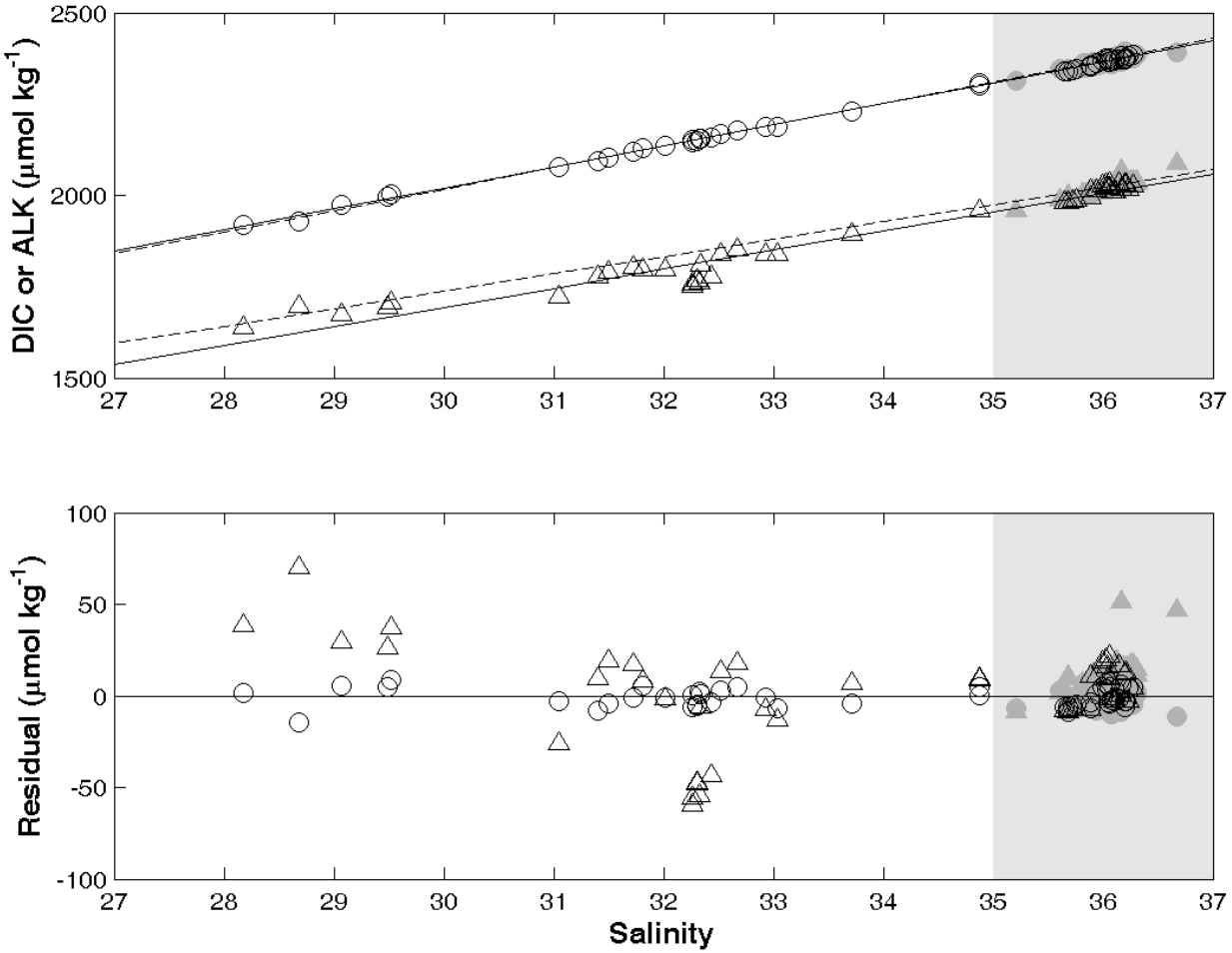

Figure 2.4.1: Winter 2001 underway sea surface temperature (SST; A), sea surface salinity (SSS; B), observed mixed layer depth (MLD; C), and windspeed (D). The dotted line in (B) indicates salinity 35, the threshold below which samples are considered "plume-influenced." The gray line in (C) at 75 m indicates the modeled MLD (see Results).

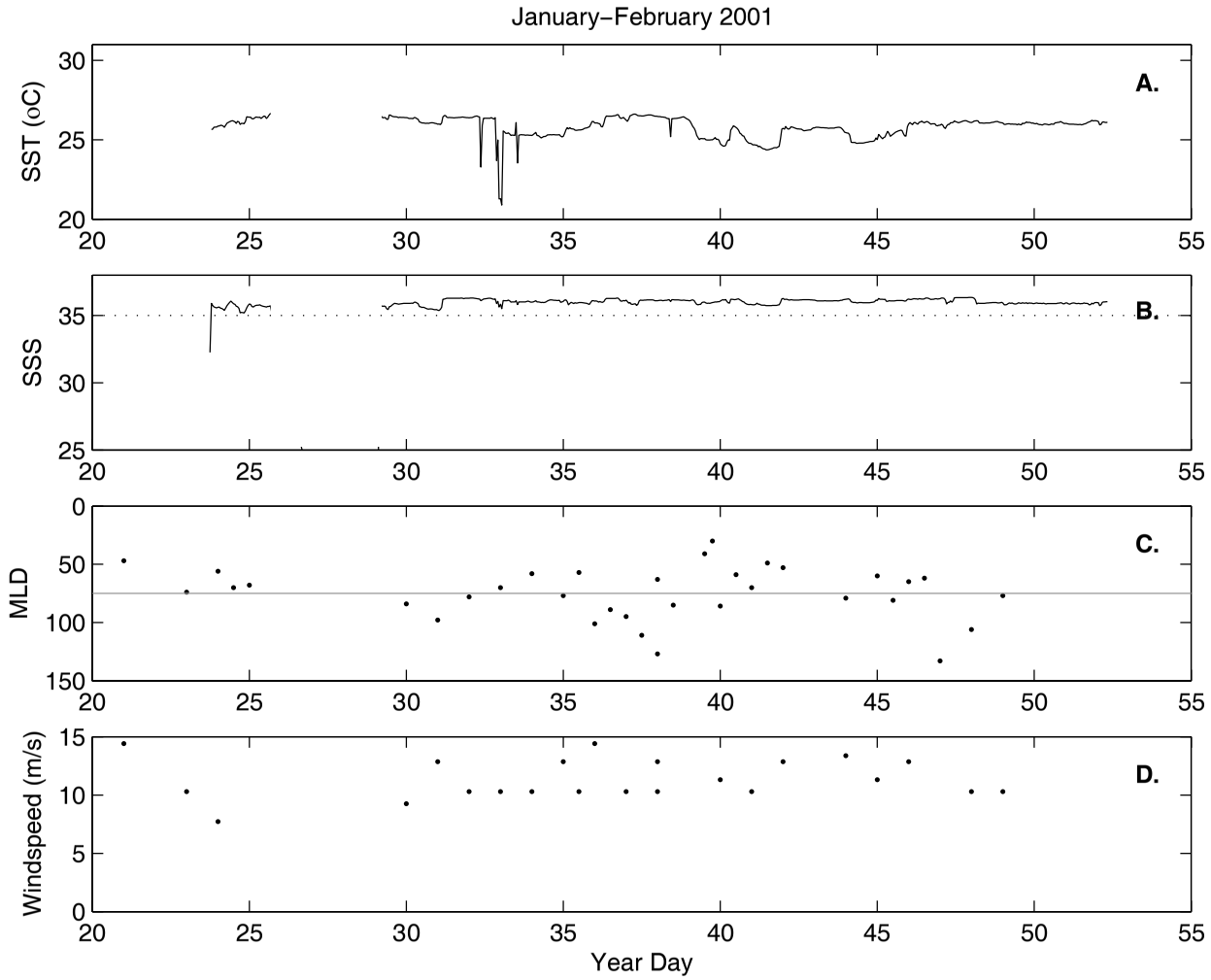

Figure 2.4.2: Summer 2001 underway sea surface temperature (SST; E), sea surface salinity (SSS; F), observed mixed layer depth (MLD; G), and windspeed (H). The dotted line in (F) indicates salinity 35, the threshold below which samples are considered "plume-influenced." The gray line in (G) at 15 m indicates the modeled MLD (see Results).

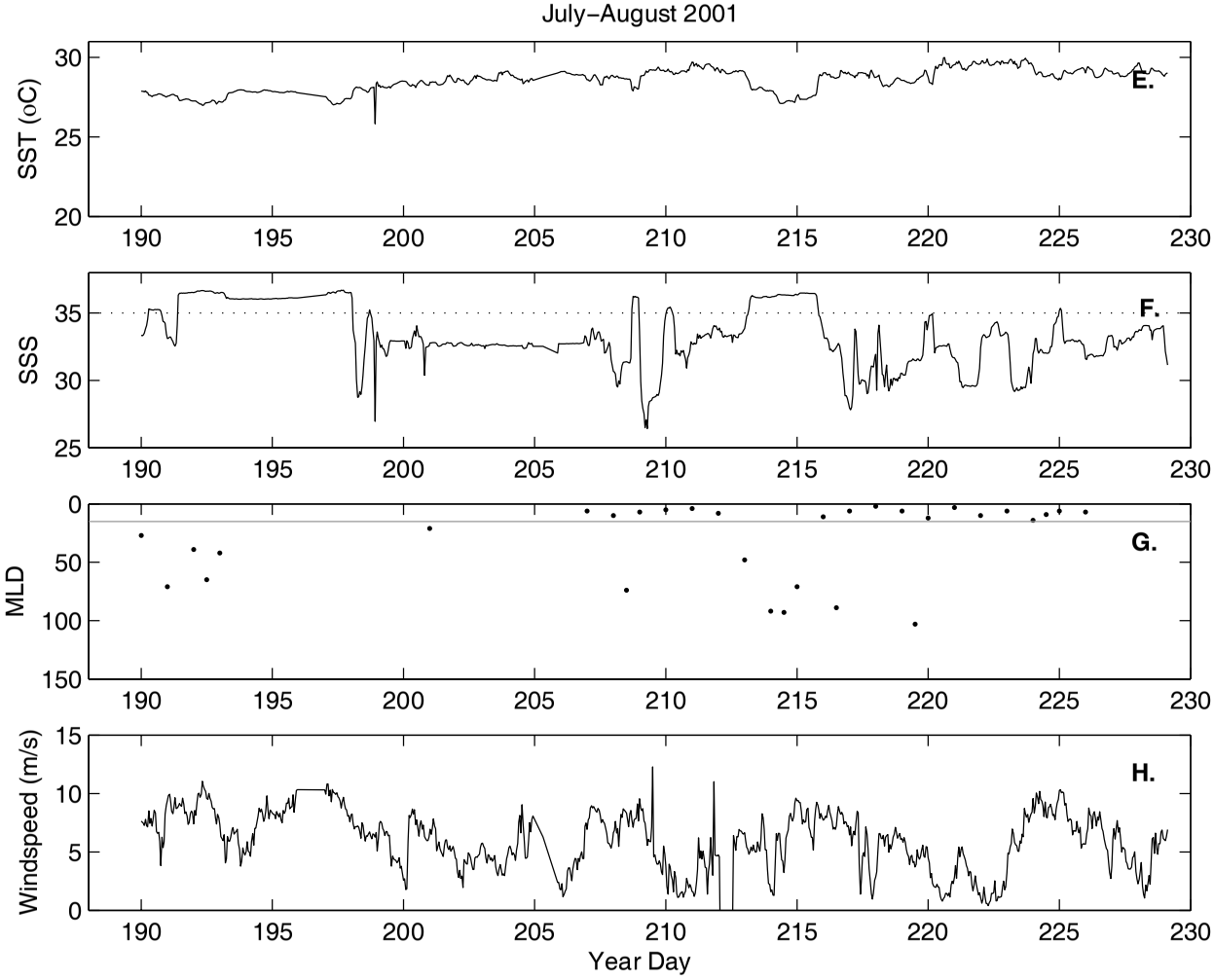

Figure 2.5: ΔpCO_2 (pCO_{2sea} (SST) - pCO_{2atm}), plotted on a map of the WTNA in (a) winter and (b) summer 2001. The gray line indicates the approximate location of the salinity 35 contour, also shown and described in Figure 1. Station numbers discussed in the text are noted. Stations with $+\Delta pCO_2$ (red-orange colors) are oversaturated with respect to the atmosphere; $-\Delta pCO_2$ (blue-green colors) represent undersaturated regions.

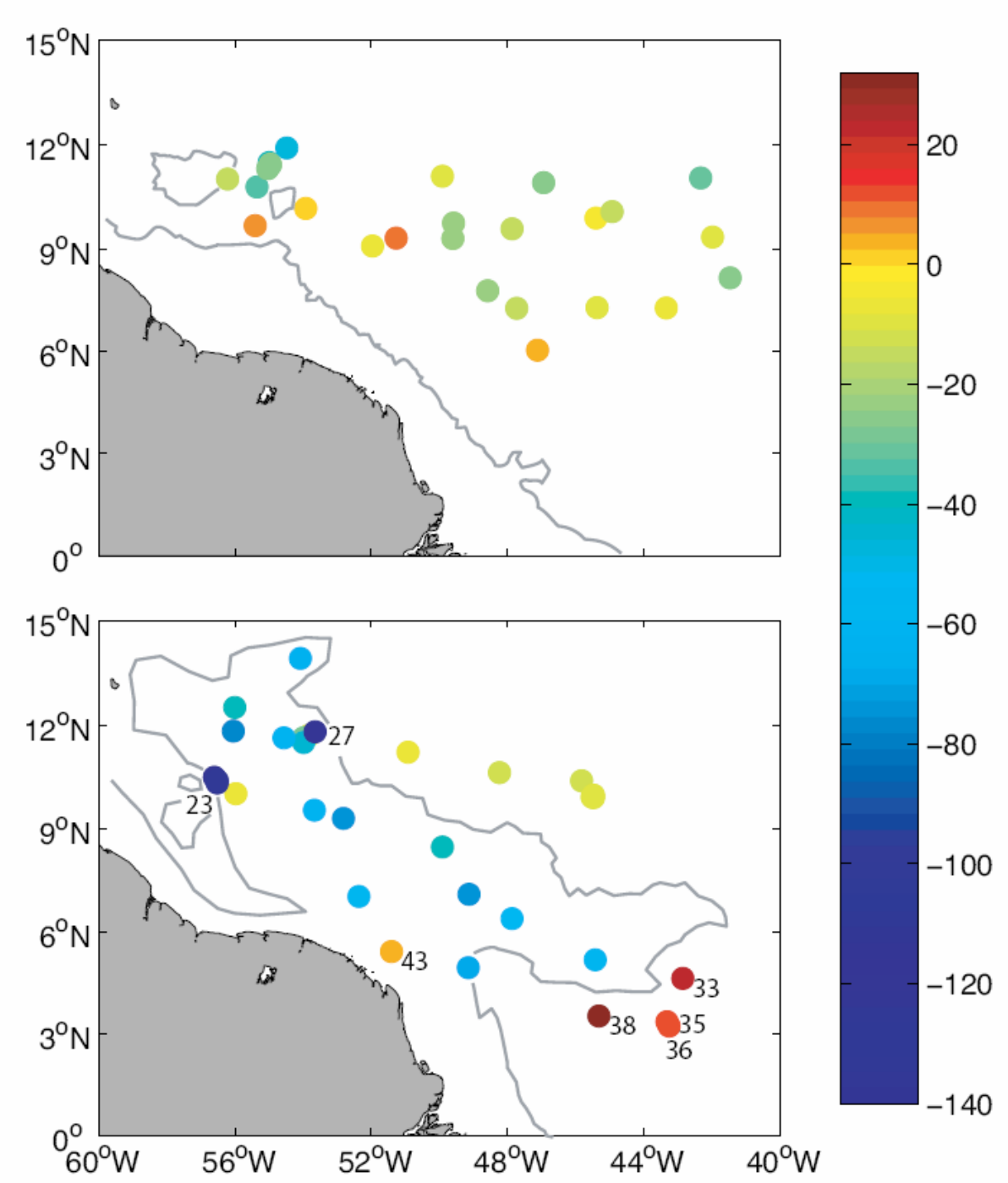

Figure 2.6: Community impact on DIC (ΔDIC_{BIO}), calculated with the mixing model, plotted against salinity. 95% confidence interval error bars are within the size of the marker. Station numbers are shown for summer samples. Endmembers used to calculate ΔDIC_{BIO} included: A_s = 2359.4 ± 5.9, S_s = 36.07 ± 0.10, DIC_s = 2024.5 ± 6.8, S_r = 0 ± 0. The shaded region above salinity 35 indicates data outside the influence of the plume. Markers indicate the prevailing macroscopic nitrogen-fixing organisms observed at a station: ■ = none, ● = *Richelia*, * = *Trichodesmium*, circle and star superimposed = *Richelia* and *Trichodesmium* together.

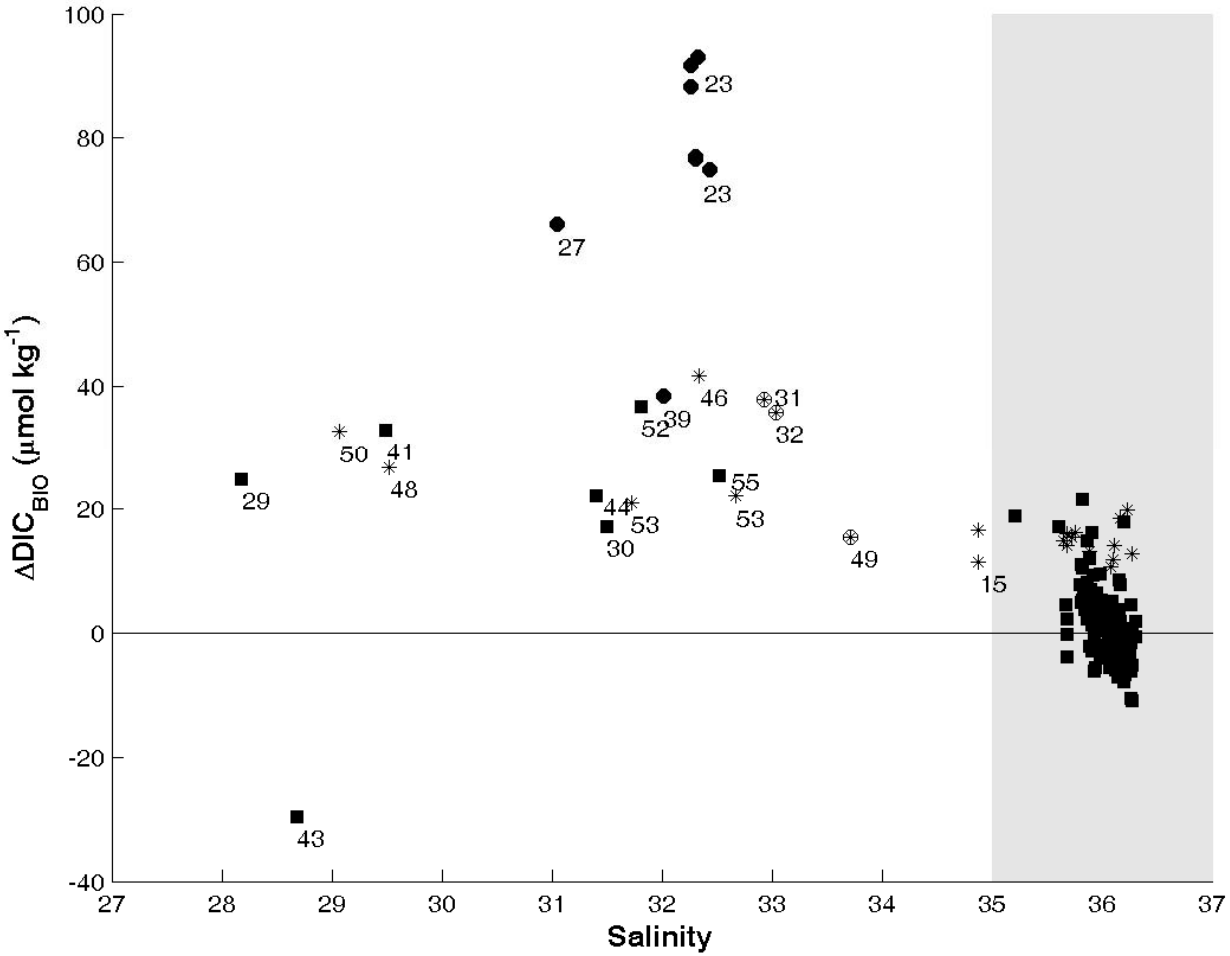

Figure 2.7: Winter (dark gray squares) and summer pCO_2 (black squares) calculated at SST are plotted against salinity. Open squares indicate expected pCO_2 (pCO_{2exp}), given conservative mixing of plume and ocean water. Regressions of ETAMBOT/SABORD data, and *Meteor* cruise 55 data are shown for comparison. The shaded region above salinity 35 indicates data outside the influence of the plume.

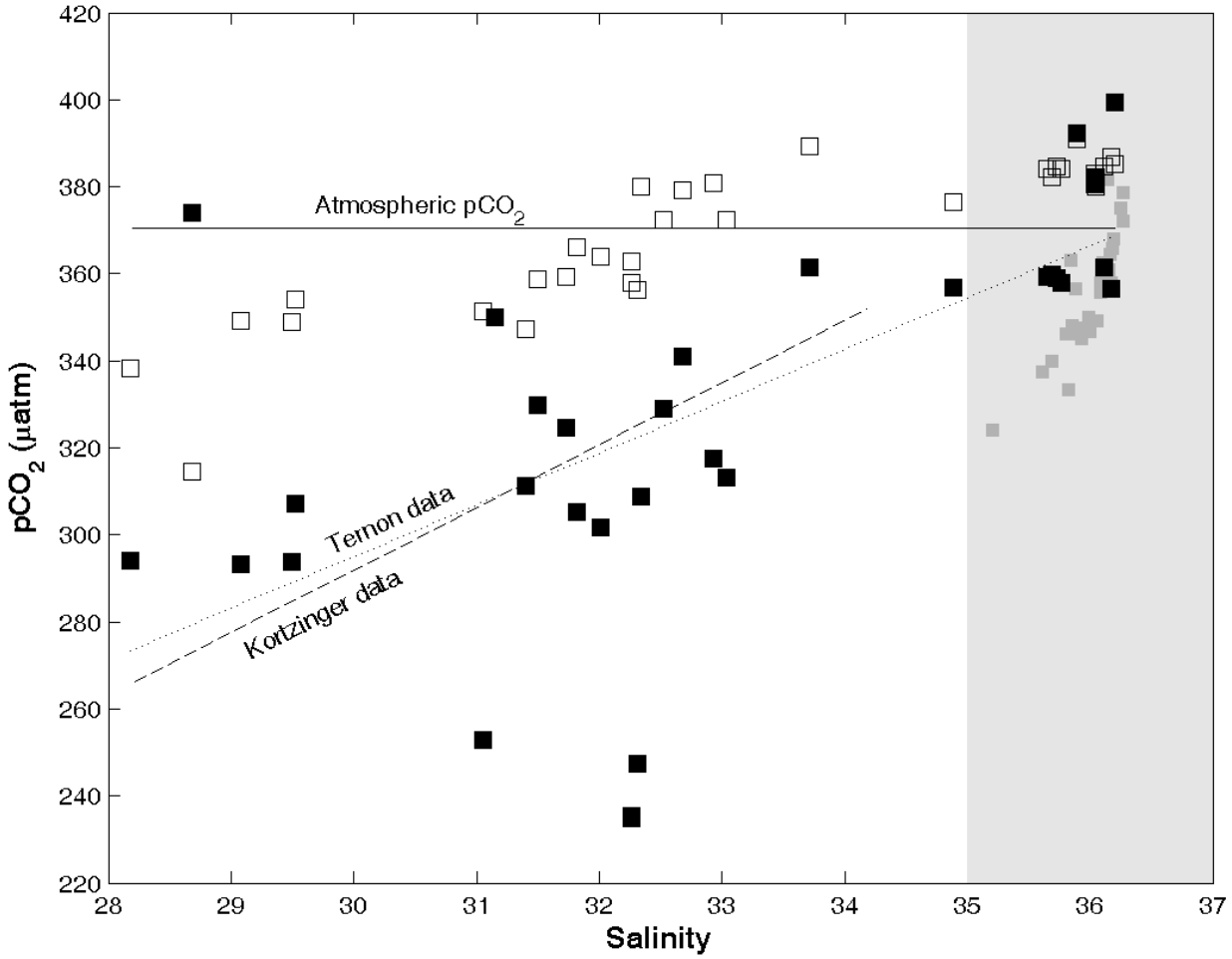

Figure 2.8: Schematic diagram of physical influences on the one-dimensional, WTNA surface mixed layer carbon budget. All fluxes are in mmol m^{-2} d^{-1}. Solid lines indicate mixed layer depth (m). White arrows represent air-sea CO_2 transfer, and gray arrows represent vertical mixing fluxes. Dashed arrows indicate net evaporation (up) or precipitation (down), and numbers in the dashed ovals indicate the associated change per day in the surface mixed layer carbon inventory (see Methods, Discussion).

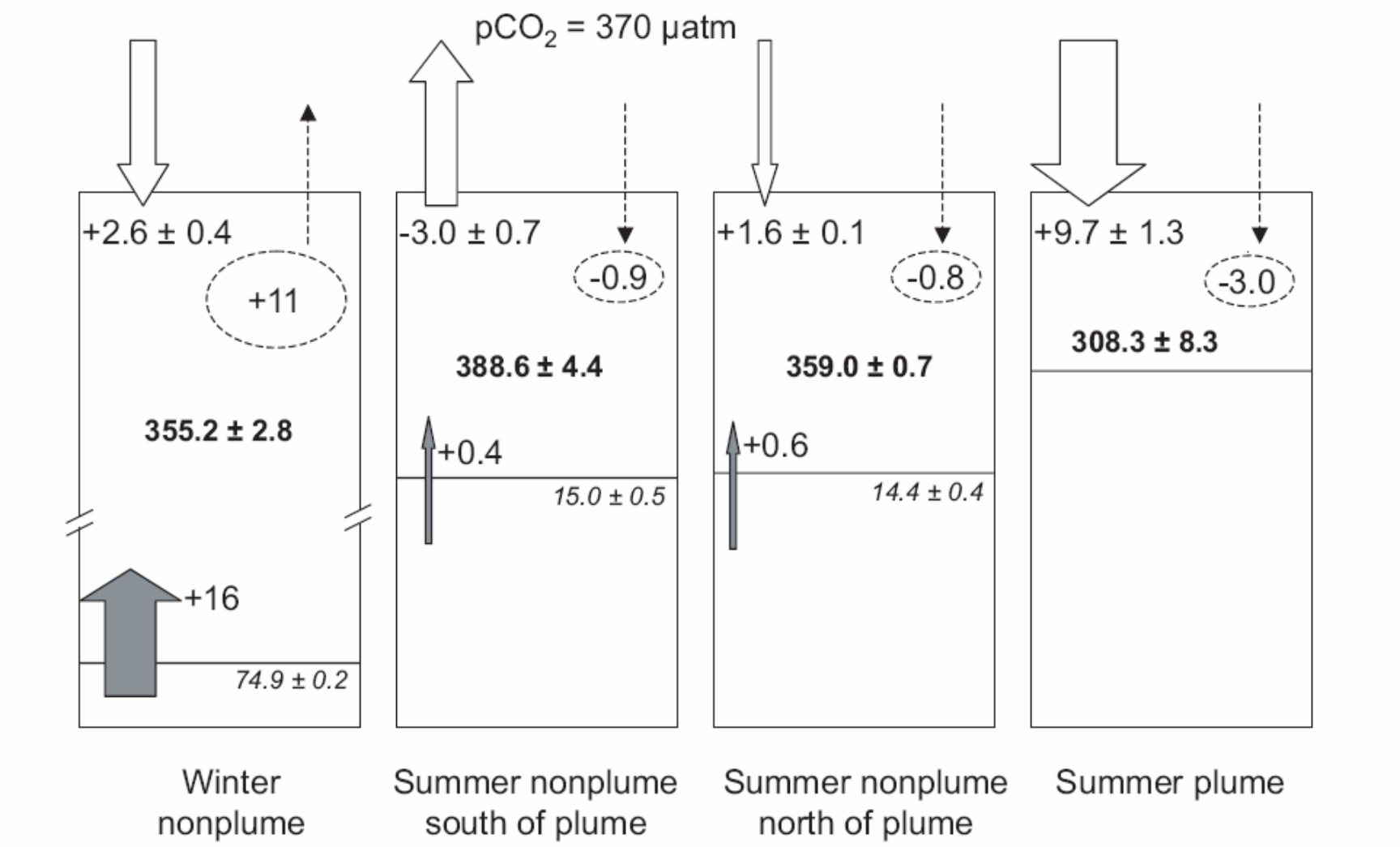

CHAPTER 3

SEASONAL VARIATIONS IN THE AMAZON PLUME-RELATED ATMOSPHERIC CARBON SINK[1]

[1] Cooley, S.R., V.J. Coles, A. Subramaniam, and P.L. Yager. To be submitted to *Global Biogeochemical Cycles.*

Abstract

The Amazon River plume is a highly seasonal feature that reaches more than halfway across the tropical Atlantic Ocean in satellite ocean color images during some parts of the year. Shipboard observations show that the seasonal presence of the plume significantly reduces ocean surface salinities and inorganic carbon values. In April-May 2003, dissolved inorganic carbon (DIC), total alkalinity (TA), and partial pressure of CO_2 (pCO_2) were measured in the upper 1000 m of the Western Tropical North Atlantic (WTNA; 48-60ºW, 6-14ºN). Plume-influenced stations exhibited pCO_2 as low as 201 µatm and inorganic carbon values up to 563 µmol C kg^{-1} (~28%) below those of non-plume surface samples. We combine our own data with those from other published investigations to understand the annual uptake and seasonal variability of the Amazon River plume-related CO_2 sink. Combining inorganic carbon data from all seasons with monthly plume areas determined by satellite, we estimate the annual carbon uptake by the outer plume ($28 < S < 35$) to be 15 ± 6 Tg C yr^{-1}. We further examine both riverine and oceanic data to quantify seasonality of river carbon supply and of the biological and physical processing of inorganic carbon within the plume. By a seasonally changing combination of Andean carbonate dissolution and lowland dilution, the Amazon River delivers 295 ± 61 (mean ± amplitude) µmol kg^{-1} TA to the plume. Upon entering the ocean, TA was a conservative tracer of Amazon water throughout the plume. Assuming that DIC was supplied to the plume in proportion to TA, DIC was significantly affected by nonconservative offshore processes. Throughout the study region ($28<S<35$), net community production associated with diazotrophy primarily drove plume DIC changes by enhancing the air-sea CO_2 disequilibrium. Decreased autumn CO_2 solubility and windspeed, however, may have limited the air-sea CO_2 flux despite biological enhancement. Not

only sensitive to diazotroph production, the Amazon plume carbon sink thus also depends on meteorological conditions that control river hydrology, CO_2 solubility, and gas exchange.

Introduction

The Amazon River generates an offshore plume each summer that covers ~$2x10^6$ km^2 of the Western Tropical North Atlantic Ocean (WTNA) with 5-10 m of low-carbon, low-salinity water (Lentz and Limeburner 1995; Körtzinger 2003; Ternon et al. 2000; Smith and DeMaster 1996; DeMaster and Pope 1996). Net community production enhances the mixing-driven air-sea CO_2 gradient, and the plume takes up an estimated 5.9 g C m^{-2} y^{-1} atmospheric CO_2 (Körtzinger 2003). In contrast, tropical Atlantic seawater releases approximately 8.2 g C m^{-2} y^{-1} (for a total of 0.15 Pg C yr^{-1}, Takahashi et al. 2002) due to solubility-driven CO_2 loss in excess of biological uptake (Goyet et al. 1998; Lee et al. 1997; Takahashi et al. 1997; Takahashi et al. 2002; Sarmiento et al. 1995). The seasonal presence of the Amazon plume offshore thus drives temporal variability in WTNA inorganic carbon values (Cooley and Yager 2006) and reverses the direction of the air-sea flux over a large region.

Initial estimates of plume carbon uptake have used surface area and inorganic carbon-salinity relationships from one or two seasons and transects to determine yearly sink magnitude (Körtzinger 2003; Ternon et al. 2000). Combining previous studies with our own three field programs may now provide great enough seasonal and spatial coverage to address temporal variability of inorganic carbon within the plume. This approach is important since predictions of future sink behavior that incorporate natural and climate-driven changes require a mechanistic understanding of the system. In this study, we use our own and other published data sets of WTNA total alkalinity (TA), dissolved inorganic carbon (DIC), and surface ocean pCO_2 to quantify natural seasonal variability in the plume inorganic carbon system.

Background:

Total alkalinity appears to be a conservative tracer of both Andean water within the river mainstem (Devol et al. 1995) and Amazon water in the offshore plume (Ternon et al. 2000; Cooley and Yager 2006). Andean runoff is the only source of alkalinity to the Amazon River, peaking in March at ~700 μmol kg^{-1} upstream (at Marchanteria, 1500 km from the river mouth, Figure 3.1, Devol et al. 1995; Devol and Hedges 2001); other Amazon tributaries that peak at different times dilute the Andean signal downstream (Richey et al. 1991; Devol and Hedges 2001; Marengo et al. 2001; Grimm 2003). As a result, monthly TA near the river midpoint (at Obidos, 800 km from the river mouth; Fig. 3.1) ranges between 400-600 μmol kg^{-1} (Devol and Hedges 2001). Seasonal TA values at the river mouth in water that supplies the offshore plume have not been published, but likely are low and seasonally variable as a function of total Amazon watershed drainage. Processes that would nonconservatively influence TA offshore, like the growth of carbonate-forming organisms, are not expected to occur in the plume, where diatoms may be favored due to nutrient levels (Iglesias-Rodriguez et al. 2002). Also, coccolithophores were not observed during our cruises (E.J. Carpenter, personal communication), and the relative abundance of coccolithophores to other phytoplankton in the tropical Atlantic is quite low (Kinkel et al. 2000). Plume TA distributions primarily reflect mixing of river and ocean water (Cooley and Yager 2006). Seasonal plume TA variations are therefore more likely due to changes in riverine supply since nonconservative processing of plume TA is minimal.

Unlike TA, dissolved inorganic carbon (DIC) is not expected to act conservatively along the mountain-ocean mixing gradient (Devol and Hedges 2001; DeMaster and Aller 2001; Ternon et al. 2000; Cooley and Yager 2006). Net respiration of mainstem organic matter releases CO_2 to the atmosphere (Devol et al. 1987; Richey et al. 2002; Mayorga et al. 2005), dominating DIC

processing until turbidity settles in the early plume (salinity 0-3, DeMaster et al. 1996; Edmond et al. 1981). Nevertheless, DIC values at the river mouth are expected to be low (363 umol L^{-1} in November 1991, Druffel et al. 2005), and water in the mid- to offshore plume has pCO_2 values far below atmospheric levels (Ternon et al. 2000; Körtzinger 2003; Cooley and Yager 2006). Nutrients in the plume support net primary production offshore (Smith and DeMaster 1996; DeMaster and Pope 1996), which enhances the water's CO_2 undersaturation and increases air-sea CO_2 transfer (Ternon et al. 2000; Körtzinger 2003; Cooley and Yager 2006). The Amazon is not a significant source of bioavailable N to the WTNA, however. Only 20-50% of the nitrogen supply to the shelf comes from the river, and only about 50% of the external nitrogen supply to the Amazon shelf is exported offshore, implying that nitrogen fixation must be important to net community production, even in the early plume (DeMaster and Aller 2001). As with TA, seasonal values of DIC at the river mouth have not been published, so analyses frequently assume that DIC supplying the plume co-occurs with TA in a fixed ratio and vary little (Ternon et al. 2000, and references therein ; Devol et al. 1995; Cooley and Yager 2006). At the same time, nonconservative biological processing in the outer plume is known to alter DIC by up to ~100 μmol kg^{-1} (Cooley and Yager 2006). We therefore hypothesize that seasonal changes in plume DIC processing such as biological production and air-sea CO_2 transfer, rather than in supply from the river, will drive seasonality in outer plume DIC.

Goal:

To examine the sources of DIC and TA seasonality and their influences on the Amazon plume-associated CO_2 sink, we posit that: 1) TA acts as a conservative tracer from the Andes to the offshore plume throughout the year, and 2) plume net primary production, evidenced by

nonconservative variations in plume DIC and CO_2 partial pressure (pCO_2), uniformly affects inorganic carbon budgets among seasons. To test our hypotheses, we report new values of WTNA surface mixed layer (SML) DIC, TA, and underway pCO_2 measured during Spring 2003, and use this data with historical WTNA and Amazon mainstem data (Ternon et al. 2000; Körtzinger 2003; Cooley and Yager 2006; Devol et al. 1995) to model TA at the river mouth by two independent methods, compare DIC and TA mixing curves between seasons, and calculate seasonal differences in the biological impact on DIC. Combining the third analysis with seasonal differences in the area of the plume quantifies the effects of observed supply/processing variations on the plume-associated carbon sink and provides an estimate of the total annual uptake by the plume.

Methods:

Sample collection and analysis

The spring 2003 dataset was collected during daily stations aboard the *R/V Seward Johnson I* during the third Atlantic MANTRA/PIRANA cruise (Spring '03; April 18 – May 22, 2003; also referred to as "MP8" by our collaborators) within 6-13 ˚N, 48-58 ˚W (Figure 3.1). Water samples for DIC and TA analysis were collected using Niskin bottles between 1 and 1000 m using standard protocol (DOE 1997). In addition, a single sample of surface Amazon water was hand-collected from a small boat near Macapá, Brazil (0 °N, 51 °W; Figure 3.1) in April 2002 using a pole sampler. The sample was sealed tightly and returned to Georgia, where it was refrigerated in the dark until analysis. Preserved samples collected on the ship were kept in the dark at a cool room temperature until they were returned to Georgia, where they were stored in the dark at 4 ˚C until analysis. Samples were analyzed within 1 year of collection. Seawater

collected and stored following this protocol was stable for DIC and TA analysis for at least 4 years (P.L. Yager, unpublished data).

During the cruise, the partial pressure of CO_2 (pCO_2) in the surface ocean was measured continuously using an automated underway analyzer plumbed into the ship's uncontaminated seawater line. The system's primary components included a 10 L showerhead-type seawater equilibrator (Bates et al. 1998; Sweeney et al. 2000; Takahashi et al. 1997) and an infrared CO_2 detector (LI-6262, Li-Cor, Lincoln, NE). Seawater flow of 8 L min^{-1} produced a system e-folding time of 35 minutes (S. Cooley, unpublished data). Sampling and calibration routines were computer automated; measurements were calibrated at least hourly against five CO_2-N_2 gas mixtures containing from 0 to 510.85 ppm CO_2 (certified by NOAA CMDL, Boulder, CO). Instrument accuracy was ± 1 μatm. pCO_2 was calculated at *in situ* temperature (Takahashi et al. 1993). The data (Nyquist frequency[2] = 0.003 Hz) were processed using a Lanczos filter (Duchon 1979, 100 weights, cutoff frequency = 9.3 x 10^{-5} Hz) to remove occasional brief high-pCO_2 excursions related to short interruptions in the ship's seawater supply during high seas.

Dissolved inorganic carbon measurements were performed on a SOMMA system (Single Operator Multiparameter Metabolic Analyzer, Johnson et al. 1993) connected to a CO_2 coulometer (UIC, model 5011). Samples were analyzed following standard protocols (Johnson et al. 1993; DOE 1997; Bates et al. 1996). Sample conductivity was measured with a Sea-Bird conductivity cell (SBE-4) plumbed into the SOMMA gas-driven delivery system. Salinity (practical salinity scale, unitless) was calculated based on cell calibration to IAPSO salinity standards. Primary system calibration was based on analysis of pure (99.995%) CO_2 gas and Certified Reference Materials (CRMs; supplied by A.G. Dickson, Scripps Institute of

[2] The Nyquist frequency, or critical frequency, is half the sampling frequency. Filters with a cutoff frequency below the Nyquist frequency will not distort the signal.

Oceanography). DIC measurements were corrected to daily standards. Instrument precision based on analysis of replicate standards (DOE 1997), was ±0.51 µmol C kg^{-1}, and precision based on replicate samples was ±1.58 µmol C kg^{-1}.

Total alkalinity was measured using a programmable open-cell potentiometric titration system (Dickson et al. 2003; Bates et al. 1996). Samples were weighed using an electronic balance accurate to within 0.06 g (0.05% of typical sample mass) with a precision of ± 0.2 mg. Samples were titrated with small additions of 0.1 N HCl in 0.7 M NaCl and total alkalinity was determined with a modified Gran calculation (Dickson et al. 2003; Goyet and Poisson 1989; Bates et al. 1996; DOE 1997; Millero et al. 1993). CRMs were used as primary alkalinity standards to back-calculate titration acid concentration. This forced the absolute accuracy of samples to CRM standards. Instrument precision based on replicate standards (DOE 1997) was ±1.93 µmol kg^{-1}, while precision based on duplicate samples was ±1.66 µmol kg^{-1}.

The Macapá sample was centrifuged at 8500 rpm for 20 minutes to remove the larger suspended sediment particles before chemical analysis. Salinity was then determined using the SOMMA conductivity cell, and alkalinity was measured as described above.

Historical observational datasets

WTNA dissolved inorganic carbon and total alkalinity datasets collected during other seasons and years were also used for this study (Figure 3.1). Fall 1995 ("Fall '95", ETAMBOT I, September-October 1995) and Spring 1996 ("Spring '96", ETAMBOT II; April-May 1996) datasets (Ternon et al. 2000) were obtained from the IFREMER FTP site (www.ifremer.fr/sismer). Meteor 55 underway pCO_2 data from October 13 – November 17, 2002 (Körtzinger 2003) were kindly provided by A. Körtzinger. Summer and winter 2001 data

from the MANTRA/ PIRANA project (Winter '01 and Summer '01, January-February and July-August 2001) were presented previously (Cooley and Yager 2006). Winter data was free of plume influence (Cooley and Yager 2006). Atmospheric pCO_2 at Ragged Point, Barbados was obtained from NOAA CMDL (www.cmdl.noaa.gov/infodata/ftpdata.html) for flux calculations.

Data Analysis

Observational data

Following previous analyses (Cooley and Yager 2006; Lentz and Limeburner 1995; Geyer et al. 1996; Lentz 1995b), plume stations in the spring 2003 dataset were identified by their low surface salinities (< 35) and shallow haloclines overlying oceanic-salinity water. SML depths used to select the plume-influenced data were calculated from CTD profiles using a density gradient criterion ($\Delta\sigma/\Delta z > 0.01$, Brainerd and Gregg 1995). The critical value throughout the analysis for statistical significance was at least $\alpha = 0.05$, and mean values are presented with their standard error unless otherwise noted.

Fall '95 and Spring '96 TA reported by Ternon (2000) were calculated from DIC and pH using the UNESCO (1987) TA definition. To ensure consistency between datasets, Fall '95 and Spring '96 TA were recalculated from measured DIC and pH (Ternon et al. 2000) with CO2SYS (Lewis and Wallace 1998), using the Dickson (1981) TA definition, carbonate dissociation constants of Mehrbach et al. (1973), refit by Dickson and Millero (1987, valid for salinities 20-40), and the KSO_4 dissociation constant of Dickson (1990). As a result of this adjustment, Fall '95 and Spring '96 fCO_2s determined using recalculated TA and measured DIC in CO2SYS (Lewis and Wallace 1998, see below) were comparable to Ternon *et al.*'s measured fCO_2s (average difference = 0.8 ± 1.5 µatm, n=20).

Modeled Mainstem TA

TA at the river mouth from 1991-2003 was modeled to help test the conservative mixing hypothesis by predicting mainstem TA at an upstream river gauging station, and propagating this TA signal downstream to the river mouth. A multiple regression equation was developed to predict Manacapuru TA (1700 km inland, Figure 3.1) from 1982-1992 using daily discharge records from Manacapuru (Q_{Man}) and percent Andean discharge (%A, e.g., Devol et al. 1995, Figure 3.2A). Andean discharge to the Amazon has been defined as mainstem discharge at Sao Paulo de Olivenca (Q_{SPdO}, Devol et al. 1995; Quay et al. 1992; Richey et al. 1990), making %A = Q_{SPdO}/Q_{Man}. River discharge for 1968-2004 at Sao Paulo de Olivenca, Manacapuru, and Obidos (towns shown in Figure 3.1) were obtained from Hidroweb (http://hidroweb.ana.gov.br), the hydrologic information system maintained by the Brazilian National Water Agency (ANA). The computer program used to generate the regression equation ("R"; www.r-project.org) also provided the error associated with each coefficient using the least squares module, based on the S function of Chambers (1992) and the implementation of Wilkinson & Rogers (1973).

For the periods in 1991-2003 where Hidroweb records of Mancapuru discharge are not continuous (1991-1996, 2002-2003) but were required to predict mainstem TA, we estimated Q_{Man} as a fraction of Obidos discharge (Q_{Obi}). Obidos is the next major station downstream of Manacapuru, and its discharge records are continuous for 1969-2005. For each day that Manacapuru and Obidos discharge records overlapped (June 1972 - December 1984, January 1996 – December 2001), we calculated the ratio of Manacapuru discharge to Obidos discharge ($M = Q_{Man}/Q_{Obi}$). Mean M for each day of the year (M_{YD}) was calculated using all 17 years, and the missing data in the $Q_{Man,\ Hidroweb}$ record were filled with $Q_{Man,\ predicted} = M_{YD} * Q_{Obi}$. (A

randomly selected 75% of $Q_{Man,\ Hidroweb}$ data was used to calculate M_{YD}, and the remaining 25% of the $Q_{Man,\ Hidroweb}$ data was plotted against $Q_{Man,\ predicted}$ to check the accuracy of the prediction, Figure 3.2B.) Daily TA at Manacapuru (TA_{Man}) was then calculated for 1991-2003 using the newly continuous Q_{Man} and %A records in the multiple regression equation.

Amazon mainstem TA at the river mouth (Macapá) was modeled by diluting the Andean signal downstream. Mean monthly TA_{Man} and Q_{Man} for 1991-2003 were calculated from daily values, and monthly TA at Macapá was predicted by the equation: $TA_{Macapá} = TA_{Man} * Q_{Man}/Q_{Total}$. Q_{Total} is modeled monthly total Amazon discharge (see below). Monthly TA_{Man} from 1995-2004 was combined into a monthly climatology to show general seasonal variability. Error associated with discharge and calculated TA values was propagated throughout the dilution model with a Monte Carlo-type error analysis (see Yager et al. 1995).

Modeled Mainstem Discharge

Previous studies of Amazonian hydrology (e.g., Zeng 1999; Labat et al. 2004) indicate that the interannual and annual signals in precipitation dominate the river discharge data. To capture as much interannual variation as possible, total Amazon discharge to the tropical Atlantic Ocean was modeled by combining a seasonal discharge climatology (Dai and Trenberth 2002) with variability from integrated precipitation over the watershed. The Dai and Trenberth (2002) climatology is based on streamflow coupled to a runoff database to extrapolate from upstream stations to the river mouth. Two climatologies based on monthly precipitation databases (NASA GPCP V2 Combined Precipitation Data Set; (Huffman 1997), and the CPC Merged Analysis of Precipitation (CMAP, Xie and Arkin 1997) were used. Precipitation was lagged by three months and linearly correlated to the Dai and Trenberth climatology. Adjusted discharge was then

calculated with the precipitation climatology and the linear relationship. The resulting two linear models coupling the discharge and precipitation climatologies were applied to interannually varying precipitation data to estimate the interannual variability in the Amazon discharge at the river mouth (Q_{tot}).

For comparison, the Obidos gauge was projected to the river mouth using a linear regression against the Amazon river mouth climatology. Data from the Obidos gauging station obtained from SAGE Global River Discharge Database, which is based on data from the RivDis 1.1 database, the United States Geological Service, and the Brazilian National Department of Water and Electrical Energy, were used to validate the model. As above, linear models were also constructed based on the relation between interannually varying precipitation and Obidos data projected to the river mouth.

Biological DIC drawdown

Biological DIC drawdown was calculated for all plume-influenced datasets as previously described (Cooley and Yager 2006) to test the hypothesis of seasonally uniform biological activity. To avoid skewing the seasonal analysis, we only used data for the outer plume, with salinities between 28 and 35. Briefly, the proportions of river (*r*) and seawater (*s*) present in an individual sample were calculated using salinity as a conservative tracer. The model assumed that TA and DIC covary in the river mainstem, and TA supply to the river is conservative. We used *r*, *s*, TA of non-plume influenced sea water (TA_s), and the observed TA of a sample (TA_{obs}) to calculate the TA of the river endmember (TA_r) and compare it to the above-described discharge model prediction for $TA_{Macapá}$ for a given time period. The TA:DIC ratio in the mainstem (DICr = TA_r/0.82, Richey et al. 1991; Devol and Hedges 2001) was used to calculate

the DIC of riverwater (DIC_r); DIC_r, r, s, and seawater DIC (DIC_s) in a sample were then used to calculate expected DIC (DIC_{exp}). DIC_{exp} is the DIC value if conservative mixing were the only influence. The difference between DIC_{exp} and measured DIC (DIC_{obs}) was attributed to biological acitivity (ΔDIC_{bio}). Positive ΔDIC_{bio} values corresponded to inorganic carbon deficits caused by net production, and negative values indicated excess inorganic carbon due to net heterotrophy.

Seawater endmembers used in the mixing model were average values of pooled nonplume (S>35) SML samples from all cruises (Fall '95, Spring '96, Winter '01, Summer '01, Spring '03; S = 36.04 ± 0.22, TA = 2367.02 ± 18.10, DIC = 2014.24 ± 18.73; mean ± s.d., n=254). Error associated with calculated parameters was propagated throughout the mixing model with a Monte Carlo-type error analysis (see Yager et al. 1995).

pCO_2 and CO_2 flux estimates

In situ pCO_2 was calculated for Winter '01 and Summer '01 (Cooley and Yager 2006) from discrete surface values of DIC and TA using CO2SYS (Lewis and Wallace 1998). Measured pCO_2 from other seasons and years (this study, and Ternon et al. 2000) was used in the rest of the analysis. In addition, the pCO_2 expected if conservative river-ocean mixing were the only influence on the system (pCO_{2mix}) was calculated for plume-influenced datasets (Spring '96, Spring '03, Summer '01, Fall '95) using CO2SYS and measured temperature, salinity, nutrients, TA, and DIC_{exp} output from the conservative mixing model (Cooley and Yager 2006). Operator-chosen CO2SYS constants included: carbonate dissociation constants of Mehrbach *et al*., refit by Dickson and Millero (Mehrbach et al. 1973; Dickson and Millero 1987), valid for salinities 20-40), and the KSO_4 dissociation constant of Dickson (1990).

Inorganic carbon fluxes into the Amazon plume were calculated for in situ data, assuming it represents the combined effects of mixing plus biology (calculations used measured or calculated *in situ* pCO_2, hereafter pCO_{2obs}) and mixing-only (using pCO_{2mix}) conditions to assess biological enhancement of the sink over spring, summer and fall. Fluxes were calculated for each plume-influenced dataset using solubility (Weiss 1974), piston velocity (short term wind formulation of Wanninkhof and McGillis 1999), and the air-sea pCO_2 gradient (ΔpCO_{2mix} or ΔpCO_{2obs}; $\Delta pCO_2 = pCO_{2,atmosphere} - pCO_{2,sea}$). Atmospheric pCO_2 was assumed to be 370 µatm, near the average value (368.4 ± 2.3 µatm, n=10) of atmospheric values at Ragged Point, Barbados during the cruises. Windspeeds used to calculate piston velocity were obtained for January 1, 1995 – July 20, 1999 from Level 3.0 SSM/I derived global ocean surface winds (Atlas et al. 1996)(available at http://podaac.jpl.nasa.gov/products/product079.html) and for July 21, 1999 – December 31, 2005 from QuikSCAT Level 3 daily gridded ocean winds (JPL SeaWinds Project, available at http://podaac.jpl.nasa.gov/products/product109.html). Gridded winds were averaged over space (4-13 ºN, 40-60 ºW) (and over the 6h timestep of SSM/I data) to yield mean daily windspeeds for the study region. Climatological daily winds for the WTNA were then determined using all 1995-2005 data. Error associated with the average windspeeds was propagated through air-sea flux calculations and plume uptake estimates (described below) using a Monte Carlo-type error analysis (see Yager et al. 1995).

Parameters influencing the air-sea CO_2 flux (ΔDIC_{bio}, ΔpCO_{2obs}, ΔpCO_{2mix}, solubility, and climatological winds) and the air-sea CO_2 fluxes were compared between 4 plume-influenced cruises and 3 salinity groups ($28 \leq S < 30$, $30 \leq S < 32$, $32 \leq S < 35$) using an ANOVA or a nonparametric Kruskal-Wallis test for differences in location of ranked data (Sokal and Rohlf,

1995) when Bartlett's test for homogeneity of variances (Sokal and Rohlf, 1995) indicated that group variances were unequal.

Outer plume surface area was obtained from SeaWiFS satellite derived maps of diffuse attenuation coefficient at 490 nm (K_{490}) using a salinity-K_{490} relationship (Del Vecchio and Subramaniam 2004; Subramaniam et al. *in revision*). Briefly, monthly climatological binned 9-km level 3 data of K_{490} for the WTNA were extracted based on the relationship between *in situ* measurements of K_{490} and salinity described by Del Vecchio and Subramaniam (Del Vecchio and Subramaniam 2004): K_{490} = -0.021 (± 0.002) * salinity + 0.768 (±0.057), (mean ± s.d., r^2=0.93). This formulation is only valid for the salinity range of 28 to 35. The area covered by each salinity group (28<S<30, 30<S<32, 32<S<35) was calculated from the satellite data. This was then summed to provide the area over the range 28<S<35.

Monthly outer plume carbon uptake for both mixing plus biology (observed) and mixing-only (expected) conditions was then calculated by multiplying the monthly plume surface area (Table 3.2) by the mean daily flux (based on climatological winds) and by the number of days in the month. Because field observations in the plume were not available for all 12 months, annual uptake estimates assumed that fluxes are similar within seasons. Therefore, Spring '96 fluxes (calculated from data collected April 12 – May 16) were assumed to approximate January-April plume conditions (see Results for justification of this assumption), while the Spring '03 fluxes (data collected April 18 – May 22) represented May-June. The Summer '01 fluxes (data collected July 9 – August 19) were used for July-August, and the Fall '95 fluxes (data collected September 9 – October 11) we applied to September-December.

Results:

DIC, TA, and pCO_2 in the spring 2003 WTNA SML were similar to those in other plume-influenced seasons (Ternon et al. 2000; Cooley and Yager 2006). Regions of low salinity (Figure 3.1), DIC, TA, and pCO_2 (Figure 3.3) extended north and northwest of the Amazon mouth for all cruises. Minimum observed Spring '03 DIC and TA values at salinity 24.3 were 555 μmol kg^{-1} and 662 μmol kg^{-1}, respectively, below mean seawater values (Figure 3.4). Surface pCO_2 in the southwestern-most study area near shore fell as low as 201 μatm where salinity was lowest, and exhibited occasional lows in the moderate salinities of the mid- to northern portion of the study zone (Figures 3.1, 3.3). Spring '03 underway pCO_2 ranged from 201.3 - 402.1 (mean = 337.4 ± 0.41, n=10169) μatm, and underway sea surface salinity ranged from 21.9 – 36.4 (mean = 33.5 ± 0.03, n=10169). The Spring '03 underway sea surface temperature range was small, from 26.3 – 28.6°C (mean = 27.7 ± 0.004°C; Figure 3.9). Low-carbon, low-salinity regions moved between seasons, but the linear relationships between DIC or TA and salinity from $28<S<35$ were highly conserved ($r^2 = 0.827$ and 0.997, respectively, Figure 3.4, Ternon et al. 2000; Cooley and Yager 2006).

River discharge model

The best regressions between the discharge and precipitation climatologies ($r^2 = 0.94$ and 0.95 for GPCP and CMAP, respectively) were obtained with a 3 month lag between variables, consistent with the findings of Zeng (1999, Figure 3.5). The climatology constructed from Obidos gauge data (1979-1995) was correlated at r = 0.99 with the Dai and Trenberth climatology. The linear models coupling precipitation and discharge climatologies (CMAP and GPCP based) closely matched the projected discharge based on the Obidos river gauge alone.

The resultant discharge timeseries were correlated at r = 0.87 and 0.86 with the Obidos data at the river mouth between 1979 and 1995. Linear models were also constructed based on the relation between interannually varying precipitation and Obidos data projected to the river mouth. The differences were modest, with mean rms error (calculated between precipitation-based and Obidos-based discharge estimates) indistinguishable between data sets and methods (rms = 0.6 (11%)). These relatively high correlation coefficients and low errors suggested that the method reasonably captured the gross variability in the seasonal cycle associated with interannual weather and climate patterns. However, the model tended to have greater errors at high precipitation and maximum discharge, where there is more scatter in the relationship (Figure 3.5).

TA prediction model

Andean discharge peaks in May and declines through the summer to its minimum in September (Fig. 3.6A). The multiple regression equation relating TA at Manacapuru (TA_{Man}, Figure 3.6B) to discharge at Manacapuru (Q_{Man}) and the proportion of Andean discharge (%A) was: TA_{Man} = 224.6 (± 69.23) + 5.981 (± 0.8435) *% A - 1.161 x 10^{-3}(± 4.983 x 10^{-3})* Q_{Man} (± s.d., r^2 = 0.42)(Figure 3.2A). The correlation was significant at α=0.05, whereas relationships between TA and other chemical or hydrographic variables were not significant (Devol et al. 1995). For the 25% of the data set withheld, values for Manacapuru discharge predicted from Obidos discharge ($Q_{Man, pred}$) were not significantly different from observed ($Q_{Man, obs}$): $Q_{Man, pred}$ = 0.967 ± 0.033 ($Q_{Man, obs}$) + 2612.1 ± 3304.6 (r^2 = 0.9442, n=53; Figure 3.2B). As with Andean discharge, total river discharge (Fig 3.6C) also peaked in the late spring, but it showed a

minimum in November. Discharge predictions made using the two models, CMAP and GPCP, were not significantly different from each other.

Dilution-modeled average monthly TAs at the Amazon mouth (Macapá) were 303 ± 45 μmol kg^{-1} and 295 ± 61 μmol kg^{-1} (mean ± amplitude; Fig. 3.6D) depending on whether GPCP or CMAP data, respectively, were used to calculate Q_{tot}; modeled values were about half of Obidos maximum values (400-600 μmol kg^{-1}, Devol and Hedges 2001). The bimodal pattern of dilution-modeled Macapa TA (Figure 3.6D) was a product of the May river discharge peak (Figures 3.6A and C) and the sinusoidal Andean TA supply (maxima in March and December, Figure 3.6B, Devol et al. 1995).

Interannual variability in discharge caused some small interannual variability in TA predicted at Macapa. Andean discharge in 1991 and 1995 was significantly below the lower 95% confidence interval of the interannual average (Figure 3.6A), and total river discharge in those years was near or below the lower 95% confidence interval (Figure 3.6C). As a result, dilution-modeled alkalinity at Macapa (Figure 3.6D) for 1995 and 1991 were below the lower 95% confidence interval. In 1996, 2001, and 2002, Andean discharges were near the interannual average (Figure 3.6A), but 1996 and 2002 total discharges were above average (Figure 3.6C) and potentially diluted the Andean signal, lowering TA at Macapa to average or slightly below average levels (Figure 3.6D).

The dilution model does not completely capture all interannual variation, however. Dilution-modeled TA (average of values preceding cruise dates by one month, to permit time for river water to reach offshore sampling locations) plotted against mixing-modeled Macapa TA (or observed Macapa TA in 2002) does not lie exactly along the 1:1 line (Figure 3.7A), although the 95% confidence intervals of three datasets overlap the 1:1 line. The fit between offshore datasets

and dilution-modeled TA was improved by using dilution-modeled Macapa TA one month preceding the offshore data collection. Dilution-modeled TAs corresponding to the 1991 (Druffel et al. 2005) and 2002 hand samples were not lagged.

Although interannual variability is not completely described by the above approach, mixing-modeled average Macapa TA_r values (individual points with errorbars, Figure 3.7B) nicely overlapped with dilution-modeled, Macapá TA interannual average values (continuous lines, Figure 3.7B). Our single measured April '02 Macapá TA sample (440.71 ± 0.37 μmol kg^{-1}; ± s.d., n=2 at salinity 0.0 ± 0.0, n=3) was higher than predicted mean TAs (314.0 ± 45.7 μmol kg^{-1}, GPCP, and 353.5 ± 45.7 μmol kg^{-1} CMAP, ± s.d.) (Figure 3.7B). The Macapá DIC sample from November 1991 (363 μmol L^{-1}; (Druffel et al. 2005) agreed well (298 μmol kg^{-1}; Figure 3.7B) with dilution-modeled TA, however, after applying the TA = 0.82*DIC relationship (Devol et al. 1995; Devol and Hedges 2001).

Biological DIC drawdown

The observed variations in WTNA plume DIC that were not attributable to conservative mixing (ΔDIC_{bio})(Cooley and Yager 2006) averaged 26.1 ± 3.0 μmol C kg^{-1} for all seasons, with individual deficits as much as 109 μmol C kg^{-1} (Figure 3.8A). A Model I linear regression (Sokal and Rohlf 2000) of individual data plotted against sampling day of year indicates no significant increase in ΔDIC_{bio} with time ($r = 0.20$, n=76, $p=0.09$) although we did see a significant difference between cruises (Table 3.1; KW) due to the low values observed in Spring '96; the mean values for ΔDIC_{bio} during Spring '03, Summer '01, and Fall '95 were not significantly different ($p = 0.16$) although the distributions varied (KW $p = 0.05$). As in Summer '01 (Cooley and Yager 2006; Subramaniam et al. *in revision*), ΔDIC_{bio} was greatest in Spring '03

when *Richelia intracellularis/Hemiaulus hauckii* diatom-diazotroph associations (DDAs) were found; ΔDIC_{bio} in the plume correlated significantly with the integrated *Richelia* abundance ($r = 0.45$, $n = 26$, $p = 0.02$) at a given station (e.g., Subramaniam et al. *in revision*). Large ΔDIC_{bio} values in Fall '95 were found in the same general area and salinity range as those we found associated with diatom-diazotroph associations (Subramaniam et al. *in revision*) in Spring '03 and Summer '01, suggesting that DDAs may also have contributed to the large individual inorganic carbon deficits observed in Fall '95.

Plume uptake of CO_2

As with ΔDIC_{bio}, significant differences ($p<0.01$) were observed among cruises for solubility, observed and mixing-only ΔpCO_2, climatological winds, and the observed and mixing-only CO_2 fluxes (Table 3.1); but in the case of ΔpCO_{2obs} and the changes in the gradient ($\Delta\Delta pCO_{2bio}$, the difference between ΔpCO_{2obs} and ΔpCO_{2mix}) and the flux attributable to biology ($\Delta Flux_{bio}$, the difference between $Flux_{obs}$ and $Flux_{mix}$) this result was due to the very different Spring '96 dataset (see Fig. 3.8). Differences between Spring '03, Summer '01, and Fall '95 were not significant for ΔpCO_{2obs}, $\Delta\Delta pCO_{2bio}$, or $\Delta Flux_{bio}$ (Table 3.1). Significant differences were found among salinity groups for ΔpCO_{2mix}, and CO_2 $flux_{mix}$ only (Table 3.1), suggesting that the biological impact was not sensitive to salinity, at least for $28<S<35$. Because we detected few significant salinity-associated differences in most variables, mean values for each season are presented for the entire $28<S<35$ zone.

Solubility of CO_2 (Fig. 3.7B; Table 3.1) was higher in the Spring '03 than in Summer '01 or Fall '95 due to warming. Spring '03 solubility was also higher than Spring '96 solubility, which was collected during a period of anomalously warm sea surface temperatures related to

Pacific-Atlantic atmospheric connections (Illig et al. 2006). This meant that for a similar ΔDIC_{bio}, the ΔpCO_{2obs} was reduced later in the year. Values for ΔpCO_{2obs} dropped slightly between summer and fall (Figure 3.8C; Table 3.1).

Except for Spring '96, values for cruise-averaged ΔpCO_{2obs} were positive ($pCO_{2atm} > pCO_{2sea}$; Figure 3.8C) and favored plume uptake from the atmosphere. The air-sea pCO_2 gradient expected from mixing only (ΔpCO_{2mix}) was near zero or slightly positive (Figure 6C), favoring very little CO_2 uptake in the outer plume. Climatological winds were highly seasonal (Fig 3.8D) and dropped by about 20% between spring and summer.

Air-sea CO_2 fluxes calculated for observed conditions ($Flux_{obs}$, using ΔpCO_{2obs}, to which both mixing and biology contribute) were significantly higher than fluxes expected if mixing were the only influence ($Flux_{mix}$, calculated using ΔpCO_{2mix}) in Spring '03, Summer '01 and Fall '95 by 4-7 mmol m^{-2} d^{-1} (Figure 3.8D). Although the differences between observed and predicted CO_2 fluxes varied somewhat across seasons (with a maximum in Spring '03), the main difference was due to Sp96; neither $\Delta\Delta pCO_{2bio}$ or $Flux_{bio}$ differed significantly between Sp03, Su01, and F95 (Table 1, Fig 3.8C, 3.8E). Observed fluxes were generally into the plume (positive) within the 28<S<35 zone (Figure 3.10) and there was no salinity effect (Table 3.1) on either $Flux_{obs}$ or the difference between expected and observed fluxes. Only $Flux_{mix}$ varied significantly with salinity. Without significant seasonal change in biology, the seasonal change in observed flux could be attributed entirely to the decrease in solubility and wind speed between spring and fall.

Choosing which data to apply to each month for uptake estimates was guided by monthly climatological salinity contours shown in Figures 3.1 and 3.3. Spring '03, Summer '01, and Fall '95 salinities coincided well with April-November climatological salinities (Figure 3.1).

Although Spring '96 salinities do not exactly overlap monthly climatological salinities from December-March (Figure 3.1), we used Spring '96 data to represent this period because its low salinities east of the Amazon mouth correspond to conditions intermittently observed in February and March, when northerly winds impede along-shelf plume movement (this plume conditions in indicated in Figures 3.1A and 3.3A by dashed lines, as in Geyer et al. 1996). When summed over the entire plume area across all seasons, biological activity enhanced the Amazon outer plume CO_2 sink by nearly 100x (Table 3.2). If mixing were the only influence, the outer plume would take up 15 ± 163 Gmol C yr^{-1} (0.0002 ± 0.002 Pg yr^{-1}; mean ± s.d.); under observed conditions, however, the outer plume will take up 1245 ± 474 Gmol C yr^{-1} (0.015 ± 0.006 Pg C yr^{-1}; Table 3.2) for a difference of 15 Tg C y^{-1}.

Discussion

Our approach has focused on quantifying atmospheric carbon dioxide uptake by the Amazon River plume and identifying its potential for a perturbation response to anthropogenic change. Since the enhanced drawdown of inorganic carbon in the WTNA has been associated with diazotrophy (Cooley and Yager 2006; Subramaniam et al. *in revision*), we anticipated that enhanced gas exchange reflects true atmospheric drawdown associated with biological carbon sequestration (Eppley and Peterson 1979). Some of the biological material will be remineralized as it sinks into the deep ocean, adding carbon to watermasses that will be ventilated within 1000 years (the oceanic mixing time), and some will be buried resulting in sequestration for thousands of years. By investigating the sensitivity of the carbon sink to seasonal variation in either riverine supply or non-conservative processes within the plume, we aimed to quantify its potential sensitivity to projected meteorological and hydrological changes to the region.

Seasonality in riverine supply

Because dilution-modeled TA agreed well with mixing-modeled TA at Macapa (Figure 3.7B), we conclude that TA did travel conservatively from the mountains to the offshore plume, and that seasonal changes in plume TA were related to variations in either Andean or lower Amazon basin drainage, rather than nonconservative processing in the plume. Small differences between spring observed TA, mixing-modeled TA, and dilution-modeled TA (Figure 3.7B) were likely related to interannual variability in both Andean contributions (Figures 3.6A, B) and total Amazon River discharge (Figure 3.6C), although negative ions such as silicic acid or phosphate that behave nonconservatively in the early plume may have further contributed to the discrepancy between modeled and measured TA at the river mouth.

The conservative mixing model indicates that outer plume samples with $28<S<35$ contain only a small proportion of river water (average $r = 0.09 \pm 0.005$, n=76), however, seasonal changes in river TA and DIC would appear to cause only very small changes in outer plume distributions. Increasing river TA and DIC 3 standard deviations from the mixing-modeled mean, for example, would increase measured plume TA by an average of 2.9 ± 0.01% (n=76), and increase expected plume DIC by 4.2 ± 0.03%; these effects are small compared to biological processes within the plume (see below). We expect, however, that supply-driven DIC changes compete more evenly with plume biology to influence DIC in the nearshore plume ($S<28$), where the proportion of river water present is much higher.

Our calculations of the flux were sensitive, however, to our assumptions about DIC at the river mouth. In this study, we made the common assumption that the river delivers DIC to the plume in proportion with TA (Richey et al. 1991; Ternon et al. 2000; Cooley and Yager 2006).

Carbonate equilibria may shift when river and ocean water meet (Körtzinger 2003), changing the TA:DIC ratio in the low-salinity early plume, but the ratio is not likely to exceed 1 before salinity rises above zero. The closer the TA:DIC ratio of water supplying the plume is to 1, the lower its pCO_2. If we had used a ratio of 1, estimated mixing-only fluxes would be 151 ± 154% (n=76) greater, decreasing the mean difference between mixing-only and mixing + biology fluxes to 3.3 ± 0.5 mmol C m^{-2} d^{-1} (n=76) from the current 4.8 ± 0.5 mmol C m^{-2} d^{-1} (n=76), and subsequently decreasing our estimated annual biological enhancement of the Amazon plume carbon sink. If the supply ratio had been 1, however, DIC at the river mouth would have varied between 234-343 μmol kg^{-1}, below the published zero-salinity DIC value at Macapa (363 μmol L^{-1} in November 1991, Druffel et al. 2005). A ratio of DIC = TA/0.82 (Richey et al. 1991) would deliver between 286-418 μmol kg^{-1} DIC to the plume, with the Druffel *et al*. DIC value in the center of this range. This assumption is lower than endmembers used previously, but is greater than the DIC value at the river mouth based on published fluxes; the average DIC flux from the Amazon mouth ($72x10^8$ mol d^{-1}, Richey et al. 1990; Richey et al. 1991) divided by the average river discharge (218.4 km^3 d^{-1}, Dai and Trenberth 2002) yields a river-mouth value of 33 μmol kg^{-1}. Without more observational data from the early plume, it thus seems reasonable to assume the ratio was 0.82 and infer that 286-420 μmol kg^{-1} DIC was supplied to the plume through the year with an amplitude of 55-73 μmol kg^{-1}.

Seasonality in offshore processing

Inorganic carbon in the Amazon plume is influenced by both biological and physical processing, which vary enough in other estuarine and coastal systems to affect regional carbon source/sink status over time (Cai et al. 2003; Frankignoulle and Borges 2001; Thomas et al.

2004; Tsunogai et al. 1999). Seasonal variations in WTNA biological processes will affect the carbon sink by variably enhancing the air-sea gradient of pCO_2 initially created by mixing, while changes in physical processes will influence the mechanics of gas transfer by changing piston velocity, solubility, or the amount of time surface water spends in contact with the atmosphere.

Our measure of ΔDIC_{bio} at a given point in time reflects the instantaneous balance between biological drawdown and its replacement by physical processes (Cooley and Yager 2006). Primary production in the oligotrophic ocean can surpass (2-30 mmol C m^{-2} d^{-1}, Maranon et al. 2003) physical replacement by air-sea CO_2 exchange (0-10 mmol C m^{-2} d^{-1}, Figure 3.8E). Changes in ΔDIC_{bio} over time, though, could be the result of some combination of changing net community production and/or air-sea replacement. Conversely, no change in ΔDIC_{bio} over time likely reflects the net effect of seasonally steady air-sea CO_2 transfer and net community production. No change could also theoretically reflect balanced decreases in net community production and gas exchange, but the likelihood of these changes perfectly balancing each other seems low. Spring '03 total primary production rates from stations in the 28-35 salinity range (D. Capone, personal communication) tended to be somewhat (~15%) higher than in Summer '01 but were not significantly different (T-test; p=0.26). We have no primary production data from Fall '95 or Spring '96. Gas exchange rates slowed from spring to fall, but this effect seemed to be driven by physical processes and not biology. Thus, the only real biologically linked seasonality in inorganic carbon distributions we detected was related to the size of the plume (when scaling biologically influenced fluxes up to the seasonally changing surface area) and not the effect of biological activity on inorganic carbon per meter. Conditions favorable to diazotrophy and net community production must be linked to processes more complex than

season or salinity alone such as nutrient supply, regeneration, or biological community succession (Subramaniam et al. *in revision*).

Mixing additionally affects plume inorganic carbon processing primarily by altering air-sea pCO_2 gradients. The vertical flux of CO_2 into the plume from below was assumed to be zero, because the strong pycnocline separating the Amazon plume from the underlying ocean water discourages vertical mixing and attenuates most of the normal upward carbon flux (Cooley and Yager 2006; Pailler et al. 1999; Sprintall and Tomczak 1992)[3]. On the other hand, lateral mixing between river and ocean water dominates plume inorganic carbon distributions (Cooley and Yager 2006) and causes a seaward decrease in both air-sea pCO_2 gradients and fluxes. In general, the plume moves quickly (0.54 m s^{-1}) from the river mouth to the retroflection zone (6 ºN) and slows thereafter (0.12 m s^{-1}, Hellweger and Gordon 2002, and references therein), with additional plume speed changes due to seasonal winds and currents (Lentz 1995a). WTNA air-sea CO_2 transfer is slow overall and can lag biological production (Cooley and Yager 2006); the more quickly an individual water parcel travels from the Amazon mouth to the retroflection zone, the less time is available for replacing inorganic carbon deficits at an air-sea CO_2 flux rate comparable to the net community production rate. Therefore, faster plume speeds increase the likelihood that a biologically induced carbon deficit will outlast the plume's physical structure.

Implications of results on sink

Esimated DIC supply to the plume ($72x10^8$ mol d^{-1}, Richey et al. 1990; Richey et al. 1991) at an average discharge of 6,642 km^3 mo^{-1} (Dai and Trenberth 2002) yields a low value for early plume DIC (32 μmol kg^{-1}). To eliminate the plume-driven WTNA DIC deficit completely and reach nonplume seawater DIC levels (2017 μmol kg^{-1}, Cooley and Yager 2006) in 80 days of

[3] See chapter 4 for an exploration of this assumption.

travel from the Amazon mouth to the nonplume WTNA (Hellweger and Gordon 2002), a 10 m deep plume water must acquire 254 mmol m^{-2} d^{-1}. Part of the deficit is remediated by horizontal mixing and entrainment of nonplume water, which is an important mechanism for increasing plume salinity (and presumably DIC, Lentz 1995b). Air-sea CO_2 transfer into the plume is the other main mechanism replacing the inorganic carbon deficit in the plume. Outer plume air-sea CO_2 transfer (0-8 mmol m^{-2} d^{-1} on average, Figure 3.8E) provides up to about 5% of the carbon per day required to remediate the plume-related deficit. Until future studies can sample the biological/chemical system in the near-shore, low-salinity Amazon plume, outer plume studies will necessarily examine only a small portion of the Amazon-created inorganic carbon deficit.

Biological activity permits uptake of significantly non-zero quantities of atmospheric carbon by the offshore Amazon plume. Without enhanced CO_2 drawdown by net production, the outer 20% of the S = 0-35 mixing curve would take up only 15 ± 163 Gmol C yr^{-1} (0.0002 ± 0.002 Pg C yr^{-1}; Table 3.1), 0.1% of the 0.15 Pg C yr^{-1} tropical Atlantic carbon evasion (Takahashi et al. 2002). We estimate the 28<S<35 plume spanned a maximum surface area of 1.3 x 10^6 km^2, yielding a mixing-only flux of 0.03 mmol C m^{-2} d^{-1} into the plume. Under observed conditions that include positive net community production, the enhanced sink took up 1245 ± 474 Gmol C yr^{-1} (0.015 ± 0.006 Pg C yr^{-1}; Table 3.1), offsetting 10% of tropical CO_2 loss. This corresponds to an average flux of 2.63 mmol C m^{-2} d^{-1}, which is nearly double Körtzinger's estimate of 1.35 mmol C m^{-2} d^{-1} (0.014 Pg C yr^{-1} over 15<S<35 and 2x10^6 km^2, Körtzinger 2003). Our study area spanned a smaller portion of the river-ocean salinity gradient (28-35), and our flux estimates were greater. In contrast, the Körtzinger estimate did not appear particularly influenced by patchy changes in net community production; we believe sampling DDA-rich waters in Spring '03 and Summer '01 increased our mean flux estimates, given that

DDA production (averaging 93 mmol C m^{-2} d^{-1}, Carpenter et al. 1999) is several times greater than oligotrophic primary production (2-30 mmol C m^{-2} d^{-1}, Maranon et al. 2003). Because we generalize results from just a few cruises across many years, our uptake should be taken as a first order estimate only. Improving Amazon plume carbon uptake precision requires better quantification of biological effects with sampling that includes both irregular, patchy offshore blooms and inshore plume waters below S=28 where production and respiration rates are much higher.

Our modeled river endmembers seem to provide a more realistic view of the conditions at the river mouth than previous studies which used higher river endmembers (TA_r = 600 μmol kg^{-1} and DIC_r = 600-744 μmol kg^{-1}, Ternon et al. 2000; Körtzinger 2003) that set expected carbonate system mixing lines far above observed data. To account for the difference, large production-related DIC losses from the early plume (Ternon et al. 2000), possibly supplemented by carbonate equilibria shifts (Körtzinger 2003), were invoked. On the continental shelf, apparent DIC deficits of 200μmol kg^{-1} (almost twice the maximum ΔDIC_{bio} in the outer plume) can indeed be created with observed inner-plume transit speeds and primary production rates (Ternon et al. 2000). Off the shelf, however, we believe that changes in plume TA attributed to biological carbonate production/dissolution (Ternon et al. 2000) are unlikely, due to the low levels of coccolithophorids and foraminifera in the WTNA (Iglesias-Rodriguez et al. 2002; Aller and Aller 1986, and E.J. Carpenter, personal communication), but changes in DIC due to the balance of production/respiration continue to be quite likely (DeMaster and Pope 1996; DeMaster and Aller 2001). We assumed that plume TA was conservative because of its high correlation with salinity (e.g., Spring '03 samples from 28<S<35 were correlated at r^2 = 0.997). Therefore, our mixing model for the outer plume was designed only to diagnose nonconservative

variations of DIC. Our modeled value for average net community production (26 ±3 μmol kg^{-1}) over the outer 20% of the 0-36 salinity gradient is slightly higher than 20% of the DIC removal expected from phosphate depletion along the entire plume-ocean mixing gradient, which can remove at least 96 μmol kg^{-1} DIC (Körtzinger 2003). Thus, with our endmembers, the calculated enhanced fluxes due to biology are much more in line with what geochemists predict and biologists observe.

Interannual variability

Because these data were collected over multiple years, our analysis begins to uncover effects of interannual variability on WTNA inorganic carbon cycling. Spring '96 data was collected during an anomalously warm period (Illig et al. 2006), while Fall '95 data was collected during a slightly negative phase (El Niño) of the Southern Oscillation Index (SOI; http://www.cpc.noaa.gov/products/precip/CWlink/MJO/enso.shtml). The other datasets were collected during near-neutral periods.

Sea surface temperature conditions for the WTNA remained near normal for most of 1995 and early 1996 (Illig et al. 2006), likely resulting in normal moisture transport into the Amazon basin in the first months of 1996 (described in Marengo and Nobre 2001) and leading to near-average Amazon discharge and predicted TA in the Spring 1996 datasets (Figures 3.6, 3.7). However, the anomalously warm conditions acting during Spring '96 apparently influenced offshore processing (i.e., air-sea CO_2 transfer) of inorganic carbon by decreasing solubility and increasing windspeed variability (leading to more low-wind days in Spring '96 than in Spring '03, Figure 3.8). Without biological observations for Spring 1996, we cannot evaluate how well the mixing model's low ΔDIC_{bio} values correlate to observed, integrated phytoplankton

populations during that period as we can for Spring 2003 and Summer 2001. If the horizontal mixing model accurately describes all seasons, Spring 1996 also appeared to be a period during which biological enhancement of the sink was minimal. This could represent a period when plume respiration was greater relative to production, or when lower nutrient levels discouraged primary production.

A cooler, windier fall than that of 1995, such as those in La Niña years (Wang 2005), would increase total annual uptake by lowering plume pCO_2 and raising the air-sea transfer rate, promoting uptake for a longer period. Higher windspeeds may, however, encourage faster plume lateral mixing, reducing air-sea contact time and the air-sea CO_2 gradient, thereby countering some of the uptake due to a higher piston velocity. Drought in the Amazon basin as seen in 2005 (rain map, www.cpc.ncep.noaa.gov/products/precip/realtime/SA/annual.cycle.y2005.anom.gif) that may be linked to rising WTNA SST (e.g., Nobre and Shukla 1996) suggests that global warming could decrease the Amazon plume carbon sink by shrinking plume surface area and decreasing the air-sea CO_2 gradient via a temperature-driven pCO_{2sea} increase.

Because of the importance of processing in plume uptake behavior offshore, future climate-driven changes that affect biological activity, meteorological conditions, or plume size will most affect the WTNA carbon sink there. Unless the TA:DIC ratio changes significantly, changes in inorganic carbon supply will not likely change the sink; changes in river discharge or Amazon nutrient chemistry, however, may indirectly influence the offshore carbon sink through the biological community (Subramaniam et al. *in revision*). Enhanced blooms or export of macroscopic diazotrophs due to increases in nitrogen fixation, biogenic silica generation (Supplemental Document 2 in Subramaniam et al. *in revision*), or grazing will increase ΔDIC_{bio}.

However, such changes would increase plume CO_2 uptake only if they occurred early in the year, when prevailing meteorological conditions enable sink uptake. Spring 1996 conditions raise the possibility that other changes associated with interannual variability can decrease biological enhancement of the sink regardless of local meteorological conditions. The large number of variables affecting inorganic carbon processing in the WTNA makes quantifying specific climate change effects on the plume sink difficult at this point, because seasonality for many of those contributing factors has not been established.

Conclusion:

Although the WTNA is traditionally regarded as a CO_2 source to the atmosphere, biological activity in the Amazon plume permits uptake of an excess of 15 Tg C y^{-1} from the atmosphere due to a combination of biological and physical conditions. DIC and TA values supplied to the plume from the river mainstem are approximately 360 μmol kg^{-1} and 300 μmol kg^{-1}, respectively, and do not vary more than 75 μmol kg^{-1} seasonally. TA is a conservative tracer of Andean water all the way to the offshore plume. Assuming DIC is supplied in proportion to TA at the river mouth, nonconservative processes affecting plume DIC, and therefore plume pCO_2, can be studied. The small proportion of river water in offshore plume water means that typical variations in plume TA and DIC supply have a limited ability to influence plume TA and DIC. Biological production, primarily associated with diatom-diazotroph assemblages, enables the offshore plume to take up CO_2 throughout the year. The apparent biological enhancement of the plume carbon sink is steady throughout an annual cycle, but air-sea CO_2 fluxes are heavily governed by physical factors. As a result, fall conditions are not as conducive to carbon sequestration as those in spring and summer. Changes in

meteorological conditions later in the year that enhance plume uptake will have a greater impact on the sink than earlier in the year.

Acknowledgments:

This research was supported by the Office of Science (BER), U.S. Department of Energy, Grant No. DE-FG02-02ER63472, NOAA Office of Global Programs Grant NA16GP2689, and by faculty research support from the University of Georgia to P.L.Y. Financial support was provided to S.R.C. by the University of Georgia Presidential Graduate Fellowship and the NASA Earth System Science Fellowship. A.F. Michaels, D.G. Capone, and E.J. Carpenter graciously invited us into the MANTRA/PIRANA Biocomplexity Project. E.J. Carpenter, D.G. Capone, and M. Neumann shared data with us and provided excellent sampling access. S. Pluvinage assisted with sampling. C. M. Tilburg assisted with sample analysis. C. E. Tilburg provided technical assistance and guidance on the Lanczos data filter. F. le Hingrat at IFREMER made the ETAMBOT/SABORD datasets available. A. Körtzinger kindly provided the Meteor 55 data set.

References

Aller, J. Y. and R. C. Aller (1986). General characteristics of benthic faunas on the Amazon inner continental shelf with comparison to the shelf off the Changjiang River, East China Sea. *Continental Shelf Research 6*(1/2): 291-310.

Atlas, R., R. Hoffman, S. Bloom, J. Jusem and J. Ardizzone (1996). A Multi-Year Global Surface Wind Velocity Data Set Using SSM/I Wind Observations. *Bulletin of the American Meterological Society 77*(5): 869-882.

Bates, N. R., A. F. Michaels and A. H. Knap (1996). Seasonal and interannual variability of oceanic carbon dioxide species at the US JGOFS Bermuda Atlantic Time-series Study (BATS) site. *Deep-Sea Research Part II-Topical Studies in Oceanography 43*(2-3): 347-383.

Bates, N. R., T. Takahashi, D. W. Chipman and A. H. Knap (1998). Variability of pCO_2 on diel to seasonal timescales in the Sargasso Sea near Bermuda. *Journal of Geophysical Research 103*(C8): 15567-15585.

Brainerd, K. E. and M. C. Gregg (1995). Surface mixed and mixing layer depths. *Deep-Sea Research I 42*(9): 1521-1543.

Cai, W.-J., Z. A. Wang and Y. Wang (2003). The role of marsh-dominated heterotrophic continental margins in transport of CO_2 between the atmosphere, the land-sea interface and the ocean. *Geophysical Research Letters 30*(16): doi:10.1029/2003GL017633.

Carpenter, E. J., J. P. Montoya, J. Burns, M. R. Mulholland, A. Subramaniam and D. G. Capone (1999). Extensive bloom of a N_2-fixing diatom/cyanobacterial association in the tropical Atlantic Ocean. *Marine Ecology Progress Series 185*: 273-283.

Chambers, J. M. (1992). Linear Models. *Statistical Models in S*. J. M. Chambers and T. J. Hastie. Wadsworth and Brooks**:** Chapter 4.

Cooley, S. R. and P. L. Yager (2006). Physical and biological contributions to the western tropical North Atlantic Ocean carbon sink formed by the Amazon River plume. *Journal of Geophysical Research-Oceans (in press)*.

Dai, A. and K. E. Trenberth (2002). Estimates of Freshwater Discharge from Continents: Latitudinal and Seasonal Variations. *Journal of Hydrometeorology 3*: 660-687.

Del Vecchio, R. and A. Subramaniam (2004). Influence of the Amazon River on the surface optical properties of the Western Tropical North Atlantic Ocean. *Journal of Geophysical Research - Oceans 109*(C11): doi:10.1029/2004JC002503.

DeMaster, D. J. and R. C. Aller (2001). Biogeochemical Processes on the Amazon Shelf: Changes in Dissolved and Particulate Fluxes during River/Ocean Mixing. *The Biogeochemistry of the Amazon Basin*. M. E. McClain, R. L. Victoria and J. E. Richey. Oxford University Press**:** 328-357.

DeMaster, D. J. and R. H. Pope (1996). Nutrient Dynamics in Amazon Shelf Waters - Results from AMASSEDS. *Continental Shelf Research 16*(3): 263-289.

DeMaster, D. J., W. O. Smith, D. M. Nelson and J. Y. Aller (1996). Biogeochemical processes in Amazon shelf waters: chemical distributions and uptake rates of silicon, carbon and nitrogen. *Continental Shelf Research 16*(5-6): 617-643.

Devol, A. H., B. R. Forsberg, J. E. Richey and T. P. Pimentel (1995). Seasonal variation in chemical distributions in the Amazon (Solimões) River: a multiyear time series. *Global Biogeochemical Cycles 9*: 307-328.

Devol, A. H. and J. I. Hedges (2001). Organic Matter and Nutrients in the Mainstem Amazon River. *The Biogeochemistry of the Amazon Basin*. M. E. McClain, R. L. Victoria and J. E. Richey. Oxford University Press, New York**:** 275-306.

Devol, A. H., P. D. Quay, J. E. Richey and L. A. Martinelli (1987). The role of gas exchange in the inorganic carbon, oxygen, and ^{222}Rn budgets of the Amazon River. *Limnology and Oceanography 32*(1): 235-248.

Dickson, A. G. (1981). An exact definition of total alkalinity and a procedure for the estimation of alkalinity and total inorganic carbon from titration data. *Deep Sea Research Part I 28A*: 609-623.

Dickson, A. G., J. D. Afghan and G. C. Anderson (2003). Reference materials for oceanic CO_2 analysis: a method for the certification of total alkalinity. *Marine Chemistry 80*: 185-197.

Dickson, A. G. and F. J. Millero (1987). A comparison of the equilibrium constants for the dissociation of carbonic acid in seawater media. *Deep-Sea Research Part A-Oceanographic Research Papers 34*(10): 1733-1743.

DOE (1997). Handbook of methods for the analysis of the various parameters of the carbon dioxide system in sea water. A. G. Dickson and C. Goyet, eds., ORNL/CDIAC-74.

Druffel, E. R. M., J. E. Bauer and S. Griffin (2005). Input of particulate organic and dissolved inorganic carbon from the Amazon to the Atlantic Ocean. *Geochemistry Geophysics Geosystems 6*(3): doi: 10.1029/2004GC000842.

Duchon, C. E. (1979). Lanczos Filtering in One and Two Dimensions. *Journal of Applied Meteorology 18*: 1016-1022.

Edmond, J. M., E. A. Boyle, B. Grant and R. F. Stallard (1981). The chemical mass balance in the Amazon plume - I. The nutrients. *Deep-Sea Resarch 28A*(11): 1339-1374.

Eppley, R. W. and B. J. Peterson (1979). Particulate organic matter flux and planktonic new production in the deep ocean. *Nature 282*: 677-680.

Frankignoulle, M. and A. V. Borges (2001). European continental shelf as a significant sink for atmospheric carbon dioxide. *Global Biogeochemical Cycles 15*(3): 569-576.

Geyer, W. R., R. C. Beardsley, S. J. Lentz, J. Candela, R. Limeburner, W. E. Johns, B. M. Castro and I. D. Soares (1996). Physical oceanography of the Amazon shelf. *Continental Shelf Research 16*(5-6): 575-616.

Goyet, C., R. Adams and G. Eischeid (1998). Observations of the CO_2 system properties in the tropical Atlantic Ocean. *Marine Chemistry 60*(1-2): 49-61.

Goyet, C. and A. Poisson (1989). New determination of carbonic acid dissociation constants in seawater as a function of temperature and salinity. *Deep-Sea Resarch 36*(11): 1635-1654.

Grimm, A. M. (2003). The El Niño Impact on the Summer Monsoon in Brazil: Regional Processes versus Remote Influences. *Journal of Climate 16*: 263-280.

Hellweger, F. L. and A. L. Gordon (2002). Tracing Amazon River water into the Caribbean Sea. *Journal of Marine Research 60*(4): 537-549.

Huffman, G. J., ed. (1997). The Global Precipitation Climatology Project monthly mean precipitation data set. Geneva, Switzerland, WMO**:** 37pp.

Iglesias-Rodriguez, M. D., C. W. Brown, S. C. Doney, J. A. Kleypas, D. Kolber, Z. S. Kolber, P. K. Hayes and P. G. Falkowski (2002). Representing key phytoplankton functional groups in ocean carbon cycle models: Coccolithophorids. *Global Biogeochemical Cycles 16*(4): doi:10.1029/2001GB001454.

Illig, S., D. Gushschina, B. Dewitte, N. Ayoub and Y. du Penhoat (2006). The 1996 equatorial Atlantic warm event: Origin and mechanisms. *Geophysical Research Letters 33*: doi: 10.1029/2005GL025632.

Johnson, K. M., K. D. Wills, D. B. Butler, W. K. Johnson and C. S. Wong (1993). Coulometric total carbon-dioxide analysis for marine studies: Maximizing the performance of an automated gas extraction system and coulometric detector. *Marine Chemistry 44*: 167-187.

Kinkel, H., K.-H. Baumann and M. Cepek (2000). Coccolithophores in the equatorial Atlantic Ocean: response to seasonal and Late Quaternary surface water variability. *Marine Micropaleontology 39*: 87-112.

Körtzinger, A. (2003). A significant CO_2 sink in the tropical Atlantic Ocean associated with the Amazon River plume. *Geophysical Research Letters 30*(24): 2287-2290.

Labat, D., J. Ronchail, J. Callede, J. L. Guyot, E. De Oliveira and W. Guimaraes (2004). Wavelet analysis of Amazon hydrological regime variability. *Geophysical Research Letters 31*: doi:10.1029/2003GL018741.

Lee, K., F. J. Millero and R. Wanninkhof (1997). The carbon dioxide system in the Atlantic Ocean. *Journal of Geophysical Research 102*(C7): 15,693-15,707.

Lentz, S. J. (1995a). The Amazon river plume during AMASSEDS- subtidal current variability and the importance of wind forcing. *Journal of Geophysical Research-Oceans 100*(C2): 2377-2390.

Lentz, S. J. (1995b). Seasonal Variations in the Horizontal Structure of the Amazon Plume Inferred from Historical Hydrographic Data. *Journal of Geophysical Research-Oceans 100*(C2): 2391-2400.

Lentz, S. J. and R. Limeburner (1995). The Amazon River Plume During AMASSEDS - Spatial Characteristics and Salinity Variability. *Journal of Geophysical Research-Oceans 100*(C2): 2355-2375.

Lewis, E. and D. W. R. Wallace (1998). *Program developed for CO_2 System Calculations. Version 1.05.* ORNL/CDIAC-105. Carbon Dioxide Information Analysis Center, Oak Ridge National Laboratory, U.S. Department of Energy, Oak Ridge, Tennesee.

Maranon, E., M. J. Behrenfeld, N. González, B. Mouriño and M. V. Zubkov (2003). High variability of primary production in oligotrophic waters of the Atlantic Ocean: uncoupling from phytoplankton biomass and size structure. *Marine Ecology - Progress Series 257*: 1-11.

Marengo, J. A., B. Liebmann, V. E. Kousky, N. P. Filizola and I. C. Wainer (2001). Onset and End of the Rainy Season in the Brazilian Amazon Basin. *Journal of Climate 14*: 833-852.

Marengo, J. A. and C. A. Nobre (2001). General characteristics and variability of climate in the Amazon basin and its links to the global climate system. *The Biogeochemistry of the Amazon Basin*. C. R. McClain, R. L. Victoria and J. E. Richey. Oxford University Press**:** 17-41.

Mayorga, E., A. K. Aufdenkampe, C. A. Masiello, A. V. Krusche, J. I. Hedges, P. D. Quay, J. E. Richey and T. A. Brown (2005). Young organic matter as a source of carbon dioxide outgassing from Amazonian rivers. *Nature 436*: 538-541.

Mehrbach, C., C. H. Culberson, J. E. Hawley and R. M. Pytkowicz (1973). Measurement of apparent dissociation constants of carbonic acid in seawater at atmospheric pressure. *Limnology and Oceanography 18*(6): 897-907.

Millero, F. J., J.-Z. Zhang, K. Lee and D. M. Campbell (1993). Titration alkalinity of seawater. *Marine Chemistry 44*: 153-165.

Nobre, P. and J. Shukla (1996). Variations of Sea Surface Temperature, Wind Stress, and Rainfall over the Tropical Atlantic and South America. *Journal of Climate 9*: 2464-2479.

Pailler, K., B. Bourles and Y. Gouriou (1999). The barrier layer in the Western Tropical Atlantic Ocean. *Geophysical Research Letters 26*(14): 2069-2072.

Quay, P. D., B. Tilbrook and C. S. Wong (1992). Oceanic Uptake of Fossil Fuel CO_2: Carbon-13 Evidence. *Science 256*: 74-78.

Richey, J. E., J. I. Hedges, A. H. Devol, P. D. Quay, R. L. Victoria, L. A. Martinelli and B. R. Forsberg (1990). Biogeochemistry of carbon in the Amazon River. *Limnology and Oceanography 35*(2): 352-371.

Richey, J. E., J. M. Melack, A. K. Aufdenkampe, V. M. Ballester and L. L. Hess (2002). Outgassing from Amazonian rivers and wetlands as a large tropical source of atmospheric CO_2. *Nature 416*: 617-620.

Richey, J. E., R. L. Victoria, E. Salati and B. R. Forsberg (1991). The Biogeochemistry of a Major River System: The Amazon Case Study. *Biogeochemistry of Major World Rivers*. E. T. Degens, S. Kempe and J. E. Richey. John Wiley & Sons, New York. *42***:** 57-74.

Sarmiento, J. L., R. Murnane and C. LeQuere (1995). Air-Sea CO_2 Transfer and the Carbon Budget of the North- Atlantic. *Philosophical Transactions of the Royal Society of London Series B-Biological Sciences 348*(1324): 211-219.

Smith, W., O., Jr. and D. J. DeMaster (1996). Phytoplankton biomass and productivity in the Amazon River plume: correlation with seasonal river discharge. *Continental Shelf Research 16*(3): 291-319.

Sokal, R. R. and F. J. Rohlf (2000). *Biometry: The Principles and Practice of Statistics in Biological Research*. W.H. Freeman and Co., New York.

Sprintall, J. and M. Tomczak (1992). Evidence of the Barrier Layer in the Surface Layer of the Tropics. *Journal of Geophysical Research 97*(C5): 7305-7316.

Subramaniam, A., E. J. Carpenter, P. L. Yager, S. R. Cooley, R. Del Vecchio, D. Karl, C. Mahaffey, S. A. Sanudo-Wilhelmy, R. Shipe, A. Tovar-Sanchez and D. G. Capone (*in revision*). Amazon River amplifies C and N cycles in the Tropical North Atlantic Ocean.

Sweeney, C., D. A. Hansell, C. A. Carlson, L. Codispoti, L. I. Gordon, J. Marra, F. J. Millero, W. O. Smith and T. Takahashi (2000). Biogeochemical regimes, net community production and carbon export in the Ross Sea, Antarctica. *Deep Sea Research Part II 47*(15-16): 3369-3394.

Takahashi, T., R. A. Feely, R. F. Weiss, R. H. Wanninkhof, D. W. Chipman, S. C. Sutherland and T. T. Takahashi (1997). Global air-sea flux of CO_2: An estimate based on measurements of sea-air pCO_2 difference. *Proceedings of the National Academy of Sciences of the United States of America 94*(16): 8292-8299.

Takahashi, T., J. Olafsson, J. G. Goddard, D. Chipman and S. C. Sutherland (1993). Seasonal variation of CO_2 and nutrients in the high-latitude surface oceans: A comparative study. *Global Biogeochemical Cycles 7*(4): 843-878.

Takahashi, T., S. C. Sutherland, C. Sweeney, A. Poisson, N. Metzl, B. Tilbrook, N. R. Bates, R. Wanninkhof, R. A. Feely, C. L. Sabine, J. Olafsson and Y. Nojiri (2002). Global sea-air CO_2 flux based on climatological surface ocean pCO_2, and seasonal biological and temperature effects. *Deep-Sea Resarch II 49*: 1601-1622.

Ternon, J. F., C. Oudot, A. Dessier and D. Diverres (2000). A seasonal tropical sink for atmospheric CO_2 in the Atlantic Ocean: the role of the Amazon River discharge. *Marine Chemistry 68*: 183-201.

Thomas, H., Y. Bozec, K. Elkalay and H. J. W. de Baar (2004). Enhanced open ocean storage of CO_2 from shelf-sea pumping. *Science 304*: 1005-1008.

Tsunogai, S., S. Watanabe and T. Sato (1999). Is there a "continental shelf pump" for the absorption of atmospheric CO_2? *Tellus Series B-Chemical and Physical Meteorology 51*(3): 701-712.

UNESCO (1987). Thermodynamics of the carbon dioxide system in seawater. Report by the carbon dioxide sub-panel of the joint panel on oceanographic tables and standards. Technical papers in Marine Science, vol. 51. UNESCO.

Wang, C. (2005). ENSO, Atlantic climate variability, and the Walker and Hadley circulations. *The Hadley Circulation: Present, Past and Future*. H. F. Diaz and R. S. Bradley. Kluwer Academic Publishers, The Netherlands**:** 173–202.

Wanninkhof, R. and W. R. McGillis (1999). A cubic relationship between air-sea CO_2 exchange and wind speed. *Geophysical Research Letters 26*(13): 1889-1892.

Weiss, R. F. (1974). Carbon dioxide in water and seawater: The solubility of a nonideal gas. *Marine Chemistry 2*: 203-215.

Wilkinson, G. N. and C. E. Rogers (1973). Symbolic descriptions of factorial models for analysis of variance. *Applied Statistics 22*: 392-9.

Xie, P. P. and P. Arkin (1997). Global precipitation: a 17-year monthly analysis based on gauge observations, satellite estimates, and numerical model outputs. *Bulletin of the American Meterological Society 78*(11): 2539-2558.

Yager, P. L., D. W. R. Wallace, K. M. Johnson, W. O. J. Smith, P. J. Minnett and J. W. Deming (1995). The Northeast Water Polynya as an atmospheric CO_2 sink: A seasonal rectification hypothesis. *Journal of Geophysical Research 100*(C3): 4389-4398.

Zeng, N. (1999). Seasonal cycle and interannual variability in the Amazon hydrologic cycle. *Journal of Geophysical Research - Atmospheres 104*(D8): 9097-9106.

Table 3.1: Testing for differences in mean (ANOVA) or data distributions (Kruskal-Wallis; KW) between cruises or salinity groups (28-30, 30-32, 32-35) for parameters related to air-sea CO_2 transfer. Top part of table includes all four cruises. Bottom part of table tests for differences between Spring '03, Summer '01, and Fall '95 only.

	Cruise groups			Salinity groups		
	Variances	ANOVA P value	KW P value	Variances	ANOVA P value	KW P value
All data						
ΔDIC_{bio}	≠		**0.0004**[1]	=	0.9688	0.9231
Solubility	≠		**<0.0001**	=	0.8421	0.9062
ΔpCO_{2obs}	≠		**0.0005**	=	0.2377	0.0515
ΔpCO_{2mix}	=	**0.0263**	**0.0428**	=	**0.0002**	**0.0009**
$\Delta\Delta pCO_{2bio}$	≠		**0.0007**	≠		0.9540
Clim. winds	=	**<0.0001**	**<0.0001**	=	0.5611	0.7838
$Flux_{obs}$	≠		**0.0001**	=	0.8180	0.3212
$Flux_{mix}$	=	**0.0371**	0.0657	=	**0.0007**	**0.0038**
$\Delta Flux_{bio}$	≠		**0.0016**	≠		0.9098
Sp03, Su01, F95						
ΔDIC_{bio}	=	0.1580	0.0470	=	0.9720	0.9282
Solubility	≠		**<0.0001**	=	0.9140	0.9249
ΔpCO_{2obs}	=	0.3340	0.2598	=	0.4642	0.1212
ΔpCO_{2mix}	=	**0.0179**	**0.0315**	=	**0.0004**	**0.0012**
$\Delta\Delta pCO_{2bio}$	=	0.6651	0.4402	≠		0.9493
Clim. winds	=	**<0.0001**	**<0.0001**	=	0.6373	0.8644
$Flux_{obs}$	≠		**0.0119**	=	0.9398	0.6171
$Flux_{mix}$	=	**0.0394**	**0.0431**	=	**0.0010**	**0.0044**
$\Delta Flux_{bio}$	=	0.8310	0.2533	≠		0.6482

[1] Significant effects at the >95% confidence level are indicated in boldface.

Table 3.2: Plume surface area and mean monthly plume CO_2 uptake (± s.d.)

Month[2]	Surface area (km^2)	Uptake, mixing only (Gmol mo^{-1})	Uptake, mixing + biology (Gmol mo^{-1})
January	315900	-9.1 ± 22.5	-4.5 ± 22.8
February	320031	-8.3 ± 20.6	-4.2 ± 20.8
March	388152	-11.1 ± 27.7	-5.6 ± 28.0
April	745686	12.6 ± 49.1	176.8 ± 150.6
May	1096821	19.2 ± 74.6	268.7 ± 228.9
June	1330263	17.6 ± 65.0	207.8 ± 208.4
July	1337958	18.3 ± 67.6	216.0 ± 216.6
August	1265463	17.3 ± 63.9	204.3 ± 204.9
September	906633	-17.7 ± 50.0	99.6 ± 103.9
October	507384	-10.2 ± 28.9	57.6 ± 60.1
November	291033	-5.7 ± 16.1	32.0 ± 33.4
December	268434	-7.7 ± 19.1	-3.9 ± 19.4
Total (Gmol y^{-1})		15.2 ± 162.8	1244.5 ± 474.3

[2] December-March uptakes were calculated using Spring '96 fluxes; April-May uptakes used Spring '03 fluxes; June-August used Summer '01 fluxes; September-November used Fall '95 fluxes.

Figure 3.1: Sea surface salinity (practical salinity scale, unitless) for each dataset superimposed over monthly Amazon plume (S<35) areas derived from satellite data (see Methods for description of S=35 contours, and Results for grouping rationale). A) Spring 1996 data (Ternon et al., 1999) are marked with circles, and Winter 2001 data (Cooley and Yager, 2006) are marked with triangles. The dashed line in A indicates the possible location of the plume during periods of northerly winds (see Results). C) Fall 1995 data (Ternon et al., 1999) are marked with circles, and Fall 2002 (Körtzinger 2003) data are marked with triangles. Stations sampled during other cruises and upriver gauging stations discussed in the analysis are also plotted for reference.

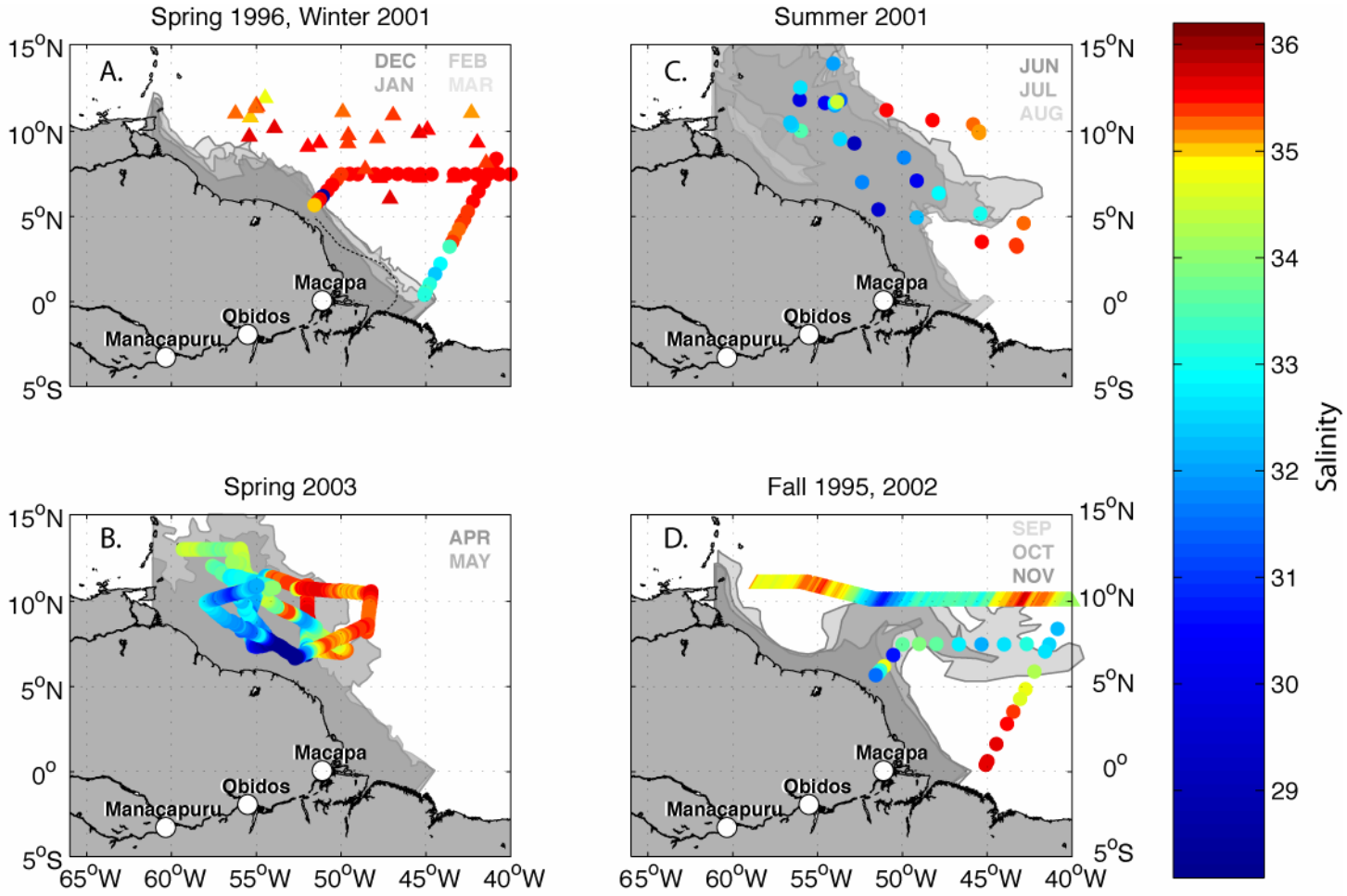

Figure 3.2 A) Predicted Manacapuru alkalinity is calculated using the multiple regression equation based on % Andean discharge and Manacapuru discharge (see Results). B) Modeled Manacapuru discharge vs. Manacapuru discharge from the Hidroweb database for a randomly selected 25% of the data, with the regression line. In both (A) and (B), The gray diagonals represent the 1:1 line.

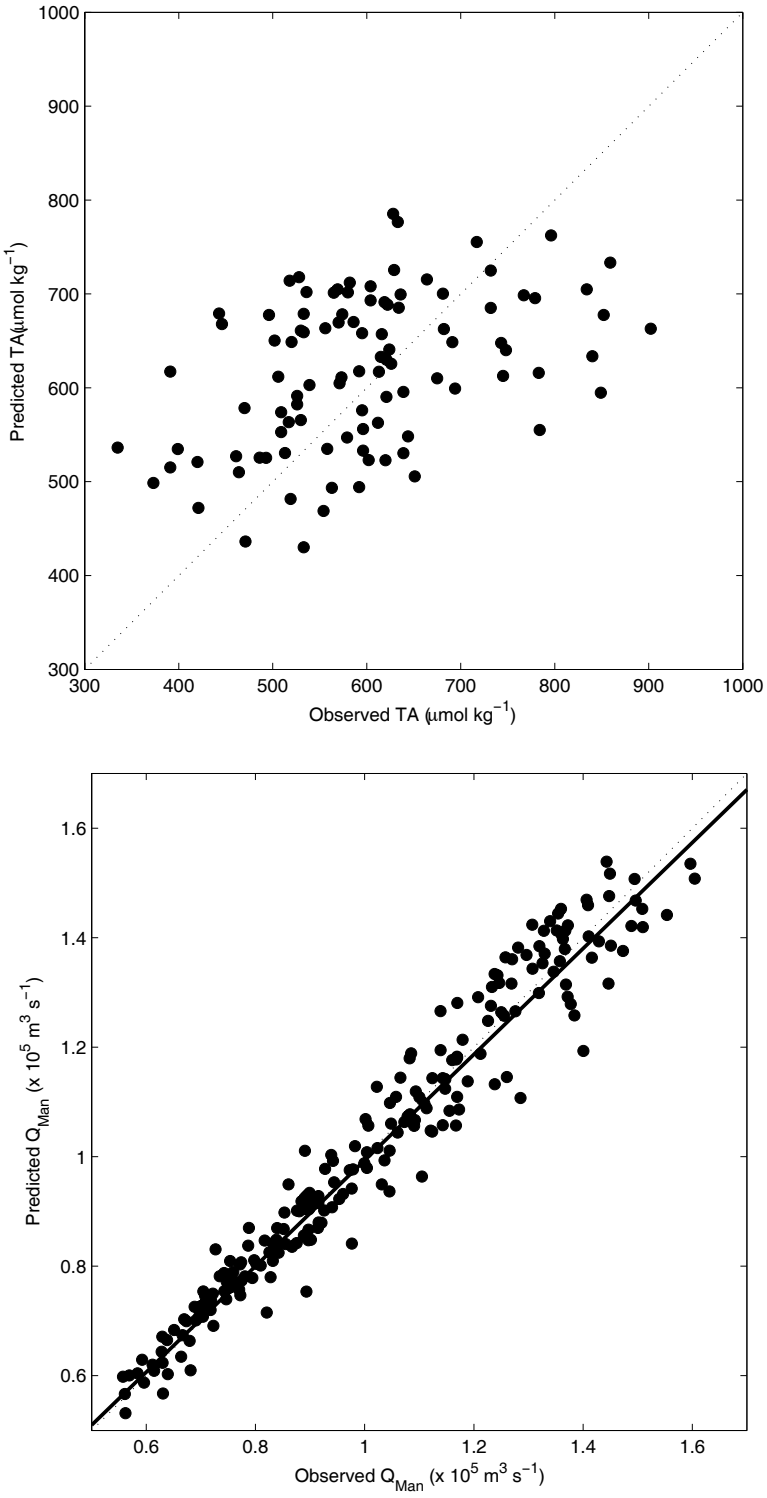

Figure 3.3: Sea surface pCO_2 (µatm) for each dataset superimposed over monthly Amazon plume (S<35) areas derived from satellite data (see Methods for description of S=35 contours, and Results for grouping rationale). A) Spring 1996 data (Ternon et al., 1999) are marked with circles, and Winter 2001 data (Cooley and Yager, 2006) are marked with triangles. The dashed line in A indicates the possible location of the plume during periods of northerly winds (see Results). C) Fall 1995 data (Ternon et al., 1999) are marked with circles, and Fall 2002 (Körtzinger 2003) data are marked with triangles. Stations sampled during other cruises and upriver gauging stations discussed in the analysis are also plotted for reference.

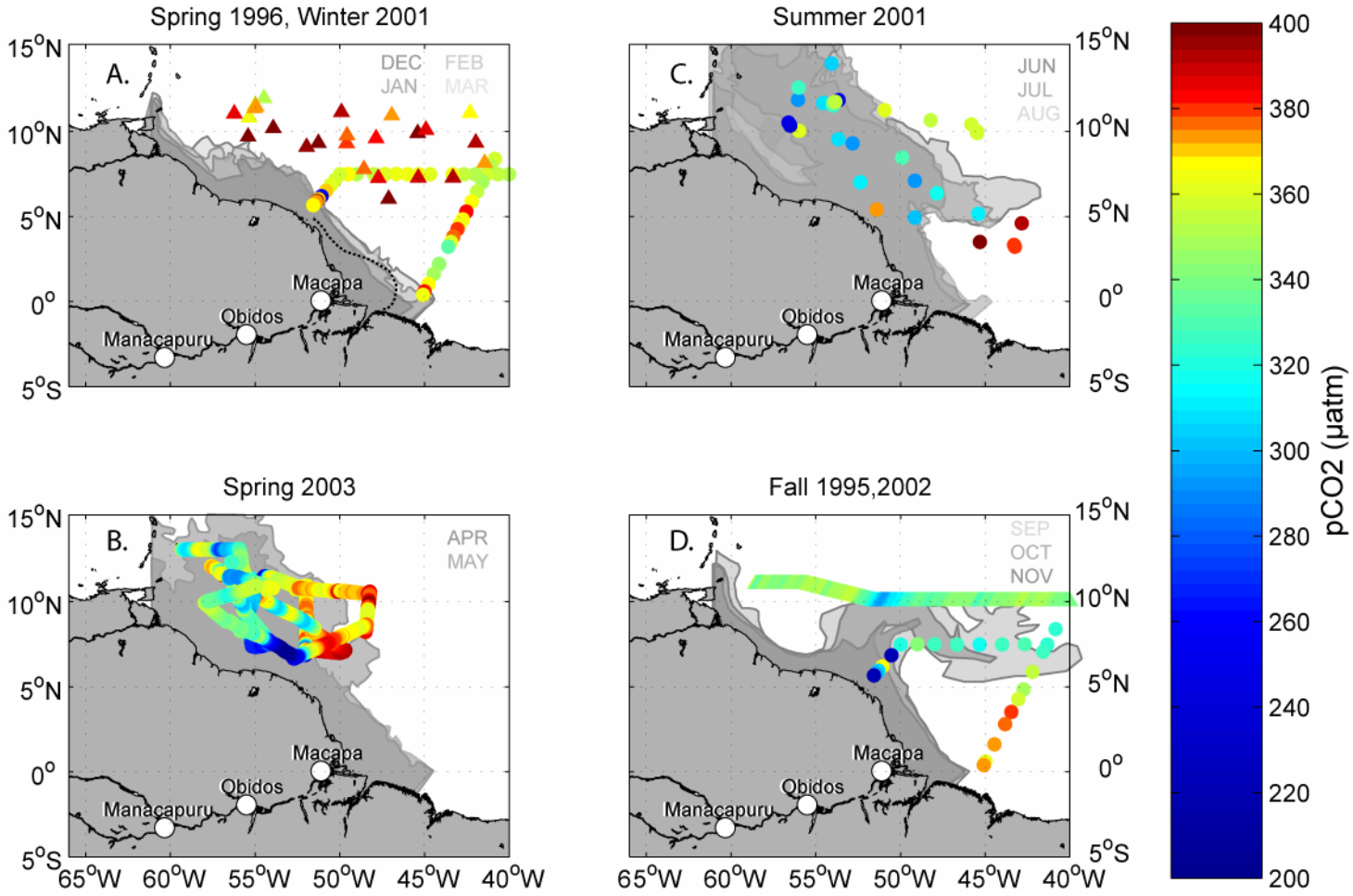

Figure 3.4: TA (filled symbols) and DIC (open symbols) plotted against salinity for all datasets. Boxed data was used in the analysis; oceanic samples had S>35, whereas only spring samples were collected below S=28.

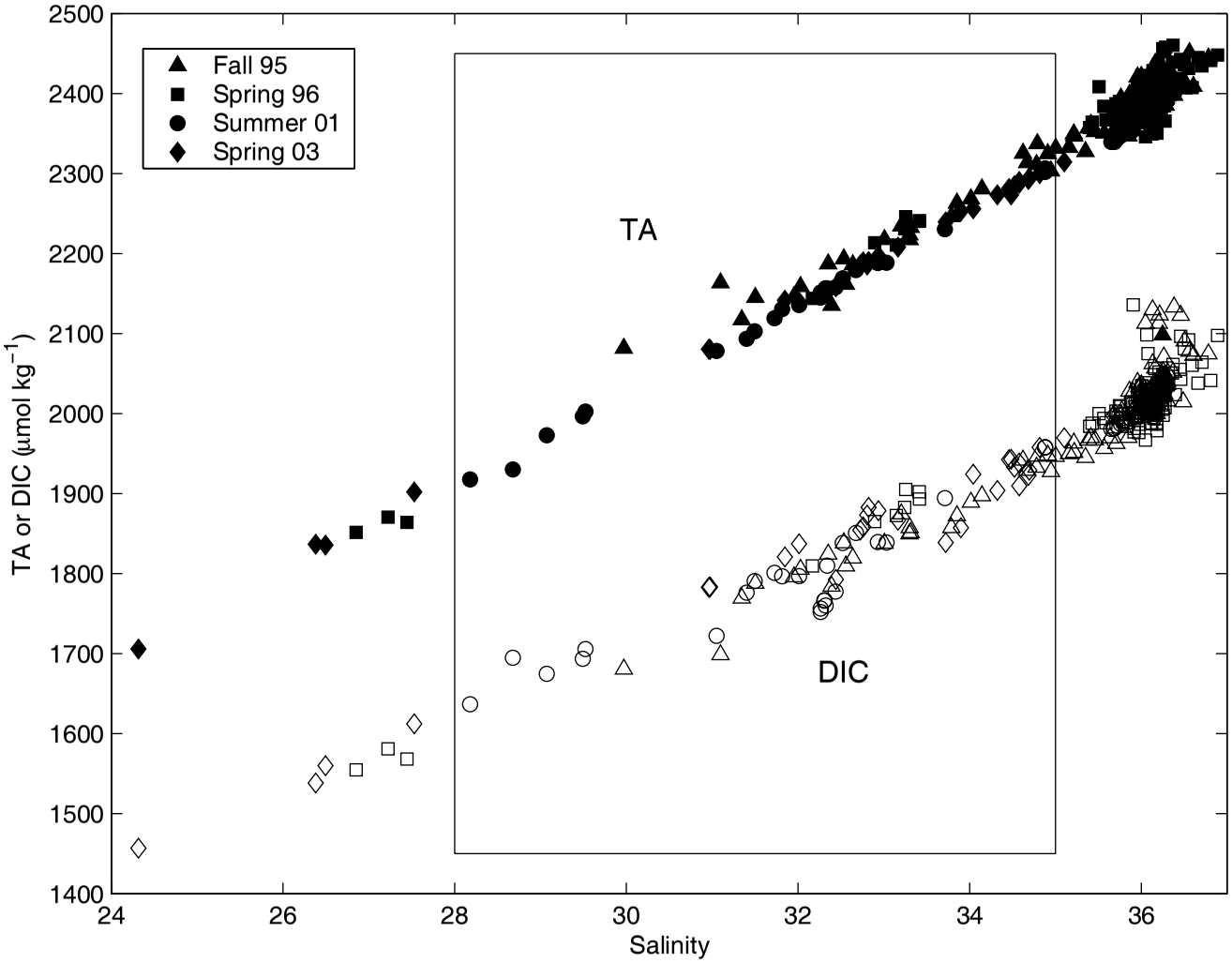

Figure 3.5: Amazon discharge climatology versus climatological precipitation, lagged three months. Triangles represent the CMAP precipitation dataset (dashed regression line), and squares represent the GPCP precipitation dataset (solid regression line).

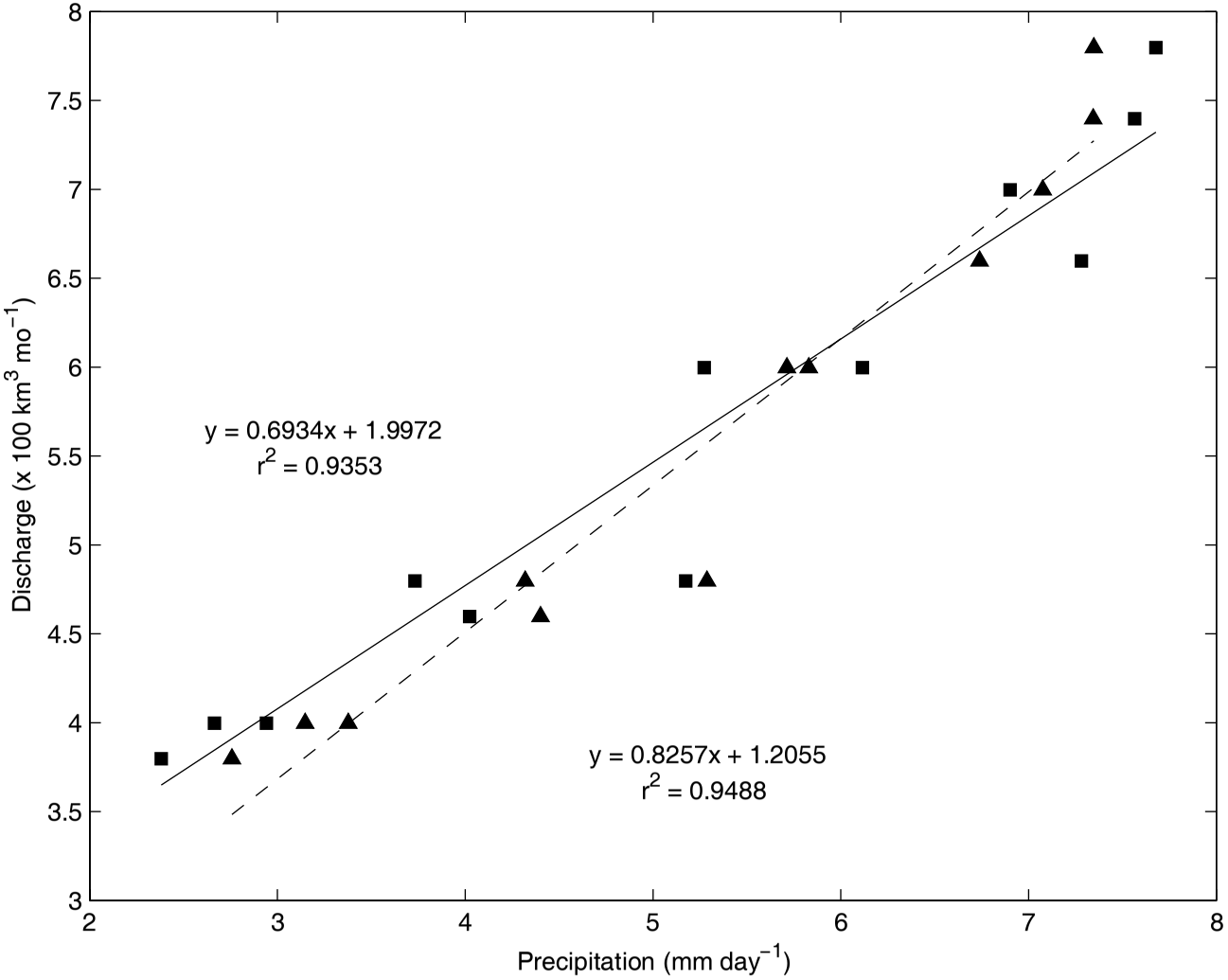

Figure 3.6: a) Monthly mean Andean discharge (m^3 s^{-1}; Sao Paulo de Olivenca) from Hidroweb. B) Measured Manacapuru TA, January 1983-November 1992, plotted over one year; adapted from Devol et al. (1995). C) Monthly modeled mean Amazon total discharge (m^3 s^{-1}) adjusted to include precipitation, using either the CMAP (black) or GPCP (gray) datasets. D). Modeled TA at Macapá (Amazon mouth) calculated using CMAP (black)- or GPCP (gray)- derived total discharge. Continuous lines plot interannual mean values, and dashed lines show 95% confidence intervals. Values for time periods discussed in the text plus one month prior are plotted in A, C, D using individual points.

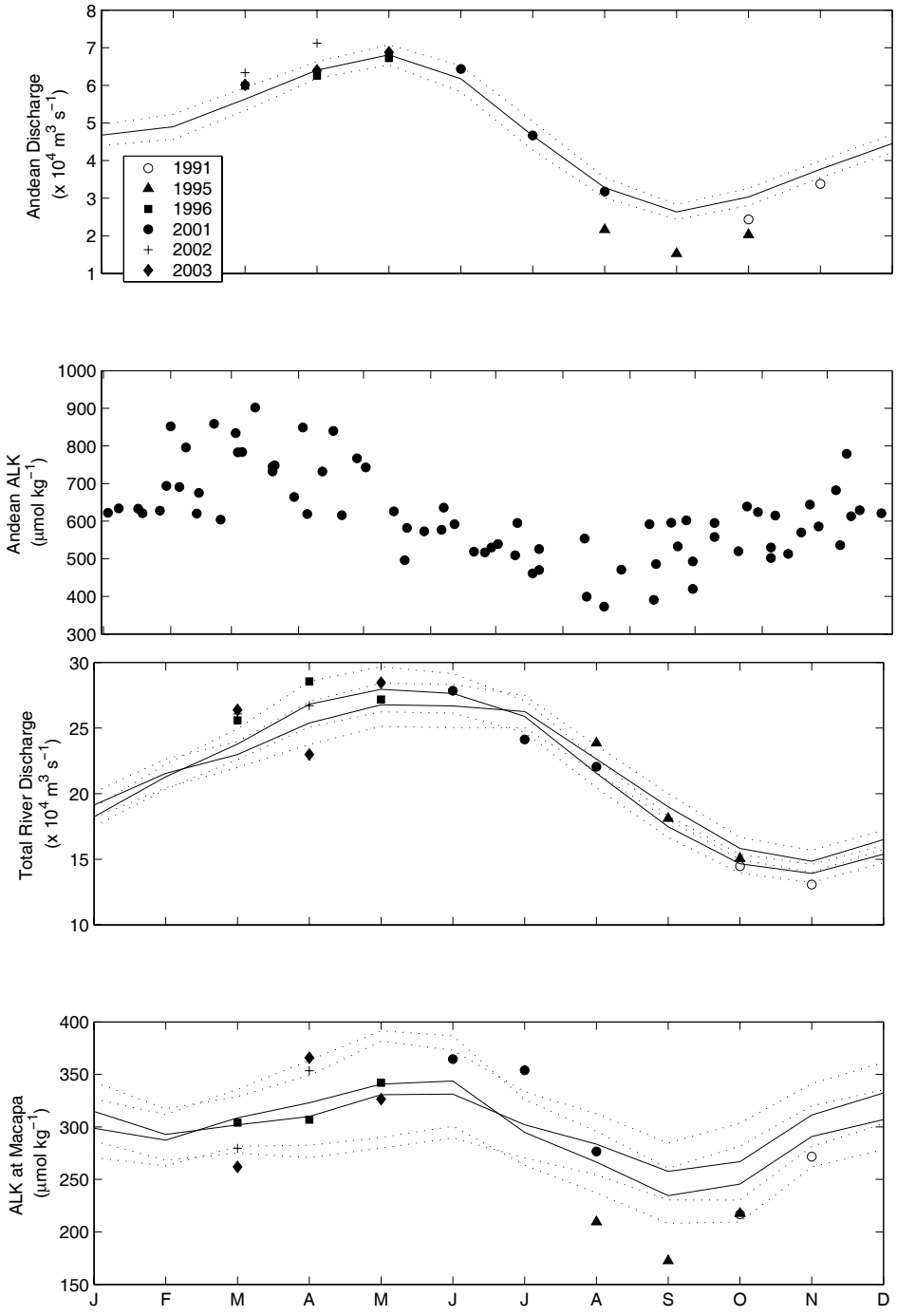

Figure 3.7. A) Dilution-modeled Macapa TA (using CMAP prediction) vs. mixing-modeled (or measured) TA. Dilution-modeled values are averages of the Macapa value one month prior to the cruise (if a cruise occurred in April-May 1996, the plotted value is the average for March-April 1996) to allow for plume movement offshore. Mixing-modeled TA is the average TA_r returned by the mixing model. Errorbars indicate 95% confidence intervals. The 1:1 line is indicated by the gray diagonal. B) Mean monthly TA at Macapa (solid lines), calculated using the multiple regression equation relating TA to discharge (adjusted with either CMAP, black, or GPCP, gray, precipitation climatologies). Individual points indicate mean mixing-modeled Macapa TA during each offshore cruise; vertical errorbars indicate 95% confidence intervals. Error bars for the 2002 hand sample are smaller than the marker. Horizontal bars indicate the length of the cruise. The open circle indicates the predicted November 1991 TA based on Druffel (2005) DIC (see Results).

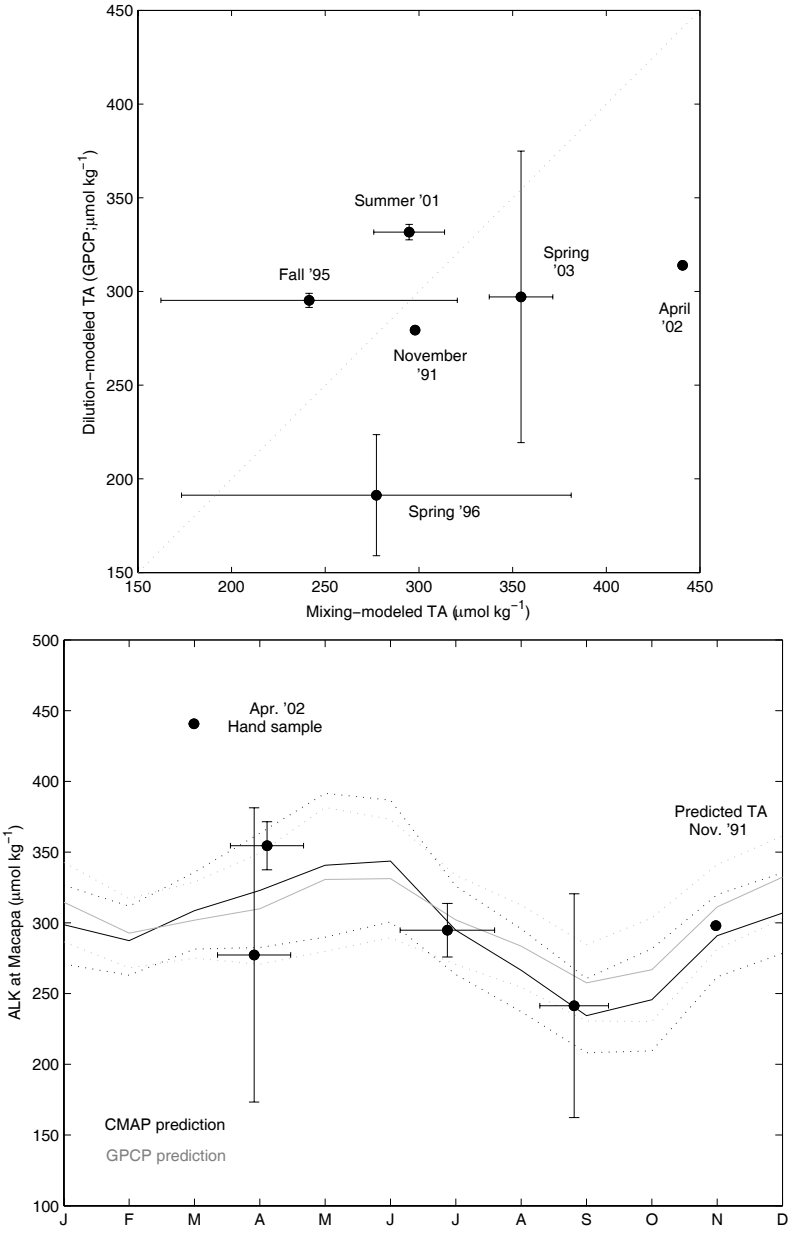

Figure 3.8: Data distributions (small points) and mean values (large black diamonds with 95% confidence intervals shown) for 28<S<35 surface mixed layer samples from the four cruises. A) ΔDIC_{bio} (µmol kg^{-1}); B) Solubility (mol L^{-1} atm^{-1}); C) Air-sea pCO_2 gradient ($pCO_{2atm} - pCO_{2sea}$), for both mixing-only (open) and observed/mixing plus biology (filled); D) Average windspeeds, calculated from WTNA wind climatologies (see Methods); E) Solved CO_2 flux rates for mixing-only (open symbols) or mixing plus biology/observed conditions (filled symbols). Positive fluxes indicate movement into the plume. B) C) Calculated CO_2 solubility for observational data at *in situ* temperature and salinity.

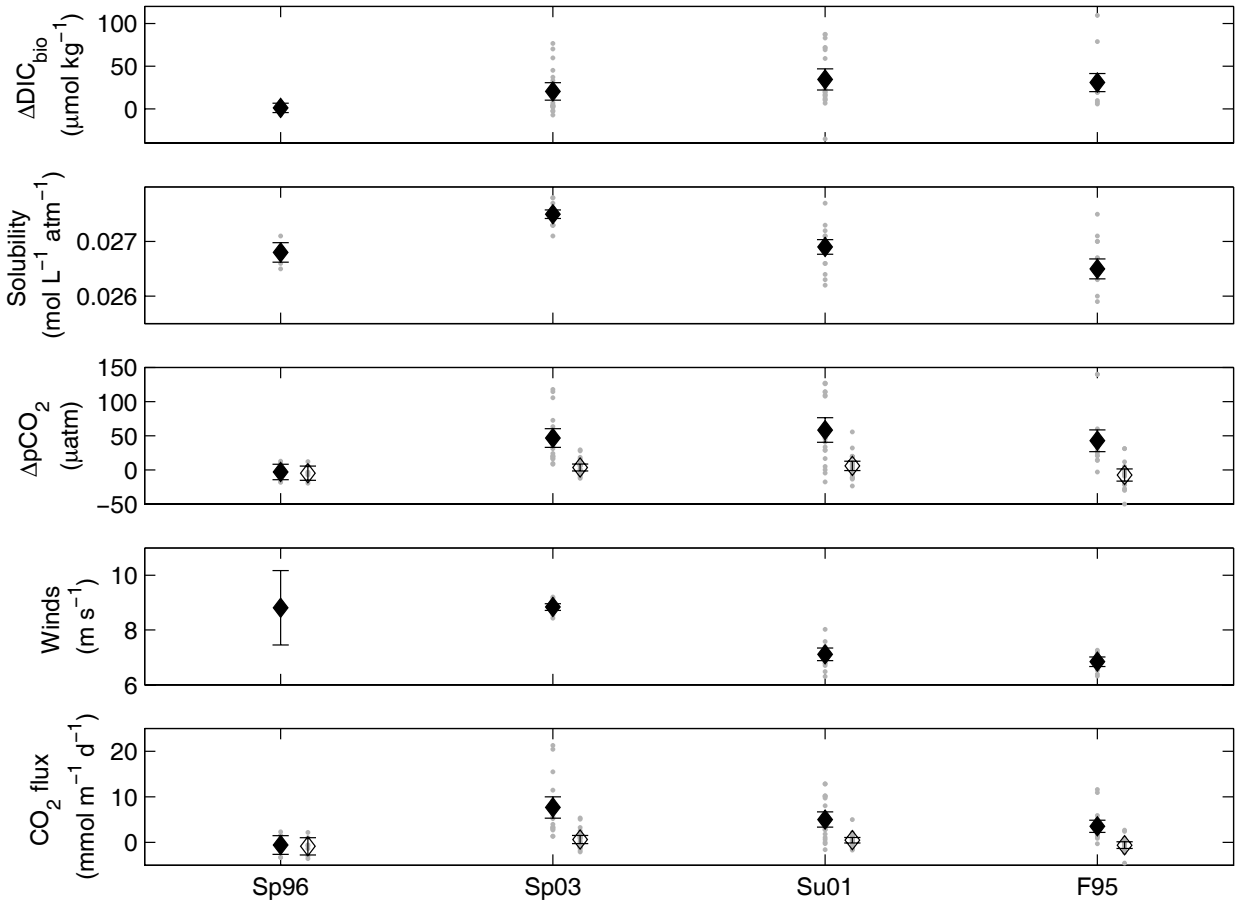

Figure 3.9: Underway salinity, temperature, and in situ pCO_2 for Spring 2003. Salinities above 35 (dashed line, middle panel) are considered oceanic samples; plume-influenced samples have salinities below 35. Atmospheric pCO_2 is 370 µatm (dashed line, bottom panel).

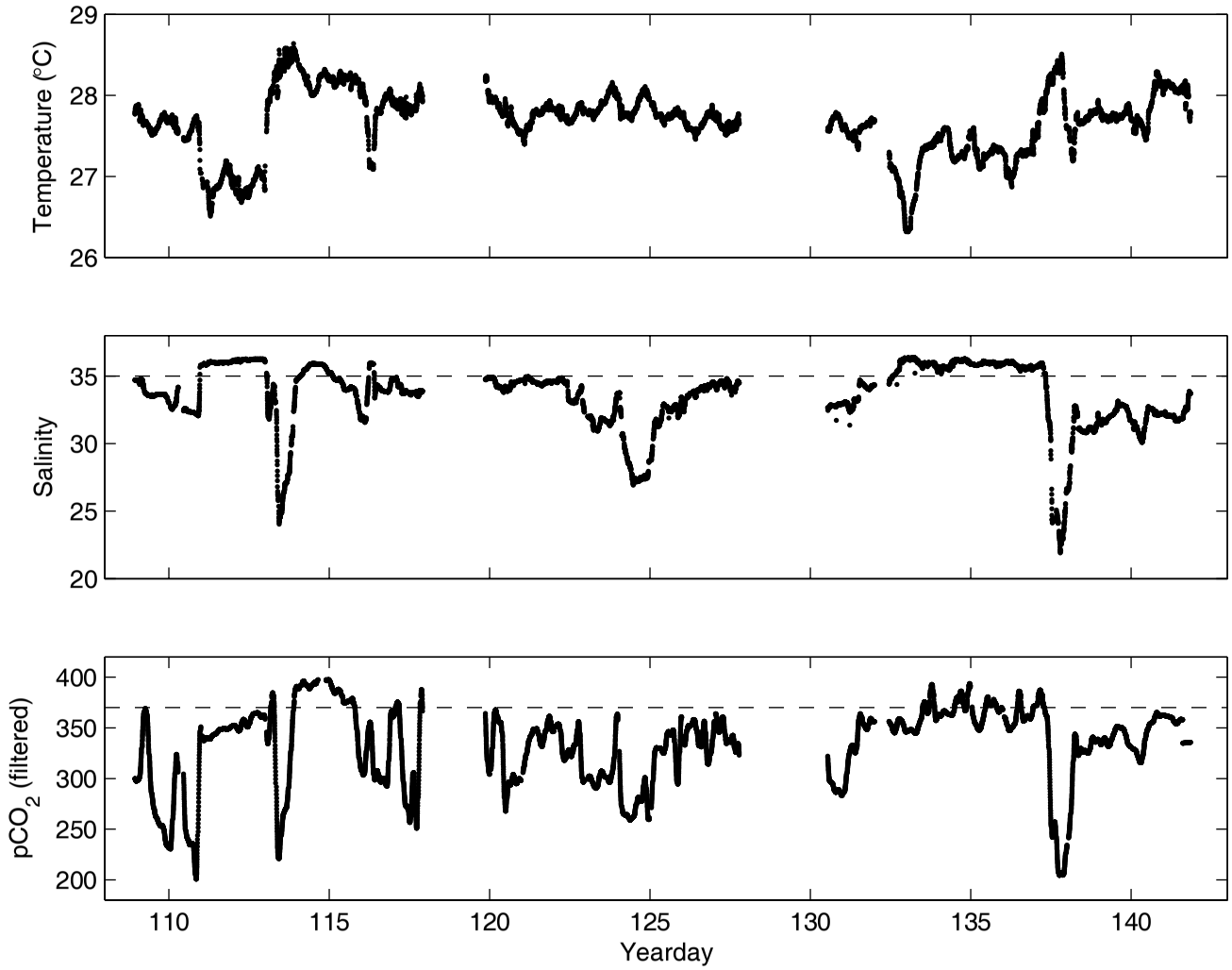

Figure 3.10: Calculated CO_2 flux rates for individual samples. Filled symbols indicate in situ (mixing + biology) values, and open symbols indicate mixing-only fluxes.

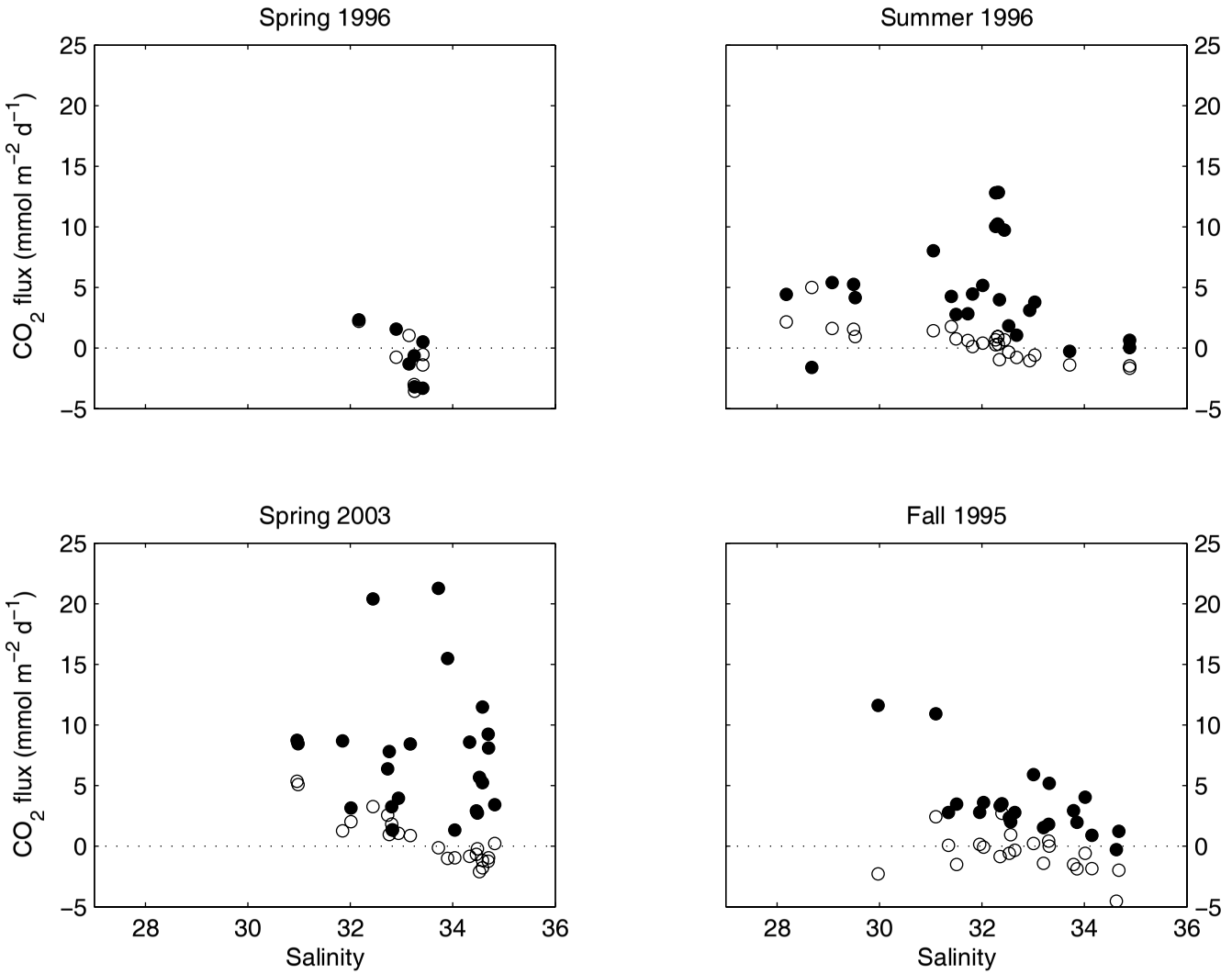

CHAPTER 4

RESIDUAL EFFECTS OF THE AMAZON PLUME ON WESTERN TROPICAL NORTH ATLANTIC INORGANIC CARBON CYCLING[1]

[1] Cooley, S.R., V. Coles, A. Burd, P.L. Yager. To be submitted to *Geophysical Research Letters*.

Abstract

The Amazon River plume reaches far into the Western Tropical Atlantic Ocean (WTNA) during boreal summer, and its low-salinity, low-carbon waters create an atmospheric CO_2 sink through a combination of mixing and net community production. Slow air-sea CO_2 exchange in the area may leave residual inorganic carbon deficits in plume water, created by either mixing or biology, that become even more difficult to replace when diluted over a deeper SML and the air-sea CO_2 flux becomes even weaker. In this study, we use both observed data and a vertical mixing model to quantify the breakdown of the plume structure, and determine that vertical fluxes of carbon into the plume are insufficient for replacing the plume-associated carbon deficit. Instead, horizontal advection must be invoked to return plume conditions to nonplume conditions in the timescales observed.

Introduction

The Amazon River releases 16% of worldwide river runoff to the Western Tropical North Atlantic (WTNA, Oltman 1968), creating a 5-10m deep lens (Lentz and Limeburner 1995) of low-salinity (S<35, Cooley and Yager 2006), low-inorganic-carbon water (Ternon et al. 2000) that covers two million square kilometers of the ocean (Körtzinger 2003). Net community production enhances the mixing-generated CO_2 undersaturation in the Amazon plume, and permits uptake of an estimated 0.015 Pg C yr^{-1} from the atmosphere (Cooley et al. 2006), which is 10% of the WTNA's usual solubility-driven CO_2 release (total tropical Atlantic efflux = 0.15 Pg C yr^{-1}, Takahashi et al. 2002; Sarmiento et al. 1995). Slow tropical air-sea exchange rates and small vertical fluxes hamper replacement of the plume-related deficit, which is eliminated either by these processes or by mixing. Just as large heat and salt fluxes must be quantified to describe ocean mixing accurately, the disappearance of the plume-associated inorganic carbon deficit must be understood to quantify basin-scale WTNA inorganic carbon cycling.

In the absence of the plume, vertical mixing deepens the winter mixed layer to ~80m (Cooley and Yager 2006) while stratified summer conditions hamper vertical mixing, and modeled mixed layer depths (15m, Cooley and Yager 2006) are near levels normally found at plume stations (5-15m, Lentz and Limeburner 1995; Cooley and Yager 2006). When summer winds (Lentz 1995; Lentz and Limeburner 1995; Geyer et al. 1996) and currents (Stramma and Schott 1999) spread the offshore plume north and east (as seen in the satellite images of Hochman et al. 1994; Muller-Karger et al. 1988; Muller-Karger et al. 1995), low-carbon river water directly mixes into the oligotrophic WTNA. Throughout most of the plume (0<S<30), lateral mixing dominates plume-ocean mixing because the strong halocline

between the plume and the ocean inhibits turbulent vertical mixing (Lentz and Limeburner 1995). The halocline weakens as plume salinity rises, and the plume thins (observed over 0<S<30, Lentz and Limeburner 1995). Beyond S=30, however, summer 2001 plume mixed layer depths did not decrease as salinity increased, and were not less than 4m (MANTRA/PIRANA Biocomplexity Project, unpublished data). Turbulent vertical mixing therefore seems to overcome plume stratification when the halocline is weak enough.

Salinity changes in the WTNA are expected to be especially important influences on vertical mixing due to the presence of a tropical isothermal barrier layer (Sprintall and Tomczak 1992), which prevents cooling from below of any shallow low-salinity layer present (caused by either precipitation or river discharge, Pailler et al. 1999). Lacking quantitative data on how mixing occurs between the plume edge and the ocean, we used a 1D model to quantify the contribution of vertical mixing to the breakdown of the plume. We initialized the model with starting conditions that represented nonplume conditions or plume conditions at discrete points along the outer edge of the plume-ocean horizontal mixing gradient. Initial conditions are based on Summer 2001 WTNA dissolved inorganic carbon, total alkalinity, salinity, and temperature data (Cooley and Yager 2006). Nonplume conditions do not significantly vary between seasons; natural variability in nonplume dissolved constituents is small and possibly related to sampling location (Cooley and Yager 2006). Therefore, nonplume stations south and east of the plume (Cooley and Yager 2006) in the North Brazil Current (Stramma and Schott 1999) were chosen as the control condition because significantly lower surface pCO_2 was observed at nonplume stations north and east of the plume (Cooley and Yager 2006), which may have been caused by mixing retroflected plume water with nonplume ocean water. Alternatively, a different watermass altogether

may have been present at northeastern nonplume stations. Initial runs examined the role of vertical mixing only on late-plume and nonplume conditions, and a relaxation term was added to the model in subsequent runs to simulate the effects of horizontal advection on plume water.

Methods

We created a series of synthetic plume profiles along the outer-plume mixing gradient, based on Summer 2001 (July 9 – August 19) WTNA dissolved inorganic carbon (DIC), total alkalinity (ALK), salinity, and temperature data from the MANTRA/PIRANA Biocomplexity project (available at http://cdiac.ornl.gov/oceans/RepeatSections/MP_cruises.html) (Cooley and Yager 2006). Winter 2001 and Spring 2003 data from the same project (Cooley and Yager 2006; Cooley et al. 2006) are included in results plots for context. Synthetic plume profiles contained regularly decreasing proportions of riverwater, which also decreased surface salinity, DIC, and TA. Actual plume profiles were not used because they were not collected evenly along the river-ocean gradient, and because net diazotroph-associated community production often lowered plume DIC nonconservatively (Subramaniam et al. *in revision;* Cooley and Yager 2006; Cooley et al. 2006). Synthetic profiles' surface mixed layer (SML) salinity, ALK, and DIC were calculated using:

$$C_r r + C_s s = C_{SML} \qquad (4.1)$$

where r and s are proportions of river and seawater in the sample (r: 10%, 7.5%, 5%, 2.5%, 0, s = 100 %- r), C_r and C_s are river and seawater endmembers of salinity, ALK, or DIC, and C_{SML} is the solved surface mixed layer value. River endmembers were calculated previously with a system of conservative mixing equations ($S_r = 0 \pm 0$, $ALK_r = 253.3 \pm 9.5$ μmol kg^{-1},

DIC_r = 308.8 ± 11.6 µmol kg^{-1}; n = 25)(Cooley and Yager 2006), and seawater endmembers were average surface mixed layer values for the summer southeastern nonplume station group (S_s = 36.0 ± 0.1, ALK_s = 2369.4 ± 5.9 µmol kg^{-1}, DIC_s = 2024.5 ± 6.8 µmol kg^{-1}; n=12)(Cooley and Yager 2006). Synthetic plume profiles were assumed to be homogenous to 10m, near the average plume mixed layer depth (MLD, 7.3m, Lentz and Limeburner 1995; 9.2 m, Cooley and Yager 2006), and DIC, ALK, and salinity values at 15m were interpolated linearly between the 10m value and the 20m oceanic endmember (Figure 4.2). In this paper, we refer to the surface mixed layer (SML) to indicate the homogenous surface layer bordered at its bottom by the mixed layer depth (MLD). Input profiles from 20-200m were composed of southeastern nonplume group averages interpolated linearly at 1m intervals; southeastern group salinity and alkalinity profiles were not significantly different from deep profiles of other groups. The overall average summer temperature profile (Figure 4.1D) was used throughout the analysis, as no significant differences were observed among the temperature profiles of different groupings of summer stations (e.g., plume/nonplume, nonplume southeastern/northeastern, etc.).

PWP Mixed layer model

Vertical inorganic carbon movement in the upper 200 m of the WTNA was simulated using a Price-Weller-Pinkel-type mixed layer model (PWP, Price et al. 1986) for Matlab v. 5.X by P. Lazarevich and S. Stoermer, URI (Version 1.4; http://www.po.gso.uri.edu/rafos/research/pwp/). Background vertical eddy diffusivity was set at 1 x 10^{-4} m^2 s^{-1} (Hood et al. 2001); depth increments were 1m, and total depth was 200m. The model timestep was 3600s (1 hour). The MLD criteria was $\Delta\sigma_t/\Delta z$ = 0.01 (Brainerd and Gregg 1995; Cooley and

Yager 2006; Cooley et al. 2006). DIC and ALK were added to the physical model as passive tracers whose controlling equations were based on those for salinity. Evaporation and precipitation concentrated or diluted DIC and ALK in the surface box only. Surface DIC was additionally influenced by air-sea CO_2 transfer (see below).

Surface pCO_2 was calculated from DIC and ALK at each timestep using the method of Lewis and Wallace (1998) with equations adapted from CO2SYS, Version 11 for Visual Basic, written by G. Pelletier, E. Lewis, and D. Wallace, (http://www.ecy.wa.gov/programs/eap/models/). Total concentrations of boron, fluorine, and sulfate were assumed to be proportional to salinity (Lewis and Wallace 1998, and references therein), and the following quantities were calculated using T, S, DIC, or ALK: CO_2 solubility (K_o, Weiss 1974); ionic strength (DOE 1997); the dissociation constant for sulfide, K_S (Dickson 1990a); fluoride, K_F (Dickson and Riley 1979); the free concentration of hydrogen ions, *f*H (Takahashi et al. 1982); the dissociation constants for borate, K_B (Dickson 1990b), water, K_w (Millero 1995), phosphate, K_{P1}, K_{P2}, K_{P3}, silicate, K_{Si} (Millero 1995); the dissociation constants for the carbonate system, K_1, K_2 (Dickson and Millero 1987; Dickson and Millero 1989); and the vapor pressure factor (Weiss and Price 1980). pH was then calculated from ALK and DIC using a Newton-Raphson solver (Lewis and Wallace 1998). Lastly, pCO_2 was calculated from DIC, pH, and the Mehrbach refit dissociation constants (Dickson and Millero 1987; Dickson and Millero 1989; DOE 1997).

The air-sea CO_2 flux was also calculated at each timestep using CO_2 solubility (K_o, Weiss 1974), total wind speed derived from wind stress (Yelland and Taylor 1996), piston velocity (short-term wind formulation, (Wanninkhof and McGillis 1999), and the air-sea

pCO_2 gradient ($pCO_{2,atmosphere} - pCO_{2,sea}$; $pCO_{2,\ atmosphere}$ = 370 µatm). DIC in the uppermost grid cell was adjusted with the modeled flux at the end of each time step.

The model was forced with monthly climatological heat, momentum, and freshwater fluxes from the Southampton Oceanography Center (SOC) Global Air-Sea Climatology (GASC97) dataset (Josey and Taylor 1999)(IRI-LDEO Climate Data Library, http://ingrid.ldeo.columbia.edu/), and short-wave radiation was scaled by a constant factor (0.85) so input conditions for the control run would return annually repeated modeled ocean temperatures and mixed layer depths. The model was initialized with synthetic profiles of DIC, ALK, temperature, and salinity described above (where r = 0% generated the mean nonplume southeastern profile). Runs began on yearday 195 (July 14), because starting profiles are based on July-August conditions, and were continued for 5 years (control) or 500 days (plume initial conditions).

After running the model for each input profile (R = 0-10%) to quantify the effects of vertical mixing on replacing the plume inorganic carbon deficit, we added a Newtonian relaxation term to simulate the contributions of horizontal mixing between plume water and the nonplume water surrounding it at any time t:

$$C_{t+1} = C_t + \Delta t\gamma(\hat{C}_t - C_t) \qquad (4.2)$$

where C was the value of an item at a given depth, C(hat) was the modeled nonplume value for the same depth and time (the "reference state" to which we relaxed), Δt was the model timestep, and γ was the relaxation factor (1/60 $days^{-1}$), chosen to approximate the expected transit time of water from the Amazon mouth to Barbados (57-80 d at speeds in Hellweger and Gordon 2002). The relaxation term, or the second term on the right hand side of the equation, was output from the model to track the dynamics of relaxation.

Changes in mixed layer carbon are due to the summed effects of the vertical mixing flux, air-sea exchange, the concentrating/diluting effects of evaporation and precipitation (Cooley and Yager 2006), and horizontal advection (Foltz et al. 2004). The effects of air-sea exchange and evaporation/precipitation on carbon and salt in the surface mixed layer were determined using the relaxation-free, vertical-mixing-only model to generate output for successive runs in which air-sea exchange was turned off, and then the effects of evaporation and precipitation on DIC and ALK were also eliminated. The difference in surface mixed layer carbon was then calculated between model outputs to evaluate the size of each process.

Results

Temperature profiles for Summer 2001 southeastern and northeastern groups were not significantly different, so (as mentioned in the Methods) average temperatures for all summer data were used to generate the mean profile (Figure 4.1D). The southeastern group of nonplume samples had salinity, DIC, and ALK similar to the nonplume groups of other cruises (Winter 2001 and Spring 2003), whereas the northeastern group of nonplume samples had slightly lower salinity, DIC, and TA than other groups (Figures 4.1A-C), which led to a significant difference at 40 m. The level of significance for all comparisons in this paper is α=0.05. These conditions resulted in mean northeastern surface pCO_2 (364.4 ± 1.9 μatm; n=6, mean ± s.e.) that was significantly below southeastern surface pCO_2 (388.6 ± 4.4 μatm, n=4)(Cooley and Yager 2006). Synthetic plume profiles were not significantly different from average observed plume profiles (Figure 4.2). Surface values of synthetic plume profiles represented the more oceanic end (32<S) of the observational gradient (Table 4.1), which spanned salinity 28-35 (Cooley and Yager 2006). At and below 50m, TA and salinity

of northeastern and southeastern nonplume profiles were not significantly different (Figures 4.1 A, C).

The model was initially run with the r = 0% input profile for five years to examine whether it returned to initial conditions. Model output produced repeating annual cycles for mixed layer depth (MLD), sea surface temperature (SST), sea surface salinity (SSS), surface DIC (sDIC), surface alkalinity (sALK), and surface pCO_2 (Figure 4.3 A-F). Modeled summer conditions were heavily stratified, with shallow summer MLDs (calculated every 12 hours over YD 210-244; July 29 – September 1 = 18.9 ± 0.2 m, n=67, mean ± s.e.; Figure 4.3A). The large summer heat surplus (where heat absorbed, Q_i, exceeded heat lost, Q_o, Figure 4.3H), low winds, and net summer precipitation (Figure 4.3H) maintained strong stratification; vertical mixing began when autumn winds increased and net evaporation became positive (Figure 4.3H, November), narrowing the heat imbalance ($Q_i - Q_o < 20$ W m^{-2}; Figure 4.3G).

Model runs initialized with plume profiles showed the importance of the salt balance in WTNA mixing. Plume initial conditions generated a highly stratified water column, starting with shallow MLDs. The nonplume profile began with a deeper calculated mixed layer depth at 75 m. Both plume and nonplume conditions experienced late summer mixed layer shoaling related to the late summer wind minimum and high temperatures, but after the onset of vertical mixing in late winter and spring, salinity-driven density changes modulated stratification: less salty initial plume conditions (10% r -2.5% r) resisted vertical mixing longer than nonplume conditions (0% r; Figure 4.4A). During mixed layer deepening, modeled sea surface temperatures diverged, with greater proportions of river water yielding lower sea surface temperatures. At the same time, surface pCO_2 at river-influenced stations

remained below nonplume pCO_2 (Figure 4.4C). Output for stations with higher proportions of river water appears to be more sensitive to precipitation; when precipitation peaks in November, pCO_2 (Figure 4.4 C; and the associated air-sea CO_2 flux, Figure 4.4 D) exhibits a local minimum (maximum). Vertical mixing and air-sea CO_2 exchange did not replace deficits after more than a year; at the end of the modeled period, SST, pCO_2, and the air-sea CO_2 flux for plume conditions never reached nonplume levels (Figure 4.4). Plume air-sea CO_2 effluxes were depressed relative to the nonplume rate after one year by up to 0.3 mmol m^{-2} d^{-1} (10% R condition, Figure 4.4C). The reduction in efflux was great enough for runs started with 7.5 % and 10% plume profiles that the net fluxes were into the plume for approximately half the year.

Below the surface, values of salinity, DIC, or ALK in the upper water column for nonplume analyses also remained greater than those initialized with plume conditions (positive values in difference plots, Figures 4.5-7). Difference plots only show the upper portion of the water column, as residuals below the nonplume MLD to 200m are not significantly different from zero. Three processes cause the observed distributions in Figures 4.5-7. First, mixed layer deepening through the fall and winter mixes the plume-associated carbon deficit over a greater volume and entrains subsurface water, with oceanic levels of carbon and salt; both processes reduce plume-associated carbon and salt deficits per unit of seawater. Meanwhile, nonplume surface mixed layer values of DIC, ALK and salinity are high throughout the year (initial conditions shown in Figures 4.1 A-C), causing predominantly small positive residuals in difference plots (Figures 4.5-4.7; nonplume minus plume conditions). Second, nonplume MLDs are deeper than plume MLDs for most of the year (September – July, Figure 4.4A). DIC, ALK, and salinity just below the shallow plume

ML remain at oceanic levels, whereas those depths are above the nonplume mixed layer and experience surface conditions. SML DIC, ALK and salinity values are lowered by the third process, net precipitation, which affects both plume and nonplume model runs. Precipitation-driven decreases in these constituents, however, are restricted to the SML (Figure 4.11B), and the MLD mismatches between plume and nonplume permit the precipitation-driven, SML-localized decreases in nonplume DIC, ALK, and salinity to be visible (negative values in the difference plots from October to March, between 10-80 m). By the end of a year, these differences have become homogeneous over the SML. When the mixed layer shoals (August), precipitation introduces small salt, carbon, and density changes in the water column from above (noise in upper right hand corner of each subplot, Figures 4.5-4.7) and the annual vertical mixing cycle begins again on a deficit that has not been completely eliminated.

Adding the relaxation term to the vertical model forced full recovery of deficits associated with the plume to enable us to evaluate the potential role of horizontal advection in the area. Modeled mixed layer depths in runs with relaxation recovered to nonplume conditions within 5-6 months due to the relaxation timescale selected (Figures 4.9-4.11). Sea surface temperatures showed the same tendency to diverge in relation to plume proportion (Figure 4.8B) as seen in the vertical mixing-only run, but the difference was recovered sooner in these runs by relaxation. Surface pCO_2 and the air-sea CO_2 flux took about 6 months to return completely to nonplume values (Figures 4.8B, C). The relaxation terms plotted in Figures 4.9-4.11 (second term in Equation 4.2) show the amount of carbon or salinity added at each timestep to regain nonplume conditions in 60 days. As expected, the relaxation term was greatest for salinity, DIC, and TA in the upper water column (0-15m) at

the start of the model run, at the times and depths where plume conditions were most different from nonplume conditions (Figures 4.5-4.7). Trailing threads of nonzero relaxation terms that follow mixed layer deepening in these plots are related to small differences in mixing between runs.

The magnitudes of processes acting on modeled water column DIC differ greatly. Air-sea exchange removes DIC from the SML, causing a cumulative difference (loss) of up to 5 μmol kg^{-1} DIC after 1.5 years (Figure 4.12A; results from nonplume run without air-sea exchange minus results from full nonplume run). In contrast, net fall precipitation, peaking in November, alters (reduces) DIC by 0-30 μmol kg^{-1} (positive values in Figure 4.11B; results from nonplume run without air-sea exchange or evaporation/precipitation minus results from nonplume run without air-sea exchange). Subsequent net evaporation removes the precipitation-added freshwater and then concentrates DIC (negative values) in spring by up to 5 μmol kg (Figure 4.11B). Lastly, the relaxation term calculated to bring even the 5% river water initial condition to the nonplume conditions is the largest of the three processes, adding up to 80 μmol kg^{-1} (Figure 4.11C).

Discussion

Modeled surface mixed layer characteristics for the southeastern nonplume profile, or control (r = 0%) conditions, replicated observed conditions well. Like WTNA pCO_2, whose average at southeastern nonplume stations was 388.6 ± 4.4 μatm (n=4, mean ± s.e.)(Cooley and Yager 2006), modeled pCO_2 remains oversaturated year round (Cooley and Yager 2006; Cooley et al. 2006; Körtzinger 2003; Ternon et al. 2000; Takahashi et al. 2002). Other modeled surface conditions throughout the year span observed conditions in nonplume water

(mean nonplume SST = 26.13 ± 0.08 ºC, SSS = 36.05 ± 0.02, DIC = 2017.2 ± 1.5 μmol kg^{-1}, TA=2365.7 ± 1.2 μmol kg^{-1}, n=123) (Cooley and Yager 2006), and seasonal variations are small. The slight decrease in pCO_2 towards the end of the model run is due to the gradual change in the DIC/ALK ratio caused by air-sea DIC efflux without an accompanying change in ALK. For simplicity, we did not explicitly parameterize re-equilibration between DIC and ALK, assuming instead that the nonconservative changes in DIC were negligible in changing the DIC:ALK ratio over one year, our time period of interest. The assumption appears to be valid, as the consequences of this assumption are barely visible at the end of a five-year run.

Modeled mixed layer depth was calculated using $\Delta\sigma/\Delta z = 0.01$ for consistency with the other observational portions of this project (Cooley et al. 2006; Cooley and Yager 2006). Modeled nonplume winter mixed layer depths (75.4 ± 0.4, n=58) were not significantly different from observed winter mixed layer depths (78.5 ± 4.5 m ; n=24, ± s.e.)(Cooley and Yager 2006), but summer nonplume modeled mixed layer depths tended to be shallower than those observed outside the plume (northeastern group 76.0 ± 10.6, n=4, southeastern group 54.3 ± 8.1, n=4, mean ± s.e.)(Cooley and Yager 2006) even when real-time meteorological data or daily climatologies (e.g., NCEP) were used to force the model (as in Cooley and Yager 2006).

Preliminary model runs in this study with the mixed layer depth threshold set at $\Delta\sigma/\Delta z = 1x10^{-4}$ generated an extremely noisy mixed layer depth whose values were approximately equal to as those generated with the higher threshold. The addition of fresh water by precipitation caused this instability; as fresh water mixed downwards, it created small density variations that exceeded the smaller mixed layer depth threshold and caused apparent oscillations in the mixed layer depth. The lack of change with depth in upper water

column temperature (Figure 4.1D), a common feature of tropical regions (Sprintall and Tomczak 1992), causes water column stability to depend greatly on small changes in salinity (Pailler et al. 1999). This sensitivity to freshwater can be seen in both the mixed layer oscillations and the annually repeated mixed layer shoaling; as late summer precipitation begins (Figure 4.12C; salinity appears essentially identical to this plot of DIC), the mixed layer depth shoals quickly (Figure 4.4A). Adding plume water to this already stratified summer system further discourages vertical mixing.

Vertical fluxes of carbon from below in this modeled system are small. An air-sea CO_2 loss of approximately 1 mmol C m^{-2} d^{-1} (Figure 4.4C) from nonplume water is sufficient to prevent a buildup of inorganic carbon in the SML; without horizontal advection or biological export, the air-sea loss from nonplume water indicates the approximate vertical flux of carbon from below. The vertical flux of carbon from below in plume-initialized conditions must be less than or equal to that of nonplume conditions, because the plume-initialized mixed layer deepen as much as in nonplume-initialized runs. Plume conditions therefore do not entrain deep subsurface water with DIC, TA, and salinity that are any higher than when the nonplume mixed layer deepens (i.e., water below 80m, Figure 4.1, A-C). Furthermore, the later onset of deep mixing lessens the time to acquire carbon and salt from below. Instead of somehow encouraging vertical movement of carbon by setting a low-carbon watermass atop a high-carbon watermass, the Amazon plume indeed inhibits vertical carbon and salinity movement.

Air-sea fluxes in the WTNA are also small (Figure 4.12A) and heavily governed by prevailing meterological conditions (Cooley et al. 2006), so the plume-associated carbon deficit is also not largely replaced by air-sea transfer. We added the relaxation term into the

model to show the potential role of horizontal advection for "replacing" carbon to the system. The relaxation term is not exactly like horizontal advection, because it assumes the system can provide an infinite amount of carbon, salt, or heat, and it occurs on an arbitrary time scale. As a result, introducing the relaxation term may decrease the magnitude of the modeled vertical flux from below or the air-sea CO_2 transfer flux by replacing the carbon or salt more quickly than the slower vertical processes would be able to.

In the real WTNA, horizontal advection of ocean water followed by mixing between the river and ocean cannot be an infinite source of carbon, salt, or heat, but horizontal advection and mixing of watermasses is expected to be very important in the WTNA salt and heat budgets. By the time the plume reaches salinity 30, it has entrained five time the river discharge as it moves off the shelf (Lentz 1995). Horizontal advection changes monthly in the tropical Atlantic, adding or removing up to half the salt in the mixed layer budget (Foltz et al. 2004). Finally, heat transport in a barrier layer region requires horizontal advection to remove excess heat, because it cannot be disspated to cooler subsurface waters below (Sprintall and Tomczak 1992); advection prevents runaway sea surface temperature increases (Sprintall and Tomczak 1992). One dimensional models, therefore, are more prone to extreme behavior that may be prevented by the inclusion of more types of mixing and advection in multidimensional models (Schudlich and Price 1992).

By parameterizing our three-dimensional system in one dimension, our model required some assumptions and adjustments that ultimately underscored the need for a more detailed treatment. Although previous PWP studies have scaled input fluxes to return a realistic model output (e.g., Christian 2005) and global heat fluxes are often out of balance (Josey and Taylor 1999), thus necessitating regional scaling. We scaled the SOC solar flux

by a constant factor (0.85) to prevent runaway heating of the water column, which is an expected result in situations without advection.

In the WTNA, plume waters can be identified by SST, which is on average a degree or two higher than nonplume water (Pailler et al. 1999, also see Table 2.1 and Figure 3.9 in this document). However, modeled sea surface temperature for plume waters was incorrect; plume waters with lower salinity and higher stratification developed lower SST than nonplume waters. The plume SST decrease appears related to the lower density of plume stations – the lower the density, the faster the heat gain or loss of the water. Because the low-density plume is stratified for longer in the model, it may be more sensitive decreasing solar shortwave radiation from September to November. The model used the same climatological heat loss fluxes for each input condition, the relationship between sea surface temperature and heat loss to the atmosphere was not included. A more accurate solution would be to adjust outgoing heat fluxes at every timestep to reflect modeled sea surface temperature. Future work with this model should also use the constrained SOC fluxes, in which several fluxes (not just the solar flux) have been scaled (Grist and Josey 2003).

This one-dimensional model was also likely influenced by our use of average meterological climatologies. Interpolating monthly data to the model's hourly timestep prevented us from modeling diurnal mixing, which was the original purpose of the model (Price et al. 1986), and it excluded short-timescale variations that could perturb the low-stability WTNA water column. For example, peak wind conditions are not usually well accounted for in climatologies or shipboard data because of their relative spatial and temporal rarity, and this causes modeled estimates to err on the conservative side (for example, see justification for using long-term wind formulation in CO_2 flux calculations,

Wanninkhof and McGillis 1999). Such isolated wind events could homogenize and deepen the mixed layer below where the model would place it using the climatological average inputs, and bring pulses of carbon up from below. Similarly, because WTNA mixed layer stability is so sensitive to salinity, isolated precipitation events could temporarily stratify the water column and cut off the vertical flux. Neither of these processes would be modeled with average climatological forcing.

Modeled vertical fluxes in the WTNA are not sufficient to replace even the smallest plume-related inorganic carbon deficits after one year, although the plume lasts only 60-80 days. Without horizontal mixing or advection, removing up to 1000L of fresh water from a 10m plume (the equivalent of 10% river water) in 60 days would take sustained net evaporation of 16 mm d^{-1}, four times as large as maximum in situ rates (0.05 mm s^{-1} = 4.3 mm d^{-1}; Figure 4.3H). Conversely, an unrealistically large precipitation event would be required to create the low-salinity signature (Hu et al. 2004).

Net primary production in the plume would further lower SML DIC and increase air-sea CO_2 fluxes (up to 5 mmol C m^{-2} d^{-1}, Cooley et al. 2006). The change in SML DIC due to the biologically enhanced air-sea CO_2 flux in the outer plume could be up to 25 μmol kg^{-1} after 1.5 years (5 times the change in Figure 4.12A, which was generated using a 1 mmol m^{-2} air-sea flux, Figure 4.4D). This would be a permanent enhancement of the air-sea flux that would be approximately the same magnitude as the cyclical effects on DIC of evaporation and precipitation. The change in DIC due to biologically enhanced air-sea exchange would still be smaller than the relaxation term (Figure 4.12C), so the safest interpretation of the potential role of biology on the breakdown of the plume is that the enhanced air-sea flux can increase DIC as much as net evaporation does. However, evaporation and precipitation act

cyclically through an annual cycle in the WTNA, whereas biology acts cumulatively; the total effect of biological enhancement will decrease or reverse the air-sea efflux in the region permanently, in comparison to the seasonal changes in air-sea efflux related to meteorology. Relaxation of biologically enhanced plume conditions back to nonplume conditions would take longer, and reduce the CO_2 efflux for longer. Our modeled efflux reductions provide a background related only to mixing, and are likely enhanced by additional biological activity.

Conclusion:

Even though WTNA plume water is more likely to take up CO_2 than nonplume water due to its lowered pCO_2 and enhanced air-sea fluxes (Figures 4.8, 4.10), the majority of deficit remediation comes from horizontal advection (Figure 4.11) because vertical fluxes are not sufficient to even replace the deficit associated with 2.5% river water (Figures 4.4-4.7). Evaporation and precipitation (and potentially biological activity) are large influences on surface mixed layer salinity, DIC, and TA, but they cause changes that are still smaller than the relaxation terms. Unless horizontal advection brings water with higher DIC, TA, and salinity to the plume region (for example, if it brings water that has been recently upwelled) and cancels the plume-related carbon deficit, the deficit is likely to become mixed into the rest of the WTNA and slightly reduce the air-sea CO_2 efflux.

Acknowledgements

This research was supported by the Office of Science (BER), U.S. Department of Energy, Grant No. DE-FG02-02ER63472, NOAA Office of Global Programs Grant NA16GP2689, and by faculty research support from the University of Georgia to P.L.Y.

Financial support was provided to S.R.C. by the University of Georgia Presidential Graduate Fellowship and the NASA Earth System Science Fellowship.

References

Brainerd, K. E. and M. C. Gregg (1995). Surface mixed and mixing layer depths. *Deep-Sea Research I 42*(9): 1521-1543.

Christian, J. R. (2005). Biogeochemical cycling in the oligotrophic ocean: Redfield and non-Redfield models. *Limnology and Oceanography 50*(2): 646-657.

Cooley, S. R., V. J. Coles, A. Subramaniam and P. L. Yager (2006). Seasonal variations in the Amazon plume-related atmospheric carbon sink. *in prep.*

Cooley, S. R. and P. L. Yager (2006). Physical and biological contributions to the western tropical North Atlantic Ocean carbon sink formed by the Amazon River plume. *Journal of Geophysical Research-Oceans (in press).*

Dickson, A. G. (1990a). Standard potential of the reaction: $AgCl_{(s)} + 1/2\ H_{2(g)} = Ag_{(s)} + HCl_{(aq)}$, and the standard acidity constant of the ion $HSO_4^{(-)}$ in synthetic seawater from 273.15 to 318.15K. *Journal of Chemical Thermodynamics 22*: 113-127.

Dickson, A. G. (1990b). Thermodynamics of the dissociation of boric acid in synthetic seawater from 273.15 to 318.15K. *Deep Sea Research 37*: 755-766.

Dickson, A. G. and F. J. Millero (1987). A comparison of the equilibrium constants for the dissociation of carbonic acid in seawater media. *Deep-Sea Research Part A-Oceanographic Research Papers 34*(10): 1733-1743.

Dickson, A. G. and F. J. Millero (1989). Corrigenda. *Deep-Sea Resarch 36*: 983.

Dickson, A. G. and J. P. Riley (1979). The estimation of acid dissociation constants in seawater media from potentiometric titrations with strong base. I. The ionic product of water - Kw. *Marine Chemistry 7*: 89-99.

DOE (1997). Handbook of methods for the analysis of the various parameters of the carbon dioxide system in sea water. A. G. Dickson and C. Goyet, eds., ORNL/CDIAC-74.

Foltz, G. R., S. A. Grodsky, J. A. Carton and M. J. McPhaden (2004). Seasonal salt budget of the northwestern tropical Atlantic Ocean along 38W. *Journal of Geophysical Research 109*: doi:10.1029/2003JC002111.

Geyer, W. R., R. C. Beardsley, S. J. Lentz, J. Candela, R. Limeburner, W. E. Johns, B. M. Castro and I. D. Soares (1996). Physical oceanography of the Amazon shelf. *Continental Shelf Research 16*(5-6): 575-616.

Grist, J. P. and S. A. Josey (2003). Inverse Analysis Adjustment of the SOC Air–Sea Flux Climatology Using Ocean Heat Transport Constraints. *Journal of Climate 16*(20): 3274-3295.

Hellweger, F. L. and A. L. Gordon (2002). Tracing Amazon River water into the Caribbean Sea. *Journal of Marine Research 60*(4): 537-549.

Hochman, H. T., F. E. Muller-Karger and J. J. Walsh (1994). Interpretation of the coastal zone color scanner signature of the Orinoco River plume. *Journal of Geophysical Research-Oceans 99*(C4): 7443-7455.

Hood, R. R., N. R. Bates, D. G. Capone and D. B. Olson (2001). Modeling the effect of nitrogen fixation on carbon and nitrogen fluxes at BATS. *Deep-Sea Research Part II-Topical Studies in Oceanography 48*(8-9): 1609-1648.

Hu, C., E. T. Montgomery, R. W. Schmitt and F. E. Muller-Karger (2004). The dispersal of the Amazon and Orinoco River water in the tropical Atlantic and Caribbean Sea: Observation from space and S-PALACE floats. *Deep-Sea Resarch Part II: Topical Studies in Oceanography 51*(10-11): 1151-1171.

Josey, S. and P. Taylor (1999). New insights into the ocean heat budget closure problem from analysis of the SOC air-sea flux climatology. *Journal of Climate 12*(9): 2856-2880.

Körtzinger, A. (2003). A significant CO_2 sink in the tropical Atlantic Ocean associated with the Amazon River plume. *Geophysical Research Letters 30*(24): 2287-2290.

Lentz, S. J. (1995). Seasonal Variations in the Horizontal Structure of the Amazon Plume Inferred from Historical Hydrographic Data. *Journal of Geophysical Research-Oceans 100*(C2): 2391-2400.

Lentz, S. J. and R. Limeburner (1995). The Amazon River Plume During AMASSEDS - Spatial Characteristics and Salinity Variability. *Journal of Geophysical Research-Oceans 100*(C2): 2355-2375.

Lewis, E. and D. W. R. Wallace (1998). *Program developed for CO_2 System Calculations. Version 1.05.* ORNL/CDIAC-105. Carbon Dioxide Information Analysis Center, Oak Ridge National Laboratory, U.S. Department of Energy, Oak Ridge, Tennesee.

Millero, F. J. (1995). Thermodynamics of the carbon dioxide system in the oceans. *Geochimica et Cosmochimica Acta 59*: 661-677.

Muller-Karger, F. E., C. R. McClain and P. L. Richardson (1988). The dispersal of the Amazon's water. *Nature 333*(56-59).

Muller-Karger, F. E., P. L. Richardson and D. J. McGillicuddy (1995). On the offshore dispersal of the Amazon's plume in the North Atlantic: Comments. *Deep-Sea Research Part I-Oceanographic Research Papers 42*(11-12): 2127-2137.

Oltman, R. E. (1968). *Reconnaissance investigations of the discharge and water quality of the Amazon River*. U.S. Geological Survey, Washington, D.C.

Pailler, K., B. Bourles and Y. Gouriou (1999). The barrier layer in the Western Tropical Atlantic Ocean. *Geophysical Research Letters 26*(14): 2069-2072.

Price, J. F., R. A. Weller and R. Pinkel (1986). Diurnal Cycling: Observations and Models of the Upper Ocean Response to Diurnal Heating, Cooling, and Wind Mixing. *Journal of Geophysical Research 91*: 8411-8427.

Sarmiento, J. L., R. Murnane and C. LeQuere (1995). Air-Sea CO_2 Transfer and the Carbon Budget of the North- Atlantic. *Philosophical Transactions of the Royal Society of London Series B-Biological Sciences 348*(1324): 211-219.

Schudlich, R. and J. F. Price (1992). Diurnal cycles of current, temperature, and turbulent dissipation in a model of the equatorial upper ocean. *Journal of Geophysical Research 97*(C4): 5409-5422.

Sprintall, J. and M. Tomczak (1992). Evidence of the Barrier Layer in the Surface Layer of the Tropics. *Journal of Geophysical Research 97*(C5): 7305-7316.

Stramma, L. and F. Schott (1999). The mean flow field of the tropical Atlantic Ocean. *Deep-Sea Research Part Ii-Topical Studies in Oceanography 46*(1-2): 279-303.

Subramaniam, A., E. J. Carpenter, P. L. Yager, S. R. Cooley, R. Del Vecchio, D. Karl, C. Mahaffey, S. A. Sanudo-Wilhelmy, R. Shipe, A. Tovar-Sanchez and D. G. Capone (*in revision*). Amazon River amplifies C and N cycles in the Tropical North Atlantic Ocean.

Takahashi, T., S. C. Sutherland, C. Sweeney, A. Poisson, N. Metzl, B. Tilbrook, N. R. Bates, R. Wanninkhof, R. A. Feely, C. L. Sabine, J. Olafsson and Y. Nojiri (2002). Global sea-air CO_2 flux based on climatological surface ocean pCO_2, and seasonal biological and temperature effects. *Deep-Sea Resarch II 49*: 1601-1622.

Takahashi, T., R. T. Williams and D. L. Bos (1982). Carbonate chemistry. *GEOSECS Pacific Expedition, Hydrographic Data 1973-1974*. W. S. Broecker, D. W. Spencer and H. Craig. National Science Foundation, Washington, DC. *13*.

Ternon, J. F., C. Oudot, A. Dessier and D. Diverres (2000). A seasonal tropical sink for atmospheric CO_2 in the Atlantic Ocean: the role of the Amazon River discharge. *Marine Chemistry 68*: 183-201.

Wanninkhof, R. and W. R. McGillis (1999). A cubic relationship between air-sea CO_2 exchange and wind speed. *Geophysical Research Letters 26*(13): 1889-1892.

Weiss, R. F. (1974). Carbon dioxide in water and seawater: The solubility of a nonideal gas. *Marine Chemistry 2*: 203-215.

Weiss, R. F. and B. A. Price (1980). Nitrous oxide solubility in water and seawater. *Marine Chemistry 8*: 347-359.

Yelland, M. and P. K. Taylor (1996). Wind stress measurements from the open ocean. *Journal of Physical Oceanography 26*(4): 541-558.

Table 4.1: SML values for synthetic plume profiles and nonplume groups.

	SML values (mean ± s.d., observed data)			*Surface*
% r[1]	*Salt*	*DIC (µmol kg^{-1})*	*ALK (µeq kg^{-1})*	*pCO_2 (µatm)*
10	32.4	1852.9	2157.8	348.2
7.5	33.3	1895.8	2210.7	357.8
5	34.2	1938.7	2263.6	367.6
2.5	35.1	1981.6	2316.5	377.7
NE Group	35.9 ± 0.2	1999.7 ± 16.3	2360.3 ± 18.2	359.0 ± 0.7
SE Group[2], r=0.0	36.0 ± 0.1	2024.5 ± 6.8	2369.4 ± 5.9	388.6 ± 4.4

[1] Percent riverwater found in synthetic plume surface mixed value (see Methods).
[2] The southeastern group profile was the same as the r = 0% synthetic profile.

Figure 4.1: Average profiles of a) Salinity, b) DIC, c) and TA for nonplume summer 2001 (Red; northeastern stations plotted with □, and southeastern stations plotted with O), spring 2003 (green Δ), and winter 2001 (blue ◊). D) Temperature profiles group all data for each season, as no significant temperature differences were found between subgroups within a season. Errorbars indicate 95% confidence intervals. Solid black line plots the mean profile used in the model.

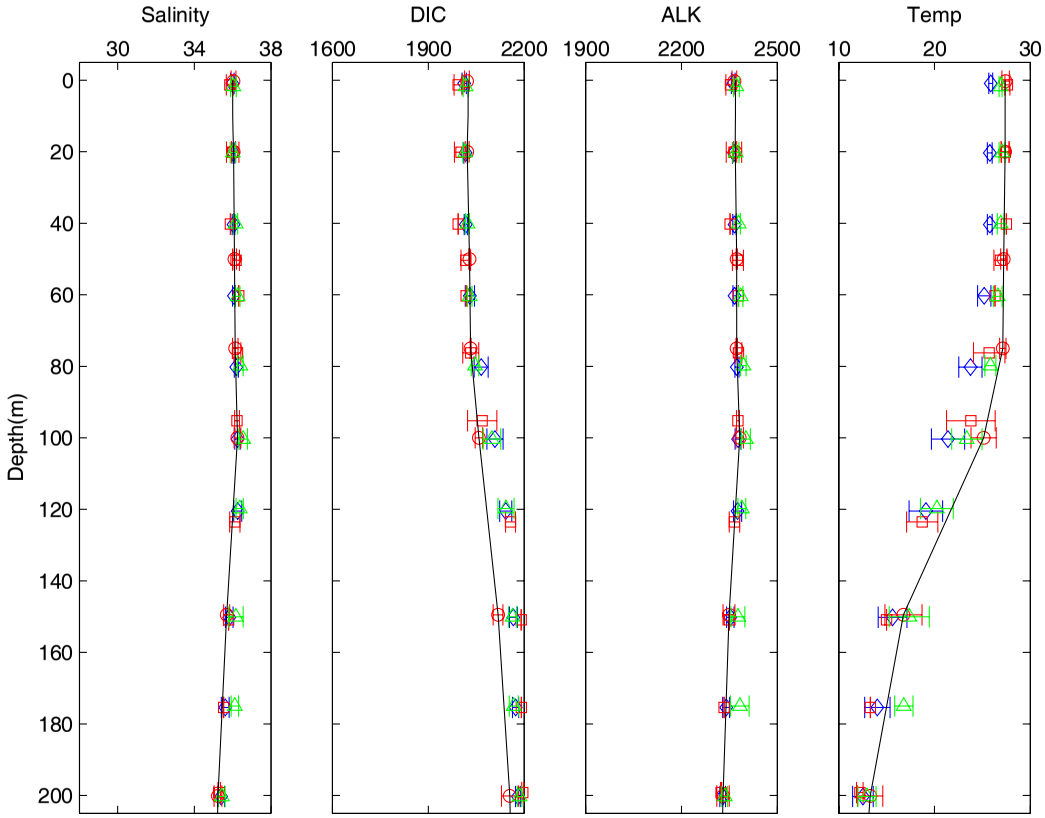

Figure 4.2: Average profiles of a) Salinity, b) DIC, c) and TA for plume summer 2001 (red O) and spring 2003 (green Δ). Errorbars indicate 95% confidence intervals. Solid black lines plot the R=10, 5, and 0% river profiles (left to right in plots) used in the model.

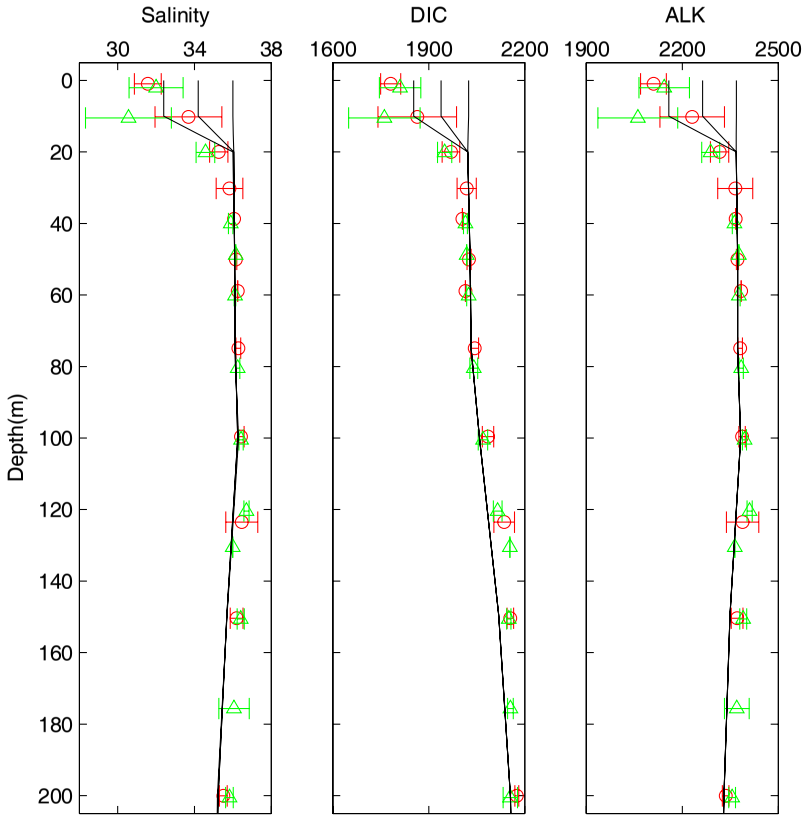

Figure 4.3: Model output for a five-year control run begun in July with the r=0% (nonplume) initial conditions. A) mixed layer depth (m), B) sea surface temperature (ºC), C) sea surface salinity (unitless), D) surface DIC (µmol kg^{-1}). E) surface ALK (ueq kg^{-1}), F) pCO2 (µatm), G) net heat flux (W m^{-2}, where Q_i is heat absorbed and Q_o is heat lost. H) Evaporation minus precipitation (mm s^{-1}. solid line, left axis), and total wind stress (N m^{-2}, dashed line, right axis). The X-axis increment is 2 months, starting in July.

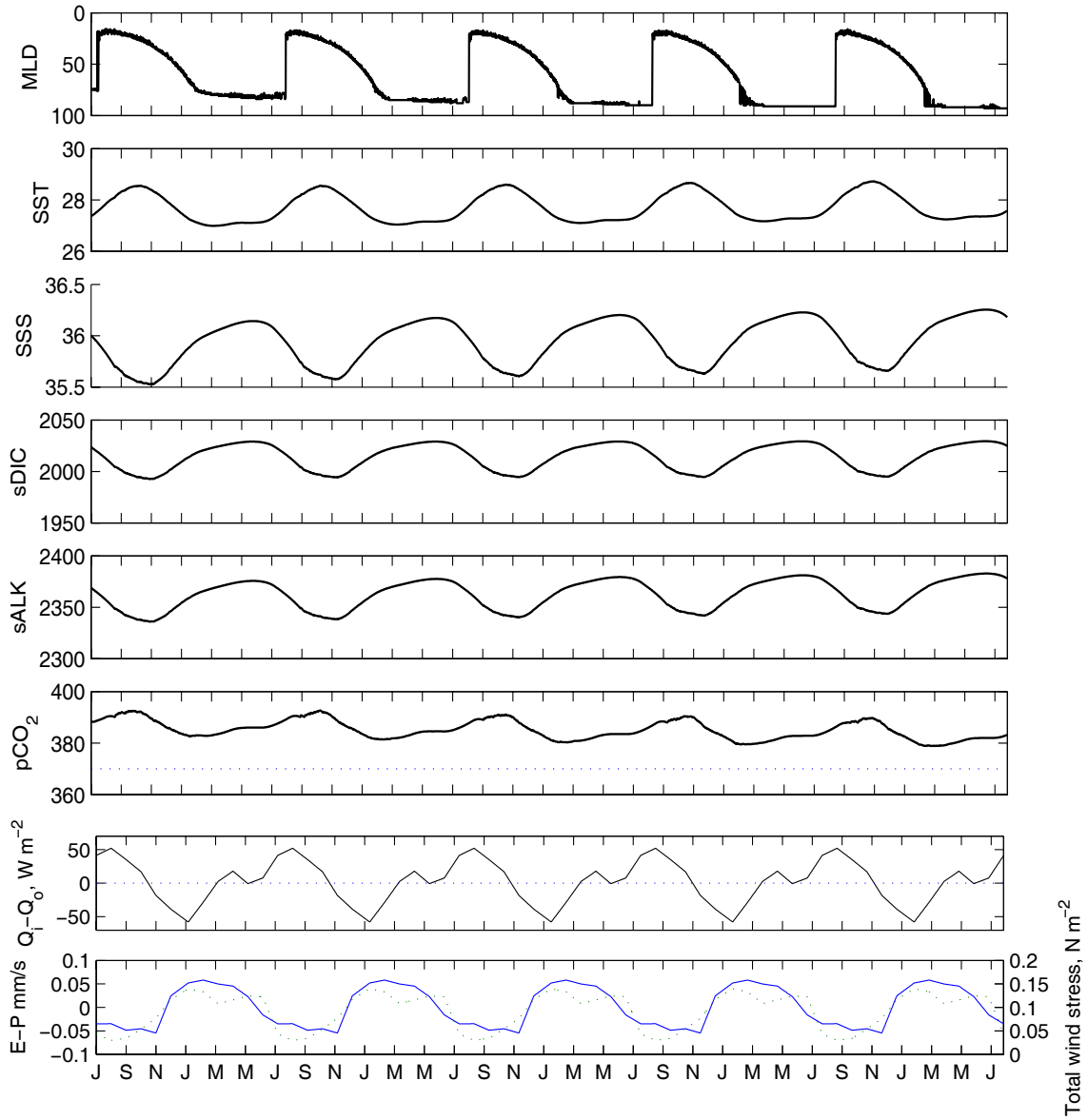

Figure 4.4: Vertical mixing-only modeled values for A) mixed layer depth (m), B) pCO_2 (µatm), and C) air-sea CO_2 flux (mmol m^{-2} d^{-1}). Negative fluxes indicate CO_2 loss to the atmosphere. Colors indicate initial conditions: R = 0%, black; R = 2.5%, blue; R = 5%, green; R = 7.5%, yellow; R=10%, red. X-axis indicates month.

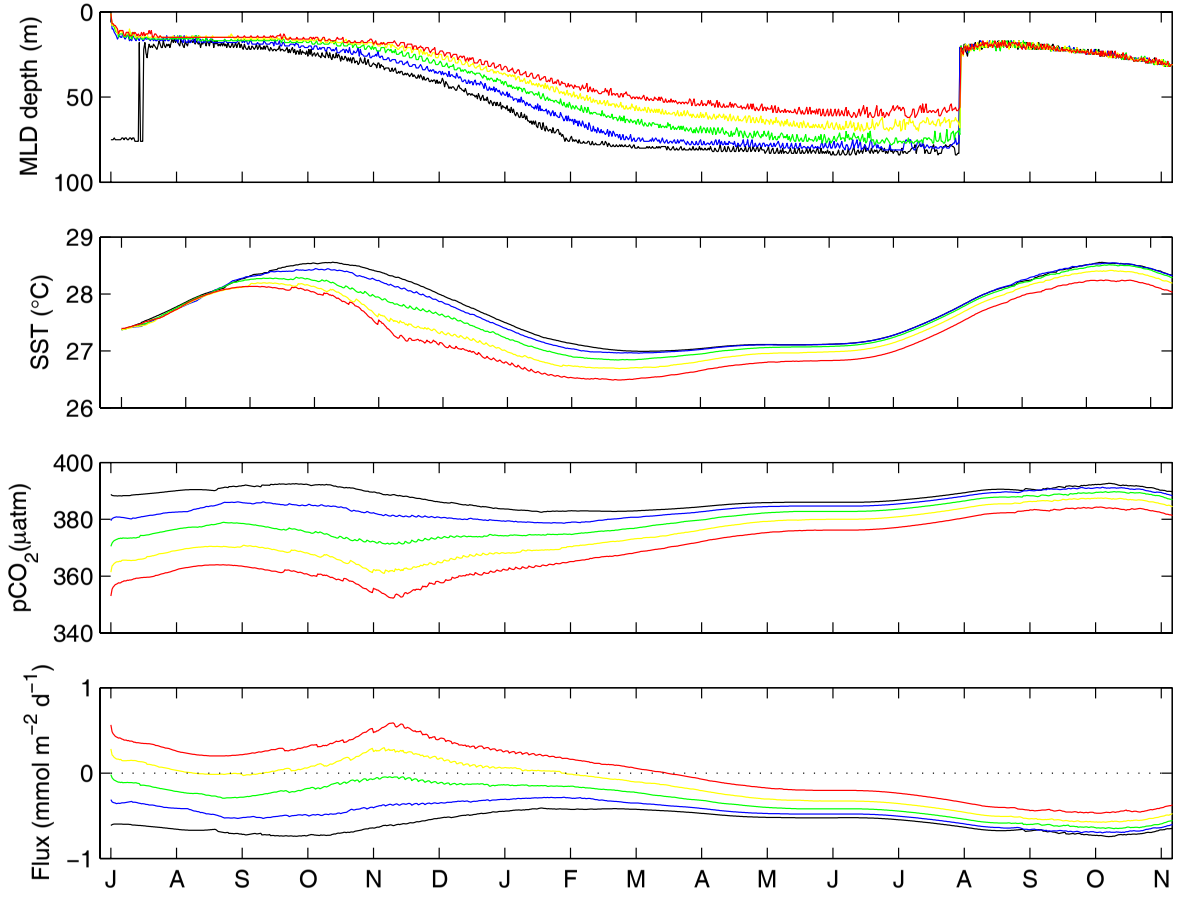

Figure 4.5: Difference through time between modeled salinity for the control and an initial plume condition, where R = 0%. X-axis indicates month. Salinity is unitless.

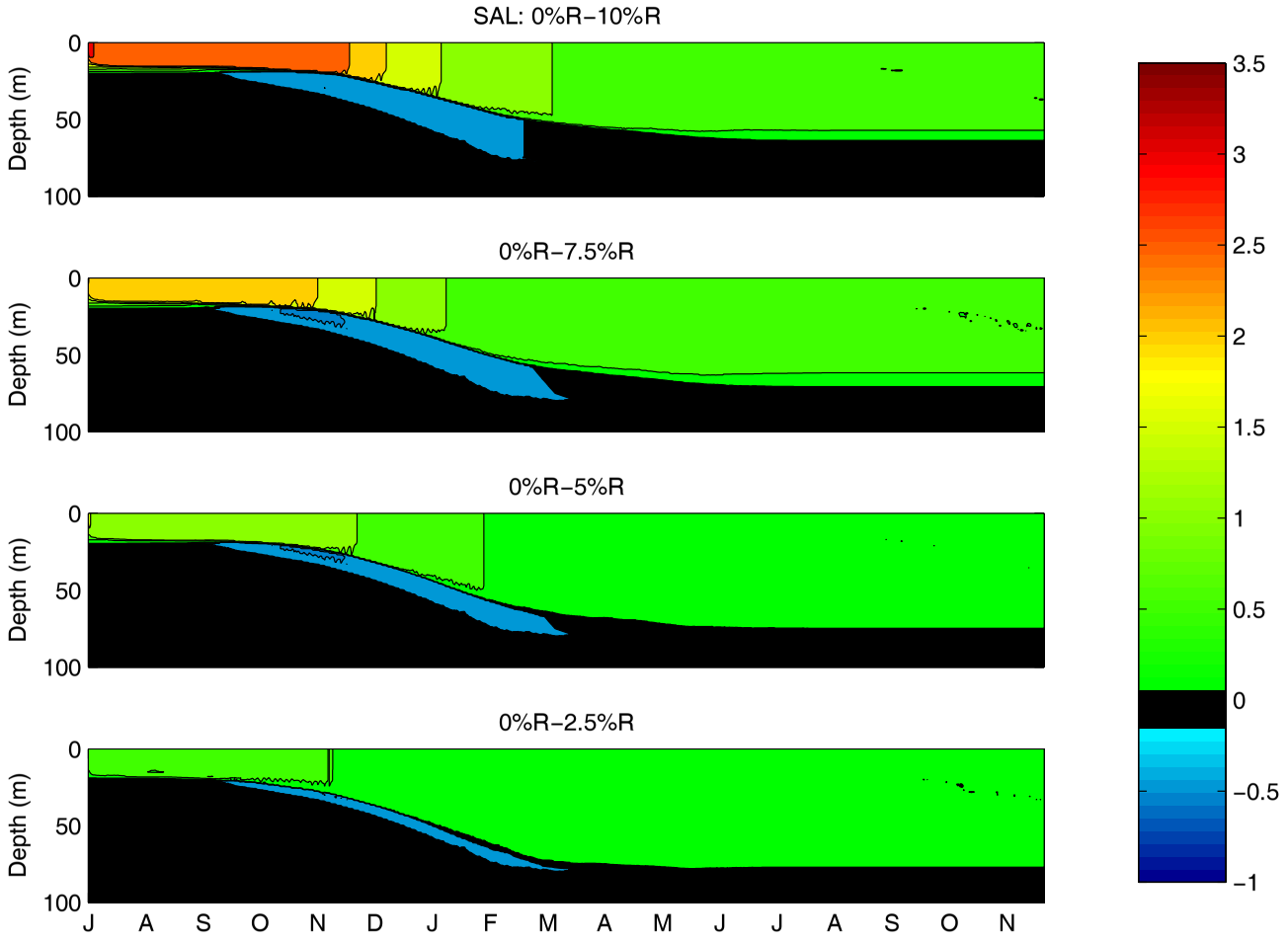

Figure 4.6: Difference through time between modeled DIC for the control and an initial plume condition, where R = 0%. X-axis indicates month. DIC is in µmol kg^{-1}.

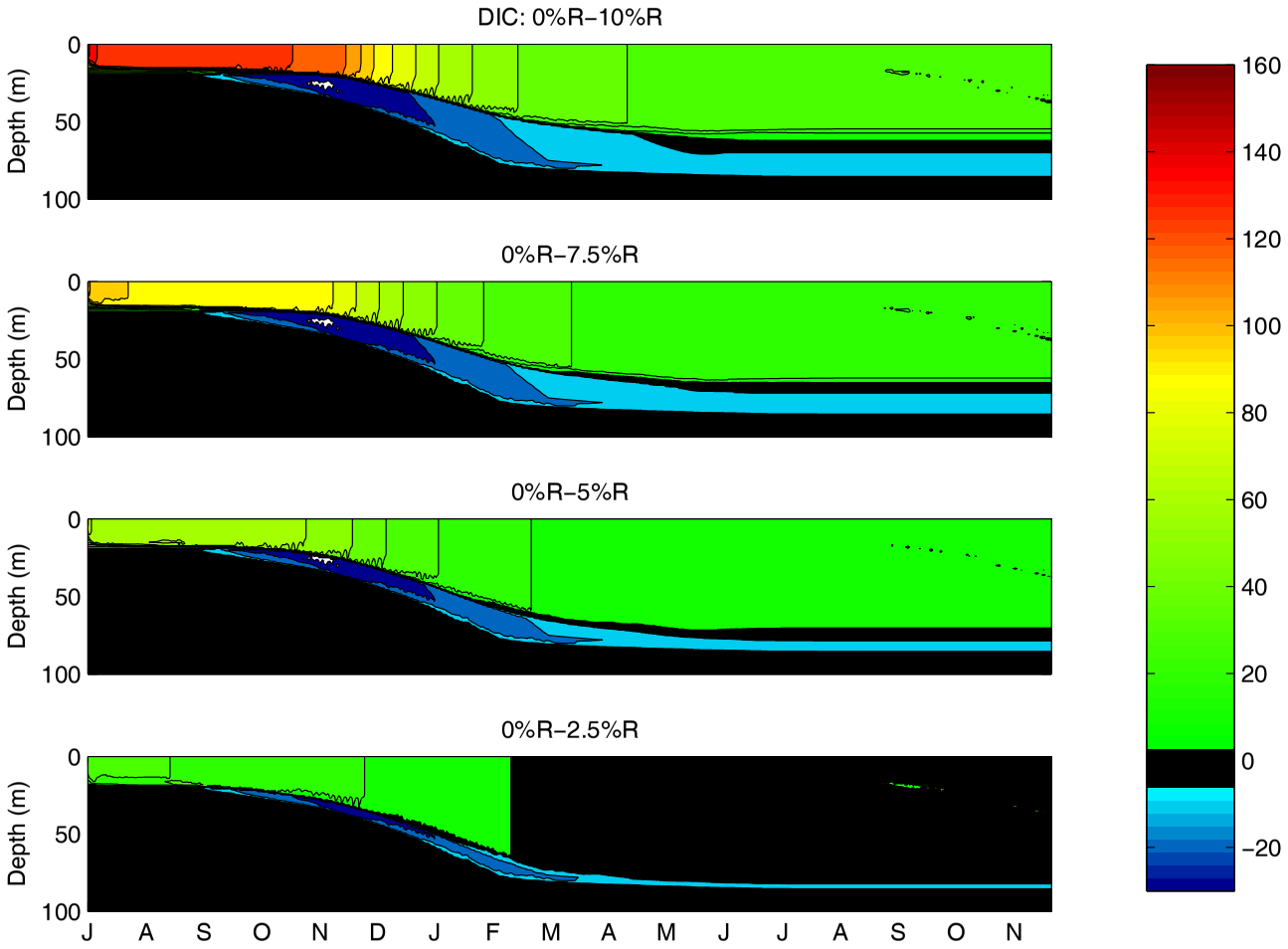

Figure 4.7: Difference through time between modeled ALK for the control and an initial plume condition, where R = 0%. X-axis indicates month. ALK is in µmol kg^{-1}.

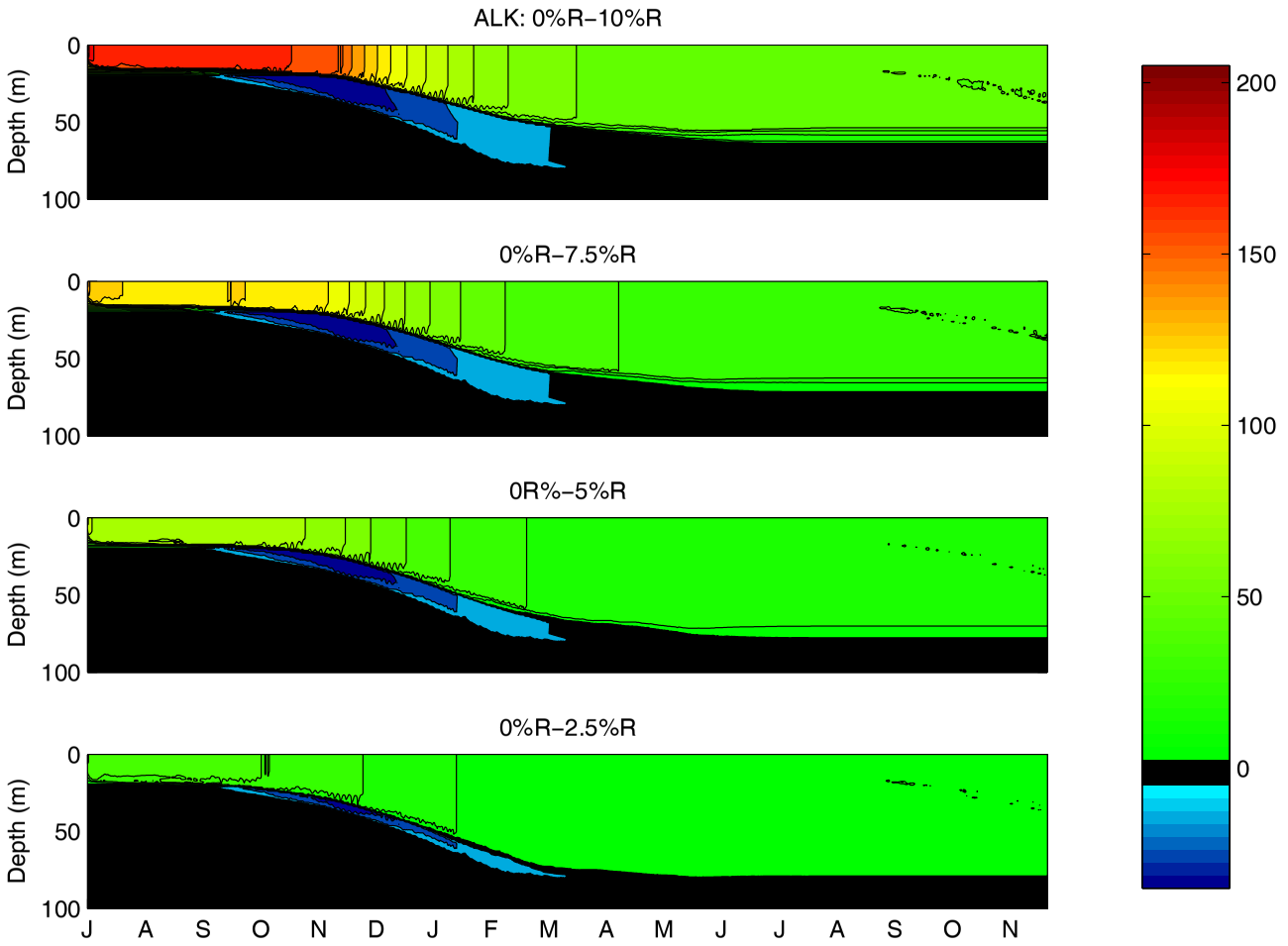

Figure 4.8: Vertical mixing plus relaxation (to R = 0%) modeled values for A) mixed layer depth (m), B) pCO_2 (µatm), and C) air-sea CO_2 flux (mmol m^{-2} d^{-1}). Negative fluxes indicate CO_2 loss to the atmosphere. Colors indicate initial conditions: R = 0%, black; R = 2.5%, blue; R = 5%, green; R = 7.5%, yellow; R=10%, red. X-axis indicates month.

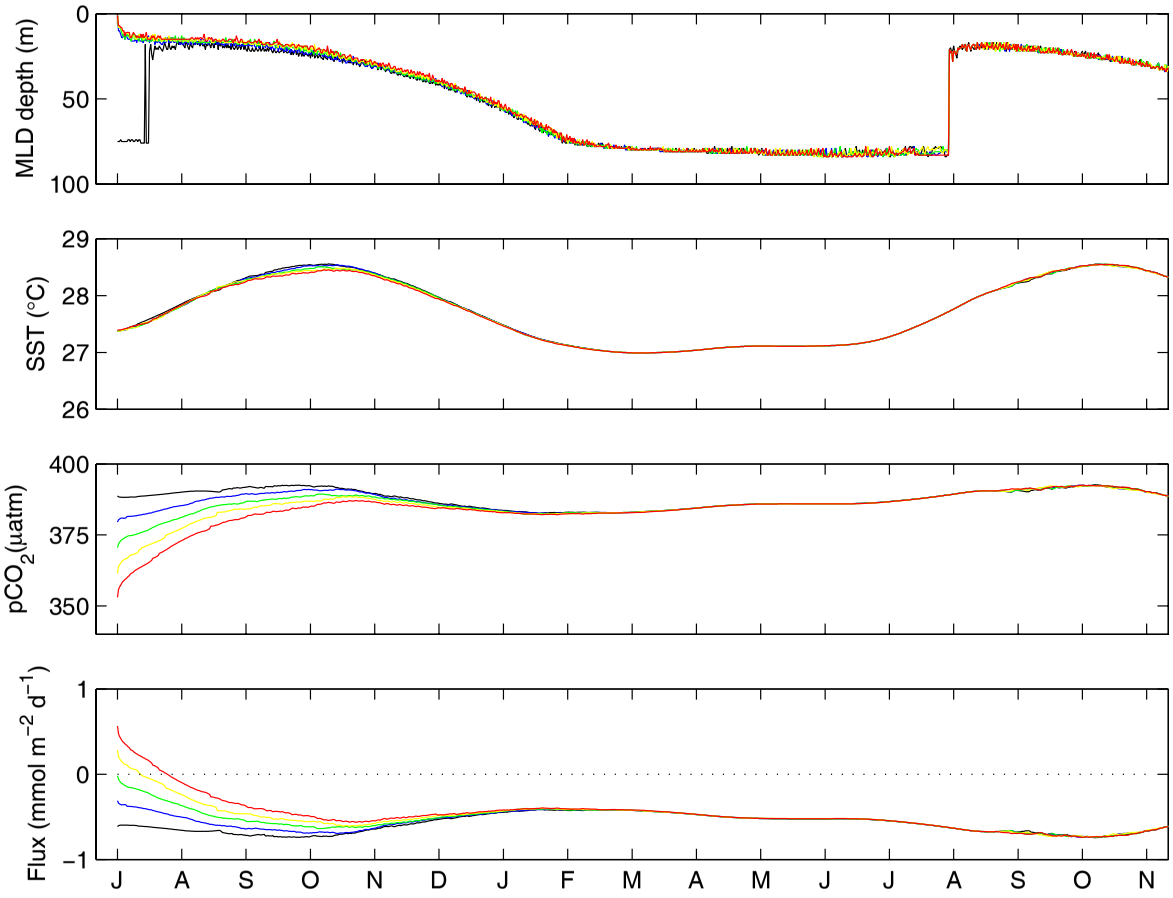

Figure 4.9: Relaxation term for salinity through time when an initial plume condition is relaxed to the control, where R = 0%. X-axis indicates month. Salinity is unitless.

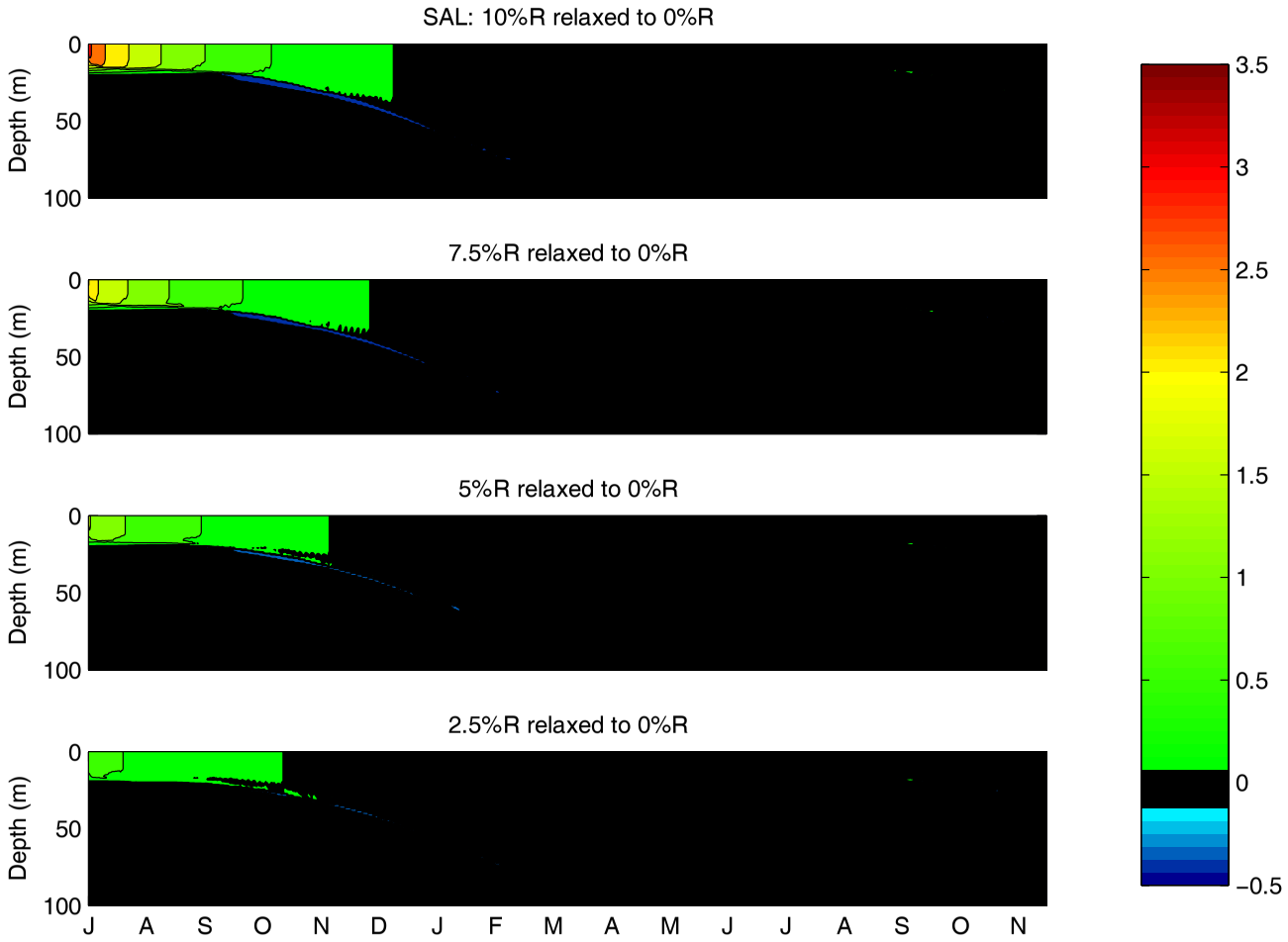

Figure 4.10: Relaxation term for DIC through time when an initial plume condition is relaxed to the control, where R = 0%. X-axis indicates month. DIC is in μmol kg^{-1}.

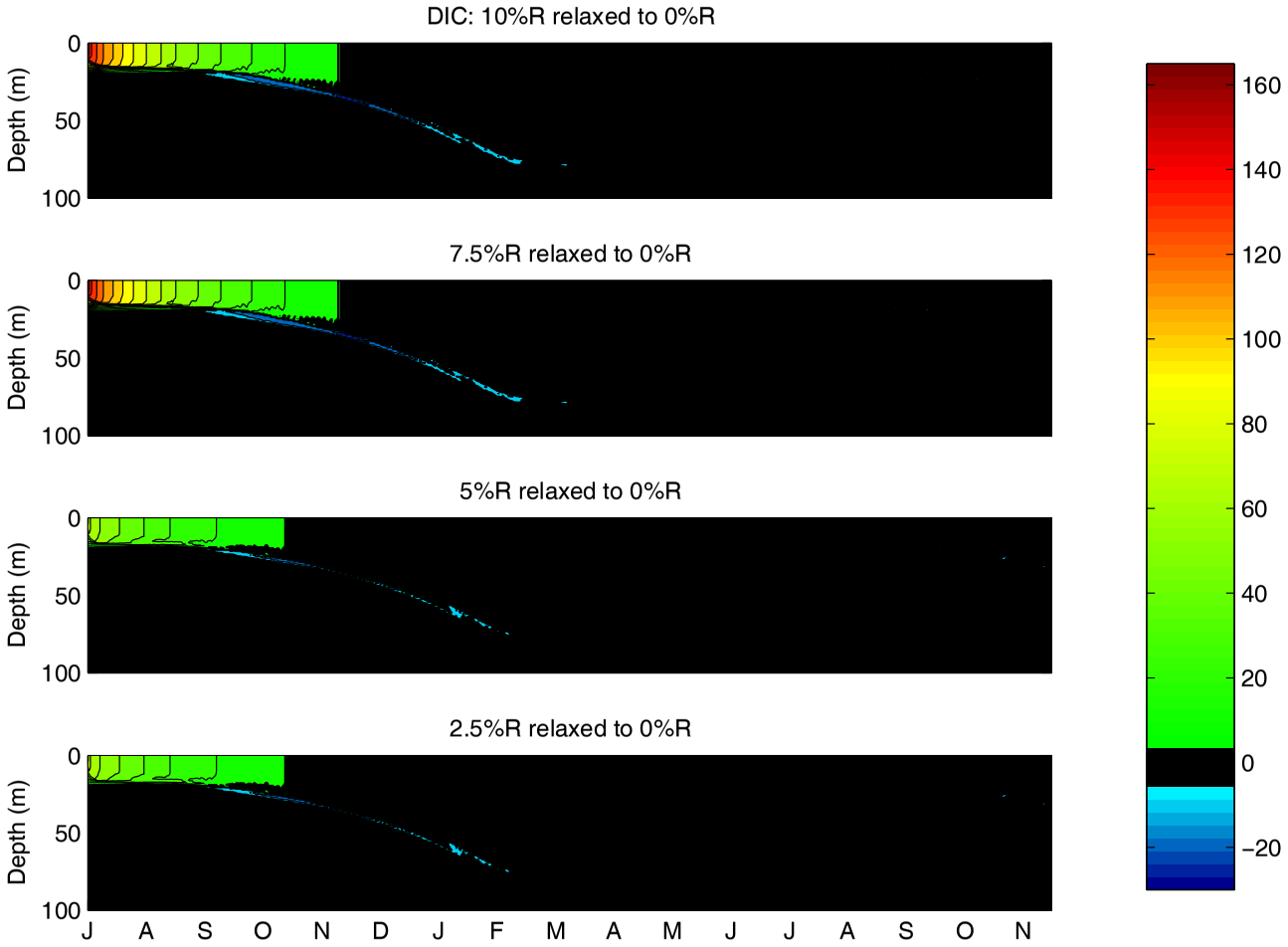

Figure 4.11: Relaxation term for ALK through time when an initial plume condition is relaxed to the control, where R = 0%. X-axis indicates month. ALK is in µmol kg^{-1}.

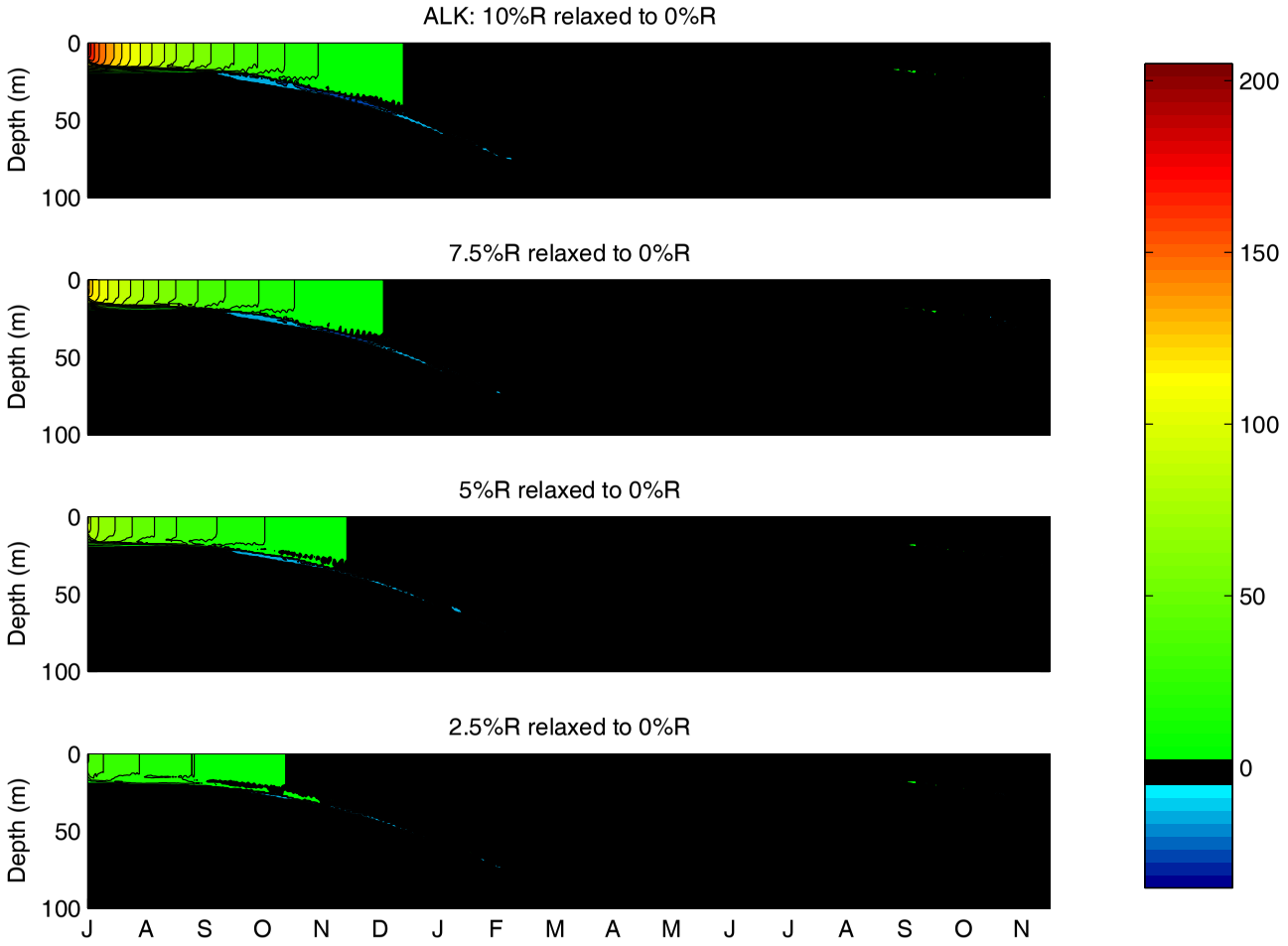

Figure 4.12: Comparison of the magnitudes of influences on modeled DIC (µmol kg^{-1}, see Results). X-axis indicates month. DIC is in µmol kg^{-1}.

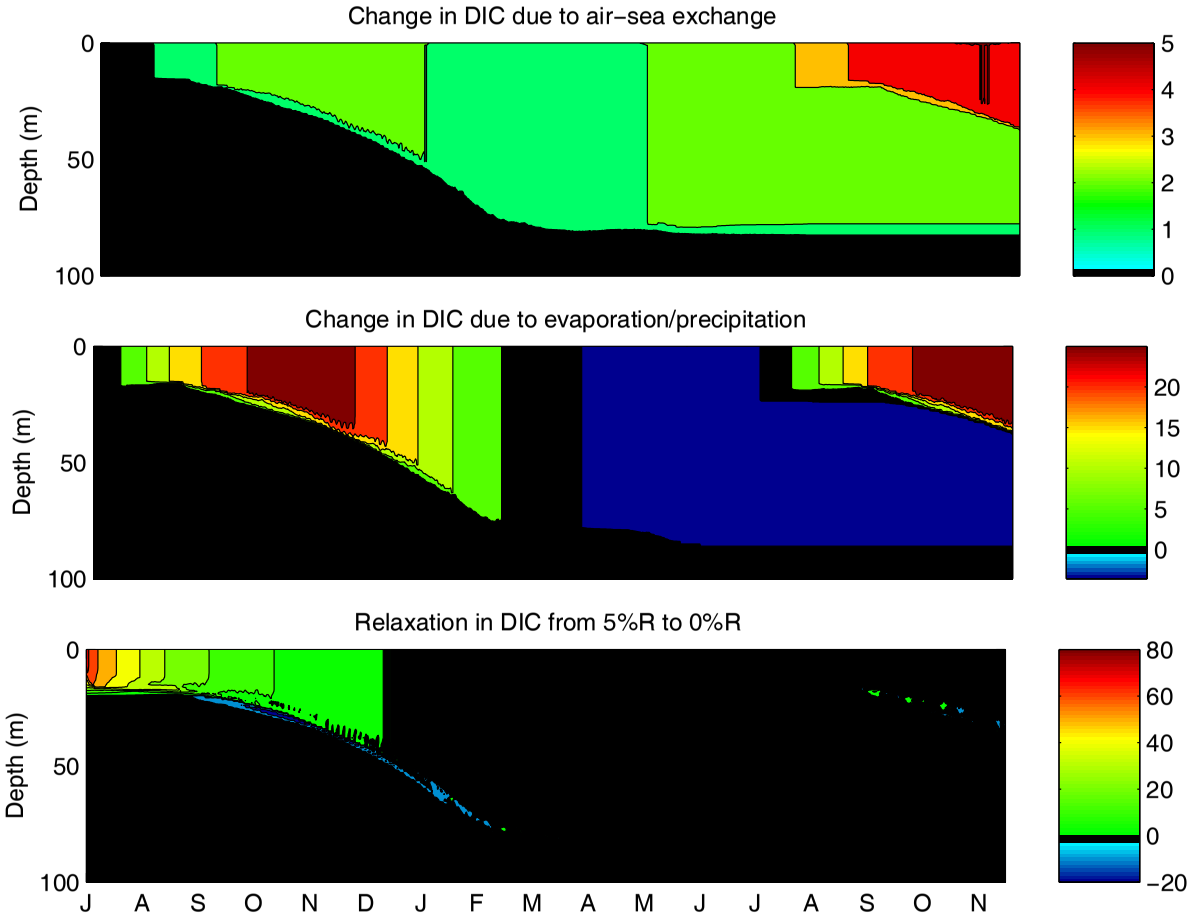

CHAPTER 5

CONCLUSIONS

Quantifying physical, chemical, biological, and geological influences on dissolved inorganic carbon cycling in coastal and riverine systems will constrain uncertainties in the global carbon cycle by clarifying the timescales and magnitudes with which they act. Although the Amazon River is the largest river system in the world, the large inorganic carbon fluxes in its offshore plume have not been mechanistically quantified even though the plume is large enough to influence the entire western tropical North Atlantic Ocean (WTNA) carbon budget. To begin improving current understanding of this undersampled system, my goals in this project were to 1) quantify physical mixing and biological effects of the Amazon plume on WTNA inorganic carbon cycling, 2) to quantify seasonal variability in both supplies of inorganic carbon and alkalinity to the river plume and in offshore processing of those pools, and 3) determine the fate of the river-associated inorganic carbon deficit in the WTNA.

A conservative mixing model separated physical mixing from biological effects in the Amazon plume inorganic carbon budget and showed that net community production removes a significant amount of inorganic carbon from plume waters that creates an undersaturation with the potential to outlast the plume structure. Net community production was greatest where diatoms containing diazotrophic symbionts were numerous. Even so, physical processes dominate the region's inorganic carbon cycle, with lateral mixing primarily dictating plume inorganic carbon distributions. A vertical mixing model indicated that evaporation and

precipitation dominated changes in surface mixed layer inorganic carbon conentrations in the absence of the plume.

Inorganic carbon and total alkalinity data for the early plume at the river mouth have not been published. To constrain seasonality of the alkalinity supply to the river plume, we modeled total alkalinity at the river mouth using previously published upriver TA data and a precipitation-adjusted modeled river discharge. At the same time, we used a conservative mixing model to determine alkalinity values at the river mouth using offshore data. Model results indicated that TA travels conservatively throughout the river-ocean mixing continuum and is supplied to the plume with low, seasonally varying levels of alkalinity, below approximate values used in previous studies. We assumed that DIC was supplied in a constant ratio with TA and examined the relative effects of seasonality in supply vs. seasonality in offshore processing. Offshore processing is the more important adjustment of plume DIC, because biological activity there creates the large drawdown of carbon observed. With biological activity, the outer 20% of the plume takes up 15 Tg C y^{-1}; otherwise, it would take up less than 1 Tg C y^{-1}.

The Amazon River plume creates a large deficit in inorganic carbon that disappears approximately at the same time as the stratified plume salinity structure. Regional evaporation is not sufficient to obliterate the river plume, and air-sea gas exchange in the area is too slow to replace the DIC deficit from the atmosphere. We use a vertical mixing model with starting conditions set along the outer edge of the plume to determine how the plume structure disappears, with the goal of quantifying the contributions of vertical carbon replacement from above and below and comparing to see if they compete with the estimated effects of horizontal advection in eliminating the deficit. We found that the vertical fluxes of carbon are so small that horizontal advection is necessary to return WTNA waters to nonplume conditions in a realistic

period of time. This means that if a residual plume-associated carbon deficit remains, it will contribute to lowering CO_2 efflux in the WTNA and may offset CO_2 release in the river basin.

The air-sea carbon fluxes investigated in this dissertation represent a small fraction of the carbon deficit introduced to the WTNA by the Amazon plume. Inorganic carbon supply from the Amazon is estimated at 32 Tg C y^{-1} (Devol and Hedges 2001), and average total discharge is estimated at 79,704 km^3 y^{-1} (Dai and Trenberth 2002), implying plume water enters the WTNA with 32 µmol C kg^{-1}. At the same time, the Amazon River supplies 19 Tg C y^{-1} DOC and 9 Tg C y^{-1} POC (Devol and Hedges 2001). If all the organic carbon were completely respired during the plume transit, it would add 29 µmol kg^{-1} DIC, for a total load of 61 µmol C kg^{-1}. Bringing this water to oceanic DIC levels requires an addition of 1956 µmol C kg^{-1} (250 mmol m^{-2} d^{-1} to a 10 m plume over 80 d). These flux rates correspond to a plumewide uptake of 7.3 Tg C d^{-1} to remediate the deficit in 80 days (over a 10m deep plume with surface area of 2.4 x 10^6 km^2), which is far greater than we found was regionally likely in Chapter 3. The mixing-only air-sea flux of carbon into the outer plume is no match for the plume-linked deficit at 1 mmol C m^{-2} d^{-1}, but even the biologically enhanced, outer plume air-sea flux of 5 mmol C m^{-2} d^{-1} flux is still no match for the plume-associated deficit. Furthermore, biological enhancement of the air-sea flux would require removing carbon from the plume, worsening the deficit. In comparison, the mixing-only air-sea carbon flux into the plume (1 mmol C m^{-2} d^{-1}) is slightly greater than the CO_2 efflux from Amazonian rivers and wetlands (0.5 Gt C yr^{-1} over a 1.8x10^6 km^2 basin, corresponding to a 0.07 mmol C m^{-2} d^{-1} loss, Richey et al. 2002).

The Amazon plume's offshore location and production-enhanced air-sea CO_2 sink is unusual given its tropical latitude, yet is a characteristic seen in other large river systems. Low-latitude tropical to subtropical continental shelves emit CO_2 to the atmosphere (Cai et al. 2006).

At the same time, the few rivers with large enough discharge can affect air-sea CO_2 fluxes off the continental shelf. The plumes of the Amazon, Mississippi, and Yangtze are known to act as CO_2 sinks (Ternon et al. 2000; Körtzinger 2003; Cai 2003; Wang et al. 2000). Other large-discharge rivers may also exhibit this behavior, but the chemistry of their plumes has not been as well studied.

Like the Amazon, the Mississippi River plume supports biological production in the offshore plume, except production occurs farther offshore in the Mississippi plume salinity gradient (Cai 2003). The key characteristic in common for both rivers is that discharge is large enough to drive estuarine mixing outside the physical boundaries of the estuary, where turbidity can settle, decreasing light limitation and allowing primary production to take advantage of the riverine nutrient loads. When the plumes are located off the continental shelf, the deep water column prevents any sediment-associated respiration from overcoming the production-related signal from the upper water column. Although specific values for the Yangtze River carbon cycle are not readily available, this river appears to have similar characteristics as the Amazon and Mississippi, as the low salinity region associated with the Yangtze river plume is also associated with low carbon water that extends at least 200 km offshore (Wang et al. 2000).

The findings of this dissertation promote understanding of inorganic carbon cycling in several ways. First, our method to distinguish physical mixing from net community production in river plume inorganic carbon distributions can be applied in the future to other low-latitude river systems where biological carbonate formation is expected to be minimal. The findings from this model are consistent with a linkage between nitrogen fixation and carbon drawdown in the WTNA. Second, we created a working model of TA and DIC supply to the Amazon plume that incorporates regional processes. Fluxes calculated from this effort are in line with

geochemical predictions and biological observations. Until samples at the river mouth can be collected to develop an observationally based model for TA and DIC seasonality, we feel that our endmembers do a very good job of parameterizing mixing in the river-ocean system. We determined that biological activity is crucial for creating and maintaining the carbon sink in the Amazon plume. Although the Amazon plume is undersaturated with respect to atmospheric levels of inorganic carbon, the net effect of mixing this large volume of low-carbon water on the regional carbon cycle may result in small-magnitude changes in DIC and TA throughout the WTNA basin, which may be difficult to distinguish from seasonal or spatial variability using current sampling intensity and distribution. This work highlights the need to understand the variables controlling biology in the plume, because future changes in the plume uptake will undoubtedly depend on changes in biological cycling of carbon there.

Shipboard sampling of the Amazon plume, from oceanic salinities right into the river mouth at salinity zero would be an ideal continuation of this project. Little is known about inorganic carbon cycling in the lower salinity zones of the plume, except that fluxes must be much larger than we observed offshore, because biological production and respiration rates inshore are very high, and the mixing-driven undersaturation is quite large. Improved understanding of the relationship between TA and DIC at the river mouth would greatly constrain estimates of biological carbon drawdown in the entire plume. Finally, understanding the multivariate controls on biological activity in the entire plume will be critical for constraining predictions of the Amazon plume carbon sink's future behavior in situations of climate change.

References:

Cai, W.-J. (2003). Riverine inorganic carbon flux and rate of biological uptake in the Mississippi River plume. *Geophysical Research Letters 30*(2): doi:10.1029/2002GL016312.

Cai, W.-J., M. Dai and Y. Wang (2006). Air-sea exchange of carbon dioxide in ocean margins: A province-based synthesis. *Geophysical Research Letters 33*: doi: 10.1029/2006GL02619.

Dai, A. and K. E. Trenberth (2002). Estimates of Freshwater Discharge from Continents: Latitudinal and Seasonal Variations. *Journal of Hydrometeorology 3*: 660-687.

Devol, A. H. and J. I. Hedges (2001). Organic Matter and Nutrients in the Mainstem Amazon River. *The Biogeochemistry of the Amazon Basin*. M. E. McClain, R. L. Victoria and J. E. Richey. Oxford University Press, New York**:** 275-306.

Körtzinger, A. (2003). A significant CO_2 sink in the tropical Atlantic Ocean associated with the Amazon River plume. *Geophysical Research Letters 30*(24): 2287-2290.

Richey, J. E., J. M. Melack, A. K. Aufdenkampe, V. M. Ballester and L. L. Hess (2002). Outgassing from Amazonian rivers and wetlands as a large tropical source of atmospheric CO_2. *Nature 416*: 617-620.

Ternon, J. F., C. Oudot, A. Dessier and D. Diverres (2000). A seasonal tropical sink for atmospheric CO_2 in the Atlantic Ocean: the role of the Amazon River discharge. *Marine Chemistry 68*: 183-201.

Wang, S. L., C. T. A. Chen, G. H. Hong and C. S. Chung (2000). Carbon dioxide and related parameters in the East China Sea. *Continental Shelf Research 20*(4-5): 525-544.

Appendix A: Bottle data for Winter 2001, Summer 2001, and Spring 2003 cruises. Salinity, DIC, or TA values with standard deviations (s.d.) are average measured values for duplicate samples (n=2). Mixed layer depths (MLDs) were obtained from the Biocomplexity project FTP site (http://biology.usc.edu/bc/) on 5/21/2004.

Date sampled	Total Latitude (degrees)	Total Longitude (degrees)	STATION	CAST #	Niskin #	Bottle depth (m)	CTD Temp (°C)	CTD Salinity	MLD (m)	Salinity	s.d. Salinity	DIC (µmol kg^{-1})	s.d DIC	Sigma T(Somma Sal, t, 0m)	s.d. sigma t	Alk (µmol kg^{-1})	s.d. ALK
											n=2 for all s.d.'s and averages						
1/21/01	9.892	45.400	16	01	23	3.9	25.915	36.252	47	36.192	0.037	2031.334	0.229	23.9615	0.028	2377.981	2.370
1/21/01	09.892	45.400	16	01	20	20.6	25.923	36.250	47	36.184		2032.205		23.9530		2376.325	
1/21/01	09.892	45.400	16	01	17	40.5	25.921	36.247	47	36.199		2031.503		23.9649		2393.891	
1/21/01	09.892	45.400	16	01	14	60.8	20.711	36.360	47	36.289		2131.470		25.5558		2391.130	
1/21/01	09.892	45.400	16	01	11	80.9	19.140	36.342	47	36.277		2155.196		25.9627		2377.005	
1/21/01	09.892	45.400	16	01	08	100.5	17.191	36.143	47	36.071		2171.710		26.2917		2368.493	
1/21/01	09.892	45.400	16	01	05	120.1	14.871	35.740	47	35.696		2184.028		26.5380		2345.075	
1/21/01	09.892	45.400	16	01	03	150.4	12.028	35.316	47	35.255		2188.545		26.7824		2327.599	
1/21/01	09.895	45.404	16	06	21	175.9	11.100	35.150	47	35.065		2188.615		26.8085		2316.715	
1/21/01	09.895	45.404	16	06	19	199.0	10.510	35.060	47	34.968		2189.983		26.8388		2314.204	
1/21/01	09.895	45.404	16	06	17	297.5	9.840	34.990	47	34.929		2200.631		26.9242		2312.374	
1/21/01	09.895	45.404	16	06	15	408.0	8.700	34.860	47	34.725		2206.633		26.9508		2306.822	
1/21/01	9.895	45.404	16	06	13	500.1	7.880	34.780	47	34.723	0.020	2212.241	1.214	27.0745	0.016	2305.851	3.141
1/21/01	09.895	45.404	16	06	11	752.1	5.710	34.650	47	34.533		2221.740		27.2202		2312.694	
1/21/01	09.895	45.404	16	06	09	998.9	5.180	34.710	47	34.603		2217.544		27.3396		2308.512	
1/21/01	09.895	45.404	16	06	07	1500.4	4.480	34.990	47	34.924		2172.730		27.6742		2322.797	
1/21/01	09.895	45.404	16	06	05	1999.4	3.590	34.980	47	34.885		2160.905		27.7367		2318.756	
1/21/01	09.895	45.404	16	06	03	2500.8	3.100	34.950	47	34.890		2165.895		27.7881		2337.952	
1/21/01	09.895	45.404	16	06	01	3000.2	2.780	34.930	47	34.857		2174.493		27.7911		2329.309	
1/23/01	11.103	49.907	17	03	23	3.5	26.645	35.824	74	35.846	0.004	2002.020	0.584	23.4701	0.003	2350.587	2.278
1/23/01	11.103	49.907	17	03	20	20.2	25.662	35.882	74	35.905		2006.140		23.8235		2354.208	
1/23/01	11.103	49.907	17	03	17	40.6	25.668	35.882	74	35.896		2005.726		23.8149		2357.439	

1/23/01	11.103	49.907	17	03	14	60.1	25.670	35.882	74	35.910		2005.598		23.8248		2365.522	
1/23/01	11.103	49.907	17	03	11	80.3	25.660	35.893	74	35.899		2007.365		23.8196		2363.631	
1/23/01	11.103	49.907	17	03	08	100.7	22.905	36.950	74	36.969	0.001	2094.623	0.675	25.4570	0.001	2427.778	0.007
1/23/01	11.103	49.907	17	03	05	120.2	20.195	36.733	74	36.759		2144.592		26.0534		2407.096	
1/23/01	11.103	49.907	17	03	02	150.5	15.770	36.047	74	36.080		2177.107		26.6325		2357.509	
1/23/01	11.103	49.907	17	01	20	175.1	14.358	35.779	74	35.797		2183.667		26.7276		2346.945	
1/23/01	11.103	49.907	17	01	17	200.9	12.814	35.503	74	35.536		2196.802		26.8464		2338.662	
1/23/01	11.103	49.907	17	01	14	300.3	10.246	35.079	74	35.087		2211.791		26.9779		2311.773	
1/23/01	11.103	49.907	17	01	11	400.5	9.102	34.947	74	34.956		2219.659		27.0676		2312.514	
1/23/01	11.103	49.907	17	01	08	501.9	8.228	34.878	74	34.885	0.001	2223.087	0.266	27.1494	0.001	2309.623	0.948
1/23/01	11.103	49.907	17	01	05	749.2	6.041	34.697	74	34.708		2220.421		27.3169		2305.921	
1/23/01	11.103	49.907	17	01	02	1000.1	5.349	34.814	74	34.815		2213.816		27.4875		2318.256	
1/24/01	11.918	54.483	18	01	23	4.5	26.041	35.189	56	35.206	0.006	1956.825	0.013	23.1775	0.005	2313.669	1.450
1/30/01	10.792	55.353	20	01	23	0.0	26.103	35.524	84	35.607	0.008	1988.319	0.309	23.4611	0.006	2346.140	3.473
1/30/01	10.792	55.353	20	01	20	20.5	26.188	35.664	84	35.667		1991.079		23.4797		2339.463	
1/30/01	10.792	55.353	20	01	17	40.4	26.315	35.840	84	35.825		2003.697		23.5590		2353.057	
1/30/01	10.792	55.353	20	01	14	60.5	26.313	35.840	84	35.853		2003.230		23.5808		2352.677	
1/30/01	10.792	55.353	20	01	11	80.2	26.314	35.839	84	35.816		2004.373		23.5525		2353.257	
1/30/01	10.792	55.353	20	01	08	100.3	25.753	36.503	84	36.468	0.008	2049.555	0.160	24.2202	0.006	2399.208	5.920
1/30/01	10.792	55.353	20	01	05	121.1	22.978	36.811	84	36.839		2112.334		25.3371		2413.018	
1/30/01	10.792	55.353	20	01	02	149.2	19.088	36.270	84	36.291		2141.515		25.9868		2380.107	
1/30/01	10.945	55.132	20	14	20	176.5	17.545	36.403	84	36.434		2150.512		26.4843		2379.946	
1/30/01	10.945	55.132	20	14	17	200.8	16.110	36.148	84	36.185		2156.451		26.6350		2365.101	
1/30/01	10.945	55.132	20	14	14	300.9	11.259	35.292	84	35.318		2187.431		26.9763		2324.708	
1/30/01	10.945	55.132	20	14	11	400.5	8.769	34.904	84	34.917		2201.740		27.0904		2309.283	
1/30/01	10.945	55.132	20	14	08	500.9	7.487	34.745	84	34.756		2209.772		27.1579		2305.041	
1/30/01	10.945	55.132	20	14	05	749.2	5.725	34.626	84	34.618		2221.547		27.2856		2306.262	
1/30/01	10.945	55.132	20	14	02	1001.8	5.156	34.778	84	34.805		2211.075		27.5026		2311.123	
1/31/01	10.175	53.926	21	01	23	1.9	26.389	36.253	98	36.265	0.001	2030.976	0.021	23.8676	0.001	2380.272	2.638
1/31/01	10.175	53.926	21	01	21	20.7	26.389	36.253	98	36.250		2031.739		23.8563		2378.966	
1/31/01	10.175	53.926	21	01	19	41.4	26.394	36.251	98	36.250		2030.315		23.8547		2379.956	
1/31/01	10.175	53.926	21	01	17	59.8	26.394	36.251	98	36.254		2031.441		23.8577		2379.806	
1/31/01	10.175	53.926	21	01	15	79.3	26.398	36.250	98	36.255		2031.476		23.8572		2376.895	
1/31/01	10.175	53.926	21	01	13	100.2	25.393	36.282	98	36.277	0.012	2048.502	0.546	24.1875	0.009	2383.723	3.657
1/31/01	10.175	53.926	21	01	11	119.8	23.714	36.352	98	36.378		2080.547		24.7716		2389.150	
1/31/01	10.175	53.926	21	01	09	148.9	21.750	36.318	98	36.328		2100.660		25.2990		2386.809	
1/31/01	10.175	53.926	21	01	07	174.9	20.664	36.267	98	36.266		2112.098		25.5510		2378.936	
1/31/01	10.175	53.926	21	01	05	199.7	15.205	35.717	98	35.723		2152.533		26.4849		2350.286	
1/31/01	10.175	53.926	21	01	03	249.5	11.876	35.190	98	35.166		2165.330		26.7423		2327.819	
1/31/01	10.175	53.926	21	01	01	299.1	10.975	35.104	98	35.104		2176.433		26.8616		2314.824	

2/1/01	9.317	51.268	22	01	23	0.5	26.349	36.190	78	36.146	0.040	2031.250	0.480	23.7901	0.030	2372.059	1.111
2/1/01	09.317	51.268	22	01	21	19.5	26.355	36.190	78	36.124		2032.229		23.7720		2381.027	
2/1/01	09.317	51.268	22	01	19	40.4	26.357	36.189	78	36.123		2029.951		23.7706		2373.604	
2/1/01	09.317	51.268	22	01	17	59.8	26.359	36.189	78	36.183		2030.469		23.8152		2372.214	
2/1/01	09.317	51.268	22	01	15	79.3	25.901	36.185	78	36.142		2034.030		23.9281		2374.605	
2/1/01	9.317	51.268	22	01	13	101.4	23.154	36.397	78	36.228	0.035	2088.176	0.994	24.8222	0.027	2380.457	0.566
2/1/01	09.317	51.268	22	01	11	120.7	21.734	36.911	78	36.728		2127.805		25.6079		2406.556	
2/1/01	09.317	51.268	22	01	09	149.1	17.931	36.484	78	36.520		2155.749		26.4551		2382.978	
2/1/01	09.317	51.268	22	01	07	176.5	16.222	36.159	78	36.101		2169.085		26.5444		2361.870	
2/1/01	09.317	51.268	22	01	05	199.7	14.653	35.875	78	35.936		2179.675		26.7710		2348.216	
2/1/01	09.317	51.268	22	01	03	250.1	11.274	35.271	78	35.234		2195.297		26.9081		2327.179	
2/1/01	09.317	51.268	22	01	01	301.6	10.382	35.129	78	35.050		2195.593		26.9252		2311.823	
2/1/01	09.316	51.282	22	12	14	400.7	8.486	34.893	78	34.810		2206.996		27.0508		2304.081	
2/1/01	09.316	51.282	22	12	11	501.7	7.324	34.737	78	34.732		2213.374		27.1624		2304.531	
2/1/01	09.316	51.282	22	12	08	750.9	5.196	34.599	78	34.527		2220.049		27.2775		2307.312	
2/1/01	09.316	51.282	22	12	05	1000.4	5.047	34.800	78	34.721		2210.953		27.4488		2305.571	
2/1/01	09.316	51.282	22	12	02	2000.2	3.491	34.974	78	34.903		2161.111		27.7609		2314.264	
2/2/01	9.301	49.601	23	01	23	1.0	25.266	35.980	70	35.992	0.001	2014.327	0.694	24.0112	0.001	2361.870	2.829
2/2/01	09.301	49.601	23	01	21	20.1	25.266	35.979	70	35.999		2014.194		24.0168		2362.811	
2/2/01	09.301	49.601	23	01	19	40.3	25.276	35.978	70	35.993		2014.847		24.0092		2365.762	
2/2/01	09.301	49.601	23	01	17	60.7	25.275	35.977	70	36.003		2014.657		24.0171		2363.761	
2/2/01	09.301	49.601	23	01	15	81.2	21.905	36.557	70	36.497		2112.464		25.3841		2393.101	
2/2/01	9.301	49.601	23	01	13	100.1	19.720	36.417	70	36.429	0.010	2151.351	0.815	25.9276	0.008	2381.492	1.648
2/2/01	09.301	49.601	23	01	11	120.3	17.158	36.103	70	36.123		2166.201		26.3396		2370.003	
2/2/01	09.301	49.601	23	01	09	150.3	14.111	35.651	70	35.661		2175.050		26.6753		2349.916	
2/2/01	09.301	49.601	23	01	07	175.6	12.965	35.474	70	35.493		2180.941		26.7827		2330.410	
2/2/01	09.301	49.601	23	01	05	200.9	11.448	35.225	70	35.233		2184.705		26.8751		2327.559	
2/2/01	09.301	49.601	23	01	03	251.9	10.555	35.130	70	35.146		2195.107		26.9696		2320.366	
2/2/01	09.301	49.601	23	01	01	300.0	9.557	34.987	70	35.007		2203.671		27.0328		2311.733	
2/3/01	09.583	47.860	24	01	11	400.8	8.057	34.746	58	34.774		2201.974		27.0881		2303.431	
2/3/01	09.583	47.860	24	01	08	500.1	7.415	34.710	58	34.738		2211.777		27.1541		2302.920	
2/3/01	09.583	47.860	24	01	05	750.5	5.694	34.618	58	34.630		2220.735		27.2989		2301.650	
2/3/01	09.583	47.860	24	01	02	1000.5	4.977	34.668	58	34.689		2218.840		27.4315		2318.806	
2/3/01	9.583	47.860	24	04	23	0.2	25.345	36.060	58	36.084	0.013	2019.514	0.640	24.0568	0.010	2365.482	0.297
2/3/01	09.583	47.860	24	04	21	20.5	25.344	36.054	58	36.088		2018.994		24.0601		2363.781	
2/3/01	09.583	47.860	24	04	19	39.9	25.344	36.049	58	36.085		2018.027		24.0578		2366.542	
2/3/01	09.583	47.860	24	04	17	61.2	22.206	36.145	58	36.178		2083.893		25.0565		2375.365	
2/3/01	09.583	47.860	24	04	15	80.2	18.214	36.020	58	36.075		2163.539		26.0435		2365.762	
2/3/01	9.583	47.860	24	04	13	100.4	15.160	35.675	58	35.694	0.011	2172.162	0.341	26.4726	0.009	2344.444	1.443
2/3/01	09.583	47.860	24	04	11	121.0	13.454	35.508	58	35.536		2176.693		26.7163		2329.489	

2/3/01	09.583	47.860	24	04	09	150.1	11.972	35.292	58	35.307		2179.861		26.8336		2326.098	
2/3/01	09.583	47.860	24	04	07	174.8	10.942	35.119	58	35.124		2183.275		26.8832		2316.645	
2/3/01	09.583	47.860	24	04	05	199.5	10.331	35.020	58	35.032		2187.693		26.9201		2312.224	
2/3/01	09.583	47.860	24	04	03	251.1	9.360	34.883	58	34.891		2192.388		26.9746		2306.021	
2/3/01	09.583	47.860	24	04	01	300.1	8.850	34.831	58	34.838		2200.266		27.0156		2304.181	
2/4/01	07.767	48.655	25	01	03	1000.4	4.777	34.646	77	34.678		2218.778		27.4457		2323.657	
2/4/01	07.767	48.655	25	01	07	749.1	5.302	34.607	77	34.628		2221.254		27.3450		2306.492	
2/4/01	07.767	48.655	25	01	11	500.1	6.850	34.655	77	34.688		2212.460		27.1939		2299.749	
2/4/01	07.767	48.655	25	01	15	399.2	7.752	34.729	77	34.735		2208.468		27.1028		2320.416	
2/4/01	07.785	48.583	25	04	01	300.0	9.195	34.909	77	34.912		2202.876		27.0181		2305.851	
2/4/01	07.785	48.583	25	04	03	250.1	10.053	35.023	77	35.031		2191.035		26.9675		2310.473	
2/4/01	07.785	48.583	25	04	05	199.8	11.266	35.204	77	35.216		2188.290		26.8956		2325.628	
2/4/01	07.785	48.583	25	04	07	175.2	12.405	35.408	77	35.426		2185.793		26.8421		2333.961	
2/4/01	07.785	48.583	25	04	09	150.9	13.476	35.519	77	35.556		2182.058		26.7272		2337.452	
2/4/01	07.785	48.583	25	04	11	120.8	17.593	36.208	77	36.234		2166.915		26.3191		2376.255	
2/4/01	7.785	48.583	25	04	13	100.4	20.499	36.446	77	36.486	0.006	2142.636	0.141	25.7634	0.004	2390.000	0.481
2/4/01	07.785	48.583	25	04	15	79.5	24.957	36.339	77	36.408		2049.014		24.4208		2397.472	
2/4/01	07.785	48.583	25	04	17	60.4	25.628	35.931	77	35.950		2005.654		23.8681		2358.389	
2/4/01	07.785	48.583	25	04	19	40.0	25.627	35.929	77	35.924		2005.523		23.8487		2359.540	
2/4/01	07.785	48.583	25	04	21	20.2	25.622	35.932	77	35.979		2004.951		23.8918		2360.580	
2/4/01	7.785	48.583	25	04	23	1.0	25.619	35.932	77	35.952	0.006	2005.747	0.106	23.8724	0.004	2356.699	3.042
2/4/01	07.269	47.728	26	01	17	0.1	26.135	36.066	57	36.088		2015.594		23.8141		2367.702	
2/5/01	06.015	47.147	27	01	03	1001.2	4.837	34.656	101	34.688		2217.877		27.4468		2308.312	
2/5/01	06.015	47.147	27	01	07	750.1	5.313	34.568	101	34.586		2219.863		27.3104		2301.570	
2/5/01	06.015	47.147	27	01	11	500.1	6.907	34.623	101	34.632		2203.237		27.1420		2309.993	
2/5/01	06.015	47.147	27	01	15	400.4	8.043	34.749	101	34.766		2202.052		27.0839		2303.451	
2/5/01	06.042	47.119	27	04	01	300.4	8.902	34.823	101	34.837		2185.581		27.0066		2305.301	
2/5/01	06.042	47.119	27	04	03	250.1	10.256	35.011	101	35.035		2194.484		26.9355		2312.454	
2/5/01	06.042	47.119	27	04	05	200.4	11.714	35.251	101	35.299		2183.979		26.8765		2324.558	
2/5/01	06.042	47.119	27	04	07	175.5	13.773	35.600	101	35.670		2174.130		26.7536		2343.054	
2/5/01	06.042	47.119	27	04	09	150.5	16.201	36.024	101	36.116		2162.533		26.5608		2372.334	
2/5/01	06.042	47.119	27	04	11	120.2	22.692	36.840	101	36.883		2117.484		25.4533		2414.328	
2/5/01	6.042	47.119	27	04	13	100.5	26.335	36.287	101	36.307	0.001	2037.230	0.596	23.9160	0.001	2385.528	9.394
2/5/01	06.042	47.119	27	04	15	80.6	26.490	36.231	101	36.259		2031.222		23.8311		2383.748	
2/5/01	06.042	47.119	27	04	17	60.8	26.490	36.228	101	36.239		2030.908		23.8160		2378.286	
2/5/01	06.042	47.119	27	04	19	40.6	26.485	36.228	101	36.259		2029.655		23.8327		2377.586	
2/5/01	06.042	47.119	27	04	21	20.3	26.482	36.229	101	36.252		2030.983		23.8284		2377.166	
2/5/01	6.042	47.119	27	04	23	0.7	26.478	36.229	101	36.254	0.004	2029.969	0.040	23.8308	0.003	2377.556	1.783
2/6/01	07.293	45.360	29	01	03	1000.3	4.946	34.700	95	34.739		2218.123		27.4747		2310.163	
2/6/01	07.293	45.360	29	01	07	751.8	5.623	34.574	95	34.611		2219.532		27.2926		2295.588	

2/6/01	07.293	45.360	29	01	11	500.2	7.164	34.667	95	34.694		2221.156		27.1551		2314.624	
2/6/01	07.293	45.360	29	01	16	400.4	8.054	34.745	95	34.783		2206.856		27.0956		2311.833	
2/6/01	07.292	45.364	29	03	01	302.7	9.354	34.874	95	34.907		2189.589		26.9881		2305.131	
2/6/01	07.292	45.364	29	03	03	250.9	9.822	34.917	95	34.941		2184.232		26.9366		2308.742	
2/6/01	7.292	45.364	29	03	05	201.1	10.879	35.072	95	35.106	0.028	2177.741	0.353	26.8801	0.021	2315.530	4.393
2/6/01	07.292	45.364	29	03	07	175.2	12.697	35.371	95	35.407		2175.056		26.7697		2332.961	
2/6/01	07.292	45.364	29	03	09	150.3	15.163	35.777	95	35.813		2168.422		26.5637		2351.837	
2/6/01	07.292	45.364	29	03	11	120.1	22.635	36.641	95	36.683		2093.249		25.3178		2407.656	
2/6/01	07.292	45.364	29	03	13	100.2	26.442	36.256	95	36.297		2033.360		23.8750		2389.710	
2/6/01	07.292	45.364	29	03	15	80.2	26.466	36.264	95	36.307		2033.894		23.8749		2384.548	
2/6/01	07.292	45.364	29	03	17	60.3	26.530	36.180	95	36.231		2026.319		23.7973		2373.994	
2/6/01	07.292	45.364	29	03	19	40.1	26.353	36.121	95	36.166		2020.417		23.8043		2370.523	
2/6/01	07.292	45.364	29	03	21	20.1	26.555	36.121	95	36.151		2020.826		23.7290		2371.814	
2/6/01	7.292	45.364	29	03	23	0.4	26.556	36.123	95	36.156	0.002	2019.703	0.968	23.7321	0.002	2375.705	5.517
2/7/01	07.240	43.353	31	01	03	1002.8	4.996	34.773	127	34.797		2211.701		27.5149		2306.212	
2/7/01	07.240	43.353	31	01	07	750.1	5.949	34.656	127	34.676		2225.250		27.3033		2304.471	
2/7/01	07.240	43.353	31	01	11	500.2	8.368	34.818	127	34.848		2218.816		27.0989		2303.150	
2/7/01	07.240	43.353	31	01	15	400.5	8.716	34.795	127	34.827		2194.253		27.0282		2304.121	
2/7/01	07.285	43.329	31	05	01	300.2	9.551	34.900	127	34.916		2195.448		26.9626		2311.933	
2/7/01	07.285	43.329	31	05	03	250.3	10.352	35.001	127	35.025		2184.393		26.9110		2312.134	
2/7/01	07.285	43.329	31	05	05	200.3	12.116	35.283	127	35.314		2180.295		26.8113		2325.908	
2/7/01	07.285	43.329	31	05	07	174.8	14.601	35.657	127	35.670		2168.899		26.5769		2340.853	
2/7/01	07.285	43.329	31	05	09	150.4	18.290	36.161	127	36.183		2155.310		26.1072		2384.958	
2/7/01	07.285	43.329	31	05	11	120.8	24.037	36.550	127	36.670		2088.403		24.8970		2392.841	
2/7/01	07.285	43.329	31	05	13	100.3	26.350	36.133	127	36.177		2021.827		23.8135		2370.313	
2/7/01	07.285	43.329	31	05	15	80.1	26.349	36.136	127	36.179		2021.817		23.8154		2369.893	
2/7/01	07.285	43.329	31	05	17	60.3	26.342	36.137	127	36.144		2023.546		23.7912		2371.164	
2/7/01	07.285	43.329	31	05	19	39.7	26.341	36.138	127	36.163		2021.054		23.8058		2376.125	
2/7/01	07.285	43.329	31	05	21	20.6	26.337	36.138	127	36.168		2022.048		23.8109		2369.833	
2/7/01	7.285	43.329	31	05	23	0.4	26.331	36.139	127	36.160	0.010	2022.182	0.119	23.8067	0.007	2373.724	2.886
2/8/01	08.116	41.475	33	01	03	999.5	4.951	34.734	63	34.745		2216.161		27.4789		2311.063	
2/8/01	08.116	41.475	33	01	07	750.3	5.655	34.638	63	34.660		2222.895		27.3275		2311.013	
2/8/01	08.116	41.475	33	01	11	500.8	7.606	34.762	63	34.779		2226.760		27.1588		2302.600	
2/8/01	08.116	41.475	33	01	15	400.1	8.357	34.802	63	34.832		2218.791		27.0880		2302.690	
2/8/01	08.150	41.455	33	04	01	301.2	9.379	34.911	63	34.927		2205.928		26.9997		2306.222	
2/8/01	08.150	41.455	33	04	03	250.3	9.786	34.947	63	34.976		2197.319		26.9701		2308.672	
2/8/01	08.150	41.455	33	04	05	200.3	10.155	34.963	63	35.002		2186.558		26.9273		2312.554	
2/8/01	08.150	41.455	33	04	07	174.8	10.892	35.062	63	35.085		2179.400		26.8618		2313.974	
2/8/01	08.150	41.455	33	04	09	150.7	12.146	35.289	63	35.296		2183.790		26.7915		2323.657	
2/8/01	08.150	41.455	33	04	11	120.7	14.346	35.659	63	35.677		2184.304		26.6374		2343.684	

2/8/01	8.150	41.455	33	04	13	100.4	16.871	35.978	63	36.021	0.001	2172.866	0.517	26.3296	0.001	2360.380	4.272
2/8/01	08.150	41.455	33	04	15	81.3	22.956	36.166	63	36.191		2071.980		24.8516		2372.794	
2/8/01	08.150	41.455	33	04	17	60.2	25.061	35.960	63	35.981		2017.680		24.0660		2359.990	
2/8/01	08.150	41.455	33	04	19	39.7	25.059	35.963	63	35.984		2016.349		24.0689		2360.880	
2/8/01	08.150	41.455	33	04	21	20.1	25.056	35.965	63	35.988		2015.321		24.0729		2359.740	
2/8/01	8.150	41.455	33	04	23	1.1	25.059	35.966	63	35.996	0.025	2015.504	0.990	24.0780	0.019	2363.656	0.007
2/9/01	09.314	42.016	37	01	03	1001.3	5.127	34.740	86	34.699		2220.100		27.4220		2308.662	
2/9/01	09.314	42.016	37	01	07	750.9	5.774	34.660	86	34.617		2226.137		27.2787		2303.731	
2/9/01	09.314	42.016	37	01	11	500.7	7.270	34.736	86	34.687		2224.106		27.1346		2296.688	
2/9/01	09.314	42.016	37	01	15	399.9	8.127	34.797	86	34.734		2222.102		27.0461		2308.162	
2/9/01	09.338	41.974	37	04	01	301.3	9.304	34.922	86	34.876		2209.774		26.9721		2303.361	
2/9/01	09.338	41.974	37	04	03	250.8	9.701	34.959	86	34.912		2201.291		26.9344		2302.330	
2/9/01	09.338	41.974	37	04	05	200.3	10.397	35.047	86	34.998		2197.052		26.8820		2313.024	
2/9/01	09.338	41.974	37	04	07	175.8	10.923	35.130	86	35.088		2198.533		26.8585		2310.123	
2/9/01	09.338	41.974	37	04	09	149.5	11.953	35.275	86	35.220		2197.933		26.7696		2316.995	
2/9/01	09.338	41.974	37	04	11	120.1	14.474	35.657	86	35.619		2190.952		26.5651		2335.491	
2/9/01	9.338	41.974	37	04	13	100.6	18.418	36.088	86	36.042	0.002	2157.688	0.549	25.9666	0.002	2362.811	1.372
2/9/01	09.338	41.974	37	04	15	80.6	23.734	36.194	86	36.165		2066.585		24.6043		2371.464	
2/9/01	09.338	41.974	37	04	17	59.4	25.695	36.173	86	36.130		2028.687		23.9833		2371.194	
2/9/01	09.338	41.974	37	04	19	40.6	25.783	36.148	86	36.123		2022.998		23.9506		2365.742	
2/9/01	09.338	41.974	37	04	21	20.3	25.781	36.149	86	36.098		2023.091		23.9323		2368.943	
2/9/01	9.338	41.974	37	04	23	0.1	25.777	36.148	86	36.107	0.021	2022.540	0.464	23.9404	0.016	2368.913	0.721
2/10/01	10.995	42.355	39	01	03	1000.4	5.322	34.792	70	34.715		2220.793		27.4115		2309.253	
2/10/01	10.995	42.355	39	01	07	748.4	6.353	34.724	70	34.709		2225.789		27.2772		2306.061	
2/10/01	10.995	42.355	39	01	11	500.7	8.129	34.850	70	34.843		2225.131		27.1314		2302.610	
2/10/01	10.995	42.355	39	01	15	399.4	8.743	34.888	70	34.851		2224.213		27.0428		2301.770	
2/10/01	11.062	42.316	39	05	01	300.4	9.668	34.941	70	34.895		2211.398		26.9266		2303.361	
2/10/01	11.062	42.316	39	05	03	250.8	9.970	34.962	70	34.949		2207.326		26.9177		2305.441	
2/10/01	11.062	42.316	39	05	05	200.8	10.425	35.008	70	34.987		2197.353		26.8686		2307.172	
2/10/01	11.062	42.316	39	05	07	175.4	11.184	35.175	70	35.075		2197.129		26.8009		2314.454	
2/10/01	11.062	42.316	39	05	09	150.5	12.397	35.335	70	35.320		2197.402		26.7613		2327.669	
2/10/01	11.062	42.316	39	05	11	120.8	13.322	35.482	70	35.452		2194.838		26.6784		2329.209	
2/10/01	11.062	42.316	39	05	13	100.7	15.233	35.719	70	35.707	0.011	2183.804	1.507	26.4663	0.009	2339.188	0.460
2/10/01	11.062	42.316	39	05	15	80.1	20.418	35.884	70	35.876		2103.786		25.3200		2354.478	
2/10/01	11.062	42.316	39	05	17	59.9	24.369	35.696	70	35.687		2000.786		24.0532		2340.463	
2/10/01	11.062	42.316	39	05	19	39.6	24.365	35.699	70	35.682		2000.887		24.0506		2345.745	
2/10/01	11.062	42.316	39	05	21	20.4	24.365	35.700	70	35.680		1999.283		24.0491		2342.114	
2/10/01	11.062	42.316	39	05	23	0.4	24.636	35.702	70	35.688	0.011	2000.617	0.234	23.9736	0.009	2343.619	2.271
2/11/01	10.022	44.949	41	01	03	1000.1	5.227	34.783	53	34.815		2213.978		27.5021		2308.332	
2/11/01	10.022	44.949	41	01	07	749.9	6.188	34.699	53	34.747		2223.343		27.3288		2307.732	

2/11/01	10.022	44.949	41	01	11	500.1	8.585	34.907	53	34.939		2222.328		27.1366		2303.971	
2/11/01	10.022	44.949	41	01	15	399.8	9.340	34.943	53	34.967		2221.879		27.0374		2298.349	
2/11/01	10.079	44.921	41	04	01	300.8	10.038	35.042	53	35.081		2215.096		27.0092		2306.692	
2/11/01	10.079	44.921	41	04	03	250.4	10.861	35.155	53	35.189		2211.317		26.9484		2308.482	
2/11/01	10.079	44.921	41	04	05	199.7	11.667	35.261	53	35.291		2204.435		26.8791		2314.014	
2/11/01	10.079	44.921	41	04	07	174.9	12.428	35.367	53	35.399		2199.951		26.8166		2321.337	
2/11/01	10.079	44.921	41	04	09	150.3	13.250	35.476	53	35.489		2194.723		26.7217		2327.409	
2/11/01	10.079	44.921	41	04	11	120.4	14.802	35.788	53	35.913		2182.981		26.7206		2347.065	
2/11/01	10.079	44.921	41	04	13	99.8	16.697	35.979	53	36.028	0.010	2173.013	0.722	26.3767	0.008	2357.114	2.525
2/11/01	10.079	44.921	41	04	15	79.2	18.596	36.110	53	36.135		2151.773		25.9933		2357.159	
2/11/01	10.079	44.921	41	04	17	60.3	21.796	36.172	53	36.192		2100.420		25.1827		2369.363	
2/11/01	10.079	44.921	41	04	19	40.7	25.676	36.120	53	36.161		2018.719		24.0126		2368.713	
2/11/01	10.079	44.921	41	04	21	19.6	25.674	36.124	53	36.165		2018.759		24.0162		2368.693	
2/11/01	10.079	44.921	41	04	23	0.5	25.671	36.125	53	36.172	0.027	2018.766	0.247	24.0224	0.020	2367.117	1.026
2/13/01	10.887	46.966	42	01	03	1000.1	5.169	34.700	79	34.682		2220.790		27.4035		2302.680	
2/13/01	10.887	46.966	42	01	07	748.3	6.119	34.660	79	34.636		2217.909		27.2500		2301.140	
2/13/01	10.887	46.966	42	01	11	499.5	7.500	34.692	79	34.672		2209.411		27.0899		2295.378	
2/13/01	10.887	46.966	42	01	15	399.9	8.372	34.787	79	34.770		2206.177		27.0370		2298.099	
2/13/01	10.921	46.937	42	04	01	300.6	9.497	34.912	79	34.879		2198.486		26.9426		2301.040	
2/13/01	10.921	46.937	42	04	03	250.3	10.128	34.989	79	34.977		2194.845		26.9124		2307.482	
2/13/01	10.921	46.937	42	04	05	200.2	10.951	35.116	79	35.097		2191.792		26.8605		2311.353	
2/13/01	10.921	46.937	42	04	07	175.4	11.781	35.244	79	35.223		2187.080		26.8047		2315.605	
2/13/01	10.921	46.937	42	04	09	149.7	13.042	35.450	79	35.478		2184.106		26.7555		2327.819	
2/13/01	10.921	46.937	42	04	11	120.9	17.079	36.101	79	36.093		2175.940		26.3356		2358.569	
2/13/01	10.921	46.937	42	04	13	100.4	21.205	36.568	79	36.560	0.023	2131.526	0.214	25.6267	0.018	2388.729	0.340
2/13/01	10.921	46.937	42	04	15	80.5	24.779	35.925	79	35.914		2015.569		24.1013		2355.188	
2/13/01	10.921	46.937	42	04	17	60.3	24.795	35.924	79	35.925		2014.521		24.1047		2355.108	
2/13/01	10.921	46.937	42	04	19	40.9	24.791	35.925	79	35.945		2013.536		24.1211		2354.578	
2/13/01	10.921	46.937	42	04	21	20.6	24.787	35.926	79	35.909		2014.245		24.0950		2356.779	
2/13/01	10.921	46.937	42	04	23	0.3	24.781	35.927	79	35.934	0.017	2013.567	2.057	24.1158	0.013	2359.139	0.721
2/14/01	09.701	49.590	44	01	03	999.8	5.145	34.792	60	34.788		2211.259		27.4904		2314.344	
2/14/01	09.701	49.590	44	01	07	750.5	5.404	34.629	60	34.607		2221.432		27.3161		2299.129	
2/14/01	09.701	49.590	44	01	11	500.3	7.053	34.695	60	34.687		2214.444		27.1651		2294.798	
2/14/01	09.701	49.590	44	01	15	400.1	8.486	34.881	60	34.895		2213.235		27.1175		2299.229	
2/14/01	09.753	49.581	44	04	01	300.3	9.175	34.915	60	34.922		2203.371		27.0292		2301.040	
2/14/01	09.753	49.581	44	04	03	250.7	10.089	35.047	60	35.044		2197.790		26.9715		2308.682	
2/14/01	09.753	49.581	44	04	05	200.8	11.422	35.252	60	35.251		2190.568		26.8939		2311.163	
2/14/01	09.753	49.581	44	04	07	175.8	12.940	35.501	60	35.483		2188.269		26.7800		2327.949	
2/14/01	09.753	49.581	44	04	09	150.3	14.000	35.622	60	35.627		2176.504		26.6726		2333.581	
2/14/01	09.753	49.581	44	04	11	120.1	16.876	36.046	60	36.041		2167.730		26.3442		2358.819	

2/14/01	9.753	49.581	44	04	13	100.4	19.113	36.365	60	36.382	0.031	2156.991	1.033	26.0500	0.024	2372.584	2.730
2/14/01	09.753	49.581	44	04	15	80.9	22.342	36.518	60	36.542		2111.450		25.2945		2387.729	
2/14/01	09.753	49.581	44	04	17	61.2	25.344	36.059	60	36.068		2016.506		24.0450		2359.400	
2/14/01	09.753	49.581	44	04	19	40.7	25.354	36.059	60	36.069		2016.945		24.0427		2359.920	
2/14/01	09.753	49.581	44	04	21	20.9	25.350	36.060	60	36.085		2016.819		24.0560		2360.560	
2/14/01	9.753	49.581	44	04	23	0.3	25.349	36.060	60	36.059	0.023	2017.023	0.653	24.0366	0.017	2367.452	0.283
2/15/01	09.002	52.010	46	01	03	1000.3	5.095	34.720	65	34.691		2216.554		27.4194		2312.033	
2/15/01	09.002	52.010	46	01	07	750.5	5.304	34.571	65	34.553		2219.668		27.2853		2297.048	
2/15/01	09.002	52.010	46	01	11	500.5	6.556	34.630	65	34.599		2213.291		27.1635		2299.149	
2/15/01	09.002	52.010	46	01	15	401.1	7.595	34.715	65	34.688		2210.321		27.0888		2295.678	
2/15/01	09.080	51.962	46	04	01	299.3	9.133	34.940	65	34.913		2201.784		27.0289		2304.181	
2/15/01	09.080	51.962	46	04	03	250.7	10.500	35.123	65	35.112		2192.347		26.9529		2312.174	
2/15/01	09.080	51.962	46	04	05	201.9	11.446	35.260	65	35.234		2188.496		26.8762		2322.327	
2/15/01	09.080	51.962	46	04	07	175.3	12.337	35.409	65	35.396		2180.428		26.8321		2330.860	
2/15/01	09.080	51.962	46	04	09	149.8	13.242	35.551	65	35.536		2177.609		26.7598		2334.001	
2/15/01	09.080	51.962	46	04	11	120.5	17.325	36.224	65	36.207		2167.619		26.3637		2368.032	
2/15/01	9.080	51.962	46	04	13	99.5	18.076	36.008	65	36.002	0.023	2133.221	0.495	26.0220	0.017	2357.199	2.447
2/15/01	09.080	51.962	46	04	15	79.6	21.291	36.127	65	36.178		2094.382		25.3125		2368.493	
2/15/01	09.080	51.962	46	04	17	59.8	26.071	36.218	65	36.206		2028.262		23.9232		2371.404	
2/15/01	09.080	51.962	46	04	19	39.8	26.069	36.195	65	36.171		2027.379		23.8975		2376.185	
2/15/01	09.080	51.962	46	04	21	20.7	26.063	36.194	65	36.177		2026.815		23.9039		2373.764	
2/15/01	9.080	51.962	46	04	23	0.4	26.061	36.197	65	36.179	0.011	2027.013	0.399	23.9060	0.009	2375.705	1.287
2/16/01	09.688	55.411	48	07	03	1000.4	5.003	34.796	133	34.759		2210.042		27.4840		2318.116	
2/16/01	09.688	55.411	48	07	07	750.3	5.486	34.607	133	34.579		2220.281		27.2840		2301.010	
2/16/01	09.688	55.411	48	07	11	500.3	7.681	34.720	133	34.687		2203.539		27.0755		2301.310	
2/16/01	09.688	55.411	48	07	15	399.5	9.584	34.961	133	34.935		2198.401		26.9720		2309.002	
2/16/01	09.681	55.409	48	09	01	300.8	12.165	35.301	133	35.265		2171.368		26.7638		2326.188	
2/16/01	09.681	55.409	48	09	03	250.1	14.936	35.740	133	35.690		2163.723		26.5191		2347.225	
2/16/01	09.681	55.409	48	09	05	200.3	18.723	36.161	133	36.144		2134.657		25.9679		2369.563	
2/16/01	09.681	55.409	48	09	07	175.4	20.219	36.300	133	36.323		2120.788		25.7142		2383.158	
2/16/01	09.681	55.409	48	09	09	151.2	23.421	36.280	133	36.267		2086.413		24.7738		2389.430	
2/16/01	09.681	55.409	48	09	11	120.4	26.089	36.291	133	36.271		2037.873		23.9667		2376.955	
2/16/01	09.681	55.409	48	09	13	99.8	26.087	36.292	133	36.272		2038.356		23.9681		2386.319	
2/16/01	09.681	55.409	48	09	15	79.8	26.087	36.293	133	36.257		2037.234		23.9567		2382.317	
2/16/01	09.681	55.409	48	09	17	60.2	26.086	36.294	133	36.267		2036.826		23.9646		2379.856	
2/16/01	09.681	55.409	48	09	19	40.9	26.090	36.294	133	36.249		2036.885		23.9497		2381.217	
2/16/01	09.681	55.409	48	09	21	20.6	26.111	36.294	133	36.260		2036.937		23.9515		2376.365	
2/16/01	09.681	55.409	48	09	23	0.4	26.209	36.298	133	36.271		2036.414		23.9289		2380.237	
2/17/01	10.995	56.279	49	01	03	1000.1	5.318	34.778	106	34.750		2213.315		27.4397		2311.103	
2/17/01	10.995	56.279	49	01	07	750.3	6.035	34.662	106	34.634		2219.431		27.2592		2300.580	

2/17/01	10.995	56.279	49	01	11	500.4	8.531	34.861	106	34.828		2205.113		27.0580		2303.591	
2/17/01	10.995	56.279	49	01	15	400.5	9.122	34.856	106	34.825		2188.545		26.9618		2299.849	
2/17/01	11.022	56.227	49	04	01	300.5	10.821	35.118	106	35.077		2180.945		26.8684		2312.124	
2/17/01	11.022	56.227	49	04	03	249.3	13.748	35.646	106	35.611		2175.112		26.7132		2344.845	
2/17/01	11.022	56.227	49	04	05	200.6	17.717	36.333	106	36.313		2158.853		26.3492		2374.975	
2/17/01	11.022	56.227	49	04	07	175.6	19.235	36.530	106	36.462		2155.965		26.0796		2388.359	
2/17/01	11.022	56.227	49	04	09	150.7	21.004	36.596	106	36.539		2148.042		25.6664		2394.291	
2/17/01	11.022	56.227	49	04	11	120.8	24.048	36.810	106	36.782		2095.249		24.9786		2408.136	
2/17/01	11.022	56.227	49	04	13	100.1	26.083	36.058	106	36.027	0.006	2019.829	0.835	23.7844	0.004	2363.066	0.488
2/17/01	11.022	56.227	49	04	15	80.5	26.090	35.900	106	35.863		2007.030		23.6584		2354.328	
2/17/01	11.022	56.227	49	04	17	60.9	26.076	35.897	106	35.869		2005.552		23.6673		2357.689	
2/17/01	11.022	56.227	49	04	19	40.5	26.073	35.898	106	35.867		2005.786		23.6667		2354.238	
2/17/01	11.022	56.227	49	04	21	20.5	26.067	35.898	106	35.863		2004.003		23.6656		2362.341	
2/17/01	11.022	56.227	49	04	23	0.2	26.061	35.899	106	35.879	0.004	2005.131	0.953	23.6795	0.003	2353.217	0.637
2/18/01	11.499	55.002	51	01	23	0.3	25.939	35.853	77	35.824		1998.802		23.6762		2362.441	
2/19/01	11.429	54.969	51	19	01	300.7	10.234	34.991	77	34.957		2181.220		26.8785		2307.092	
2/19/01	11.429	54.969	51	19	03	250.1	10.710	35.021	77	34.967		2169.005		26.8025		2309.533	
2/19/01	11.429	54.969	51	19	05	199.4	13.260	35.508	77	35.474		2167.351		26.7081		2333.171	
2/19/01	11.429	54.969	51	19	07	175.2	15.468	35.930	77	35.904		2162.781		26.5655		2352.727	
2/19/01	11.429	54.969	51	19	09	150.5	17.976	36.412	77	36.432		2159.486		26.3764		2383.678	
2/19/01	11.429	54.969	51	19	11	120.5	21.723	36.995	77	36.941		2132.570		25.7731		2412.578	
2/19/01	11.429	54.969	51	19	13	100.8	23.090	36.971	77	36.885	0.002	2106.449	1.209	25.3391	0.002	2416.129	0.948
2/19/01	11.429	54.969	51	19	15	80.4	24.780	36.842	77	36.795		2074.258		24.7676		2407.306	
2/19/01	11.429	54.969	51	19	17	59.7	25.952	35.857	77	35.824		1998.113		23.6721		2353.047	
2/19/01	11.429	54.969	51	19	19	39.9	25.948	35.857	77	35.828		1997.873		23.6764		2349.996	
2/19/01	11.429	54.969	51	19	21	20.3	25.949	35.858	77	35.814		1996.803		23.6655		2352.227	
2/19/01	11.429	54.969	51	30	02	3001.0	2.794	34.933	77	34.891		2167.679		27.8170		2319.926	
2/19/01	11.429	54.969	51	30	05	2499.5	3.122	34.954	77	34.919		2163.349		27.8092		2315.815	
2/19/01	11.429	54.969	51	30	08	1998.5	3.588	34.979	77	34.941		2162.420		27.7815		2315.465	
2/19/01	11.429	54.969	51	30	11	1500.2	4.504	35.011	77	34.972		2169.179		27.7097		2311.703	
2/19/01	11.429	54.969	51	30	14	1000.6	5.132	34.745	77	34.711		2215.928		27.4309		2308.742	
2/19/01	11.429	54.969	51	30	17	749.9	5.555	34.603	77	34.554		2220.181		27.2559		2298.319	
2/19/01	11.429	54.969	51	30	20	499.6	7.678	34.762	77	34.727		2210.643		27.1074		2300.089	
2/19/01	11.429	54.969	51	30	22	400.6	8.923	34.901	77	34.865		2202.814		27.0251		2304.561	
2/19/01	11.429	54.969	51	30	24	0.1	26.115	35.913	77	35.884	0.010	2002.503	0.952	23.6664	0.007	2358.714	4.605
2/19/01	11.445	54.966	51	23	23	0.1	25.957	35.868	77	35.858	0.002	1999.340	0.169	23.6958	0.002	2351.352	0.092
2/20/01	11.321	55.038	51	40	22	0.2	25.962	35.846	77	35.804	0.000	1996.331	0.058	23.6539	0.000	2348.666	0.439
7/8/01	11.704	53.801	15	2	3	500.2	8.07	34.84	27	34.784		2211.397		27.094		2306.4	
7/8/01	11.704	53.801	15	2	6	399.8	9.35	35	27	34.95		2206.077		27.022		2309.3	

7/8/01	11.704	53.801	15	2	9	300.2	11.2	35.27	27	35.262		2197.661		26.944	2323.37	
7/8/01	11.704	53.801	15	2	12	200.2	14.55	35.82	27	35.776		2180.423		26.670	2350.77	
7/8/01	11.7077	53.8297	15	6	4	125.6	20.98	36.69	27	36.585	0.002	2145.067	0.369	25.708	2395.752	1.825
7/8/01	11.708	53.830	15	6	8	96.46	24.82	36.48	27	36.452		2049.408		24.496	2392.23	
7/8/01	11.708	53.830	15	6	12	75.1	26.58	36.45	27	36.373		2025.896		23.889	2389.15	
7/8/01	11.708	53.830	15	6	16	49.98	26.69	36.43	27	36.36		2022.539		23.844	2387.91	
7/8/01	11.708	53.830	15	6	20	20.22	27.58	34.95	27	34.881		1958.028		22.444	2306.34	
7/8/01	11.7077	53.8297	15	6	24	1.05	27.57	34.93	27	34.881	0.001	1957.435	0.943	22.447	2302.040	1.075
7/9/01	11.206	50.907	17	2	3	499.7	8.61	34.88	71	34.822		2220.948		27.041	2308.98	
7/9/01	11.206	50.907	17	2	6	401.7	8.86	34.84	71	34.759		2200.75		26.952	2305.13	
7/9/01	11.206	50.907	17	2	9	299.6	9.88	34.98	71	34.935		2201.531		26.922	2308.09	
7/9/01	11.206	50.907	17	2	12	200.2	12.51	35.57	71	35.309		2194.32		26.731	2322.79	
7/9/01	11.2291	50.9262	17	5	4	125.5	20.32	36.44	71	36.388	0.007	2145.546	0.185	25.737	2382.682	1.945
7/9/01	11.229	50.926	17	5	8	95.4	25.7	36.15	71	36.161		2034.442		24.005	2373.5	
7/9/01	11.229	50.926	17	5	12	75.2	27.24	36.15	71	36.102		2010.35		23.473	2368.24	
7/9/01	11.229	50.926	17	5	16	50.5	27.25	36.15	71	36.086		2010.009		23.458	2368.41	
7/9/01	11.229	50.926	17	5	20	20	27.28	36.15	71	36.101		2009.554		23.459	2369.1	
7/9/01	11.2291	50.9262	17	5	24	1.8	27.3	36.15	71	36.115	0.016	2010.089	0.889	23.463	2371.304	2.532
7/10/01	10.619	48.204	19	2	3	500.6	8.36	34.86	39	34.791		2219.573		27.055	2304.57	
7/10/01	10.619	48.204	19	2	6	400.1	9.17	34.93	39	34.814		2215.468		26.945	2303	
7/10/01	10.619	48.204	19	2	9	299.9	10.23	35.05	39	34.914		2209.995		26.846	2312.37	
7/10/01	10.619	48.204	19	2	12	199.8	11.91	35.33	39	35.232		2198.951		26.787	2325.58	
7/10/01	10.6350	48.2286	19	5	4	125.6	17.52	36.04	65	35.940	0.006	2172.712	0.345	26.111	2356.969	0.014
7/10/01	10.635	48.229	19	5	8	90.2	24.36	36.27	65	36.167		2058.747		24.419	2376.11	
7/10/01	10.635	48.229	19	5	12	74.2	25.55	36.37	65	36.242		2035.096		24.113	2381.96	
7/10/01	10.635	48.229	19	5	16	50.2	26.55	36.37	65	36.269		2025.245		23.820	2385.96	
7/10/01	10.635	48.229	19	5	20	20.5	27.12	36.3	65	36.231		2015.815		23.609	2383.34	
7/10/01	10.6350	48.2286	19	5	24	0.67	27.13	36.29	65	36.168	0.005	2016.220	0.163	23.558	2381.427	0.198
7/11/01	9.939	45.482	21	5	1	3000.3	2.71	34.95	42	34.776		2182.632		27.733	2336.45	
7/11/01	9.939	45.482	21	5	3	2496.5	3.08	34.95	42	34.903		2167.75		27.800	2335.75	
7/11/01	9.939	45.482	21	5	5	1997.7	3.49	34.97	42	34.936		2167.077		27.787	2314.04	
7/11/01	9.939	45.482	21	5	7	1499.4	4.32	34.98	42	34.952		2174.375		27.714	2314.74	
7/11/01	9.939	45.482	21	5	9	994.1	5.2	34.78	42	34.757		2218.462		27.459	2310.86	
7/11/01	9.939	45.482	21	5	11	748.2	6.2	34.71	42	34.672		2227.346		27.268	2309.76	
7/11/01	9.9392	45.4816	21	5	13	505.2	8.2	34.85	42	34.822	0.005	2219.785	0.480	27.104	2301.495	0.714
7/11/01	9.939	45.482	21	5	15	401.3	9.2	34.93	42	34.894		2213.608		27.003	2304.72	
7/11/01	9.939	45.482	21	5	17	298.5	9.9	35.01	42	34.997		2212.555		26.967	2307.4	
7/11/01	9.939	45.482	21	5	19	197.6	12.2	35.38	42	35.35		2194.148		26.823	2324.48	
7/11/01	9.939	45.482	21	5	21	175.4	13.3	35.56	42	35.527		2191.53		26.741	2333.66	
7/11/01	9.982	45.476	21	7	2	150.9	14.99	35.8	42	35.788		2190.898		26.583	2350.22	

7/11/01	9.982	45.476	21	7	5	119.5	18.32	36.03	42	36.025		2154.632		25.979	2358.23	
7/11/01	9.9818	45.4756	21	7	8	100.1	21.33	36.38	42	36.358	0.009	2113.240	0.621	25.438	2381.192	1.436
7/11/01	9.982	45.476	21	7	11	79.3	24.35	36.43	42	36.41		2054.227		24.606	2385.86	
7/11/01	9.982	45.476	21	7	14	60.3	26.32	36.29	42	36.314		2018.768		23.926	2378.5	
7/11/01	9.982	45.476	21	7	17	40.2	27.51	35.93	42	35.883		1993.513		23.221	2352.3	
7/11/01	9.982	45.476	21	7	20	19.9	27.79	35.72	42	35.681		1981.63		22.978	2341.32	
7/11/01	9.9818	45.4756	21	7	23	1.8	27.84	35.72	42	35.687	0.004	1981.547	0.814	22.966	2339.363	0.042
7/12/01	9.8989	45.4750	21	17	24	1.1	27.92	35.71	42	35.652	0.028	1980.841	0.358	22.913	2339.463	1.471
7/13/01	9.9318	45.5080	21	23	23	1	27.81	35.78	42	35.723	0.013	1984.770	0.226	23.002	2344.139	0.771
7/14/01	10.3995	45.8137	21	32	24	1.3	27.73	35.82	42	35.763	0.027	1987.023	0.116	23.059	2347.180	1.323
7/19/01	10.492	56.641	23	3	1	1002.1	5.29	34.73	21	34.681		2217.32		27.388	2307.38	
7/19/01	10.492	56.641	23	3	3	747.6	5.74	34.6	21	34.567		2220.755		27.243	2300.35	
7/19/01	10.492	56.641	23	3	5	498.2	7.64	34.74	21	34.701		2208.336		27.092	2300.13	
7/19/01	10.492	56.641	23	3	7	400.9	8.79	34.87	21	34.856		2202.788		27.039	2305.6	
7/19/01	10.492	56.641	23	3	9	300.7	10.94	35.19	21	35.16		2190.676		26.912	2317.54	
7/19/01	10.492	56.641	23	3	11	199.8	15.07	35.88	21	35.848		2175.364		26.611	2349.75	
7/19/01	10.492	56.641	23	3	13	150.2	20.55	36.8	21	36.804		2144.216		25.992	2405.55	
7/19/01	10.492	56.641	23	3	17	125	23.7	37.17	21	37.138		2104.093		25.352	2429.13	
7/19/01	10.4958	56.6165	23	4	1	99	25.66	36.77	21	36.666	0.011	2047.223	0.963	24.399	2402.444	0.212
7/19/01	10.496	56.617	23	4	5	74.8	26.01	36.39	21	36.361		2029.45		24.059	2385.11	
7/19/01	10.496	56.617	23	4	9	51.1	26.63	36.13	21	36.108		2010.498		23.673	2368.85	
7/19/01	10.496	56.617	23	4	13	20.9	28.23	32.34	21	32.439		1777.623		20.398	2157.69	
7/19/01	10.496	56.617	23	4	17	10.8	28.27	32.34	21	32.306		1766.173		20.285	2148.17	
7/19/01	10.4958	56.6165	23	4	21	1.8	28.27	32.34	21	32.311	0.011	1766.968	0.147	20.289	2148.738	0.778
7/20/01	10.4058	56.5310	23	21	24	1.5	28.48	32.3	21	32.265	0.016	1752.251	0.742	20.186	2145.112	0.757
7/21/01	10.329	56.525	23	27	2	200.9	14.31	35.74	21	35.624		2173.136		26.604	2346.17	
7/21/01	10.329	56.525	23	27	6	99	25.09	36.94	21	36.848		2070.384		24.713	2414.48	
7/21/01	10.329	56.525	23	27	10	50.4	26.97	36.27	21	36.157		2014.285		23.601	2379.52	
7/21/01	10.329	56.525	23	27	14	29.9	27.54	35.55	21	35.47		2003.274		22.900	2337.83	
7/21/01	10.329	56.525	23	27	18	9.9	28.44	32.41	21	32.324		1760.196		20.243	2156.72	
7/21/01	10.3285	56.5247	23	27	22	1.7	28.5	32.39	21	32.266	0.044	1756.219	0.172	20.180	2151.299	1.316
7/26/01	11.8082	53.6492	27	1	1	500	7.69	34.75	10	34.726		2208.862		27.105	2297.38	
7/26/01	11.8082	53.6492	27	1	3	400	9.07	34.92	10	34.884		2202.354		27.016	2301.21	
7/26/01	11.8082	53.6492	27	1	5	300	10.73	35.13	10	35.097		2193.057		26.900	2314.75	
7/26/01	11.8082	53.6492	27	1	7	199	13.86	35.6	10	35.574		2186.553		26.661	2338.88	
7/26/01	11.8082	53.6492	27	1	9	99	25.57	36.26	10	36.237	0.003	2039.480	0.719	24.103	2372.284	1.896
7/26/01	11.8082	53.6492	27	1	13	49	27.31	36.21	10	36.185		2016.201		23.513	2369.73	
7/26/01	11.8082	53.6492	27	1	17	20	27.69	34.57	10	34.540		1950.615		22.152	2276.64	
7/26/01	11.8082	53.6492	27	1	21	1	28.64	31.08	10	31.051	0.003	1722.178	0.066	19.223	2078.274	0.863
7/27/01	9.3013	52.8182	29	1	21	0	29.16	28.2	7	28.180	0.004	1636.829	1.090	16.903	1917.630	0.608

7/27/01	9.3013	52.8182	29	1	17	20	27.66	35.74	7	35.537		2007.647		22.912	2333.58	
7/27/01	9.3013	52.8182	29	1	13	50	26.2	36.2	7	36.170		2029.23		23.856	2370.6	
7/27/01	9.3013	52.8182	29	1	9	100	22.49	36.51	7	36.517	0.083	2111.000	0.661	25.233	2395.107	1.464
7/27/01	9.3013	52.8182	29	1	7	199	12.09	35.31	7	35.155		2177.073		26.693	2323.2	
7/27/01	9.3013	52.8182	29	1	5	300	7.62	34.66	7	34.512		2188.854		26.947	2294.39	
7/27/01	9.3013	52.8182	29	1	1	751	5.86	34.64	7	34.600		2222.528		27.254	2298.92	
7/27/01	9.3013	52.8182	29	1	3	499	6.81	34.61	7	34.511		2204.942		27.060	2295.54	
7/28/01	8.4747	49.9075	30	2	21	1	28.89	31.5	5	31.496	0.011	1790.674	0.767	19.474	2102.953	0.821
7/28/01	8.4747	49.9075	30	2	17	20	28.17	35.82	5	35.757		2005.487		22.910	2347.67	
7/28/01	8.4747	49.9075	30	2	13	50	27.46	36.17	5	36.163		2038.22		23.448	2368.95	
7/28/01	8.4747	49.9075	30	2	9	100	23.22	36.6	5	36.504	0.007	2089.891	0.044	25.012	2387.009	2.278
7/28/01	8.4747	49.9075	30	2	7	200	11.72	35.26	5	35.219		2197.103		26.813	2316.7	
7/28/01	8.4747	49.9075	30	2	5	300	9.7	34.95	5	34.924		2207.206		26.944	2307.51	
7/28/01	8.4747	49.9075	30	2	3	500	7.53	34.74	5	34.712		2212.535		27.117	2298.05	
7/28/01	8.4747	49.9075	30	2	1	750	5.39	34.59	5	34.548		2220.578		27.271	2298.39	
7/29/01	6.3778	47.8630	31	2	21	0.5	29.26	32.99	4	32.930	0.052	1839.314	0.651	20.426	2188.252	1.316
7/29/01	6.3778	47.8630	31	2	17	20	28.26	35.94	4	35.918		1994.286		23.002	2352.77	
7/29/01	6.3778	47.8630	31	2	13	50	26.79	36.25	4	36.229		2031.447		23.713	2371.35	
7/29/01	6.3778	47.8630	31	2	9	100	15.3	35.51	4	35.479	0.001	2132.032	0.213	26.276	2331.150	0.410
7/29/01	6.3778	47.8630	31	2	7	200	10.26	34.91	4	34.882		2166.458		26.815	2306.94	
7/29/01	6.3778	47.8630	31	2	5	300	9.33	34.81	4	34.774		2175.947		26.888	2299.2	
7/29/01	6.3778	47.8630	31	2	3	499	7.19	34.62	4	34.585		2199.372		27.066	2291.44	
7/29/01	6.3778	47.8630	31	2	1	751	6.22	34.55	4	34.514		2204.944		27.141	2293.02	
7/30/01	5.1802	45.4158	32	3	23	1	28.92	34.57	8	33.033	0.004	1838.778	0.569	20.616	2188.392	0.920
7/30/01	5.1802	45.4158	32	3	17	20	28.36	35.73	8	35.726		1984.333		22.825	2340.54	
7/30/01	5.1802	45.4158	32	3	13	50	27.1	36.25	8	36.209		2018.57		23.599	2369.96	
7/30/01	5.1802	45.4158	32	3	11	100	19.57	36.06	8	36.021		2146.638		25.655	2357.21	
7/30/01	5.1802	45.4158	32	3	10	120	15.78	35.71	8	35.682	0.008	2158.727	0.361	26.324	2340.663	0.523
7/30/01	5.1802	45.4158	32	3	7	200	10.21	35	8	34.956		2181.953		26.882	2307.29	
7/30/01	5.1802	45.4158	32	3	5	299	8.02	34.73	8	34.695		2194.86		27.032	2297.05	
7/30/01	5.1802	45.4158	32	3	3	499	6.15	34.56	8	34.523		2210.44		27.157	2292.81	
7/30/01	5.1802	45.4158	32	3	1	751	5	34.57	8	34.534		2221.537		27.306	2301.19	
7/31/01	4.6223	42.8430	33	3	21	0	27.94	35.96	48	35.891	0.008	2011.823	0.889	23.086	2355.778	1.245
7/31/01	4.6223	42.8430	33	3	17	20	27.97	36	48	35.941		2014.522		23.115	2363.69	
7/31/01	4.6223	42.8430	33	3	13	50	27.63	36.08	48	36.010		2026.775		23.277	2370.82	
7/31/01	4.6223	42.8430	33	3	9	100	23.29	36.03	48	35.992	0.001	2073.295	0.241	24.603	2366.127	0.516
7/31/01	4.6223	42.8430	33	3	7	200	12.08	35.15	48	35.076		2175.053		26.633	2311.98	
7/31/01	4.6223	42.8430	33	3	5	300	10.02	34.92	48	34.842		2180.504		26.826	2300.88	
7/31/01	4.6223	42.8430	33	3	3	500	7.63	34.66	48	34.595		2202.508		27.011	2295.6	
7/31/01	4.6223	42.8430	33	3	1	750	5.93	34.58	48	34.514		2218.067		27.178	2294.59	

8/1/01	3.3510	43.3137	34	3	24	0	27.06	36.12	92	36.033	0.052	2024.138	0.293	23.479	2371.154	1.740
8/1/01	3.3510	43.3137	34	3	22	20	27.06	36.12	92	35.998		2024.869		23.453	2370.37	
8/1/01	3.3510	43.3137	34	3	20	50	27.06	36.17	92	36.023		2027.689		23.471	2374.22	
8/1/01	3.3510	43.3137	34	3	18	75	26.96	36.2	92	36.064		2031.952		23.534	2374.34	
8/1/01	3.3510	43.3137	34	3	16	100	25.08	36.47	92	36.318	0.033	2060.505	0.972	24.315	2392.158	1.305
8/1/01	3.3510	43.3137	34	3	14	149	17.75	35.9	92	35.768		2110.674		25.923	2358.53	
8/1/01	3.3510	43.3137	34	3	12	200.5	13.36	35.32	92	35.186		2161.472		26.465	2346.38	
8/1/01	3.3510	43.3137	34	3	9	301	11.18	35.04	92	34.879		2173.797		26.649	2308.25	
8/1/01	3.3510	43.3137	34	3	7	499.5	8.57	34.8	92	34.668		2216.031		26.926	2299.88	
8/1/01	3.3510	43.3137	34	3	4	748.8	5.52	34.55	92	34.402		2220.958		27.140	2297.26	
8/1/01	3.3510	43.3137	34	3	1	1000	4.66	34.66	92	34.523		2216.156		27.336	2306.62	
8/1/01	3.2335	43.2450	36	1	23	1	27.19	36.07	93	36.045	0.003	2019.048	0.516	23.446	2364.981	1.358
8/1/01	3.2335	43.2450	36	1	21	20	27.04	36.04	93	36.058		2019.398		23.504	2365.19	
8/1/01	3.2335	43.2450	36	1	19	50	26.87	36.17	93	36.144		2031.153		23.623	2372.81	
8/1/01	3.2335	43.2450	36	1	17	100	25.77	36.43	93	36.411	0.004	2055.634	0.429	24.172	2390.650	4.032
8/1/01	3.2335	43.2450	36	1	15	500	8.76	34.79	93	34.771		2198.229		26.977	2300	
8/1/01	3.2335	43.2450	36	1	13	1000	4.63	34.68	93	34.649		2217.221		27.439	2306.44	
8/1/01	3.2335	43.2450	36	1	11	1500	4.31	34.97	93	34.949		2173.997		27.713	2313.29	
8/1/01	3.2335	43.2450	36	1	9	2000	3.61	34.97	93	34.933		2162.774		27.773	2313.25	
8/1/01	3.2335	43.2450	36	1	7	2500	3.08	34.95	93	34.915		2165.12		27.810	2317.94	
8/1/01	3.2335	43.2450	36	1	5	3000	2.71	34.92	93	34.886		2170.998		27.820	2323.75	
8/1/01	3.2335	43.2450	36	1	3	3497	2.52	34.91	93	34.878		2173.496		27.831	2325.43	
8/1/01	3.2335	43.2450	36	1	1	3997	2.28	34.89	93	34.875		2176.016		27.849	2326.88	
8/2/01	3.5257	45.3148	38	6	24	0	27.55	36.22	71	36.201	0.013	2029.647	0.802	23.447	2371.083	0.170
8/2/01	3.5257	45.3148	38	6	22	20	27.44	36.22	71	36.194		2028.698		23.478	2374.16	
8/2/01	3.5257	45.3148	38	6	20	50	27.39	36.23	71	36.215		2030.467		23.510	2375.19	
8/2/01	3.5257	45.3148	38	6	18	75	27.3	36.23	71	36.209		2033.321		23.534	2371.88	
8/2/01	3.5257	45.3148	38	6	16	100	26.39	36.3	71	36.294	0.001	2044.449	0.232	23.889	2381.712	0.417
8/2/01	3.5257	45.3148	38	6	14	150	15.78	35.64	71	35.610		2126.18		26.268	2339.46	
8/2/01	3.5257	45.3148	38	6	12	200	14.42	35.44	71	35.429		2129.773		26.430	2332.54	
8/2/01	3.5257	45.3148	38	6	9	300	10.95	34.99	71	34.981		2160.159		26.770	2305.86	
8/2/01	3.5257	45.3148	38	6	7	500	7.73	34.71	71	34.684		2201.376		27.066	2300.21	
8/2/01	3.5257	45.3148	38	6	4	750	5.66	34.57	71	34.549		2217.584		27.239	2293.02	
8/2/01	3.5257	45.3148	38	6	1	1000	4.76	34.72	71	34.697		2213.726		27.463	2309.25	
8/3/01	4.9443	49.1508	39	1	24	1	28.71	32.04	11	32.014	0.002	1797.021	3.947	19.921	2135.704	0.849
8/3/01	4.9443	49.1508	39	1	22	19.4	28.1	35.35	11	36.376		1995.23		23.399	2326.29	
8/3/01	4.9443	49.1508	39	1	20	49.5	27.35	36	11	35.987		2024.59		23.351	2363.71	
8/3/01	4.9443	49.1508	39	1	18	74.6	26.77	36.11	11	36.077		2028.319		23.605	2367.29	
8/3/01	4.9443	49.1508	39	1	16	99.6	26.22	36.18	11	36.164	0.004	2033.878	0.633	23.844	2372.669	0.474
8/3/01	4.9443	49.1508	39	1	14	150.5	15.72	35.78	11	35.758		2171.613		26.396	2347.97	

8/3/01	4.9443	49.1508	39	1	12	202.5	11.41	35.13	11	35.106		2168.545		26.783	2317.61	
8/3/01	4.9443	49.1508	39	1	9	301	9.64	34.92	11	34.890		2186.631		26.927	2304.22	
8/3/01	4.9443	49.1508	39	1	7	503	7.12	34.64	11	34.624		2209.086		27.106	2298.9	
8/3/01	4.9443	49.1508	39	1	4	750	5.69	34.58	11	34.574		2219.912		27.255	2302.31	
8/3/01	4.9443	49.1508	39	1	1	1000	4.86	34.62	11	34.598		2217.512		27.373	2307.5	
8/4/01	7.0932	49.1340	41	1	24	0.6	29.04	29.57	6	29.493	0.002	1693.546	0.414	17.924	1996.657	4.499
8/4/01	7.0932	49.1340	41	1	22	19.2	28.22	35.15	6	34.618		1962.581		22.038	2284.85	
8/4/01	7.0932	49.1340	41	1	20	50.4	26.06	36.08	6	35.975		2077.174		23.752	2361.4	
8/4/01	7.0932	49.1340	41	1	18	74.1	22.86	36.12	6	36.029		2096.762		24.756	2367.43	
8/4/01	7.0932	49.1340	41	1	16	98.5	18.58	36.04	6	35.960	0.008	2139.666	0.204	25.863	2365.859	1.213
8/4/01	7.0932	49.1340	41	1	14	149.5	13.57	35.47	6	35.365		2161.069		26.560	2332.05	
8/4/01	7.0932	49.1340	41	1	12	198.6	11.14	35.09	6	34.993		2170.53		26.745	2313.45	
8/4/01	7.0932	49.1340	41	1	9	300.1	9.06	34.82	6	34.707		2181.901		26.879	2302.1	
8/4/01	7.0932	49.1340	41	1	7	498.6	6.88	34.6	6	34.507		2200.6		27.047	2295.52	
8/4/01	7.0932	49.1340	41	1	4	749.5	5.52	34.55	6	34.441		2214.28		27.171	2297.18	
8/4/01	7.0932	49.1340	41	1	1	1000.9	5	34.67	6	34.561		2219.229		27.327	2305.12	
8/5/01	5.4182	51.4075	43	1	17	0.8	28	28.7	2	28.679	0.001	1694.756	0.852	17.652	1930.134	11.586
8/5/01	5.4182	51.4075	43	1	14	5.1	28.32	31.1	2	31.150		1793.512		19.401	2084.7	
8/5/01	5.4182	51.4075	43	1	11	9.9	27.8	36.18	2	36.055		2021.502		23.256	2368.58	
8/5/01	5.4182	51.4075	43	1	8	19.8	27.35	36.24	2	36.172		2032.156		23.490	2385.18	
8/5/01	5.4182	51.4075	43	1	5	30.5	27.25	36.26	2	36.178		2033.815		23.527	2393.61	
8/5/01	5.4182	51.4075	43	1	2	49.5	27.22	36.26	2	36.201	0.012	2034.739	0.235	23.554	2378.421	0.573
8/6/01	7.0253	52.3672	44	1	24	0.9	28.36	31.45	6	31.401	0.006	1776.297	0.517	19.576	2093.439	1.316
8/6/01	7.0253	52.3672	44	1	22	19.9	28.66	35.83	6	35.699		1998.28		22.705	2344.56	
8/6/01	7.0253	52.3672	44	1	20	49.6	27.49	36.18	6	36.127		2031.533		23.411	2373.23	
8/6/01	7.0253	52.3672	44	1	18	75.1	27.37	36.26	6	36.205		2035.026		23.509	2377.53	
8/6/01	7.0253	52.3672	44	1	16	99.7	26.9	36.24	6	36.188	0.020	2040.102	0.558	23.647	2376.720	1.549
8/6/01	7.0253	52.3672	44	1	14	151.4	15.14	35.61	6	35.560		2146.014		26.374	2330.91	
8/6/01	7.0253	52.3672	44	1	12	200	12.39	35.24	6	35.152		2155.468		26.632	2320.98	
8/6/01	7.0253	52.3672	44	1	10	300.6	10.43	35.05	6	34.999		2196.057		26.877	2310.06	
8/6/01	7.0253	52.3672	44	1	7	502.5	7.82	34.75	6	34.684		2208.696		27.053	2296.85	
8/6/01	7.0253	52.3672	44	1	4	752.5	5.45	34.58	6	34.519		2219.821		27.241	2291.64	
8/6/01	7.0253	52.3672	44	1	1	1001.4	4.97	34.77	6	34.708		2210.72		27.447	2306.57	
8/7/01	9.5447	53.6690	46	1	24	0	29.5	32.39	12	32.342	0.011	1809.828	2.530	19.905	2156.331	0.481
8/7/01	9.5447	53.6690	46	1	22	20	28.9	33.13	12	33.116		1852.527		20.686	2164.49	
8/7/01	9.5447	53.6690	46	1	20	50	26.69	36.14	12	36.084		2024.785		23.636	2365.01	
8/7/01	9.5447	53.6690	46	1	18	75	25.19	36.31	12	36.244		2051.188		24.225	2377.06	
8/7/01	9.5447	53.6690	46	1	16	100.7	20.81	36.51	12	36.466	0.008	2143.165	0.167	25.664	2383.108	0.439
8/7/01	9.5447	53.6690	46	1	14	150.1	15.34	35.85	12	35.774		2183.43		26.494	2344.99	
8/7/01	9.5447	53.6690	46	1	12	199.7	11.58	35.24	12	35.157		2200.911		26.791	2312.13	

8/7/01	9.5447	53.6690	46	1	9	300	9.91	34.99	12	34.928		2210.955		26.912	2303.55	
8/7/01	9.5447	53.6690	46	1	7	498.6	8.07	34.8	12	34.748		2210.562		27.066	2297.55	
8/7/01	9.5447	53.6690	46	1	4	748.5	5.79	34.63	12	34.558		2220.455		27.230	2297.22	
8/7/01	9.5447	53.6690	46	1	1	1001.5	5.28	34.76	12	34.694		2214.711		27.400	2305.31	
8/8/01	11.6370	54.5648	48	1	24	0.3	29.14	29.52	3	29.525	0.012	1705.906	0.206	17.916	2002.539	2.037
8/8/01	11.6370	54.5648	48	1	22	20.3	28.08	35.86	3	35.681		1992.206		22.883	2352.97	
8/8/01	11.6370	54.5648	48	1	20	49.9	27.18	36.21	3	36.070		2016.305		23.468	2373.33	
8/8/01	11.6370	54.5648	48	1	18	74.6	26.21	36.22	3	36.103		2029.842		23.802	2374.43	
8/8/01	11.6370	54.5648	48	1	16	99.1	25.59	36.46	3	36.324	0.042	2044.028	0.717	24.162	2389.440	0.863
8/8/01	11.6370	54.5648	48	1	14	151	20.21	36.52	3	36.325		2152.51		25.718	2381.61	
8/8/01	11.6370	54.5648	48	1	12	201.7	15.76	35.92	3	35.770		2178.146		26.396	2353.32	
8/8/01	11.6370	54.5648	48	1	9	305	11.35	35.21	3	35.035		2187.469		26.739	2316.35	
8/8/01	11.6370	54.5648	48	1	7	500	7.08	34.68	3	34.541		2212.467		27.046	2297.1	
8/8/01	11.6370	54.5648	48	1	4	747	5.26	34.61	3	34.452		2220.624		27.211	2302.3	
8/8/01	11.6370	54.5648	48	1	1	1000	5.06	34.78	3	34.609		2211.606		27.358	2309.28	
8/8/01	11.6370	54.5648	48	1	1	1000	5.06	34.78	3	34.609		2211.606		27.358	2308.17	
8/9/01	10.0228	55.9740	49	1	24	0	29.44	33.76	10	33.713	0.001	1894.197	0.859	20.953	2230.506	1.429
8/9/01	10.0228	55.9740	49	1	22	20	27.77	35.78	10	35.670		1992.505		22.976	2343.53	
8/9/01	10.0228	55.9740	49	1	20	50	26.79	36.34	10	36.327		2024.084		23.787	2380.46	
8/9/01	10.0228	55.9740	49	1	18	75	24.96	36.83	10	36.800		2064.621		24.716	2406.92	
8/9/01	10.0228	55.9740	49	1	16	100	21.51	36.6	10	36.551	0.001	2136.329	0.378	25.536	2389.750	0.552
8/9/01	10.0228	55.9740	49	1	14	150	16.43	36.16	10	36.086		2164.836		26.484	2363.92	
8/9/01	10.0228	55.9740	49	1	12	200	13.4	35.61	10	35.544		2183.296		26.734	2335.61	
8/9/01	10.0228	55.9740	49	1	9	299.6	10.25	35.09	10	35.031		2198.541		26.933	2317.29	
8/9/01	10.0228	55.9740	49	1	7	499.3	7.14	34.69	10	34.630		2211.292		27.108	2296.71	
8/9/01	10.0228	55.9740	49	1	4	748.9	5.47	34.62	10	34.542		2220.605		27.257	2311.67	
8/9/01	10.0228	55.9740	49	1	1	1001.5	5.06	34.77	10	34.714		2212.089		27.442	2306.33	
8/10/01	11.8260	56.0552	50	2	24	0.07	29.32	29.08	6	29.075	0.004	1674.688	0.112	17.520	1972.914	0.573
8/10/01	11.8260	56.0552	50	2	21	20.01	27.95	35.8	6	35.756		1992.2		22.982	2347.45	
8/10/01	11.8260	56.0552	50	2	20	50.6	27.14	36.15	6	36.091		2020.525		23.497	2367.93	
8/10/01	11.8260	56.0552	50	2	18	74.6	26.01	36.26	6	36.202		2037.511		23.939	2374.45	
8/10/01	11.8260	56.0552	50	2	16	101.5	23.14	36.54	6	36.485	0.000	2099.987	0.882	25.021	2391.700	4.329
8/10/01	11.8260	56.0552	50	2	14	150.9	18.94	36.63	6	36.560		2146.251		26.231	2394.05	
8/10/01	11.8260	56.0552	50	2	12	202.1	15.06	35.91	6	35.837		2174.702		26.605	2348.28	
8/10/01	11.8260	56.0552	50	2	9	301.3	11.73	35.38	6	35.317		2184.087		26.887	2321.56	
8/10/01	11.8260	56.0552	50	2	7	499.9	7.73	34.8	6	34.733		2209.269		27.104	2298.59	
8/10/01	11.8260	56.0552	50	2	4	748.1	5.73	34.62	6	34.562		2219.291		27.241	2299.33	
8/10/01	11.8260	56.0552	50	2	1	1001.2	5.16	34.76	6	34.704		2213.505		27.422	2308.13	
8/11/01	13.9112	54.0782	51	2	24	0.3	28.76	31.91	14	31.816	0.011	1796.590	0.443	19.757	2130.577	1.691
8/11/01	13.9112	54.0782	51	2	22	20.1	28.06	34.32	14	34.155		1921.132		21.742	2259.21	

8/11/01	13.9112	54.0782	51	2	20	49.9	26.64	36.26	14	36.177		2025.689		23.722	2374.45	
8/11/01	13.9112	54.0782	51	2	18	75.5	25.67	36.69	14	36.587		2047.361		24.336	2402.39	
8/11/01	13.9112	54.0782	51	2	16	99.7	24.67	37.12	14	36.968	0.001	2068.368	0.604	24.932	2426.547	1.408
8/11/01	13.9112	54.0782	51	2	14	149.9	21.71	37.03	14	36.950		2131.737		25.784	2417.87	
8/11/01	13.9112	54.0782	51	2	12	199.3	18.01	36.49	14	36.409		2151.629		26.350	2385.9	
8/11/01	13.9112	54.0782	51	2	9	299.8	14.04	35.84	14	35.715		2173.786		26.732	2346.89	
8/11/01	13.9112	54.0782	51	2	7	500.1	8.87	34.98	14	34.896		2205.839		27.058	2308.52	
8/11/01	13.9112	54.0782	51	2	4	749.8	6.32	34.71	14	34.618		2218.325		27.210	2301.27	
8/11/01	13.9112	54.0782	51	2	1	1000.3	5.39	34.76	14	34.673		2214.473		27.370	2310.51	
8/12/01	11.6355	53.9953	53	2	24	1	29.05	32.76	6	32.675	0.005	1850.913	0.009	20.305	2179.469	0.255
8/12/01	11.6355	53.9953	53	2	22	10.2	28.71	34.91	6	34.049		1908.068		21.449	2250.6	
8/12/01	11.6355	53.9953	53	2	20	19.4	28.32	36.08	6	35.962		2000.047		23.015	2361.91	
8/12/01	11.6355	53.9953	53	2	18	38.7	28.09	36.16	6	36.069		2005.433		23.171	2367.02	
8/12/01	11.6355	53.9953	53	2	16	58.9	27.25	36.34	6	36.249		2014.632		23.581	2383.92	
8/12/01	11.6355	53.9953	53	2	12	99.8	23.97	36.83	6	36.793	0.070	2089.896	0.614	25.010	2405.240	0.290
8/12/01	11.6355	53.9953	53	2	8	199.6	13.27	35.52	6	35.535		2179.441		26.753	2336.47	
8/12/01	11.6355	53.9953	53	2	6	299.8	10.4	35.1	6	35.125		2194.687		26.981	2313.41	
8/12/01	11.6355	53.9953	53	2	4	499.3	8.04	34.82	6	34.836		2215.882		27.139	2302.59	
8/12/01	11.6355	53.9953	53	2	2	751.7	5.54	34.61	6	34.614		2220.482		27.305	2302.3	
8/13/01	11.4992	53.9953	53	17	24	0.5	28.7	31.61	6	31.726	0.045	1801.190	0.916	19.709	2119.143	0.276
8/13/01	11.4992	53.9953	53	17	22	20.6	27.71	36.07	6	36.039		2005.248		23.273	2366.4	
8/13/01	11.4992	53.9953	53	17	20	50.9	26.81	36.25	6	36.287		2022.309		23.750	2376.34	
8/13/01	11.4992	53.9953	53	17	18	75.7	25.62	36.26	6	36.288		2057.276		24.126	2373.92	
8/13/01	11.4992	53.9953	53	17	16	100.6	24.05	36.94	6	36.966	0.004	2088.889	0.200	25.117	2418.119	1.103
8/13/01	11.4992	53.9953	53	17	14	150.3	16.63	36.02	6	36.058		2174.124		26.416	2360.25	
8/13/01	11.4992	53.9953	53	17	12	198.1	13.39	35.57	6	35.601		2183.884		26.780	2333.42	
8/13/01	11.4992	53.9953	53	17	9	301.6	10.22	35.08	6	35.031		2198.002		26.939	2314.57	
8/13/01	11.4992	53.9953	53	17	7	501.1	8.04	34.82	6	34.793		2219.948		27.106	2307.65	
8/13/01	11.4992	53.9953	53	17	4	751.2	5.87	34.64	6	34.663		2220.221		27.303	2305.45	
8/13/01	11.4992	53.9953	53	17	1	998.5	5.22	34.73	6	34.739		2215.245		27.443	2307.55	
8/14/01	12.5080	56.0147	54	3	24	1	28.78	32.56	7	32.522	0.004	1838.336	0.059	20.280	2169.043	3.073
8/14/01	12.5080	56.0147	54	3	22	20.1	27.91	36.1	7	35.958		1999.832		23.147	2368.19	
8/14/01	12.5080	56.0147	54	3	20	50.1	27.41	36.21	7	36.171		2011.632		23.470	2371.75	
8/14/01	12.5080	56.0147	54	3	18	74.5	27.06	36.24	7	36.205		2021.202		23.609	2372.55	
8/14/01	12.5080	56.0147	54	3	16	100.2	25.58	36.54	7	36.376	0.005	2049.153	0.653	24.204	2379.556	0.849
8/14/01	12.5080	56.0147	54	3	14	150.6	21.79	36.98	7	36.954		2128.471		25.764	2403.78	
8/14/01	12.5080	56.0147	54	3	12	200.8	17.78	36.47	7	36.441		2146.882		26.432	2379.62	
8/14/01	12.5080	56.0147	54	3	9	300.7	13.34	35.65	7	35.598		2179.646		26.788	2341.99	
8/14/01	12.5080	56.0147	54	3	7	500.8	8.87	35	7	34.958		2207.174		27.106	2306.1	
8/14/01	12.5080	56.0147	54	3	4	750.3	6.02	34.68	7	34.643		2216.973		27.268	2302.09	

8/14/01	12.5080	56.0147	54	3	1	1003.1	5.16	34.73	7	34.686	2213.707		27.408	2306.3	
4/18/03	11.56	56.48	1	6	23	2	27.55	33.73	10	33.723	1838.718	0.0412	21.582	2239.64	1.7778
4/18/03	11.56	56.48	1	6	20	20.5	26.81	35.95	10	35.935	2009.02		23.485	2365	
4/18/03	11.56	56.48	1	6	17	40.5	26.75	36.02	10	36.007	2011.72		23.558	2367.25	
4/18/03	11.56	56.48	1	6	14	60.5	26.23	36.12	10	36.104	2019.36		23.796	2372.25	
4/18/03	11.56	56.48	1	6	10	80.5	25.91	36.06	10	36.046	2018.113		23.853	2367.96	
4/18/03	11.56	56.48	1	6	8	102.6	26.03	36.45	10	36.435	2057.263		24.109	2391.91	
4/18/03	11.56	56.48	1	6	5	120.5	24.21	36.93	10	36.912	2102.735		25.029	2419.94	
4/18/03	11.56	56.48	1	6	2	149.5	21.27	36.75	10	36.758	2142.468		25.76	2409.39	
4/18/03	11.50	56.50	1	1	22	177.5	18.85	36.55	12	36.546	2149.851		26.243	2394.91	
4/18/03	11.50	56.50	1	1	19	201.5	17.21	36.25	12	36.251	2159.231	0.4062	26.425	2376.81	0.2137
4/18/03	11.50	56.50	1	1	16	297.5	12.29	35.43	12	35.437	2186.605		26.873	2352.27	
4/18/03	11.50	56.50	1	1	13	402.0	9.59	34.99	12	35.002	2203.327		27.023	2313.35	
4/18/03	11.50	56.50	1	1	9	502.5	7.90	34.75	12	34.769	2212.193		27.108	2308.07	
4/18/03	11.50	56.50	1	1	6	751.5	5.86	34.60	12	34.62	2224.47		27.27	2308.51	
4/18/03	11.50	56.50	1	1	2	998.0	5.07	34.68	12	34.707	2215.92		27.435	2310.98	
4/19/03	11.30	54.55	2	3	23	2	27.28	32.44	9	32.444	1792.85	0.0076	20.707	2162.75	5.7275
4/19/03	11.30	54.55	2	3	20	20.2	26.93	35.66	9	35.678	1998.325		23.253	2352.71	
4/19/03	11.30	54.55	2	3	17	40.5	26.86	35.9	9		0				
4/19/03	11.30	54.55	2	3	14	60.5	26.52	36.11	9	36.094	2018.818		23.697	2375.41	
4/19/03	11.30	54.55	2	3	11	79.0	26.11	36.12	9	36.107	2023.684		23.836	2378.69	
4/19/03	11.30	54.55	2	3	8	100.5	25.55	36.72	9	36.661	2069.217		24.429	2391.68	
4/19/03	11.30	54.55	2	3	5	119.5	23.52	36.95	9	36.941	2106.131		25.256	2425.21	
4/19/03	11.30	54.55	2	3	2	151.5	19.31	36.45	9	36.491	2157.935		26.082	2394.8	
4/19/03	11.24	54.59	2	1	22	175.5	18.27	36.38	11	36.386	2164.378		26.268	2385.02	
4/19/03	11.24	54.59	2	1	18	202.5	18.27	36.16	11	36.169	2157.252	2.0246	26.101	2373.32	2.827
4/19/03	11.24	54.59	2	1	16	300.8	10.99	35.16	11	35.159	2192.329		26.902	2324.16	
4/19/03	11.24	54.59	2	1	13	401.0	8.79	34.83	11	34.848	2205.191		27.033	2310.78	
4/19/03	11.24	54.59	2	1	9	501.5	7.41	34.67	11	34.7	2213.961		27.125	2306.17	
4/19/03	11.24	54.59	2	1	6	749.5	5.66	34.56	11	34.58	2223.872		27.264	2307.84	
4/19/03	11.24	54.59	2	1	2	999.5	5.09	34.66	11	34.683	2216.561		27.414	2314.9	
4/20/03	10.81	52.25	4	3	23	1.5	26.68	36.08	55	36.056	2012.149	0.4657	23.618	2374.35	1.5533
4/20/03	10.81	52.25	4	3	20	20.3	26.67	36.08	55	36.044	2012.795		23.612	2374.99	
4/20/03	10.81	52.25	4	3	17	39.5	26.67	36.08	55	36.056	2011.845		23.621	2375.09	
4/20/03	10.81	52.25	4	3	14	60.5	26.22	36.19	55	36.153	2016.207		23.836	2381.43	
4/20/03	10.81	52.25	4	3	11	79.5	26.04	36.23	55	36.243	2027.332		23.961	2386.38	
4/20/03	10.81	52.25	4	3	8	99.5	25.37	36.75	55	36.691	2056.029		24.508	2414.51	
4/20/03	10.81	52.25	4	3	5	119.5	21.49	36.61	55	36.645	2131.359		25.613	2409.3	
4/20/03	10.81	52.25	4	3	2	150.5	19.73	36.67	55	36.662	2152.34		26.103	2406.58	

4/20/03	10.78	52.28	4	1	22	175.5	17.29	36.25	51	36.215	2160.393		26.378	2397.88	
4/20/03	10.78	52.28	4	1	19	199.5	15.51	35.92	51	35.903	2171.628	0.6639	26.555	2361.37	0.3284
4/20/03	10.78	52.28	4	1	16	299.5	10.84	35.11	51	35.11	2191.491		26.891	2322.44	
4/20/03	10.78	52.28	4	1	13	400.5	8.02	34.67	51	34.665	2196.909		27.008	2305.21	
4/20/03	10.78	52.28	4	1	9	499.5	8.28	34.77	51	34.769	2209.151		27.05	2311.09	
4/20/03	10.78	52.28	4	1	6	750.5	5.91	34.58	51	34.589	2221.21		27.239	2310.31	
4/20/03	10.78	52.28	4	1	2	998.5	5.21	34.66	51	34.672	2218.616		27.391	2316.33	
4/21/03	8.87	52.00	5	1	24	1	26.58	36.25	63	36.233	2025.508	0.384	23.783	2385.72	0.565
4/21/03	8.87	52.00	5	1	22	20.5	26.58	36.25	63						
4/21/03	8.87	52.00	5	1	20	41.2	26.59	36.26	63	36.249	2024.941		23.792	2385.87	
4/21/03	8.87	52.00	5	1	18	60.2	26.29	36.29	63	36.235	2035.009		23.876	2385.14	
4/21/03	8.87	52.00	5	1	16	80.5	25.42	36.23	63	36.246	2049.801		24.156	2386.64	
4/21/03	8.87	52.00	5	1	14	100.5	23.67	37.07	63	37.048	2111.545		25.293	2432.35	
4/21/03	8.87	52.00	5	1	12	150.5	17.44	36.33	63	36.329	2160.142		26.429	2384.55	
4/21/03	8.87	52.00	5	1	10	200.2	13.41	35.52	63	35.517	2177.119	0.9803	26.71	2341.62	0.3478
4/21/03	8.87	52.00	5	1	8	301.5	9.59	34.88	63	34.897	2200.832		26.941	2313.21	
4/21/03	8.87	52.00	5	1	6	501.0	7.54	34.65	63	34.667	2218.394		27.08	2304.03	
4/21/03	8.87	52.00	5	1	4	750.5	5.8	34.52	63	34.538	2219.693		27.213	2305.63	
4/21/03	8.87	52.00	5	1	2	1000.5	5.19	34.62	63	34.619	2219.742		27.351	2310.9	
4/22/03	6.95	52.05	6	3	23	2	28.12	26.53	7	26.496	1559.958	0.1596	15.978	1837.86	1.5906
4/22/03	6.95	52.05	6	3	20	19.5	28.17	34.71	7	34.633	1956.458		22.065	2288.67	
4/22/03	6.95	52.05	6	3	17	39.5	26.61	36.15	7	36.098	2049.985		23.672	2376.03	
4/22/03	6.95	52.05	6	3	14	61.0	25.94	36.25	7	36.18	2067.452		23.945	2403.04	
4/22/03	6.95	52.05	6	3	11	80.2	25.01	36.4	7	36.351	2074.513		24.361	2394.73	
4/22/03	6.95	52.05	6	3	8	101.0	19.66	36.21	7	36.149	2121.557		25.729	2385.2	
4/22/03	6.95	52.05	6	3	5	120.5	18.4	36.26	7	36.178	2153.508		26.076	2378.97	
4/22/03	6.88	52.03	6	3	2	151.5	14.3	35.49	7	35.475	2149.613		26.491	2344.32	
4/22/03	6.88	52.03	6	1	22	174.0	13.2	35.31	3	35.255	2151.571		26.551	2330.76	
4/22/03	6.88	52.03	6	1	19	201	12.83	35.38	3	35.326	2177.493	0.6461	26.68	2333.08	2.9812
4/22/03	6.88	52.03	6	1	16	301.5	10.05	35.01	3	34.949	2194.284		26.904	2317.38	
4/22/03	6.88	52.03	6	1	13	401.5	8.31	34.78	3	34.722	2217.45		27.009	2307.28	
4/22/03	6.88	52.03	6	1	9	501.5	7.42	34.71	3	34.66	2221.846		27.092	2305.88	
4/22/03	6.88	52.03	6	1	6	751.5	5.68	34.64	3	34.599	2231.582		27.276	2315.89	
4/22/03	6.88	52.03	6	1	2	1006.5	5.06	34.76	3	34.697	2216.914		27.428	2315.16	
4/23/03	7.03	49.93	8	3	23	2.5	26.87	36.04	66	35.993	2020.146	5.2047	23.51	2369.21	1.091
4/23/03	7.03	49.93	8	3	20	20.5	27.85	36.04	66	35.992	2015.072		23.192	2368.43	
4/23/03	7.03	49.93	8	3	17	39.5	27.85	36.04	66	35.983	2025.867		23.185	2369.28	
4/23/03	7.03	49.93	8	3	14	60.5	27.85	36.05	66	35.971	2015.524		23.176	2369.37	
4/23/03	7.03	49.93	8	3	11	81.0	27.27	36.28	66	36.223	2029.282		23.554	2383.13	
4/23/03	7.03	49.93	8	3	8	101.5	26.38	36.36	66	36.31	2048.827		23.904	2391.49	

4/23/03	7.03	49.93	8	3	5	121.5	23.78	36.47	66	36.403	2086.207		24.771	2398.04	
4/23/03	7.03	49.93	8	3	2	149.5	22.33	36.95	66	36.941	2131.889		25.601	2423.94	
4/23/03	7.00	49.99	8	1	22	174.5	16.31	36.01	66	36.018	2174.772		26.46	2368.14	
4/23/03	7.00	49.99	8	1	19	200.5	12.84	35.37	66	35.342	2183.716	0.9232	26.69	2332.51	0.3358
4/23/03	7.00	49.99	8	1	16	301.0	9.04	34.86	66	34.818	2201.298		26.97	2312.51	
4/23/03	7.00	49.99	8	1	13	400.5	7.41	34.69	66	34.635	2210.158		27.074	2304.46	
4/23/03	7.00	49.99	8	1	9	500.5	6.58	34.62	66	34.568	2215.224		27.136	2303.61	
4/23/03	7.00	49.99	8	1	6	750.5	5.12	34.59	66	34.543	2221.621		27.299	2316.18	
4/23/03	7.00	49.99	8	1	2	998.5	4.6	34.75	66	34.688	2214.824		27.473	2316.11	
4/24/03	8.31	51.68	10	1	24	3.5	28.03	34.04	20	34.042	1924.137	0.4182	21.667	2256.01	0.5658
4/24/03	8.31	51.68	10	1	22	20.4	28.03	34.1	20	34.055	1933.407		21.677	2257.2	
4/24/03	8.31	51.68	10	1	20	40.7	27.31	35.73	20	35.663	1996.311		23.12	2352.68	
4/24/03	8.31	51.68	10	1	19	60.2	26.96	36.1	20	36.053	2013.673		23.526	2375.87	
4/24/03	8.31	51.68	10	1	17	81.2	26.39	36.2	20	36.162	2024.073		23.79	2382.01	
4/24/03	8.31	51.68	10	1	16	99.5	24.75	36.4	20	36.343	2061.396		24.435	2388.81	
4/24/03	8.31	51.68	10	1	13	121.5	21.04	36.53	20	36.488	2145.853		25.618	2400.72	
4/24/03	8.31	51.68	10	1	11	150.0	17.534	36.35	20	36.324	2156.415		26.403	2385.54	
4/24/03	8.31	51.68	10	1	10	200.36	12.991	35.492	20	35.462	2181.958	1.3573	26.753	2338.95	0.544
4/24/03	8.31	51.68	10	1	8	300.0	9.444	34.939	20	34.9	2201.072		26.968	2313.16	
4/24/03	8.31	51.68	10	1	5	602.1	6.651	34.684	20	34.669	2230.33		27.206	2306.32	
4/24/03	8.31	51.68	10	1	2	1002.0	4.98	34.69	20	34.651	2219.575		27.401	2312.99	
4/25/03	9.81	54.08	12	1	24	1.8	27.61	34.37	17	34.326	1903.862		22.015	2272.75	
4/25/03	9.81	54.08	12	1	22	20.2	27.73	34.87	17	35.093	1966.492		22.555	2337.99	
4/25/03	9.81	54.08	12	1	20	40.3	26.83	36.04	17	36	2017.874		23.528	2371.96	
4/25/03	9.81	54.08	12	1	19	60.6	26.58	36.13	17	36.065	2016.183		23.656	2376.19	
4/25/03	9.81	54.08	12	1	17	80.6	26.19	36.21	17	36.197	2026.023		23.879	2380.47	
4/25/03	9.81	54.08	12	1	16	99.2	24.67	36.79	17	36.734	2089.247		24.755	2419.59	
4/25/03	9.81	54.08	12	1	13	120.8	23.48	37.16	17	37.154	2116.702		25.429	2438.3	
4/25/03	9.81	54.08	12	1	11	151.3	19.1	36.53	17	36.479	2151.315		26.128	2394.88	
4/25/03	9.81	54.08	12	1	10	200.5	14.89	35.82	17	35.781	2170.902	0.5989	26.599	2354.89	0.0025
4/25/03	9.81	54.08	12	1	8	300.2	10.15	35.06	17	35.025	2193.202		26.946	2317.99	
4/25/03	9.81	54.08	12	1	5	599.5	6.68	34.65	17	34.599	2222.262		27.147	2312.69	
4/25/03	9.81	54.08	12	1	2	999.5	5.22	34.73	17	34.675	2217.814		27.392	2313.57	
4/26/03	11.08	56.25	14	1	24	3	27.67	33.94	17	33.899	1857.391	0.0694	27.217	2252.96	2.6859
4/26/03	11.08	56.25	14	1	22	19.5	27.1	35.076	16	35.144	1989.537		22.796	2325.49	
4/26/03	11.08	56.25	14	1	20	41.5	26.691	35.981	16	35.987	2013.825		23.562	2370.35	
4/26/03	11.08	56.25	14	1	19	60.5	26.59	36.137	16	36.089	2016.09		23.671	2374.16	
4/26/03	11.08	56.25	14	1	17	80.7	26.31	36.145	16	36.091	2016.821		23.761	2376.3	
4/26/03	11.08	56.25	14	1	16	100.7	25.78	36.263	16	36.207	2024.841		24.015	2382.4	
4/26/03	11.08	56.25	14	1	13	121.0	25.72	36.456	16	36.409	2045.683		24.186	2395.48	

4/26/03	11.08	56.25	14	1	11	150.9	22.79	37.084	16	37.035	2123.296		25.54	2430.53	
4/26/03	11.08	56.25	14	1	10	200.2	18.32	36.353	16	36.309	2161.361	0.228	26.196	2385.61	0.9931
4/26/03	11.08	56.25	14	1	8	300.8	11.45	35.245	16	35.168	2186.878		26.824	2326.05	
4/26/03	11.08	56.25	14	1	5	600.3	6.23	34.655	16	34.618	2220.707		27.221	2310.8	
4/26/03	11.08	56.25	14	1	2	999.5	5.25	34.817	16	34.773	2213.771		27.466	2300.38	
4/29/03	13.00	55.96	15	1	24	1.5	27.42	34.63	8	34.58	1909.755	0.2391	22.269	2289.09	3.4141
4/29/03	13.00	55.96	15	1	22	20.4	27.03	35.983	8	35.921	2004.182		23.404	2368.45	
4/29/03	13.00	55.96	15	1	20	39.5	26.72	36.137	8	36.091	2013.084		23.631	2377.22	
4/29/03	13.00	55.96	15	1	19	59.7	26.65	36.147	8	36.099	2013.414		23.66	2377.18	
4/29/03	13.00	55.96	15	1	17	81.5	26.55	36.193	8	36.146	2013.891		23.727	2382.56	
4/29/03	13.00	55.96	15	1	16	100.2	26.325	36.316	8	36.305	2023.357		23.918	2392.48	
4/29/03	13.00	55.96	15	1	13	119.5	25.65	36.988	8	36.956	2076.27		24.621	2426.34	
4/29/03	13.00	55.96	15	1	11	150.8	20.98	36.681	8	36.632	2146.825		25.744	2405.17	
4/29/03	13.00	55.96	15	1	10	198.5	17.34	36.274	8	36.227	2170.343	0.0608	26.375	2378.2	0.9196
4/29/03	13.00	55.96	15	1	8	299.0	12.61	35	8	35.514	2188.359		26.87	2341.92	
4/29/03	13.00	55.96	15	1	5	600.5	7.025	34.708	8	34.668	2216.652		27.154	2306.62	
4/29/03	13.00	55.96	15	1	2	999.0	5.365	34.778	8	34.731	2215.961		27.419	2323.98	
4/30/03	11.59	55.68	16	1	24	2	27.581	34.564	29	34.524	1932.932	0.2077	22.175	2284.9	1.4335
4/30/03	11.59	55.68	16	1	22	19.7	27.59	34.57	29	34.58	1938.229		22.214	2289.93	
4/30/03	11.59	55.68	16	1	20	41.5	26.82	36.004	29	35.958	2015.463		23.499	2370.33	
4/30/03	11.59	55.68	16	1	19	60.5	26.16	36.085	29	36.052	2019.109		23.779	2373.6	
4/30/03	11.59	55.68	16	1	17	80.6	25.93	36.18	29	36.126	2023.75		23.907	2377.95	
4/30/03	11.59	55.68	16	1	16	101.5	25.55	36.669	29	36.622	2067.962		24.4	2407.92	
4/30/03	11.59	55.68	16	1	13	119.7	23.94	37.033	29	36.978	2109.191		25.159	2427.14	
4/30/03	11.59	55.68	16	1	11	*150.6*	23.94	37.033	29	36.569	2151.688		24.849	2399.42	
4/30/03	11.59	55.68	16	1	10	200.6	16.31	36.162	29	36.13	2165.076		26.546	2371.63	
4/30/03	11.59	55.68	16	1	10	200.6	16.31	36.162	29						
4/30/03	11.59	55.68	16	1	8	301.5	11.96	35.392	29	35.35	2186.098		26.869	2337.2	
4/30/03	11.59	55.68	16	1	5	600.2	6.74	34.661	29	34.619	2216.466		27.155	2303.93	
4/30/03	11.59	55.68	16	1	2	1001.2	5.055	34.687	29	34.634	2235.857		27.379	2314.72	
5/1/03	10.35	55.10	18	1	24	2.5	27.49	33.198	15	33.166	1866.61	1.3897	21.183	2207.96	1.805
5/1/03	10.35	55.10	18	1	22	20.3	27.56	34.48	15	34.432	1950.975		22.112	2279.2	
5/1/03	10.35	55.10	18	1	20	40.8	27.09	35.172	15	35.635	2007.079		23.169	2344.16	
5/1/03	10.35	55.10	18	1	19	60.2	26.72	36.143	15	36.115	2032.964		23.649	2370.7	
5/1/03	10.35	55.10	18	1	17	79.6	25.98	36.202	15	36.144	2053.134		23.905	2373.44	
5/1/03	10.35	55.10	18	1	16	100.3	23.21	36.248	15	36.191	2091.948		24.778	2381.38	
5/1/03	10.35	55.10	18	1	13	120.8	20.53	36.436	15	36.387	2133.028		25.679	2386.61	
5/1/03	10.35	55.10	18	1	11	151.5	18.32	36.427	15	36.381	2156.411		26.251	2384.19	
5/1/03	10.35	55.10	18	1	10	200.4	14.38	35.722	15	35.663	2174.911	4.2055	26.619	2344.47	1.5928
5/1/03	10.35	55.10	18	1	8	301.5	10.51	35.064	15	35.017	2193.606		26.877	2315.23	

5/1/03	10.35	55.10	18	1	5	600.3	6.98	34.662	15	34.618	2220.452		27.121	2301.26	
5/1/03	10.35	55.10	18	1	2	999.5	5.05	34.65	15	34.608	2222.543		27.359	2305.09	
5/2/03	8.35	55.67	20	1	24	1.2	27.72	31.874	15	31.849	1820.861	19.129	20.119	2141.63	2.332
5/2/03	8.35	55.67	20	1	22	19.9	27.72	33.367	15	33.366	1902.671		21.259	2223.31	
5/2/03	8.35	55.67	20	1	20	39.8	27.64	35.576	15	35.562	2014.727		22.937	2345.44	
5/2/03	8.35	55.67	20	1	19	60.7	27.25	36.184	15	36.14	2027.812		23.498	2378.14	
5/2/03	8.35	55.67	20	1	17	80.2	26.678	36.239	15	36.177	2046.831		23.71	2379.14	
5/2/03	8.35	55.67	20	1	16	100.3	25.93	36.161	15	36.107	2027.884		23.893	2374.8	
5/2/03	8.35	55.67	20	1	14	121.7	23.21	36.577	15	36.553	2103.833		25.052	2402.55	
5/2/03	8.35	55.67	20	1	13	150.6	19.52	36.296	15	36.247	2136.035		25.841	2385.01	
5/2/03	8.35	55.67	20	1	11	201.41	17.172	36.207	15	36.162	2159.396	0.2048	26.366	2375.49	0.6192
5/2/03	8.35	55.67	20	1	8	300.9	11.288	35.222	15	35.196	2186.182		26.876	2326.76	
5/2/03	8.35	55.67	20	1	5	601.9	5.711	34.597	15	34.552	2221.979		27.235	2307.26	
5/2/03	8.35	55.67	20	1	2	999.0	5.17	34.793	15	34.742	2211.86		27.451	2335.39	
5/3/03	7.51	54.20	23	1	24	1.2	27.61	27.516	3	27.532	1612.363	0.1812	16.915	1902.12	0.1645
5/3/03	7.51	54.20	23	1	22	10.3	27.66	28.681	3	29.152	1711.051		18.114	1993.25	
5/3/03	7.51	54.20	23	1	20	21.2	27.27	34.92	3	34.669	1950.882		22.384	2296.14	
5/3/03	7.51	54.20	23	1	17	40.5	26.83	36.111	3	36.056	2015.32		23.57	2375.11	
5/3/03	7.51	54.20	23	1	14	59.6	25.98	36.272	3	36.205	2033.313		23.951	2382.9	
5/3/03	7.51	54.20	23	1	11	79.5	24.67	36.663	3	36.62	2087.445		24.669	2407.3	
5/3/03	7.51	54.20	23	1	8	101.7	22.63	36.5	3	36.451	2107.577		25.143	2400.84	
5/3/03	7.51	54.20	23	1	5	150.2	17.86	36.176	3	36.141	2149.392		26.182	2374.24	
5/3/03	7.51	54.20	23	1	2	201.24	13.642	35.555	3	35.511	2168.802	0.1597	26.658	2342.29	1.5807
5/4/03	9.49	55.68	26	1	24	2	27.53	32.768	20	32.728	1854.563	0.8776	20.84	2177.11	6.1815
5/4/03	9.49	55.68	26	1	22	19.7	27.53	32.79	20	32.762	1858.411		20.866	2189.41	
5/4/03	9.49	55.68	26	1	20	39.9	27.51	35.184	20	35.258	1988.167		22.75	2329.05	
5/4/03	9.49	55.68	26	1	19	60.4	26.68	36.188	20	36.072	2026.767		23.63	2376.32	
5/4/03	9.49	55.68	26	1	17	80.6	26.22	36.298	20	36.269	2044.847		23.924	2387.31	
5/4/03	9.49	55.68	26	1	16	100.4	22.99	36.391	20	36.343	2099.736		24.957	2390.35	
5/4/03	9.49	55.68	26	1	14	120.3	20.66	36.363	20	36.332	2131.447		25.602	2390.16	
5/4/03	9.49	55.68	26	1	13	150.8	19.14	36.47	20	36.382	2149.702		26.043	2390.15	
5/4/03	9.49	55.68	26	1	11	199.5	14.95	35.836	20	35.797	2166.708	0.3004	26.599	2354.82	1.1996
5/4/03	9.49	55.68	26	1	8	299.5	10.65	35.129	20	35.088	2189.552		26.908	2321.69	
5/4/03	9.49	55.68	26	1	5	600.7	6.81	34.672	20	34.627	2215.998		27.151	2304.91	
5/4/03	9.49	55.68	26	1	2	1000.5	5.31	34.732	20	34.684	2226.556		27.388	2314.86	
5/5/03	12.21	56.00	28	7	24	1	27.58	34.733	27	34.686	1922.551	0.4692	22.297	2292.51	3.4542
5/5/03	12.21	56.00	28	7	22	20.2	27.52	34.721	27	34.696	1929.17		22.324	2294.14	
5/5/03	12.21	56.00	28	7	21	39.5	26.86	35.901	27	35.835	2007.514		23.394	2365.73	
5/5/03	12.21	56.00	28	7	19	59.8	26.77	35.935	27	35.891	2009.702		23.465	2362.11	
5/5/03	12.21	56.00	28	7	17	81.8	26.46	36.117	27	36.056	2019.102		23.687	2369.57	

5/5/03	12.21	56.00	28	*7*	16	100.8	26.25	36.25	27	36.193	2031.393		23.857	2377.79	
5/5/03	12.21	56.00	28	*7*	14	119.5	25.07	36.874	27	36.867	2087.893		24.733	2421.68	
5/5/03	12.21	56.00	28	*7*	13	150.3	22.38	37.006	27	36.925	2133.175		25.575	2423.75	
5/5/03	12.21	56.00	28	7	11	201.5	16.57	36.165	27	36.133	2168.161	0.5799	26.487	2372.95	1.2556
5/5/03	12.21	56.00	28	*7*	8	300.7	11.16	35.253	27	35.225	2194.564		26.922	2330.17	
5/5/03	12.21	56.00	28	*7*	5	600.8	7.21	34.736	27	34.686	2214.976		27.142	2311.02	
5/5/03	12.21	56.00	28	*7*	2	999.7	5.11	34.687	27	34.651	2218.744		27.386	2313.77	
5/10/03	10.65	54.28	30	1	24	2	27.39	34.498	19	34.46	1942.547	0.0437	22.188	2281.05	1.0409
5/10/03	10.65	54.28	30	1	22	9.8	27.39	34.512	19	34.484	1942.848		22.206	2280.73	
5/10/03	10.65	54.28	30	1	20	19.6	27.26	34.774	19	34.795	1956.331		22.482	2299.59	
5/10/03	10.65	54.28	30	1	18	48.8	26.7	36.191	19	36.149	2018.876		23.681	2377.16	
5/10/03	10.65	54.28	30	1	16	99.5	25.51	36.348	19	36.308	2048.868		24.175	2388.96	
5/10/03	10.65	54.28	30	1	14	120.8	23.41	36.888	19	36.845	2115.316		25.215	2418.74	
5/10/03	10.65	54.28	30	1	11	199.4	15.81	36.024	19	35.987	2169.753	0.0024	26.551	2364.14	1.034
5/10/03	10.65	54.28	30	1	8	502.0	8.41	34.889	19	34.868	2212.917		27.108	2314.38	
5/10/03	10.65	54.28	30	1	5	749.3	6.21	34.686	19	34.645	2222.267		27.245	2310.45	
5/10/03	10.65	54.28	30	1	2	997.0	5.26	34.753	19	34.719	2216.103		27.422	2316.59	
5/11/03	10.70	52.53	32	1	24	2	26.96	34.859	17	34.817	1957.763	0.1674	22.595	2299.82	1.2967
5/11/03	10.70	52.53	32	1	22	19.5	26.88	35.153	17	35.102	1969.885		22.835	2314.54	
5/11/03	10.70	52.53	32	1	20	39.7	26.61	36.268	17	36.219	2021.176		23.763	2384.54	
5/11/03	10.70	52.53	32	1	19	59.4	26.55	36.282	17	36.239	2024.359		23.797	2385.58	
5/11/03	10.70	52.53	32	1	17	79.8	26.32	36.383	17	36.336	2033.265		23.943	2386.67	
5/11/03	10.70	52.53	32	1	16	100.1	25.73	36.342	17	36.295	2030.568		24.097	2384.54	
5/11/03	10.70	52.53	32	1	14	120.4	25.05	36.801	17	36.733	2074.039		24.638	2411.86	
5/11/03	10.70	52.53	32	1	13	149.6	20.09	36.689	17	36.634	2154.33		25.986	2401.91	
5/11/03	10.70	52.53	32	1	11	199.4	14.77	35.798	17	35.744	2190.572	0.4015	26.597	2347.84	0.2786
5/11/03	10.70	52.53	32	1	8	299.5	10.47	35.084	17	35.05	2192.011		26.91	2316.02	
5/11/03	10.70	52.53	32	1	5	600.1	7.18	34.714	17	34.672	2214.149		27.136	2304.5	
5/11/03	10.70	52.53	32	1	2	1000.8	5.1	34.703	17	34.667	2218.343		27.4	2315.8	
5/12/03	10.56	50.07	34	1	24	2	27.15	36.066	38	36.041	2019.295	7.4983	23.456	2371.49	0.4946
5/12/03	10.56	50.07	34	1	22	19.9	27.16	36.077	38	36.052	2024.156		23.461	2372.89	
5/12/03	10.56	50.07	34	1	20	*39.5*	27.16	36.155	38	36.164	2020.534		23.545	2378.29	
5/12/03	10.56	50.07	34	1	19	60.1	26.39	36.509	38	36.472	2039.998		24.024	2399.02	
5/12/03	10.56	50.07	34	1	17	79.2	26.12	36.493	38	36.448	2052.041		24.091	2396.85	
5/12/03	10.56	50.07	34	1	16	100.3	22.45	36.227	38	36.195	2099.668		25	2378.61	
5/12/03	10.56	50.07	34	1	14	119.8	19.18	36.05	38	36.014	2149.1		25.751	2368.59	
5/12/03	10.56	50.07	34	1	13	150.5	16.21	35.95	38	35.917	2181.118		26.406	2360.74	
5/12/03	10.56	50.07	34	1	11	200.5	12.82	35.47	38	35.437	2197.571	0.4531	26.768	2331.22	0.4319
5/12/03	10.56	50.07	34	1	8	301.8	10.05	35.016	38	34.992	2204.358		26.938	2314.44	
5/12/03	10.56	50.07	34	1	5	601.0	6.98	34.729	38	34.698	2218.285		27.184	2310.99	

5/12/03	10.56	50.07	34	1	2	1001.8	5.09	34.753	38	34.724	2213.656		27.446	2315.38	
5/13/03	10.44	48.30	36	1	24	2	27	36.341	65	36.29	2031.046	0.9241	23.692	2386.3	1.4122
5/13/03	10.44	48.30	36	1	22	20.3	27	36.342	65	36.296	2030.765		23.696	2388.18	
5/13/03	10.44	48.30	36	1	20	40.4	27.01	36.342	65	36.288	2030.61		23.687	2387.44	
5/13/03	10.44	48.30	36	1	19	60.8	26.99	36.343	65	36.303	2031.682		23.705	2388.24	
5/13/03	10.44	48.30	36	1	17	79.3	25.88	36.378	65	36.335	2040.748		24.08	2387.41	
5/13/03	10.44	48.30	36	1	16	99.8	23.61	36.426	65	36.432	2102.176		24.843	2394.9	
5/13/03	10.44	48.30	36	1	14	119.5	20.24	36.577	65	36.508	2162.344		25.85	2394.1	
5/13/03	10.44	48.30	36	1	13	149.5	15.04	35.694	65	35.642	2180.123		26.459	2346.99	
5/13/03	10.44	48.30	36	1	11	200.6	12.38	35.374	65	35.344	2188.639	2.0638	26.783	2331.4	3.4383
5/13/03	10.44	48.30	36	1	8	300.3	10.1	35.037	65	34.999	2213.233		26.934	2315.32	
5/13/03	10.44	48.30	36	1	5	599.5	6.75	34.641	65	34.591	2216.576		27.131	2302.9	
5/13/03	10.44	48.30	36	1	2	1000.9	5.118	34.724	65	34.69	2216.62		27.416	2312.21	
5/14/03	8.23	48.49	38	1	24	1.7	27.03	36.054	35	36.015	2014.028	0.907	23.475	2369.92	0.7079
5/14/03	8.23	48.49	38	1	22	20.4	27.04	36.053	35	36.014	2014.552		23.471	2370.57	
5/14/03	8.23	48.49	38	1	20	40.6	26.79	36.214	35	36.018	2013.685		23.554	2369.22	
5/14/03	8.23	48.49	38	1	19	60.7	26.21	36.378	35	36.364	2036.2		23.999	2391.05	
5/14/03	8.23	48.49	38	1	17	80.3	24.96	36.74	35	36.744	2073.469		24.674	2415.06	
5/14/03	8.23	48.49	38	1	16	100.2	19.9	36.424	35	36.389	2154.439		25.85	2388.75	
5/14/03	8.23	48.49	38	1	14	119.3	17.68	36.201	35	36.162	2174.801		26.243	2374.09	
5/14/03	8.23	48.49	38	1	13	149.2	14.14	35.657	35	35.61	2173.942		26.63	2346.22	
5/14/03	8.23	48.49	38	1	11	201.8	11.57	35.198	35	35.176	2184.247	3.1315	26.808	2325.18	0.307
5/14/03	8.23	48.49	38	1	8	300.6	9.4	34.895	35	34.866	2199.709		26.948	2310.42	
5/14/03	8.23	48.49	38	1	5	600.5	6.42	34.608	35	34.575	2224.33		27.163	2303.41	
5/14/03	8.23	48.49	38	1	2	1001.2	4.97	34.701	35	34.665	2217.949		27.413	2313.8	
5/15/03	7.86	50.07	39	1	24	1.5	27.07	35.725	26	35.675	1997.616	1.0623	23.206	2348.36	0.6776
5/15/03	7.86	50.07	39	1	22	19.6	27.07	35.725	26	35.698	1998.962		23.223	2347.63	
5/15/03	7.86	50.07	39	1	20	40.2	26.37	36.377	26	36.333	2032.766		23.925	2387.22	
5/15/03	7.86	50.07	39	1	19	60.2	26.33	36.379	26	36.326	2031.946		23.932	2387.17	
5/15/03	7.86	50.07	39	1	17	79.0	25.19	36.59	26	36.583	2052.132		24.482	2401.81	
5/15/03	7.86	50.07	39	1	16	100.5	22.29	36.843	26	36.776	2123.069		25.487	2414.02	
5/15/03	7.86	50.07	39	1	14	119.0	19.17	36.53	26	36.496	2155.963		26.122	2392	
5/15/03	7.86	50.07	39	1	13	150.7	16.66	36.157	26	36.104	2165.253		26.444	2368.56	
5/15/03	7.86	50.07	39	1	11	198.9	12.15	35.34	26	35.314	2197.473	0.9445	26.805	2325.99	0.2487
5/15/03	7.86	50.07	39	1	8	299.6	9.05	34.853	26	34.808	2202.966		26.96	2305	
5/15/03	7.86	50.07	39	1	5	599.3	6.17	34.594	26	34.558	2218.82		27.182	2304.41	
5/15/03	7.86	50.07	39	1	2	999.5	5.22	34.734	26	34.687	2216.006		27.401	2311.82	
5/16/03	6.68	52.73	41	1	20	1.8	27.99	24.334	7	24.316	1456.846	1.2975	14.389	1705.74	0.3006
5/16/03	6.68	52.73	41	1	15	12.5	28.105	30.707	7	29.144	1692.271		17.967	1971.79	
5/16/03	6.68	52.73	41	1	11	18.4	27.92	35.5	7	35.487	2000.597		22.789	2328.89	

5/16/03	6.68	52.73	41	1	7	35.5	27.13	36.193	7	36.14	2029.885		23.537	2373.07	
5/16/03	6.68	52.73	41	1	2	59.0	26.95	36.276	7	36.236	2040.529		23.667	2376.95	
5/16/03	7.65	54.15	47	1	23	2.7	26.47	27.42	7	26.382	1538.373		16.406	1836.87	
5/16/03	7.65	54.15	47	1	21	9.1	27.34	27.82	7	26.766	1556.947		16.426	1851.85	
5/16/03	7.65	54.15	47	1	19	21.5	27.14	32.54	7	32.561	1860.728		20.84	2170.7	
5/16/03	7.65	54.15	47	1	3	81.0	24.16	37.08	7	37.034	2105.87		25.136	2428.08	
5/16/03	7.65	54.15	47	1	1	130.5	16.5	36.04	7	35.996	2153.734		26.399	2364.12	
5/17/03	8.34	55.62	56	2	24	2.5	27.467	30.985	12	30.962	1782.851	0.5245	19.534	2080.32	0.148
5/17/03	8.34	55.62	56	2	22	10.7	27.48	31.009	12	30.978	1783.487		19.542	2080.15	
5/17/03	8.34	55.62	56	2	20	20.5	27.47	35.332	12	35.273	1998.007		22.774	2326.18	
5/17/03	8.34	55.62	56	2	18	40.0	27.088	36.001	12	35.948	2015.45		23.406	2363.4	
5/17/03	8.34	55.62	56	2	16	60.2	26.526	36.093	12	36.037	2019.381		23.652	2369.93	
5/17/03	8.34	55.62	56	2	14	80.6	26.011	36.406	12	36.326	2063.851		24.033	2387.8	
5/17/03	8.34	55.62	56	2	13	100.6	23.477	36.684	12	36.619	2103.707		25.024	2406.28	
5/17/03	8.34	55.62	56	2	11	120.8	20.605	36.728	12	36.667	2141.091		25.873	2403.78	
5/17/03	8.34	55.62	56	2	10	150.3	18.459	36.421	12	36.362	2154.165		26.202	2387.53	
5/17/03	8.34	55.62	56	2	8	200.32	13.805	35.641	12	35.587	2172.816	0.2321	26.682	2342.94	0.3861
5/17/03	8.34	55.62	56	2	5	500.4	7.103	34.715	12	34.652	2215.336		27.131	2302.87	
5/17/03	8.34	55.62	56	2	2	749.7	5.179	34.603	12	34.537	2221.189		27.287	2303.76	
5/18/03	9.98	57.85	66	5	24	2	27.5	32.841	24	32.807	1873.306	1.2368	20.91	2185.69	0.1306
5/18/03	9.98	57.85	66	5	22	10.4	27.56	32.854	24	32.824	1882.903		20.903	2189.99	
5/18/03	9.98	57.85	66	5	20	20.5	27.56	32.982	24	32.939	1878.73		20.99	2197.15	
5/18/03	9.98	57.85	66	5	18	40.9	27	35.777	24	35.64	2008.647		23.202	2345.61	
5/18/03	9.98	57.85	66	5	16	60.9	26.43	36.117	24	36.07	2021.03		23.708	2372	
5/18/03	9.98	57.85	66	5	14	80.6	25.93	36.228	24	36.192	2037.08		23.957	2376.77	
5/18/03	9.98	57.85	66	5	13	100.1	24.11	36.992	24	36.952	2105.892		25.089	2421.6	
5/18/03	9.98	57.85	66	5	11	119.4	21.43	36.99	24	36.912	2138.14		25.833	2417.81	
5/18/03	9.98	57.85	66	5	10	150.3	17.64	36.346	24	36.306	2151.397		26.363	2376.8	
5/18/03	9.98	57.85	66	5	8	200.7	12.41	35.215	24	35.176	2153.687	1.2904	26.647	2319.41	1.0191
5/18/03	9.98	57.85	66	5	5	496.0	8.04	34.702	24	34.679	2197.615		27.016	2300.37	
5/18/03	9.98	57.85	66	5	2	750.6	6.733	34.703	24	34.66	2216.108		27.188	2304.09	
5/19/03	10.88	54.98	69	3	24	2	27.915	32.04	9	32.013	1837.145	1.2839	20.18	2139.62	1.7736
5/19/03	10.88	54.98	69	3	22	20.9	27.574	33.254	9	33.216	1887.475		21.194	2203.05	
5/19/03	10.88	54.98	69	3	20	39.6	26.913	36.03	9	35.996	2017.626		23.498	2368.18	
5/19/03	10.88	54.98	69	3	19	60.1	26.764	36.164	9	36.134	2018.228		23.65	2375.07	
5/19/03	10.88	54.98	69	3	17	80.8	26.162	36.221	9	36.175	2029.142		23.871	2376.68	
5/19/03	10.88	54.98	69	3	16	100.3	25.689	36.417	9	36.385	2045.813		24.178	2390.16	
5/19/03	10.88	54.98	69	3	14	120.2	24.197	36.923	9	36.879	2102.992		25.007	2422.73	
5/19/03	10.88	54.98	69	3	13	150.1	20.566	36.819	9	36.759	2158.398		25.953	2404.48	
5/19/03	10.88	54.98	69	3	11	200.8	17.523	36.383	9	36.346	2151.947	0.4986	26.422	2379.35	2.6302

5/19/03	10.88	54.98	69	3	8	301.5	11.003	35.202	9	35.158	2192.448	26.899	2320.55
5/19/03	10.88	54.98	69	3	5	599.0	7.063	34.719	9	34.681	2217.613	27.159	2302.59
5/19/03	10.88	54.98	69	3	2	1000.5	5.267	34.781	9	34.753	2212.637	27.448	2311.88

Appendix B: Computer scripts for Matlab, version 6.5.0 (Mathworks, Inc.), for the horizontal mixing model. Note that material in the scripts preceded by % is ignored by Matlab.

Contents and Notes:

mc_dicprojection.m

a) Purpose: Creates input heat, momentum, and freshwater flux files for the PWP code from text files.

b) Source: Sarah Cooley, author

c) Input: plain text file with one header line, containing columns: latitude, longitude, station, cast niskin, depth, CTD temperature, salinity, DIC, s.d. DIC, ALK, s.d. ALK.

d) Output: met_input_file.mat

```
%   mc_dicprojection.m - Solves for R and S, predicts DIC

%   This program applies Monte Carlo methods to solve for R, S, and their
%   error for the MP3 dataset.  After R and S have been solved for, we
%   calculate what DIC value we would expect to see at that
%   station/site and save the output to a file.

%   Sarah Cooley, July 26, 2004

clear all
filename = input ('Space delimited file to be read:','s');

%prescribe variable names from data file
[lat long sta cas nis depth CTDt sal DIC stdevDIC ALK stdevALK] = ...
    textread(filename, '%f %f %f %f %f %f %f %f %f %f %f %f', 'headerlines',1);

% input endmember values
Sr =         input ('salinity of river plume?');
stdevSr =    input ('standard deviation of river plume salinity?');
Ss =        input ('salinity of seawater?');
stdevSs =    input ('standard deviation of seawater salinity?');
Ar =        input ('Alk. of river?');
stdevAr =   input ('stdev. of river alk?');
As =        input ('Alk of seawater?');
stdevAs =   input ('stdev. of seawater alk?')';

% choose random number from normal distribution, multiply to each s.d and
% add to each endemember.

for k= 1:1000;
    Sr1 = randn*stdevSr + Sr;
```

```
    Ss1 = randn*stdevSs + Ss;
    Ar1 = randn*stdevAr + Ar;
    As1 = randn*stdevAs + As;

    C= [Ar1 As1; Sr1 Ss1];

    %Calculate R S, assuming P and E are small

    [m,j]= size (ALK);

    for i= 1:m;
        x= [ALK(i); sal(i)];
        Q1= C\x;     % contains 2 rows and be [r;s] for each comb. of normal
dists.
        result(:,i) = Q1;  %catalogues result in horiz matrix
    end;

    RSprelim= result';; %change results to vertical matrix, 2 col's, R, S

    Rpre= RSprelim(:,1);   %isolate R into own matrix
    Spre= RSprelim(:,2);   %isolate S into own matrix

       % Create matrix for each variable where rows = # original data points(m)
and
    % columns = # of iterations (k)
    Rtot(:,k) = Rpre;
    Stot(:,k) = Spre;
 end  ;
    % Calculate mean and s.d. RSPE for each data point
    Rset = mean(Rtot, 2);
    Sset = mean(Stot, 2);
    sd_Rset = std(Rtot, 0, 2);
    sd_Sset = std(Stot, 0, 2);

    calc_RS = [Rset sd_Rset Sset sd_Sset];

    % Use solved R, S to calculate projected DIC values

    DICr    = input ('Endmember for river DIC?');
    sd_DICr = input ('St. dev. of river DIC endmember?');
    DICs    = input ('Endmember for seawater DIC?');
    sd_DICs = input ('St. dev. of seawater DIC endmember?');

%choose random number from normal distribution, multiply to each s.d and
% add to each endememberm.

for k= 1:1000;
    DICr_1 = randn*sd_DICr + DICr;
    DICs_1 = randn*sd_DICs + DICs;

    %   for the size of the dataset, calculate DIC using perturbed
    %   endmembers and R&S

    [m,j] = size(Rset);
    for i=1:m;
        Rset_1 = randn*sd_Rset + Rset;
        Sset_1 = randn*sd_Sset + Sset;
```

```
        d = DICr_1*Rset_1 + DICs_1* Sset_1;
        % calculate DICproj - DICobs, i.e. biological drawdown
        f = DICr_1*Rset_1 + DICs_1*Sset_1-DIC;
        A(:,k) = d;
        B(:,k) = f;
    end

 end

    %Clear out some unused variables
    clear  m, j, Q1, C, x, Rpre, Spre, result, RSprelim,


    % Calculate mean and s.d. RSPE for each data point
DIC_proj = mean(A,2);
sd_DIC_proj = std(A, 0, 2);
DIC_bio = mean(B,2);
sd_DIC_bio = std(B,0,2);

% apply 95% c.i. to s.d.'s, so can plot 95% c.i.
tcrit = 1.962343958;     % from excel (tinv(0.05, 999)), assumes 95% c.i. and
999 d.f.

CI_95 = tcrit*sd_DIC_proj;  %calc. 95% c.i. for each DICproj point
CI_bio_95 = tcrit*sd_DIC_bio/sqrt(k);   %calc. 95% c.i. for each DICbio
(biological drawdown)
output = [lat long sta cas nis depth CTDt sal DIC stdevDIC ALK stdevALK...
        Rset sd_Rset Sset sd_Sset DIC_proj sd_DIC_proj CI_95 DIC_bio sd_DIC_bio
CI_bio_95];

    figure
    plot(sal, DIC, 'ko');
    hold on
    errorbar(sal, DIC_proj, CI_95, 'r^');
    xlabel('Salinity (pss)');
    ylabel('DIC (\mumol C/kg SW)');
    str1(1) = {['Ar= ',num2str(Ar), ' {\pm} ', num2str(stdevAr)]};
    str1(2) = {['Sr= ',num2str(Sr), ' {\pm} ', num2str(stdevSr)]};
    str1(3) = {['DICr= ',num2str(DICr), ' {\pm} ', num2str(sd_DICr)]};
    str1(4) = {['As= ',num2str(As), ' {\pm} ', num2str(stdevAs)]};
    str1(5) = {['Ss= ',num2str(Ss), ' {\pm} ', num2str(stdevSs)]};
    str1(6) = {['DICs= ',num2str(DICs), ' {\pm} ', num2str(sd_DICs)]};
v=axis;

    text(v(1,1)+0.2, v(1,4)-50, str1)

str2(1) = {'O = DIC observed'};
str2(2) = {'{\Delta} = DIC projected'};
str2(3) = {'Errorbars represent 95% c.i.'};

text (v(1,2)-2, v(1,3)+30, str2)
station_num = num2str(sta);
text(sal, DIC, station_num, 'HorizontalAlignment', 'Center',
'VerticalAlignment', 'Top')

hold off
```

```
    figure
    hold on
    plot ([27 37], [0 0]);
    errorbar(sal, DIC_bio, CI_bio_95, 'k^');
    xlabel('Salinity (pss)');
    ylabel('Biological drawdown of DIC (\mumol C/kg SW)');
    text(sal, DIC_bio, station_num, 'HorizontalAlignment', 'Right',
'VerticalAlignment', 'Top')
str1(1) = {['Ar= ',num2str(Ar), ' {\pm} ', num2str(stdevAr)]};
    str1(2) = {['Sr= ',num2str(Sr), ' {\pm} ', num2str(stdevSr)]};
    str1(3) = {['DICr= ',num2str(DICr), ' {\pm} ', num2str(sd_DICr)]};
    str1(4) = {['As= ',num2str(As), ' {\pm} ', num2str(stdevAs)]};
    str1(5) = {['Ss= ',num2str(Ss), ' {\pm} ', num2str(stdevSs)]};
    str1(6) = {['DICs= ',num2str(DICs), ' {\pm} ', num2str(sd_DICs)]};
v=axis;

    text(v(1,1)+0.2, v(1,4)-50, str1)
    hold off

        save projectedDIC.out output -ascii;
```

Appendix C, Table 1: Salinity, alkalinity, and calculated quantities, with their standard deviations, for each bottle with 28<S<35 used in Chapter 2. Data are sorted by increasing salinity. See Chapter 2 Methods for explanations of each quantity and error propagation.

	Salinity	ALK (μmol kg^{-1})	*r*	s.d.	*s*	s.d.	A_r	s.d.	DIC_r	s.d.	DIC_{exp}	s.d.	ΔDIC_{bio}	s.d.
Summer 2001	28.180	1917.63	0.2172	0.0022	0.7828	0.0022	289.41	32.21	352.94	39.28	1661.48	8.54	24.64	8.58
	28.679	1930.13	0.2033	0.0023	0.7967	0.0023	209.63	35.51	255.65	43.30	1664.79	8.72	-29.98	8.74
	29.075	1972.91	0.1923	0.0023	0.8077	0.0023	307.17	36.74	374.60	44.80	1707.33	8.69	32.62	8.71
	29.493	1996.66	0.1807	0.0023	0.8193	0.0023	304.36	39.35	371.18	47.99	1726.22	8.65	32.67	8.71
	29.525	2002.54	0.1798	0.0023	0.8202	0.0023	328.96	38.92	401.17	47.46	1732.90	8.82	26.99	8.85
	31.051	2078.27	0.1374	0.0024	0.8626	0.0024	248.53	56.29	303.08	68.64	1788.38	9.27	66.16	9.33
	31.401	2093.44	0.1277	0.0025	0.8723	0.0025	209.35	60.50	255.31	73.78	1798.23	9.29	21.92	9.32
	31.496	2102.95	0.1251	0.0025	0.8749	0.0025	238.11	61.40	290.38	74.88	1807.65	9.29	16.97	9.28
	31.726	2119.14	0.1187	0.0025	0.8813	0.0025	256.79	63.29	313.15	77.18	1821.76	9.46	20.56	9.53
	31.816	2130.58	0.1162	0.0025	0.8838	0.0025	311.07	69.37	379.36	84.60	1833.13	9.86	36.55	9.89
	32.014	2135.70	0.1107	0.0025	0.8893	0.0025	256.55	72.75	312.87	88.72	1835.13	9.90	38.09	9.84
	32.265	2145.11	0.1037	0.0025	0.8963	0.0025	206.10	76.33	251.35	93.09	1840.59	9.18	88.33	9.18
	32.266	2151.30	0.1037	0.0025	0.8963	0.0025	267.14	75.86	325.78	92.51	1848.55	9.96	92.34	9.99
	32.306	2148.17	0.1026	0.0025	0.8974	0.0025	209.86	75.87	255.92	92.52	1843.20	9.09	77.02	9.11
	32.311	2148.74	0.1024	0.0025	0.8976	0.0025	216.15	79.64	263.59	97.12	1844.39	9.66	77.41	9.64
	32.324	2156.72	0.1021	0.0025	0.8979	0.0025	284.15	75.63	346.52	92.24	1853.05	9.63	92.84	9.65
	32.342	2156.33	0.1016	0.0025	0.8984	0.0025	268.54	78.94	327.49	96.27	1852.48	9.99	42.66	10.05
	32.439	2157.69	0.0989	0.0026	0.9011	0.0026	227.59	82.49	277.55	100.59	1851.80	9.75	74.19	9.79
	32.522	2169.04	0.0966	0.0026	0.9034	0.0026	295.90	82.30	360.85	100.37	1864.01	9.79	25.70	9.83
	32.675	2179.47	0.0923	0.0026	0.9077	0.0026	309.28	85.49	377.17	104.26	1872.47	9.70	21.58	9.72
	32.930	2188.25	0.0852	0.0026	0.9148	0.0026	239.74	99.24	292.36	121.03	1877.01	10.23	37.69	10.22
	33.033	2188.39	0.0824	0.0026	0.9176	0.0026	166.56	100.55	203.12	122.62	1874.94	10.26	36.15	10.28
	33.713	2230.51	0.0635	0.0027	0.9365	0.0027	177.25	132.50	216.16	161.59	1909.62	9.92	15.46	9.96
	34.881	2302.04	0.0310	0.0027	0.9690	0.0027	186.04	279.35	226.88	340.67	1969.60	10.29	12.15	10.34
	34.881	2306.34	0.0310	0.0027	0.9690	0.0027	316.97	274.16	386.55	334.34	1974.32	10.21	16.26	10.25
						mean	253.25		308.84				39.88	
						s.d.	47.67		58.13				30.04	
						n	25		25				25	
						s.e.	9.53		11.63				6.01	

Appendix D, Table 1: Surface mixed layer data with 28<S<35, sorted by increasing salinity, used to calculate quantities in Chapter 3. Fall 1995 and Spring 1996 data were originally published by Ternon et al., (1999), and obtained from the IFREMER FTP site (www.ifremer.fr) on 9/24/04. *f*CO_2 values in bold were not measured in the original datasets (usually because they were slightly below the surface; values listed were calculated using CO2SYS (Lewis and Wallace, 1998; see Chapter 3 Methods). Spring 2003 pCO_2 values are average underway pCO_2 values measured while on station.

	Yearday	Latitude (degrees)	Longitude (degrees)	Station	Cast	Niskin	Depth (m)	Temp. (ºC)	Salinity	DIC (µmol kg^{-1})	ALK (µmol kg^{-1})	*f*CO_2 (pCO_2, Spring 2003)
Fall 1995	254	6.863833	50.54167	10			0.596658	29.654	29.971	1680.9	2062.8	**221.3**
	252	5.674167	51.555	1			2.18779	27.935	31.099	1698.8	2075.8	**221.6**
	259	7.4995	39.99733	29			1.49162	29.645	31.345	1769.7	2092.7	316.6
	260	7.497167	38.66367	31			1.093856	29.754	31.504	1788.1	2120	319.7
	257	7.499333	45.33567	20			0	29.3	31.956	1796.1	2121.9	317.3
	280	8.394167	40.84567	84			1.690464	29.038	32.031	1805.6	2134	321.9
	261	7.5	37.33233	33			0.994415	29.216	32.354	1824.6	2161.6	326.6
	279	7.500833	41.345	82			0.696091	28.968	32.391	1784.5	2110.9	324.9
	279	7.059833	41.58333	81			2.98326	28.837	32.534	1838.6	2169	326.5
	257	7.498167	44.00267	22			0.994415	29.376	32.56	1809.7	2136.7	327.5
	256	7.5	46.66617	18			0.397766	29.313	32.64	1819.6	2160.4	326
	253	5.834667	51.41333	2			1.193339	28.182	33.009	1838	2192	**298.2**
	258	7.501667	42.67017	19			1.193297	28.917	33.204	1874.7	2215.1	330.7
	262	7.502667	34.99767	37			0.099442	28.749	33.303	1857.5	2192.9	331
	253	5.9725	51.29833	6			1.292781	28.277	33.314	1851.4	2205.7	**305.2**
	254	7.498667	50	12			0.994415	29.92	33.788	1857.6	2221.4	**321.3**
	255	7.504167	47.995	16			0	29.858	33.854	1872.4	2236.6	**325.4**
	253	5.876	51.38	4			1.292783	28.066	34.015	1889.4	2247.6	**316.4**
	255	7.501667	49.001	14			0.994415	29.662	34.145	1897.3	2254.4	**342**
	278	5.8925	42.20033	79			1.491671	29.663	34.623	1941.9	2301.2	356.2
	261	7.5	36	35			0.894973	28.716	34.672	1929.1	2287.9	341.3
Spring 1996	127	1.619333	44.45183	70			1.591198	29.077	32.169	1809.6	2121.8	349.5
	128	2.217333	44.133	71			1.491743	28.604	32.894	1865.2	2189.6	346.6
	127	0.416833	45.1015	66			1.889553	28.485	33.147	1872.8	2187.9	363.4

	127	1.035667	44.76783	69			1.193402	29	33.245	1882.9	2209.1	367.2
	127	0.620667	45.00017	68			1.193404	28.569	33.256	1905.2	2223	379.3
	127	0.499667	45.04933	67			2.5857	28.4	33.414	1902.3	2218.3	384.3
	128	3.235	43.60117	74			0.696142	28.068	33.416	1893.2	2218.1	334.2
Summer 2001	209	9.3013	52.8182	29	1	21	0	29.16	28.18	1636.829	1917.63	**293.1**
	218	5.4182	51.4075	43	1	17	0.8	28	28.679	1694.756	1930.134	**373**
	223	11.826	56.0552	50	2	24	0.07	29.32	29.075	1674.688	1972.914	**292.5**
	217	7.0932	49.134	41	1	24	0.6	29.04	29.493	1693.546	1996.657	**293**
	221	11.637	54.5648	48	1	24	0.3	29.14	29.525	1705.906	2002.539	**306.4**
	208	11.8082	53.6492	27	1	21	1	28.64	31.051	1722.178	2078.274	**252.1**
	219	7.0253	52.3672	44	1	24	0.9	28.36	31.401	1776.297	2093.439	**310.3**
	210	8.4747	49.9075	30	2	21	1	28.89	31.496	1790.674	2102.953	**328.7**
	226	11.4992	53.9953	53	17	24	0.5	28.7	31.726	1801.19	2119.143	**323.6**
	224	13.9112	54.0782	51	2	24	0.3	28.76	31.816	1796.59	2130.577	**304.2**
	216	4.9443	49.1508	39	1	24	1	28.71	32.014	1797.021	2135.704	**300.8**
	202	10.4058	56.531	23	21	24	1.5	28.48	32.265	1752.251	2145.112	**234.8**
	203	10.3285	56.5247	23	27	22	1.7	28.5	32.266	1756.219	2151.299	**234.1**
	201	10.496	56.617	23	4	17	10.8	28.27	32.306	1766.173	2148.168	**245.8**
	201	10.4958	56.6165	23	4	21	1.8	28.27	32.311	1766.968	2148.738	**246.5**
	203	10.329	56.525	23	27	18	9.9	28.44	32.324	1760.196	2156.721	**233.8**
	220	9.5447	53.669	46	1	24	0	29.5	32.342	1809.828	2156.331	**307.8**
	201	10.496	56.617	23	4	13	20.9	28.23	32.439	1777.623	2157.691	**251.1**
	227	12.508	56.0147	54	3	24	1	28.78	32.522	1838.336	2169.043	**328.1**
	225	11.6355	53.9953	53	2	24	1	29.05	32.675	1850.913	2179.469	**340**
	211	6.3778	47.863	31	2	21	0.5	29.26	32.93	1839.314	2188.252	**316.7**
	212	5.1802	45.4158	32	3	23	1	28.92	33.033	1838.778	2188.392	**312.3**
	222	10.0228	55.974	49	1	24	0	29.44	33.713	1894.197	2230.506	**360.3**
	190	11.708	53.83	15	6	20	20.22	27.58	34.881	1958.028	2306.342	**351.4**
	190	11.7077	53.8297	15	6	24	1.05	27.57	34.881	1957.435	2302.04	**355.8**
Spring 2003	138	8.34	55.62	56	2	24	2.5	27.467	30.9615	1782.851	2080.325	30.9615
	138	8.34	55.62	56	2	22	10.7	27.48	30.978	1783.487	2080.155	**30.978**
	123	8.35	55.67	20	1	24	1.2	27.72	31.849	1820.861	2141.626	31.849

140	10.88	54.98	69	3	24	2	27.915	32.013	1837.145	2139.615	32.013
110	11.3	54.55	2	3	23	2	27.28	32.4435	1792.85	2162.752	32.4435
125	9.49	55.68	26	1	24	2	27.53	32.7275	1854.563	2177.11	32.7275
125	9.49	55.68	26	1	22	19.7	27.53	32.762	1858.411	2189.412	**32.762**
139	9.98	57.85	66	5	24	2	27.5	32.807	1873.306	2185.693	32.807
139	9.98	57.85	66	5	22	10.4	27.56	32.824	1882.904	2189.992	**32.824**
139	9.98	57.85	66	5	20	20.5	27.56	32.939	1878.73	2197.155	**32.939**
122	10.35	55.1	18	1	24	2.5	27.49	33.166	1866.61	2207.961	33.166
109	11.56	56.48	1	6	23	2	27.55	33.723	1838.718	2239.644	33.723
117	11.08	56.25	14	1	24	3	27.67	33.899	1857.391	2252.959	33.899
115	8.31	51.68	10	1	24	3.5	28.03	34.042	1924.137	2256.01	34.042
116	9.81	54.08	12	1	24	1.8	27.61	34.326	1903.862	2272.754	34.326
131	10.65	54.28	30	1	24	2	27.39	34.4595	1942.547	2281.053	34.4595
131	10.65	54.28	30	1	22	9.8	27.39	34.484	1942.848	2280.733	**34.484**
121	11.59	55.68	16	1	24	2	27.581	34.524	1932.932	2284.899	34.524
120	13	55.96	15	1	24	1.5	27.42	34.58	1909.755	2289.091	34.58
121	11.59	55.68	16	1	22	19.7	27.59	34.58	1938.229	2289.926	**34.58**
126	12.21	56	28	7	24	1	27.58	34.686	1922.551	2292.512	34.686
126	12.21	56	28	7	22	20.2	27.52	34.696	1929.17	2294.137	**34.696**
132	10.7	52.53	32	1	24	2	26.96	34.817	1957.763	2299.819	34.817

Appendix 2, Table 2: Salinity, alkalinity, and calculated quantities, with their standard deviations, for each bottle with 28<S<35 used in Chapter 3. Data are sorted by increasing salinity. See Chapter 3 Methods for explanations of each quantity and error propagation.

	Salinity	ALK (μmol kg^{-1})	*r*	s.d.	*s*	s.d.	A_r	s.d.	DIC_r	s.d.	DIC_{exp}	s.d.	ΔDIC_{bio}	s.d.	fCO_{2exp}
F95	29.971	2062.8	0.1684	0.0050	0.8316	0.0050	558.73	98.48	681.38	120.10	1790.34	23.45	109.44	23.45	382.3
	31.099	2075.8	0.1371	0.0052	0.8629	0.0052	236.43	134.97	288.33	164.60	1777.49	25.12	78.69	25.12	326.2
	31.345	2092.7	0.1303	0.0052	0.8697	0.0052	256.06	148.31	312.27	180.87	1792.90	24.86	23.20	24.86	354.8
	31.504	2120	0.1259	0.0052	0.8741	0.0052	403.08	145.68	491.56	177.66	1823.58	25.54	35.48	25.54	374.1
	31.956	2121.9	0.1133	0.0053	0.8867	0.0053	204.57	172.57	249.48	210.45	1815.23	26.79	19.13	26.79	354.1
	32.031	2134	0.1113	0.0053	0.8887	0.0053	264.75	173.37	322.87	211.43	1828.12	25.88	22.52	25.88	356.8
	32.354	2161.6	0.1023	0.0054	0.8977	0.0054	344.60	192.51	420.24	234.77	1851.58	26.40	26.98	26.40	365
	32.391	2110.9	0.1013	0.0054	0.8987	0.0054	-179.06	203.49	-218.37	248.16	1789.99	25.81	5.49	25.81	325.9
	32.534	2169	0.0973	0.0054	0.9027	0.0054	321.95	200.65	392.62	244.70	1858.10	25.30	19.50	25.30	362.4
	32.56	2136.7	0.0966	0.0054	0.9034	0.0054	-22.41	209.15	-27.33	255.06	1817.51	26.23	7.81	26.23	344.5
	32.64	2160.4	0.0944	0.0054	0.9056	0.0054	177.21	213.90	216.11	260.85	1845.62	26.60	26.02	26.60	360.4
	33.009	2192	0.0841	0.0055	0.9159	0.0055	279.67	237.32	341.07	289.42	1874.09	27.40	36.09	27.40	353.8
	33.204	2215.1	0.0787	0.0055	0.9213	0.0055	421.36	265.36	513.86	323.61	1897.00	27.54	22.30	27.54	373.8
	33.303	2192.9	0.0760	0.0055	0.9240	0.0055	54.43	279.19	66.37	340.48	1867.07	27.41	9.57	27.41	351.1
	33.314	2205.7	0.0757	0.0055	0.9243	0.0055	223.31	279.21	272.33	340.50	1884.05	27.18	32.65	27.18	355.9
	33.788	2221.4	0.0625	0.0056	0.9375	0.0056	16.01	353.12	19.53	430.63	1890.33	27.37	32.73	27.37	373.7
	33.854	2236.6	0.0607	0.0056	0.9393	0.0056	201.71	351.54	245.99	428.71	1908.67	29.03	36.27	29.03	384.6
	34.015	2247.6	0.0562	0.0057	0.9438	0.0057	228.99	374.24	279.26	456.39	1918.41	28.05	29.01	28.05	361.8
	34.145	2254.4	0.0526	0.0057	0.9474	0.0057	193.70	400.10	236.22	487.92	1922.61	27.58	25.31	27.58	384.2
	34.623	2301.2	0.0393	0.0058	0.9607	0.0058	645.16	529.61	786.79	645.87	1968.71	28.50	26.81	28.50	405.3
	34.672	2287.9	0.0380	0.0058	0.9620	0.0058	239.35	573.80	291.89	699.75	1950.29	27.74	21.19	27.74	377.2
Sp96	32.169	2121.8	0.1072	0.0053	0.8928	0.0053	77.15	188.68	94.09	230.10	1809.95	25.96	0.35	25.96	344.3
	32.894	2189.6	0.0871	0.0055	0.9129	0.0055	318.33	232.55	388.21	283.59	1873.21	27.75	8.01	27.75	360.4
	33.147	2187.9	0.0801	0.0055	0.9199	0.0055	113.63	267.26	138.57	325.93	1865.56	27.37	-7.24	27.37	350.4
	33.245	2209.1	0.0773	0.0055	0.9227	0.0055	324.93	260.43	396.26	317.60	1890.05	27.15	7.15	27.15	371.8
	33.256	2223	0.0770	0.0055	0.9230	0.0055	490.77	254.62	598.50	310.52	1906.34	26.98	1.14	26.98	374.8
	33.414	2218.3	0.0726	0.0056	0.9274	0.0056	306.15	275.70	373.35	336.22	1896.51	26.94	-5.79	26.94	363.3
	33.416	2218.1	0.0726	0.0056	0.9274	0.0056	309.92	268.66	377.95	327.64	1896.81	26.05	3.61	26.05	359.1
Su01	28.18	1917.63	0.2182	0.0045	0.7818	0.0045	308.10	79.73	375.73	97.23	1656.47	22.73	19.64	22.73	325.2

	28.679	1930.134	0.2043	0.0046	0.7957	0.0046	226.53	85.03	276.26	103.70	1659.33	23.38	-35.42	23.38	302.6
	29.075	1972.914	0.1934	0.0047	0.8066	0.0047	329.67	88.09	402.03	107.43	1701.69	23.16	27.00	23.16	336.9
	29.493	1996.657	0.1818	0.0048	0.8182	0.0048	328.22	98.79	400.27	120.47	1720.87	24.17	27.33	24.17	337.3
	29.525	2002.539	0.1809	0.0048	0.8191	0.0048	352.80	98.90	430.24	120.61	1728.78	24.33	22.88	24.33	344.7
	31.051	2078.274	0.1385	0.0050	0.8615	0.0050	269.37	135.39	328.49	165.11	1781.13	25.50	58.95	25.50	337.3
	31.401	2093.439	0.1288	0.0051	0.8712	0.0051	241.17	147.71	294.12	180.14	1793.31	26.36	17.01	26.36	336.9
	31.496	2102.953	0.1262	0.0051	0.8738	0.0051	271.86	152.91	331.53	186.48	1802.87	25.57	12.20	25.57	348.4
	31.726	2119.143	0.1198	0.0051	0.8802	0.0051	292.68	156.04	356.93	190.29	1816.26	24.69	15.07	24.69	348.8
	31.816	2130.577	0.1173	0.0051	0.8827	0.0051	347.03	165.49	423.21	201.81	1827.73	26.21	31.14	26.21	354.5
	32.014	2135.704	0.1118	0.0052	0.8882	0.0052	288.79	171.86	352.18	209.58	1829.37	24.64	32.35	24.64	351.5
	32.265	2145.112	0.1049	0.0052	0.8951	0.0052	248.93	191.47	303.57	233.49	1835.21	26.66	82.96	26.66	347.8
	32.266	2151.299	0.1048	0.0052	0.8952	0.0052	306.10	187.23	373.30	228.33	1843.19	26.54	86.97	26.54	353.3
	32.306	2148.168	0.1037	0.0052	0.8963	0.0052	252.56	188.15	308.00	229.46	1837.98	26.75	71.80	26.75	345.8
	32.311	2148.738	0.1036	0.0052	0.8964	0.0052	260.83	185.42	318.08	226.12	1838.44	25.89	71.47	25.89	345.9
	32.324	2156.721	0.1032	0.0052	0.8968	0.0052	324.46	184.89	395.68	225.48	1847.43	25.70	87.24	25.70	352.9
	32.342	2156.331	0.1027	0.0052	0.8973	0.0052	312.55	189.81	381.16	231.47	1846.66	25.55	36.84	25.55	367.3
	32.439	2157.691	0.1000	0.0052	0.9000	0.0052	275.73	196.69	336.25	239.87	1846.82	25.93	69.20	25.93	348.6
	32.522	2169.043	0.0977	0.0052	0.9023	0.0052	333.34	204.60	406.52	249.52	1858.08	26.68	19.75	26.68	361
	32.675	2179.469	0.0935	0.0053	0.9065	0.0053	345.89	207.14	421.82	252.60	1866.91	26.49	16.00	26.49	367.3
	32.93	2188.252	0.0864	0.0053	0.9136	0.0053	289.95	225.21	353.60	274.65	1871.76	26.36	32.44	26.36	369
	33.033	2188.392	0.0835	0.0053	0.9165	0.0053	220.23	244.24	268.57	297.86	1870.45	27.05	31.68	27.05	362.6
	33.713	2230.506	0.0647	0.0054	0.9353	0.0054	249.64	319.94	304.43	390.17	1904.97	27.13	10.78	27.13	378.7
	34.881	2306.342	0.0323	0.0056	0.9677	0.0056	432.32	687.10	527.22	837.92	1968.24	29.02	10.21	29.02	368
	34.881	2302.04	0.0323	0.0056	0.9677	0.0056	260.44	732.41	317.61	893.19	1964.04	28.94	6.61	28.94	366.6
Sp03	30.9615	2080.325	0.1408	0.0052	0.8592	0.0052	323.01	138.40	393.92	168.78	1786.78	25.79	3.93	25.79	327.9
	30.978	2080.155	0.1404	0.0052	0.8596	0.0052	323.64	130.97	394.69	159.72	1787.32	24.85	3.84	24.85	329.3
	31.849	2141.626	0.1162	0.0053	0.8838	0.0053	425.12	167.21	518.44	203.91	1841.22	26.03	20.36	26.03	348.5
	32.013	2139.615	0.1117	0.0054	0.8883	0.0054	319.23	175.34	389.31	213.83	1834.16	25.32	-2.99	25.32	343.4
	32.4435	2162.752	0.0997	0.0054	0.9003	0.0054	311.21	211.88	379.52	258.39	1852.44	27.13	59.59	27.13	338.4
	32.7275	2177.11	0.0918	0.0055	0.9082	0.0055	282.97	218.13	345.09	266.02	1861.61	26.61	7.04	26.61	340.6
	32.762	2189.412	0.0909	0.0055	0.9091	0.0055	401.26	224.07	489.34	273.26	1877.00	26.63	18.59	26.63	350.2
	32.807	2185.693	0.0896	0.0055	0.9104	0.0055	330.55	224.77	403.11	274.11	1871.10	26.59	-2.20	26.59	345.4
	32.824	2189.992	0.0892	0.0055	0.9108	0.0055	376.78	224.45	459.49	273.72	1875.62	27.21	-7.29	27.21	348.1
	32.939	2197.155	0.0860	0.0055	0.9140	0.0055	389.05	229.33	474.46	279.67	1881.71	26.02	2.98	26.02	349.8
	33.166	2207.961	0.0797	0.0056	0.9203	0.0056	365.82	247.80	446.12	302.20	1890.02	26.64	23.41	26.64	350.5

33.723	2239.644	0.0642	0.0057	0.9358	0.0057	373.08	320.83	454.97	391.26	1915.32	26.80	76.60	26.80	356.7
33.899	2252.959	0.0593	0.0057	0.9407	0.0057	424.14	373.94	517.25	456.02	1927.42	29.91	70.03	29.91	362.6
34.042	2256.01	0.0554	0.0057	0.9446	0.0057	321.13	390.46	391.62	476.17	1925.83	28.37	1.69	28.37	362.4
34.326	2272.754	0.0475	0.0058	0.9525	0.0058	358.37	444.26	437.03	541.78	1940.81	26.93	36.95	26.93	361.9
34.4595	2281.053	0.0438	0.0058	0.9562	0.0058	349.15	490.54	425.79	598.22	1947.26	28.84	4.71	28.84	359.8
34.484	2280.733	0.0431	0.0058	0.9569	0.0058	316.32	514.20	385.75	627.07	1945.32	28.78	2.47	28.78	357.2
34.524	2284.899	0.0420	0.0058	0.9580	0.0058	390.03	512.42	475.64	624.90	1953.18	27.35	20.25	27.35	368
34.58	2289.091	0.0404	0.0058	0.9596	0.0058	408.27	527.16	497.89	642.88	1954.76	27.60	45.01	27.60	363.2
34.58	2289.926	0.0404	0.0058	0.9596	0.0058	403.33	549.18	491.86	669.73	1955.78	28.97	17.55	28.97	366.2
34.686	2292.512	0.0375	0.0058	0.9625	0.0058	327.23	593.68	399.06	724.00	1955.55	27.89	33.00	27.89	363.3
34.696	2294.137	0.0372	0.0058	0.9628	0.0058	331.04	614.83	403.70	749.79	1956.31	29.43	27.14	29.43	361.6
34.817	2299.819	0.0338	0.0058	0.9662	0.0058	301.94	658.67	368.22	803.26	1960.85	28.45	3.09	28.45	354.9

Appendix E: Computer scripts for Matlab, version 6.5.0 (Mathworks, Inc.), for the PWP model. Note that material in the scripts preceded by % is ignored by Matlab.

Contents and Notes:

1) make_met.m
    a) Purpose: Creates input heat, momentum, and freshwater flux files for the PWP code from text files.
    b) Source: http://www.po.gso.uri.edu/rafos/research/pwp/index.html
    c) Input: text file with columns: time, shortwave radiation, longwave radiation, sensible heat flux, latent heat flux, zonal wind stress, meridional wind stress, precipitation
    d) Output: met_input_file.mat
2) make_profile_c.m
    a) Purpose: Creates input vertical profiles for the PWP code from text files, removes static instability in the water column.
    b) Source: modified from http://www.po.gso.uri.edu/rafos/research/pwp/index.html
    c) Input: text file with columns: depth, temperature, salinity, DIC, ALK
    d) Output: profile_input_file.mat
3) pwp_airsea4.m
    a) Purpose: Calculates surface mixed layer characteristics using a Price-Weller Pinkel (1986) one-dimensional mixing model.
    b) Source: modified from http://www.po.gso.uri.edu/rafos/research/pwp/index.html
    c) Input: met_input_file.mat, profile_input_file.mat, relax_input_file.mat*
        i) *relax_input file.mat is the renamed output of PWP_airsea2 (pwp_output_file.mat), and an input unique to PWP_airsea4.m.
    d) Output: pwp_output_file.mat

e) Note: Includes all commands from earlier versions of the PWP for Matlab, which are distinguished by typeface:

(1) PWP_carbon.m (Ch. 2, containing carbon and alkalinity) = plain text.

(2) PWP_airsea2.m (Ch. 4, containing above and calculating pCO_2, air-sea CO_2 flux) = *italic*.

(3) PWP_airsea4.m (Ch. 4, containing all above plus a relaxation term) = **bold**.

1. make_met.m

```
function make_met(met_input_file)

%  -- Load the air/sea flux data. --

%  The file must be saved as an ascii file and in column format,
%  with each line containing 8 values: time, sw, lw, qlat, qsens, tx, ty,
precip.

met.data = load(met_input_file);

%  Extract the following parameters:
%  time,          sample time in yearday
%  sw,            short wave radiation (W/m^2)
%  lw,            long wave radiation (W/m^2)
%  qlat,          latent heat flux (W/m^2)
%  qsens,         sensible heat flux (W/m^2)
%  tx,            east stress (N/m^2)
%  ty,            north stress (N/m^2)
%  precip,  precipitaion rate (m/s)

%  The heat fluxes are defined positive for
%  sw: flux into the ocean
%  lw, qlat, qsens: flux out of the ocean

met.time          = met.data(:,1);
met.sw            = met.data(:,2);
met.lw            = met.data(:,3);
met.qlat          = met.data(:,4);
met.qsens         = met.data(:,5);
met.tx            = met.data(:,6);
met.ty            = met.data(:,7);
met.precip  = met.data(:,8);

clear met.data

%  Save as a Matlab file

if ismember('.', met_input_file)
      met_input_file = met_input_file(1:min(find(met_input_file=='.'))-1);
end

eval(['save ' met_input_file ' met'])
```

2. make_profile.m

```
function make_profile_c(profile_input_file)

%  -- Load the air/sea flux data. --

%  The data must be saved as an ascii file and in column format,
%  with each line containing 5 values: z, t,  s, DIC, ALK.
%  The first record should be the surface value,
%  and the last value should be deep enough to avoid
%  entering into the caluclation (unless intentional).

% Modified June 30. 2005 by Sarah Cooley, UGA

profile.data = load (profile_input_file);

%  Extract the following parameters:
%  z,       initial depth(m)
%  t,       initial temperature(C)
%  s,       initial salinity(o/oo)
%  dic,     dissolved inorganic carbon (umol/kg)
%  alk,     total alkalinity  (ueq/kg)

profile.z   = profile.data(:,1);
profile.t   = profile.data(:,2);
profile.s   = profile.data(:,3);
profile.d = sw_dens0(profile.s,profile.t);
profile.dic = profile.data(:,4);
profile.alk = profile.data(:,5);


%  -- Remove static instability in the profiles. --

t = profile.t;
s = profile.s;
d = profile.d;
dic = profile.dic;
alk = profile.alk;

for j = 1:length(d)
      stop_index = min(find(d-d(j)>0));
      t_step= (t(stop_index)-t(j))/(stop_index-j);
      s_step= (s(stop_index)-s(j))/(stop_index-j);
      d_step= (d(stop_index)-d(j))/(stop_index-j);
    dic_step= (dic(stop_index)-dic(j))/(stop_index-j);
    alk_step= (alk(stop_index)-alk(j))/(stop_index-j);
      if isempty(stop_index)
            break
      else
            t(j:stop_index-1) = t(j)+t_step*(0:stop_index-j-1);
            s(j:stop_index-1) = s(j)+s_step*(0:stop_index-j-1);
            d(j:stop_index-1) = sw_dens0(s(j:stop_index-1),t(j:stop_index-1));
        dic(j:stop_index-1) = dic(j)+dic_step*(0:stop_index-j-1);
        alk(j:stop_index-1) = alk(j)+alk_step*(0:stop_index-j-1);
      end
end

profile.t = t;
profile.s = s;
profile.d = d;
profile.z = profile.z(1:length(profile.d));
profile.dic = dic;
profile.alk = alk;
```

```
%  Save as a Matlab file

if ismember('.', profile_input_file)
      profile_input_file =
profile_input_file(1:min(find(profile_input_file=='.'))-1);
end

eval(['save ' profile_input_file ' profile'])

% insert subfunction SW_dens0  and sw_SMOW from PWP code from web (SRC 6-23-05)

function dens = sw_dens0(S,T)

% SW_DENS0   Denisty of sea water at atmospheric pressure
%===========================================================================
% SW_DENS0  $Revision: 1.3 $  $Date: 1994/10/10 04:54:09 $
%           Copyright (C) CSIRO, Phil Morgan 1992
%
% USAGE:  dens0 = sw_dens0(S,T)
%
% DESCRIPTION:
%    Density of Sea Water at atmospheric pressure using
%    UNESCO 1983 (EOS 1980) polynomial.
%
% INPUT:  (all must have same dimensions)
%   S = salinity    [psu      (PSS-78)]
%   T = temperature [degree C (IPTS-68)]
%
% OUTPUT:
%   dens0 = density  [kg/m^3] of salt water with properties S,T,
%           P=0 (0 db gauge pressure)
%
% AUTHOR:  Phil Morgan 92-11-05  (morgan@ml.csiro.au)
%
% DISCLAIMER:
%   This software is provided "as is" without warranty of any kind.
%   See the file sw_copy.m for conditions of use and licence.
%
% REFERENCES:
%     Unesco 1983. Algorithms for computation of fundamental properties of
%     seawater, 1983. _Unesco Tech. Pap. in Mar. Sci._, No. 44, 53 pp.
%
%     Millero, F.J. and  Poisson, A.
%     International one-atmosphere equation of state of seawater.
%     Deep-Sea Res. 1981. Vol28A(6) pp625-629.
%===========================================================================

% CALLER: general purpose, sw_dens.m
% CALLEE: sw_smow.m

%----------------------
% CHECK INPUT ARGUMENTS
%----------------------
if nargin ~=2
   error('sw_dens0.m: Must pass 2 parameters')
end %if

[mS,nS] = size(S);
[mT,nT] = size(T);

if (mS~=mT) | (nS~=nT)
   error('sw_dens0.m: S,T inputs must have the same dimensions')
end %if
```

```
Transpose = 0;
if mS == 1  % a row vector
  S = S(:);
  T = T(:);
  Transpose = 1;
end %if

%----------------------
% DEFINE CONSTANTS
%----------------------
%     UNESCO 1983 eqn(13) p17.

b0 =  8.24493e-1;
b1 = -4.0899e-3;
b2 =  7.6438e-5;
b3 = -8.2467e-7;
b4 =  5.3875e-9;

c0 = -5.72466e-3;
c1 = +1.0227e-4;
c2 = -1.6546e-6;

d0 = 4.8314e-4;

%$$$ dens = sw_smow(T) + (b0 + b1*T + b2*T.^2 + b3*T.^3 + b4*T.^4).*S  ...
%$$$                   + (c0 + c1*T + c2*T.^2).*S.*sqrt(S) + d0*S.^2;

dens = sw_smow(T) + (b0 + (b1 + (b2 + (b3 + b4*T).*T).*T).*T).*S  ...
                  + (c0 + (c1 + c2*T).*T).*S.*sqrt(S) + d0*S.^2;

if Transpose
  dens = dens';
end %if

return
% ------------------------------------------------------------------------


function dens = sw_smow(T)

% SW_SMOW    Denisty of standard mean ocean water (pure water)
%==========================================================================
% SW_SMOW  $Revision: 1.3 $  $Date: 1994/10/10 05:51:46 $
%          Copyright (C) CSIRO, Phil Morgan 1992.
%
% USAGE:  dens = sw_smow(T)
%
% DESCRIPTION:
%    Denisty of Standard Mean Ocean Water (Pure Water) using EOS 1980.
%
% INPUT:
%   T = temperature [degree C (IPTS-68)]
%
% OUTPUT:
%   dens = density  [kg/m^3]
%
% AUTHOR:  Phil Morgan 92-11-05  (morgan@ml.csiro.au)
%
% DISCLAIMER:
%   This software is provided "as is" without warranty of any kind.
%   See the file sw_copy.m for conditions of use and licence.
%
% REFERENCES:
```

```
%     Unesco 1983. Algorithms for computation of fundamental properties of
%     seawater, 1983. _Unesco Tech. Pap. in Mar. Sci._, No. 44, 53 pp.
%     UNESCO 1983 p17  Eqn(14)
%
%     Millero, F.J & Poisson, A.
%     INternational one-atmosphere equation of state for seawater.
%     Deep-Sea Research Vol28A No.6. 1981 625-629.    Eqn (6)
%=========================================================================

%----------------------
% CHECK INPUT ARGUMENTS
%----------------------
% TEST INPUTS
if nargin ~= 1
   error('sw_smow.m: Only one input argument allowed')
end %if

Transpose = 0;
[mT,nT] = size(T);
if mT == 1 % a row vector
   T = T(:);
   Tranpose = 1;
end %if

%----------------------
% DEFINE CONSTANTS
%----------------------
a0 = 999.842594;
a1 =   6.793952e-2;
a2 =  -9.095290e-3;
a3 =   1.001685e-4;
a4 =  -1.120083e-6;
a5 =   6.536332e-9;

dens = a0 + (a1 + (a2 + (a3 + (a4 + a5*T).*T).*T).*T).*T;

if Transpose
  dens = dens';
end %if

return
```

3. PWP_airsea.m

```
function PWP_airsea4(met_input_file, profile_input_file, relax_input_file)

% met_input_file = surface heat, FW fluxes that force the model
% profile_input_file = initial conditions profile
% relax_input_file = modeled profile to relax to at each timestep.
%

%  MATLAB version 1.4 (8 Oct 2001)

%  This main program is used to drive the pwp subroutine (pwpgo)
%  with a daily cycle of heating, or, an arbitrary (observed) time
%  series of surface flux data.

%  Written by Jim Price, april 27, 1989. Please direct any
%  comments or questions to Jim Price, WHOI, Woods Hole, MA
%  02543, USA, tel. 508-289-2526.

%  Version 2:  changed the gradient Ri relaxation method.
%  Version 3:  clarified the bulk Ri relaxation.
%  Version 4:  fixed an error that disabled background diffusion.

%  Last editted on 20 Jan, 1999 by JFP.

%  Translated for MATLAB 5.X by Peter Lazarevich and Scott Stoermer,
%  GSO/URI, 11 July 2001.

%  Added carbon as passive tracer June 30, 2005 by Sarah Cooley, UGA
%  Air-sea flux added 12/13/05, SRC
%  Diffusion, interpolation fixed 3/27/06, SRC (see notes on PWP_carbon3
%  for details)

%  -- Option to display output during run. --

diagnostics = 0;

%  -- Initialize the user-defined variables. --

global dt dz days depth dt_save lat g cpw rb rg rkz beta1 beta2 udrag

%  dt,                  time-step increment (seconds)
%  dz,                  depth increment (meters)
%  days,    the number of days to run
%  depth,         the depth to run
%  dt_save, time-step increment for saving to file (multiples of dt)
%  lat,           latitude (degrees)
%  g,                   gravity (9.8 m/s^2)
%  cpw,                 specific heat of water (4183.3 J/kgC)
%  rb,                  critical bulk richardson number (0.65)
%  rg,                  critical gradient richardson number (0.25)
%  rkz,                 background diffusion (0)
%  beta1,   longwave extinction coefficient (0.6 m)
%  beta2,   shortwave extinction coefficient (20 m)

dt               = 3600;         %900
```

```
dz                = 1;           %10
days        = 495;           % 300
depth       = 200 ;         %1000
dt_save     = 12;                % 4
lat         = 9.63  ;          % 60
g                       = 9.8;
cpw               = 4183.3;
rb                = 0.65;         %0.65
rg                = 0.25;         %0.25
rkz               = 1e-4;         % 10x ledwell et al 1993 value
beta1       = 0.6;
beta2       = 20;

%  -- Initialize additional variables. ---

global f ucon

%  f,             Coriolis parameter
%  ucon,    coefficient of inertial-internal wave dissipation

f = 2*7.29E-5*sin(lat*pi/180);

%  -- Load the air/sea flux data. --

disp(['loading ' met_input_file])

load(met_input_file);

%  -- Interpolate the air/sea flux variables at dt resolution. --

%  Set nmet equal to the number of time increments using a resolution of dt.

nmet  = days*8.64E4/dt;
time  = met.time(1)+(0:(nmet-1))*dt/8.64E4;

% Check record length

if time(end) > met.time(end)
      time = time(time<met.time(end));
      nmet = length(time);
      disp(['Met input shorter than # of days selected, truncating run to '
num2str(nmet*dt/8.64E4) ' day(s)'])
      pause
end

% Check the time-resolution of the inertial period

if dt > 1/10*2*pi/f
      ans = input('Time step, dt, too large to accurately resolve the inertial
period. Is this okay? (y/n)','s');
      if ans == 'n'
            disp(['Please restart PWP.m with a new dt <= ' num2str(1/(10*f))])
            return
      end
end
```

```
qi                = interp1(met.time,met.sw,time,'linear'); %all these
interpolation routines were fixed 3/27/06
qo                = interp1(met.time,met.lw+met.qlat+met.qsens,time,'linear');
tx                = interp1(met.time,met.tx,time,'linear');
ty                = interp1(met.time,met.ty,time,'linear');
precip      = interp1(met.time,met.precip,time,'linear');

global xstress ystress  % introduce variables of surface wind stress for flux
calc's, SRC
xstress= tx(1);        %SRC
ystress= ty(1);        % SRC
disp('loading complete')

%  -- Load initial t,s, dic, alk profile data. --
%  for pwp_carbon, must use make_profile_c to handle input file including
%  DIC, ALK -- SRC

disp(['loading ' profile_input_file])

load(profile_input_file);

%  -- Interpolate the profile variables at dz resolution. --

global nz z t s d dic alk So DICo ALKo

%  Set nz equal to the number of depth increments + 1 using a resolution of dz.

nz    = 1+depth/dz;
z           = ((0:nz-1)*dz)';

% Check record length

if z(end) > profile.z(end)
      z = z(z<=profile.z(end));
      nz = length(z);
      disp(['Profile input shorter than depth selected, truncating to '
num2str(z(end)) ' meters'])
      pause
end

% Check the depth-resolution of the profile file

profile_increment = (profile.z(end)-profile.z(1))/(length(profile.z)-1);
if dz < profile_increment/5
      ans = input('Depth increment, dz, is much smaller than profile
resolution. Is this okay? (y/n)','s');
      if ans == 'n'
            disp(['Please restart PWP.m with a new dz >= '
num2str(profile_increment/5)])
            return
      end
end

t     = interp1(profile.z,profile.t,z);
s     = interp1(profile.z,profile.s,z);
d     = sw_dens0(s,t);
dic   = interp1(profile.z,profile.dic,z);
```

```
alk   = interp1(profile.z,profile.alk,z);

% load profile to relax to
disp(['loading ' relax_input_file])
load(relax_input_file);
relax_state = pwp_output;

% Interpolate relax_state at dt resolution


To    = interp2(relax_state.time, relax_state.z, relax_state.t, time, z,
'linear');
So    = interp2(relax_state.time, relax_state.z, relax_state.s, time, z,
'linear');
Do    = interp2(relax_state.time, relax_state.z, relax_state.d, time, z,
'linear');
DICo  = interp2(relax_state.time, relax_state.z, relax_state.dic, time, z,
'linear');
ALKo  = interp2(relax_state.time, relax_state.z, relax_state.alk, time, z,
'linear');

disp('loading complete')
%  -- Interpolate evaporation minus precipitaion at dt resolution. --

evap  = (0.03456/(86400*1000))*interp1(met.time,met.qlat,time,'linear'); %SRC
repaired 3/27/06
emp         = evap - precip;

%  -- Initialize additional profile variables at dz resolution. --

global u v absrb

%  u and v,       east and north current
%  absrb,               absorbtion fraction

u                 = zeros(nz,1);
v                 = zeros(nz,1);
absrb = absorb(beta1,beta2);

% --  Initialize MLD variable at nmet resolution -- SRC
global mld fCO2 pCO2 Flux Srlx DICrlx ALKrlx Trlx

% Initiate variables calculated later , SRC added
mld = zeros(1,nmet);        %mixed layer depth
fCO2 = zeros(1,nmet);
pCO2 = zeros(1,nmet);
Flux = zeros(1,nmet);       % air-sea carbon flux

%  -- Specify a simple "background" diffusion to be applied to the profiles. --

dstab = dt*rkz/dz^2;

if dstab > 0.5
      disp('Warning, this value of rkz will be unstable')
end

%  -- Define the variables to be saved. --
```

```
pwp_output.dt                 = dt;
pwp_output.dz                 = dz;
pwp_output.lat                = lat;
pwp_output.z                        = z;
pwp_output.time               = [];
pwp_output.t                        = [];
pwp_output.s                        = [];
pwp_output.d                        = [];
pwp_output.u                        = [];
pwp_output.v                        = [];
pwp_output.mld               = [];      %SRC
pwp_output.dic                      = [];       %SRC
pwp_output.alk                      = [];       %SRC
pwp_output.qi               = [];       %SRC
pwp_output.qo               = [];       %SRC
pwp_output.tx               = [];       %SRC
pwp_output.ty               = [];       %SRC
pwp_output.precip           = [];       %SRC
pwp_output.emp              = [];       %SRC
pwp_output.fCO2             = [];       %SRC
pwp_output.pCO2             = [];       %SRC
pwp_output.Flux             = [];       %SRC
pwp_output.Srlx             =[];
pwp_output.DICrlx           =[];
pwp_output.ALKrlx           =[];
pwp_output.Trlx             =[];

%  -- Step through the PWP model. --

disp(['STATUS (out of ' int2str(nmet) ' steps):'])

for m = 1:nmet

      pwpgo(qi(m),qo(m),emp(m),tx(m),ty(m),m, So(:,m), DICo(:,m), ALKo(:,m),
To(:,m)); %src added So, DICo, ALko


%  Apply a "background" diffusion if rkz is non-zero.

      if rkz > 0
            diffus(dstab,t);
            diffus(dstab,s);
            d = sw_dens0(s,t);
            diffus(dstab,u);
            diffus(dstab,v);
        diffus(dstab,dic);
        diffus(dstab,alk);
      end

%  -- Store variables. --

      if mod(m-1,dt_save) == 0
            pwp_output.time(:,end+1)      = time(m);
            pwp_output.t(:,end+1)               = t;
            pwp_output.s(:,end+1)               = s;
    pwp_output.d(:,end+1)                 = d;
```

```
    pwp_output.u(:,end+1)                = u;
    pwp_output.v(:,end+1)                = v;
        pwp_output.mld(:,end+1)                 = mld;  %SRC
        pwp_output.dic(:,end+1)                 = dic;  %SRC
        pwp_output.alk(:,end+1)                 = alk;  %SRC
        pwp_output.qi(:,end+1)          =qi(m);  %SRC
        pwp_output.qo(:,end+1)          =qo(m);  %SRC
        pwp_output.tx(:,end+1)          =tx(m);  %SRC
        pwp_output.ty(:,end+1)          =ty(m);  %SRC
        pwp_output.precip(:,end+1)      =precip(m);  %SRC
        pwp_output.emp(:,end+1)         =emp(m);  %SRC
        pwp_output.fCO2(:,end+1)        =fCO2;    %SRC
        pwp_output.pCO2(:,end+1)        =pCO2;   %SRC
        pwp_output.Flux(:,end+1)        =Flux;    %SRC
        pwp_output.Srlx(:,end+1)        =Srlx;
        pwp_output.DICrlx(:,end+1)      =DICrlx;
        pwp_output.ALKrlx(:,end+1)      =ALKrlx;
        pwp_output.Trlx(:,end+1)        =Trlx;

    end

%  -- Save variables. --

      if mod(m, 100) == 0
            disp([int2str(m), ' (' sprintf('%2.1f',100*m/nmet), '%)'])
      end

%  -- Diagnostics. --

      if ~exist('x')
            x = u(1)*dt;
            y = v(1)*dt;
            U = mean(u)*depth;
            V = mean(v)*depth;
      else
            x = [x x(end)+u(1)*dt];
            y = [y y(end)+v(1)*dt];
            U = [U mean(u)*depth];
            V = [V mean(v)*depth];
      end

      if diagnostics

            figure(1)

            subplot(1,3,1)
            plot(d,z,'k')
            set(gca,'ydir','reverse')
            hold on
            plot(d,z,'k.')
            hold off
            grid on
            title('Density')
            ylabel('Depth (m)')

            subplot(1,3,2)
            plot(t,z,'k')
```

```
set(gca,'ydir','reverse')
hold on
plot(t,z,'k.')
hold off
grid on
title('Temp.')

subplot(1,3,3)
plot(sqrt(u.^2+v.^2),z,'k')
set(gca,'ydir','reverse')
hold on
plot(sqrt(u.^2+v.^2),z,'k.')
hold off
grid on
title('Speed (m/s)') %currents, not winds

figure(2)

subplot(1,2,1)
plot(x,y,'k')
hold on
plot(x,y,'k.')
plot(x(end),y(end),'ko')
hold off
grid on
title('Trajectory at surface')
ylabel('y (m)')
xlabel('x (m)')

subplot(1,2,2)
compass(U(end),V(end),'k')
hold on
plot(U,V,'k.')
hold off
grid on
title('Net transport (m^3/s)')

figure(3)

subplot(2,1,1)
plot(time(1:m),qi(1:m),'k*')
hold on
plot(time(1:m),qo(1:m),'ko')
hold off
grid on
title('qi(*) and qo(o)')
ylabel('Heat flux (W/m^2)')

subplot(2,1,2)
plot(time(1:m),tx(1:m),'k*')
hold on
plot(time(1:m),ty(1:m),'ko')
hold off
grid on
title('tx(*) and ty(o)')
ylabel('Wind stress (N/m^2)')
xlabel('Time (days)')
```

```
            %pause(0.2)


      end

 end
save pwp_output_file.mat pwp_output       %SRC
disp(['Model Run Completed - Selected variables saved in file:
pwp_output_file'])% pwp_output_file])

pwp_output
load pwp_output_file.mat

figure(4)
subplot(3,1,1)
[C,h] = contour(pwp_output.time, pwp_output.z, pwp_output.s, 'k');
hold on
clabel(C,h)
set(gca,'YDir','reverse')
title('Salinity')
ylabel('Depth (m)')

subplot(3,1,2)
[C,h] = contour(pwp_output.time, pwp_output.z, pwp_output.t, 'k');
hold on
clabel(C,h)
set(gca,'YDir','reverse')
title('Temperature')
ylabel('Depth (m)')

subplot(3,1,3)
[C,h] = contour(pwp_output.time, pwp_output.z, pwp_output.d, 'k');
hold on
clabel(C,h)
set(gca,'YDir','reverse')
title('Density')
xlabel('Julian Date')
ylabel('Depth (m)')

figure(5)
subplot(2,1,1)
[C,h] = contourf(pwp_output.time, pwp_output.z, pwp_output.dic);
hold on
clabel(C,h)
set(gca,'YDir','reverse')
title('DIC')
ylabel('Depth (m)')

subplot(2,1,2)
[C,h] = contourf(pwp_output.time, pwp_output.z, pwp_output.alk);
hold on
clabel(C,h)
set(gca,'YDir','reverse')
title('Alkalinity')
xlabel('Julian Date')
ylabel('Depth (m)')
```

```
figure(6)
subplot(3,1,1)
plot(pwp_output.time, pwp_output.mld);
hold on
ylabel ('MLD')
set(gca,'YDir','reverse')

subplot (3,1,2)
plot(pwp_output.time, pwp_output.pCO2);
hold on
plot(pwp_output.time, 370e-6, 'k');
ylabel ('pCO2, atm')

subplot (3,1,3)
plot(pwp_output.time, pwp_output.Flux);
hold on
ylabel ('air-sea flux, mol m^{-2} d^{-1}')
% --------------------------------------------------------------------


function pwpgo(qi,qo,emp,tx,ty,m,So, DICo, ALKo, To) % SRC added So, DICo, ALKo

%  This subroutine is an implementation of the Price, Weller,
%  Pinkel upper ocean model described in JGR 91, C7 8411-8427
%  July 15, 1986 (PWP). This version was coded and documented by
%  Jim Price in April 1989.

%  Edited on 20 September 1993 by JFP to allow for a critical
%  gradient Richardson number other than 1/4, and to implement a
%  different and a priori better means of achieving convergence
%  of gradient ri mixing (see subroutine stir for details).
%  The major difference is that the revised scheme gives a more
%  smoothly varying mixed layer depth over a diurnal cycle.
%  Edited on 14 December 1998 by JFP to clarify the bulk Ri
%  relaxation.

%  This model also implements an energy budget form of an
%  entrainment parameterization that is very similar to that
%  described in Price, Mooers, Van Leer, JPO 8, 4, 582-599 (and
%  references therein). This part of the model should be
%  treated as developmental only, as there are several features
%  that are arbitrary to this model (i.e., the depth of the ml
%  during times of heating can be the grid interval, dz). To
%  use this parameterization set the bulk Richardson number to
%  zero, and set em1, or em2, or em3 to non-zero. The gradient
%  Richardson number can be zero or not.

global dt dz days depth dt_save lat g cpw rb rg beta1 beta2 udrag
global nz z t s d dic alk fCO2 pCO2 Flux xstress ystress
global u v absrb mld
global f ucon
global Srlx DICrlx ALKrlx Trlx

%  Apply heat and fresh water fluxes to the top most grid cell.

t(1) = t(1)+(qi*absrb(1)-qo)*dt./(dz*d(1)*cpw);
s(1) = s(1)/(1-emp*dt/dz);
```

```
dic(1) = dic(1)/(1-emp*dt/dz);
alk(1) = alk(1)/(1-emp*dt/dz);

%  Absorb solar radiation at depth.

t(2:nz) = t(2:nz)+qi*absrb(2:nz)*dt./(dz*d(2:nz)*cpw);

%  Compute the density, and relieve static instability, if it occurs.

d = sw_dens0(s,t);
remove_si;

%  At this point the density proifile should be statically stable.

%  Find the index of the surfacd mixed-layer right after the heat/salt fluxes.

ml_index = min(find(diff(d)>1E-2));

if isempty(ml_index)
      error_text = ['Error reached in PWP.m (line 346): the mixed layer is too
deep!' sprintf('\n') ...
      'Possible reasons:' sprintf('\n') ...
      '1) tempearature inversion at surface is too strong' sprintf('\n') ...
      '2) wind is too strong' sprintf('\n') ...
      '3) evaporation is too great'];
      error([ sprintf('\n') error_text])
end

%  Get the depth of the surfacd mixed-layer.
if ml_index<2
    ml_index=2;
end
mld = z(ml_index);

%  Time step the momentum equation.

%  Rotate the current throughout the water column through an
%  angle equal to inertial rotation for half a time step.

ang = -f*dt/2;

rot(ang);

%  Apply the wind stress to the mixed layer as it now exists.
du = (tx/(mld*d(1)))*dt;
dv = (ty/(mld*d(1)))*dt;
u(1:ml_index) = u(1:ml_index)+du;
v(1:ml_index) = v(1:ml_index)+dv;

%  Apply drag to the current (this is a horrible parameterization of
%  inertial-internal wave dispersion).

if ucon > 1E-10
      u = u*(1-dt*ucon);
      v = v*(1-dt*ucon);
end
```

```
%  Rotate another half time step.

rot(ang);

%  Finished with the momentum equation for this time step.

%  Do the bulk Richardson number instability form of mixing (as in PWP).

if rb > 1E-5
      bulk_mix(ml_index)
end

%  Do the gradient Richardson number instability form of mixing.

if rg > 0
      grad_mix;
end

%bio_DIC = "export" DIC from SML via biology by subtracting fixed amount,
%added SRC 5-12-06
% export = 0.0e-3; % mol m-2 d-1, 10% of Maranon primary prod range 2-30 mmol
m-2 d-1;
% export = export./mld./d./86400 ; % mol kg-1 s-1
%
% changeDIC = zeros(nz,1);
% l = length(changeDIC);
% for i=1:l;
%     if z(i)<= mld;
%     changeDIC(i) = 1;  % flags which boxes are in ML and which are not
% end
% end
% newDIC = dic - export.*10^6.*changeDIC*dt;    %export related change in ML
DIC applied over timestep
% dic = newDIC; % end bio_DIC


calc_pCO2;      %SRC 12/8/05
calc_flux;      %SRC 12/8/05
adj_DIC;        % SRC 12/13/05

% relax back to some unperturbed profile (relax_input_file)
 gamma = 1/(60.*86400); % timescale of decay, d * s/d = s-1
 Srlx = So-s;
 s  = s + (Srlx).* gamma.*dt;
 DICrlx = DICo-dic;
 dic = dic + (DICrlx).*gamma.*dt;
 ALKrlx = ALKo-alk;
 alk = alk + (ALKrlx).*gamma.*dt;
 Trlx = To - t;
 t = t + (Trlx).*gamma.*dt;

% ------------------------------------------------------------------------


function bulk_mix(ml_index)

global g rb
```

```
global nz z d
global u v

rvc = rb;
for j = ml_index+1:nz

      h     = z(j);
      dd    = (d(j)-d(1))/d(1);
      dv    = (u(j)-u(1))^2+(v(j)-v(1))^2;
      if dv == 0
            rv = Inf;
      else
            rv = g*h*dd/dv;
      end
      if rv > rvc
            break
      else
            mix5(j);
      end
end


% ------------------------------------------------------------------------


function grad_mix

%  This function performs the gradeint Richardson Number relaxation
%  by mixing adjacent cells just enough to bring them to a new
%  Richardson Number.

global dz g rg
global nz z t s d
global u v

rc    = rg;

%  Compute the gradeint Richardson Number, taking care to avoid dividing by
%  zero in the mixed layer.  The numerical values of the minimum allowable
%  density and velocity differences are entirely arbitrary, and should not
%  effect the calculations (except that on some occasions they evidnetly have!)

j1 = 1;
j2 = nz-1;

while 1
      for j = j1:j2
            if j <= 0
                  keyboard
            end
            dd = (d(j+1)-d(j))/d(j);
            dv = (u(j+1)-u(j))^2+(v(j+1)-v(j))^2;
            if dv == 0
                  r(j) = Inf;
            else
                  r(j) = g*dz*dd/dv;
            end
```

```
      end

      %  Find the smallest value of r in profile

      rs = min(r);
      js = min(find(r==rs));

      %  Check to see whether the smallest r is critical or not.

      if rs > rc
            return
      end

      %  Mix the cells js and js+1 that had the smallest Richardson Number

      stir(rc,rs,js);

      %  Recompute the Richardson Number over the part of the profile that has
changed

      j1 = js-2;
      if j1 < 1
             j1 = 1;
      end
      j2 = js+2;
      if j2 > nz-1
             j2 = nz-1;
      end
end


% ------------------------------------------------------------------------


function a = stir(rc,r,j)

%  This subroutine mixes cells j and j+1 just enough so that
%  the Richardson number after the mixing is brought up to
%  the value rnew. In order to have this mixing process
%  converge, rnew must exceed the critical value of the
%  richardson number where mixing is presumed to start. If
%  r critical = rc = 0.25 (the nominal value), and r = 0.20, then
%  rnew = 0.3 would be reasonable. If r were smaller, then a
%  larger value of rnew - rc is used to hasten convergence.

%  This subroutine was modified by JFP in Sep 93 to allow for an
%  aribtrary rc and to achieve faster convergence.

global t s d u v dic alk

rcon              = 0.02+(rc-r)/2;
rnew              = rc+rcon/5;
f                       = 1-r/rnew;
dt                      = (t(j+1)-t(j))*f/2;
t(j+1)            = t(j+1)-dt;
t(j)              = t(j)+dt;
ds                      = (s(j+1)-s(j))*f/2;
```

```
s(j+1)            = s(j+1)-ds;
s(j)              = s(j)+ds;
d(j:j+1)    = sw_dens0(s(j:j+1),t(j:j+1));
du                      = (u(j+1)-u(j))*f/2;
u(j+1)            = u(j+1)-du;
u(j)              = u(j)+du;
dv                      = (v(j+1)-v(j))*f/2;
v(j+1)            = v(j+1)-dv;
v(j)              = v(j)+dv;
ddic                    = (dic(j+1)-dic(j))*f/2;    %SRC
dic(j+1)          = dic(j+1)-ddic;                %SRC
dic(j)                  = dic(j)+ddic;                  %SRC
dalk                    = (alk(j+1)-alk(j))*f/2;    %SRC
alk(j+1)          = alk(j+1)-dalk;                %SRC
alk(j)                  = alk(j)+dalk;                  %SRC


% ------------------------------------------------------------------------


function mix5(j)

%  This subroutine mixes the arrays t, s, u, v, dic, alk down to level j.

global t s d u v dic alk

t(1:j) = mean(t(1:j));
s(1:j) = mean(s(1:j));
d(1:j) = sw_dens0(s(1:j),t(1:j));
u(1:j) = mean(u(1:j));
v(1:j) = mean(v(1:j));
dic(1:j) = mean(dic(1:j));      %SRC
alk(1:j) = mean(alk(1:j));      %SRC


% ------------------------------------------------------------------------


function rot(ang)

%  This subroutine rotates the vector (u,v) through an angle, ang

global u v

r = (u+i*v)*exp(i*ang);
u = real(r);
v = imag(r);


% ------------------------------------------------------------------------


function remove_si

%  Find and relieve static instability that may occur in the
%  density array d. This simulates free convection.
```

```
%  ml_index is the index of the depth of the surface mixed layer after
adjustment,

global d

while 1
      ml_index = min(find(diff(d)<0));
      if isempty(ml_index)
            break
      end
      mix5(ml_index+1);
end


% ------------------------------------------------------------------------


function absrb = absorb(beta1,beta2)

%  Compute solar radiation absorption profile. This
%  subroutine assumes two wavelengths, and a double
%  exponential depth dependence for absorption.

%  Subscript 1 is for red, non-penetrating light, and
%  2 is for blue, penetrating light. rs1 is the fraction
%  assumed to be red.

global nz dz

rs1 = 0.6;
rs2 = 1.0-rs1;
absrb = zeros(nz,1);
z1 = (0:nz-1)*dz;
z2 = z1 + dz;
z1b1 = z1/beta1;
z2b1 = z2/beta1;
z1b2 = z1/beta2;
z2b2 = z2/beta2;
absrb = (rs1*(exp(-z1b1)-exp(-z2b1))+rs2*(exp(-z1b2)-exp(-z2b2)))';

% ------------------------------------------------------------------------


function a = diffus(dstab,a)

%  This subroutine applies a simple diffusion
%  operation to the array a. It leaves the endpoints
%  unchanged (assumes nothing about the
%  boundary conditions).

global nz

a(2:nz-1) = a(2:nz-1)+dstab*(a(1:nz-2)-2*a(2:nz-1)+a(3:nz));


% ------------------------------------------------------------------------
```

```
function dens = sw_dens0(S,T)

% SW_DENS0   Denisty of sea water at atmospheric pressure
%==========================================================================
% SW_DENS0  $Revision: 1.3 $  $Date: 1994/10/10 04:54:09 $
%           Copyright (C) CSIRO, Phil Morgan 1992
%
% USAGE:  dens0 = sw_dens0(S,T)
%
% DESCRIPTION:
%    Density of Sea Water at atmospheric pressure using
%    UNESCO 1983 (EOS 1980) polynomial.
%
% INPUT:  (all must have same dimensions)
%   S = salinity    [psu      (PSS-78)]
%   T = temperature [degree C (IPTS-68)]
%
% OUTPUT:
%   dens0 = density  [kg/m^3] of salt water with properties S,T,
%           P=0 (0 db gauge pressure)
%
% AUTHOR:  Phil Morgan 92-11-05  (morgan@ml.csiro.au)
%
% DISCLAIMER:
%   This software is provided "as is" without warranty of any kind.
%   See the file sw_copy.m for conditions of use and licence.
%
% REFERENCES:
%     Unesco 1983. Algorithms for computation of fundamental properties of
%     seawater, 1983. _Unesco Tech. Pap. in Mar. Sci._, No. 44, 53 pp.
%
%     Millero, F.J. and  Poisson, A.
%     International one-atmosphere equation of state of seawater.
%     Deep-Sea Res. 1981. Vol28A(6) pp625-629.
%==========================================================================

% CALLER: general purpose, sw_dens.m
% CALLEE: sw_smow.m

%---------------------
% CHECK INPUT ARGUMENTS
%---------------------
if nargin ~=2
   error('sw_dens0.m: Must pass 2 parameters')
end %if

[mS,nS] = size(S);
[mT,nT] = size(T);

if (mS~=mT) | (nS~=nT)
   error('sw_dens0.m: S,T inputs must have the same dimensions')
end %if

Transpose = 0;
if mS == 1  % a row vector
  S = S(:);
```

```
  T = T(:);
  Transpose = 1;
end %if

%----------------------
% DEFINE CONSTANTS
%----------------------
%     UNESCO 1983 eqn(13) p17.

b0 =  8.24493e-1;
b1 = -4.0899e-3;
b2 =  7.6438e-5;
b3 = -8.2467e-7;
b4 =  5.3875e-9;

c0 = -5.72466e-3;
c1 = +1.0227e-4;
c2 = -1.6546e-6;

d0 = 4.8314e-4;

%$$$ dens = sw_smow(T) + (b0 + b1*T + b2*T.^2 + b3*T.^3 + b4*T.^4).*S  ...
%$$$                   + (c0 + c1*T + c2*T.^2).*S.*sqrt(S) + d0*S.^2;

dens = sw_smow(T) + (b0 + (b1 + (b2 + (b3 + b4*T).*T).*T).*T).*S  ...
                  + (c0 + (c1 + c2*T).*T).*S.*sqrt(S) + d0*S.^2;

if Transpose
  dens = dens';
end %if

return


% ------------------------------------------------------------------------


function dens = sw_smow(T)

% SW_SMOW    Denisty of standard mean ocean water (pure water)
%==========================================================================
% SW_SMOW  $Revision: 1.3 $  $Date: 1994/10/10 05:51:46 $
%          Copyright (C) CSIRO, Phil Morgan 1992.
%
% USAGE:  dens = sw_smow(T)
%
% DESCRIPTION:
%    Denisty of Standard Mean Ocean Water (Pure Water) using EOS 1980.
%
% INPUT:
%   T = temperature [degree C (IPTS-68)]
%
% OUTPUT:
%   dens = density  [kg/m^3]
%
% AUTHOR:  Phil Morgan 92-11-05  (morgan@ml.csiro.au)
%
```

```
% DISCLAIMER:
%   This software is provided "as is" without warranty of any kind.
%   See the file sw_copy.m for conditions of use and licence.
%
% REFERENCES:
%     Unesco 1983. Algorithms for computation of fundamental properties of
%     seawater, 1983. _Unesco Tech. Pap. in Mar. Sci._, No. 44, 53 pp.
%     UNESCO 1983 p17  Eqn(14)
%
%     Millero, F.J & Poisson, A.
%     INternational one-atmosphere equation of state for seawater.
%     Deep-Sea Research Vol28A No.6. 1981 625-629.    Eqn (6)
%=========================================================================

%----------------------
% CHECK INPUT ARGUMENTS
%----------------------
% TEST INPUTS
if nargin ~= 1
   error('sw_smow.m: Only one input argument allowed')
end %if

Transpose = 0;
[mT,nT] = size(T);
if mT == 1 % a row vector
   T = T(:)
   Tranpose = 1;
end %if

%----------------------
% DEFINE CONSTANTS
%----------------------
a0 = 999.842594;
a1 =   6.793952e-2;
a2 =  -9.095290e-3;
a3 =   1.001685e-4;
a4 =  -1.120083e-6;
a5 =   6.536332e-9;

dens = a0 + (a1 + (a2 + (a3 + (a4 + a5*T).*T).*T).*T).*T;

if Transpose
  dens = dens';
end %if

return

%-------------------------------------------------------------------------
function calc_pCO2;
% SRC added code based almost entirely on CO2SYS code for Visual Basic.
% http://www.ecy.wa.gov/programs/eap/models/;   CO2SYS_ver11.

%format long g
global dic alk t s fCO2 pCO2
TA = alk(1)*10^-6;  % convert to mol
TC = dic(1)*10^-6;  % convert to mol
```

```
% Constants and useful things
RGasConstant = 83.1451; % bar-cm^3/(mol-K), 1 bar approx 1 atm, 8.31451 N-
m/(mol-K)
%RGasConstant = RGasConstant*0.9869232; % atm/bar conversion factor
TempK = t(1) + 273.15;
RT = RGasConstant * TempK;
sqrSal = sqrt(s(1));
logTempK = log(TempK);
%Pbar = Pdbar/10;
TP = 0; % assume no phosphorus or silicate for now
TSi = 0;

% Total concentrations of boron, fluorine, and sulfate are all proportional
% to salinity

TB = (0.000232 / 10.811) * (s(1) / 1.80655); %mol/kgSW, from Uppstrom, DSR
21:161-162, 1974.
TF = (0.000067 / 18.998) * (s(1) / 1.80655); % mol/kgSW, from Riley, DSR 12:
219-220, 1965.
TS = (0.14 / 96.062) * (s(1) / 1.80655);% mol/kgSW from Morris & Riley, DSR 13:
699-705, 1966.

% CO2 solubility from Weiss 1974
TTT = TempK/100;
lnKo = -60.2409 + 93.4517 / TTT + 23.3585 * log(TTT);
lnKo = lnKo + s(1) * (0.023517 - 0.023656 * TTT + 0.0047036 * TTT^2); % Weiss
Mar Chem 2: 203-215, 1974.
Ko = exp(lnKo); % mol/kg-SW/atm;

IonS = 19.924 * s(1) / (1000 - 1.005 * s(1)); % DOE handbook, ch. 5, p. 13/22,
eq 7.2.4

%Dickson's KSO4 equations, J. Chem. Thermo., 22:113-127, 1990.
lnKS = -4276.1 / TempK + 141.328 - 23.093 * logTempK;
lnKS = lnKS + (-13856 / TempK + 324.57 - 47.986 * logTempK) * sqrt(IonS);
lnKS = lnKS + (35474 / TempK - 771.54 + 114.723 * logTempK) * IonS;
lnKS = lnKS + (-2698 / TempK) * sqrt(IonS) * IonS;
lnKS = lnKS + (1776 / TempK) * IonS^2;
KS = exp(lnKS) ; % free pH scale in mol/kg-H2O);
KS = KS* (1 - 0.001005 * s(1)); % convert to mol/kg SW;

% Calculate KF - Dickson and Riley, Mar Chem 7:89-99, 1979.
lnKF = 1590.2 / TempK - 12.641 + 1.525 * sqrt(IonS);
KF = exp(lnKF); % on free pH scale in mol/kg H20
KF = KF * (1 - 0.001005 * s(1));  % convert to mol/kg SW;

% pH scale conversion factors
SWStoTOT = (1 + TS / KS) / (1 + TS / KS + TF / KF);
FREEtoTOT = 1 + TS / KS;

%Calculate fH from Takahashi et al, ch. 3 in Geosecs Pacific Expedition,
%v3, 1982 (p. 80)
fH = 1.2948 - 0.002036 * TempK;
fH = fH + (0.0004607 - 0.000001475 * TempK) * s(1)^2;

% Calculate KB, Dickson, DSR 37:755-766, 1990
lnKBtop = -8966.9 - 2890.53 * sqrSal - 77.942 * s(1);
```

```
lnKBtop = lnKBtop + 1.728 * sqrSal * s(1) - 0.0996 * s(1)^2;
lnKB = lnKBtop / TempK;
lnKB = lnKB + 148.0248 + 137.1942 * sqrSal + 1.62142 * s(1);
lnKB = lnKB + (-24.4344 - 25.085 * sqrSal - 0.2474 * s(1)) * logTempK;
lnKB = lnKB + 0.053105 * sqrSal * TempK;
KB = exp(lnKB); % this is on the total pH scale in mol/kg SW
KB = KB / SWStoTOT;   % converts to SWS pH scale

% Calculate Kw, according to Millero, Geochim. Cosmo. Acta 59:661-677,
% 1995

lnKW = 148.9802 - 13847.26 / TempK - 23.6521 * logTempK;
lnKW = lnKW + (-5.977 + 118.67 / TempK + 1.0495 * logTempK) * sqrSal;
lnKW = lnKW - 0.1615 * s(1);
Kw = exp(lnKW); % on the SWS pH scale in (mol/kg SW)^2

% calculate KP1 Kp2 KP3, KSi; Yao and Millero, Aquat Geochem. 1: 53-88,
% 1995

lnKP1 = -4576.752 / TempK + 115.54 - 18.453 * logTempK;
lnKP1 = lnKP1 + (-106.736 / TempK + 0.69171) * sqrSal;
lnKP1 = lnKP1 + (-0.65643 / TempK - 0.01844) * s(1);
KP1 = exp(lnKP1);

lnKP2 = -8814.715 / TempK + 172.1033 - 27.927 * logTempK;
lnKP2 = lnKP2 + (-160.34 / TempK + 1.3566) * sqrSal;
lnKP2 = lnKP2 + (0.37335 / TempK - 0.05778) * s(1);
KP2 = exp(lnKP2);

lnKP3 = -3070.75 / TempK - 18.126;
lnKP3 = lnKP3 + (17.27039 / TempK + 2.81197) * sqrSal;
lnKP3 = lnKP3 + (-44.99486 / TempK - 0.09984) * s(1);
KP3 = exp(lnKP3);

lnKSi = -8904.2 / TempK + 117.4 - 19.334 * logTempK;
lnKSi = lnKSi + (-458.79 / TempK + 3.5913) * sqrt(IonS);
lnKSi = lnKSi + (188.74 / TempK - 1.5998) * IonS;
lnKSi = lnKSi + (-12.1652 / TempK + 0.07871) * IonS^2;
KSi = exp(lnKSi);   % on the SWS pH scale in mol/kg H2o
KSi = KSi * (1 - 0.001005 * s(1));  % convert to mol/kg SW

% Calculate K1, K2 using Mehrbach refit by Dickson and Millero (for
% starters) Dickson/Millero, DSR 34(10):1733:1743, 1987, and DSR 36:983,
% 1989, Mehrbach et al L&I, 18(6) 897-907, 1973

% table 4, p. 1739.
pK1 = 3670.7 / TempK - 62.008 + 9.7944 * logTempK;
pK1 = pK1 - 0.0118 * s(1) + 0.000116 * s(1)^2;
K1 = 10^(-pK1); % on the SWS pH scale in mol/kg SW;

pK2 = 1394.7 / TempK + 4.777 - 0.0184 * s(1) + 0.000118 * s(1)^2;
K2 = 10^(-pK2); % on the SWS pH scale in mol/kg SW;

% SRC Note: CO2SYS then calculates pressure effects, which I am leaving out
% since I am going to calculate pCO2 only for the surface at each step.

% pH output scales... make decision then mask out others
```

```
% pH
% pHfactor = 1;
% % pH SWS
% pHfactor = 1;
% pH tot
pHfactor = SWStoTOT;
% % pH free
% pHfactor = SWStoTOT/ FREEtoTOT;
% % pH NBS
% pHfactor = fH;

% Convert from SWS pH scale to chosen scale
K1 = K1*pHfactor;
K2 = K2*pHfactor;
Kw = Kw*pHfactor;
KB = KB*pHfactor;
KP1 = KP1*pHfactor;
KP2 = KP2*pHfactor;
KP3 = KP3*pHfactor;
KSi = KSi*pHfactor;

% Fugacity constants (assumes pressure is near 1 atm)
% Weiss, Mar Chem 2:203-215, 1974.
Delta = (57.7 - 0.118 * TempK); % cm^3/mol
B = -1636.75 + 12.0408 * TempK - 0.0327957 * TempK^2;
B = B + 3.16528 * 0.00001 * TempK^3;

% For a mixture of Co2 and air at 1 atm (at low CO2 conc's):
P1atm = 1.01325; % in bar
FugFac = exp((B + 2 * Delta) * P1atm / RT);

%Calculate vapor pressure factor
% Weiss and Price, Mar Chem 8: 347-359, 1980;
% Goff and Gradic(1)h, Trans of Amer Soc Heating Vent Engrs 52:95-122, 1946
% Robinson, J. Mar Biol Assoc. UK 33: 449-455, 1954.

VPWP = exp(24.4543 - 67.4509 * (100 / TempK) - 4.8489 * log(TempK/100));
VPCorrWP = exp(-0.000544 * s(1));
VPSWWP = VPWP * VPCorrWP;
VPfac = 1 - VPSWWP;

% Calculate pH from TA and TC
% uses TA, TC, K (all K for each dissociation, calculated above), T, pH
% uses Newton's method, solves for pH at which residual = 0, starting guess
% pH = 8.

pHGuess = 8;
pHTol = 0.0001; %this is 0.0001 pH units;
ln10 = log(10);
pH = pHGuess;

deltapH = 0.0002; % just to define delta pH going into loop below
iter = 0;

%VBasic start of a "Do" command - matching "while" at end says:
%Loop while abs(deltapH)>pHtol
```

```
while abs(deltapH)>pHTol
    H = 10^(-pH);
Denom = (H^2 + K1*H + K1*K2);
CAlk = TC*K1*(H + 2 * K2) / Denom;
Balk = TB * KB / (KB + H);
OH = Kw / H;
PhosTop = KP1 * KP2 * H + 2 * KP1 * KP2 * KP3 - H^3;
PhosBot = H^3 + KP1 * H^2 + KP1 * KP2 * H + KP1 * KP2 * KP3;
PAlk = TP * PhosTop / PhosBot;
SiALK = TSi * KSi / (KSi + H);
FREEtoTOT = (1+TS/KS); % pH scale conversion factor
Hfree = H / FREEtoTOT;    % for H on the total scale
HSO4 = TS / (1 + KS / Hfree); % since KS is on the free scale
HF = TF / (1 + KF / Hfree); % since KF is on the free scale
Residual = TA - CAlk - Balk - OH - PAlk - SiALK + Hfree + HSO4 + HF;
% find slope dTA/dPH: (this is not exact but keeps all important terms)
Slope = ln10 * (TC * K1 * H *(H^2 + K1 * K2 + 4 * H * K2) / Denom / Denom +
Balk * H / (KB + H) + OH + H);
deltapH = Residual/Slope; % this is newton's method

% to keep the jump from being too big:
      while abs(deltapH)>1
        deltapH = deltapH/2
      end
pH = pH + deltapH;
iter = iter + 1;
      if pH<0 || pH> 14 || iter>=100
        disp ('The Newton-Raphson pH solver is not converging.  Check for bad
inputs.')
      end
end

% for fCO2: uses TC, pH, Ko, K1, K2, fCO2, where pCO2 = fCO2/FugFac

H = 10 ^ (-pH);
fCO2 = TC*H^2/(H^2 + K1*H + K1*K2)/Ko;
% there is a difference between this modeled pco2 and CO2SYS pCO2.  can't
% tell what from, but seems like from pH solver.  In lieu of finding the
% problem and fixing it... see 060206analysis.xls  this is valid for r% = 0
% through 10%
fCO2 = 0.945.*(fCO2) + 33.648*10^-6;
pCO2 = fCO2/FugFac;

return

%-------------------------------------------------------------------------

% Calculate air-sea flux,  possibly adjust DIC(surface) to reflect new DIC
% SRC wrote this function from scratch, 12/05, updated/streamlined 3/27/06

function calc_flux;
format long g
global t s pCO2 d Flux xstress ystress %T = celsius, s = ppt, pCO2 = atm

TempK = t(1) + 273.15;
pCO2atm = 370e-6; % atmospheric pCO2 in atm
```

```
% CO2 solubility from Weiss 1974
TTT = TempK/100;
lnKo = -60.2409 + 93.4517 / TTT + 23.3585 * log(TTT);
lnKo = lnKo + s(1) * (0.023517 - 0.023656 * TTT + 0.0047036 * TTT^2); % Weiss
Mar Chem 2: 203-215, 1974.
Ko = exp(lnKo); % mol/kg-SW/atm;

Sc = 2073.1 - 125.62*t(1) + 3.6276*(t(1))^2 - 0.043219*(t(1))^3; % Coefficients
from Wanninkhof '92 appendix


% Calculate wind speed from wind stress (updated 3/27/06)

% I used a cheaty method to avoid solving cubic polynomial equations:
% I created a table of wind stress = windspeed from 0-26 m/s based on Yelland
and
% Taylor '96, and then use interp1 in a table lookup to determine windspeed
% from windstress.(note: Yelland and Taylor '96 is only
% valid for 3-26, but to avoid error msg I extended it to cover 0-3 m/s
% also, should not be a big effect in WTNA)

windlo = [0.1:0.1:6]';
windhi = [6:0.1:26]';

dens = 1.3; % kg m^-3, air density
Cdlo = (0.29 + 3.1./(windlo) + 7.7./(windlo).^2)./1000;     %drag coefficient
Cdhi = (0.60 + 0.070.*(windhi))./1000;

Tlo = dens.* Cdlo.* windlo.^2;          % wind stress
Thi = dens.* Cdhi.* windhi.^2;

clear dens Cdlo Cdhi

table = [windlo Tlo; windhi Thi];

U10 = interp1(table(:,2), table(:,1), abs(xstress), 'spline');
V10 = interp1(table(:,2), table(:,1), abs(ystress), 'spline');


 % done calculating windspeeds in x and y direction ...
 % total windspeed:
 Wtot = sqrt(U10^2 + V10^2);

k = 0.0283*Wtot^3*(Sc/660)^-0.5;     % piston velocity: cm h^-1 short-term wind
formulation, Wanninkhof and McGillis 1999
k=k * 24 / 100; % piston velocity in m/d

Flux = Ko*k*(pCO2atm-pCO2)*d(1)*10^-3 *1000; % + into the water, - out
% units: mol kg^-1 atm^-1 * m d^-1 * atm* g L^-1 *0.001 kg g^-1* 1000L m^-3 =
mol m^-2 d^-1
return

%-------------------------------------------------------------------------
% Adjust DIC(1) for time interval and gas increase or loss
% SRC wrote this fuction 12/05, updated 3/27/06

function adj_DIC;
```

```
format long g
global t s pCO2 d Flux dt mld dic z nz dz

deltaDIC = Flux/ 86400.*dt; % change in top box DIC over timestep due to air-
sea,  mol m^-2

topDIC = dic(1,:).*d(1,:).*dz.*1e-6;  % DIC in top box, in mol m-2
% Assumes air-sea driven changes are instantly applied to whole top box SRC
060506
newDIC = (topDIC + deltaDIC)./dz./d(1,:).*1e6;    %air-sea change in ML DIC
applied over timestep
dic(1,:) = newDIC;
return
```

Appendix F, Table 1: Raw underway data from the R/V Knorr meteorological data system for summer 2001. From this data, net solar radiation (W m^{-2}), the precipitation rate (mm s^{-1}), long wave radiation (W m^{-2}, Q_b), latent heat flux (W m^{-2}, Q_{lat}), and the zonal and meridional wind stresses (N m^{-1}) were calculated following Gill (1982) and Yelland and Taylor (1996). These quantities were then used to force the PWP mixed layer model in Chapter 2.

	raw data from R/V Knorr underway meterological system						
JD	Net solar radiation	Surface precip rate	Surface temperature	Above ground temperature	U	V	Relative Humidity
juliandate	Wm^-2	mm min^-1	deg C	deg C	m/s	m/s	percent
190	0.39833333	0	27.880335	27.215133	5.39121778	5.39121778	78.6602
190.0417	0.17166667	0	27.866308	27.169717	5.33264579	5.33264579	78.273133
190.0833	0.27333333	0	27.865033	27.083183	5.27725578	5.27725578	79.868667
190.125	0.46166667	0	27.82917	27.0868	5.135363	5.135363	81.19515
190.1667	0.51666667	-0.0001667	27.888992	26.76125	5.50777259	5.50777259	83.871417
190.2083	0.625	-0.0003333	27.799423	26.627617	5.12404929	5.12404929	84.433583
190.25	0.27166667	0	27.78618	26.423317	5.04874242	5.04874242	88.018383
190.2917	0.6	0	27.621328	25.75655	6.01983571	6.01983571	90.157067
190.3333	0.755	0.01366667	27.622818	26.13455	5.2575746	5.2575746	88.048717
190.375	2.195	0.015	27.58156	25.44635	5.55467732	5.55467732	90.637
190.4167	62.943333	0.0045	27.52906	25.56845	5.10153975	5.10153975	89.612317
190.4583	271.055	0	27.597245	25.906917	5.55114179	5.55114179	91.094683
190.5	440.93	-0.001	27.610655	26.047683	6.0554268	6.0554268	90.770867
190.5417	729.71	-0.0003333	27.626768	26.282067	5.8998633	5.8998633	89.042317
190.5833	627.78167	0.00016667	27.628187	26.2995	4.77627063	4.77627063	87.800117
190.625	775.995	-0.0001667	27.665583	26.29715	4.66006937	4.66006937	84.86375
190.6667	482.62833	0	27.710303	26.363683	4.72040919	4.72040919	86.154717
190.7083	472.13833	0.00016667	27.697897	26.353567	4.16945514	4.16945514	87.278267
190.75	462.09833	0	27.688643	26.349467	2.70609765	2.70609765	87.679067
190.7917	68.356667	0.079	27.653152	24.97185	4.42542779	4.42542779	93.522233
190.8333	87.018333	0.00483333	27.59725	25.663183	3.79186011	3.79186011	92.05825
190.875	13.023333	0.00666667	27.590042	25.58545	4.12443598	4.12443598	93.948533
190.9167	1.2183333	0.00016667	27.54779	26.952817	5.81477474	5.81477474	87.987233
190.9583	0.45	0	27.50886	27.240583	6.36737869	6.36737869	86.258633

191	0.45666667	-0.0001667	27.549663	27.190583	6.64421099	6.64421099	86.508933
191.0417	0.43	0.00016667	27.57398	27.128533	6.93518544	6.93518544	85.15435
191.0833	0.395	-0.0001667	27.598175	27.211267	7.02404521	7.02404521	83.1585
191.125	0.445	0	27.628897	27.144283	6.57998215	6.57998215	83.07755
191.1667	0.41166667	0.00016667	27.656845	27.002933	5.99885825	5.99885825	81.40665
191.2083	0.46333333	-0.0001667	27.666075	26.951783	5.84117344	5.84117344	84.57375
191.25	0.485	0.00016667	27.661067	26.9395	6.24858475	6.24858475	84.597883
191.2917	0.42666667	0	27.603402	26.9486	6.81144175	6.81144175	80.950433
191.3333	0.525	-0.0003333	27.573805	26.803433	6.1548931	6.1548931	80.65355
191.375	41.605	-0.0001667	27.584123	26.957467	6.19637672	6.19637672	79.267833
191.4167	204.96667	0	27.438927	26.767667	6.28016888	6.28016888	81.17035
191.4583	422.78333	0	27.28211	26.803633	6.46378096	6.46378096	79.81615
191.5	678.045	0	27.279897	26.899717	6.3604255	6.3604255	79.235983
191.5417	813.32333	0	27.29362	26.995167	6.28853628	6.28853628	79.147433
191.5833	857.93833	0	27.317738	26.983483	6.78751799	6.78751799	79.22425
191.625	973.30333	0	27.343312	26.82935	6.41180861	6.41180861	80.021517
191.6667	925.20667	0	27.366357	26.841133	5.85837968	5.85837968	79.490967
191.7083	807.35	0	27.386418	26.857583	5.95666752	5.95666752	78.533583
191.75	611.46667	0	27.378455	26.857567	5.70293406	5.70293406	78.477267
191.7917	432.74667	-0.0001667	27.380372	26.867533	5.19381718	5.19381718	77.23875
191.8333	132.565	0.00033333	27.346265	26.83315	5.31084335	5.31084335	79.793867
191.875	19.086667	0.00016667	27.299968	26.767517	5.8575547	5.8575547	80.288383
191.9167	0.46833333	0	27.272213	26.732383	6.00486866	6.00486866	74.215583
191.9583	0.50333333	0	27.259765	26.76365	5.90575584	5.90575584	77.124667
192	0.96833333	0.00233333	27.257092	25.9597	5.23011531	5.23011531	88.91405
192.0417	0.56333333	-0.0006667	27.254898	26.229967	6.040224	6.040224	89.099433
192.0833	0.48	0	27.256828	26.495467	5.75325645	5.75325645	89.00555
192.125	0.575	-0.0006667	27.190637	26.856883	6.52895259	6.52895259	88.549667
192.1667	0.52166667	-0.0003333	27.155897	26.881683	7.05492223	7.05492223	86.652617
192.2083	0.41666667	0	27.102317	26.76065	7.08685963	7.08685963	85.640117
192.25	0.47333333	0.00016667	27.064352	26.689783	6.83854756	6.83854756	85.452833
192.2917	0.41	0.00016667	27.063998	26.659117	7.02157034	7.02157034	79.595217
192.3333	0.70333333	0.00016667	26.985313	26.70955	7.81400157	7.81400157	84.15125
192.375	64.541667	0.00016667	26.99033	26.574383	7.50770625	7.50770625	84.5648
192.4167	162.09	0.00016667	27.078587	26.667417	7.31949776	7.31949776	83.478017
192.4583	456.44333	-0.0001667	27.13592	26.782583	7.20588974	7.20588974	83.663817

192.5	688.08333	-0.0001667	27.142763	26.827933	6.77655784	6.77655784	83.4803
192.5417	808.44833	-0.0001667	27.15194	26.818633	6.72152138	6.72152138	84.177433
192.5833	902.26	0.00016667	27.161403	26.9306	7.08332409	7.08332409	81.83595
192.625	968.455	-0.0001667	27.18086	27.1772	6.78633946	6.78633946	79.580367
192.6667	909.59167	-0.0001667	27.230657	27.025067	6.59235652	6.59235652	81.891233
192.7083	727.37	-0.0001667	27.304968	26.93425	6.23397126	6.23397126	84.100183
192.75	586.055	0.00016667	27.298563	26.893333	6.14664357	6.14664357	83.65435
192.7917	360.425	0.00016667	27.267683	27.037967	6.15147544	6.15147544	81.692167
192.8333	149.675	0	27.17794	26.891	5.5790725	5.5790725	83.99945
192.875	21.135	0.00016667	27.06353	26.8506	5.22292636	5.22292636	83.544983
192.9167	0.465	0.00016667	27.139713	26.850133	5.80699657	5.80699657	83.705467
192.9583	0.45	0	27.236575	26.7092	5.60606044	5.60606044	84.299417
193	0.43333333	0.00016667	27.218468	26.741533	5.18191417	5.18191417	85.5735
193.0417	0.42333333	-0.0001667	27.19359	26.843883	4.46207947	4.46207947	82.92025
193.0833	0.41166667	0	27.185373	26.942633	4.32549006	4.32549006	86.475667
193.125	0.44666667	0	27.22121	26.821817	4.20893524	4.20893524	87.3604
193.1667	0.805	0.027	27.290883	25.9956	4.57627721	4.57627721	90.324633
193.2083	1.24	0.01366667	27.326435	25.071683	2.87273917	2.87273917	93.506917
193.25	1.31	0.02133333	27.483475	24.764433	3.11150552	3.11150552	94.066317
193.2917	1.5983333	0.03366667	27.654732	25.218333	4.46820775	4.46820775	91.324617
193.3333	3.7683333	0	27.761362	26.37015	4.17746899	4.17746899	87.651883
193.375	50.51	-0.0001667	27.774972	26.297683	4.18913625	4.18913625	88.660033
193.4167	247.285	0	27.779087	26.645983	4.42530992	4.42530992	80.100683
193.4583	296.31167	0.00033333	27.785698	26.65195	4.86725165	4.86725165	86.580983
193.5	727.18333	-0.0001667	27.802745	26.885	5.01067653	5.01067653	85.309417
193.5417	775.06333	-0.0005	27.841418	27.015267	4.60903987	4.60903987	84.028017
193.5833	701.295	0.00033333	27.860773	26.797933	4.71498802	4.71498802	87.175
193.625	791.79667	0	27.893718	26.778817	4.78310595	4.78310595	87.122517
193.6667	813.16333	-0.0003333	27.925767	26.999083	4.91097447	4.91097447	85.913767
193.7083	631.82167	0	27.939732	26.9623	4.06150348	4.06150348	86.058683
193.75	478.745	0	27.95105	27.027433	3.68178713	3.68178713	84.744467
193.7917	226.81167	0.00033333	27.950912	27.05475	2.66555689	2.66555689	84.563333
193.8333	114.31333	0.00033333	27.958877	26.528617	2.95641345	2.95641345	83.133867
193.875	11.773333	0	27.944028	26.947683	3.78337483	3.78337483	86.109433
193.9167	0.23	-0.0006667	27.94019	26.9418	3.49758582	3.49758582	82.54325
193.9583	0.2	0	27.891452	26.956467	3.3397832	3.3397832	85.783983

194	0.325	0.00016667	27.862052	26.9531	3.55521502	3.55521502	86.369633
194.0417	0.32166667	0	27.846668	26.978567	4.15708077	4.15708077	84.897017
194.0833	0.18666667	0	27.854862	26.99595	3.58585636	3.58585636	84.00715
194.125	0.155	0	27.846635	26.955283	3.50465689	3.50465689	77.405483
194.1667	0.025	-0.0001667	27.840248	26.911083	3.26188358	3.26188358	85.914533
194.2083	0.17666667	0.00016667	27.82455	26.672367	4.14883116	4.14883116	89.360917
194.25	0.15666667	-0.0006667	27.80926	26.605967	4.63449572	4.63449572	89.3248
194.2917	0.46166667	0.006	27.823722	25.327467	3.93575634	3.93575634	91.590683
194.3333	11.711667	0.039	27.828245	25.410433	4.9555222	4.9555222	94.0949
194.375	54.123333	0.04666667	27.825287	25.384817	4.97426053	4.97426053	93.992633
194.4167	142.31167	0.008	27.789193	26.284283	5.3750722	5.3750722	86.2893
194.4583	554.195	0.00016667	27.799962	26.711667	5.70246264	5.70246264	81.7298
194.5	742.65	0	27.813822	26.713767	6.1805847	6.1805847	79.82095
194.5417	883.29333	0	27.841558	26.73625	5.95254276	5.95254276	79.1666
194.5833	875.08833	0	27.866367	26.764083	6.13391565	6.13391565	79.605783
194.625	935.54667	-0.0001667	27.906382	26.85765	5.88454263	5.88454263	78.7495
194.6667	891.85833	0	27.93747	26.922417	5.38721089	5.38721089	79.305367
194.7083	766.835	0	27.950552	27.006383	5.55503087	5.55503087	79.574633
194.75	574.94167	0	27.935918	27.08145	5.97634864	5.97634864	80.138017
194.7917	349.85333	0	27.940678	27.115883	6.93282844	6.93282844	81.174917
194.8333	144.66333	0	27.919255	27.013633	6.08689305	6.08689305	82.343467
194.875	10.028333	0.00016667	27.906035	27.009817	5.55196677	5.55196677	81.648183
194.9167	0.25	0	27.898065	27.096117	6.06509054	6.06509054	80.659033
194.9583	0.315	0	27.874673	27.1933	5.98082703	5.98082703	80.26685
195	0.2	0	27.848207	27.125767	5.87723589	5.87723589	77.7288
195.0417	0.205	0	27.83944	26.972267	5.82019592	5.82019592	81.849217
195.0833	0.24166667	0.00016667	27.84955	26.945867	5.79073311	5.79073311	81.970667
195.125	0.235	0.00016667	27.842753	26.892083	5.54890259	5.54890259	82.3803
195.1667	0.33833333	0	27.823155	26.829717	5.98318403	5.98318403	83.444533
195.2083	0.21666667	-0.0001667	27.83063	26.78345	5.79815773	5.79815773	83.813367
195.25	0.43	0	27.800692	26.805367	5.65980055	5.65980055	84.879783
195.2917	0.32833333	0	27.782995	26.80135	5.86686496	5.86686496	84.799
195.3333	2.2016667	0	27.790333	26.793033	5.44660786	5.44660786	84.526583
195.375	56.008333	0.00066667	27.788205	26.63285	5.29705477	5.29705477	86.258417
195.4167	227.15167	0	27.776772	26.943817	6.04894496	6.04894496	84.988083
195.4583	465.76333	0	27.793953	27.02365	5.86521507	5.86521507	83.899533

195.5	613.575	0	27.817252	38.710733	6.01830369	6.01830369	84.8606
195.5417	827.04333	0	27.83974	27.134383	6.48605483	6.48605483	84.75375
195.5833	711.04667	0	27.860238	27.184833	6.46495943	6.46495943	84.1493
195.625	878.92167	0	27.83055	27.135433	6.78657521	6.78657521	84.3013
195.6667	864.195	0	27.836607	27.19205	6.1389832	6.1389832	83.612017
195.7083	718.93333	0	27.859517	27.268083	6.24398856	6.24398856	83.929
195.75	544.30333	0	27.858745	27.232583	6.27085861	6.27085861	77.867083
195.7917	291.05	0	27.83718	27.222567	6.988572	6.988572	82.32155
195.8333	114.27667	0	27.823285	27.220867	5.93132956	5.93132956	85.445917
195.875	8.9316667	0	27.833645	27.132317	6.67473446	6.67473446	85.641183
195.9167	0.42833333	0	27.79043	27.1226	7.24595865	7.24595865	85.872167
195.9583	0.39	0	27.769692	27.121183	7.30712339	7.30712339	85.3965
196.9998	0.25333333	0	27.525747	26.916567	7.28685347	7.28685347	81.0598
197.0414	0.27166667	0	27.529832	26.8693	7.03300192	7.03300192	82.2222
197.0831	0.17	0	27.441152	26.851517	7.64924569	7.64924569	81.746
197.1248	0.21833333	0	27.351023	26.782717	7.6552561	7.6552561	80.807483
197.1664	0.11	0	27.28216	26.722317	6.93141422	6.93141422	79.54685
197.2081	0.23333333	0	27.242428	26.6608	7.27624687	7.27624687	80.069933
197.2498	0.11833333	0	27.159137	26.590283	6.56230448	6.56230448	80.1282
197.2914	1.5433333	0	27.057772	26.342917	7.3093628	7.3093628	84.533417
197.3331	0.78666667	0	27.014537	26.46935	7.12374727	7.12374727	81.348117
197.3748	43.713333	0	27.033583	26.5201	7.10783736	7.10783736	80.744583
197.4164	191.4	0	27.056403	26.687617	7.01261363	7.01261363	79.465317
197.4581	443.34333	0	27.117488	26.98615	7.11608718	7.11608718	77.195367
197.4998	639.935	0	27.095422	27.0394	6.87979543	6.87979543	76.8091
197.5414	823.84333	0	27.077633	27.135033	6.80425288	6.80425288	76.79845
197.5831	920.925	0	27.074285	27.0424	6.60449521	6.60449521	78.5403
197.6248	821.91	0	27.134803	27.006667	6.19319474	6.19319474	80.23745
197.6664	411.89667	0	27.192543	26.8467	6.56077239	6.56077239	80.305117
197.7081	740.50833	0	27.262102	27.0555	6.83713334	6.83713334	78.906433
197.7498	676.57167	0	27.380332	27.211367	6.42123668	6.42123668	77.682633
197.7914	471.61167	0	27.405455	27.3031	6.14275448	6.14275448	77.337167
197.8331	233.57833	0	27.415137	27.189633	6.08418242	6.08418242	78.215217
197.8748	44.648333	0	27.403547	26.91005	5.69904498	5.69904498	79.83285
197.9164	0.10666667	0	27.408303	26.8033	5.73098259	5.73098259	80.094767
197.9581	-0.0383333	0	27.38953	26.774717	5.35939797	5.35939797	81.38305

197.9998	0.07333333	-0.0001667	27.427745	26.736167	5.77670885	5.77670885	81.71845
198.0414	0.08333333	0	27.569412	26.771683	5.83209886	5.83209886	81.458683
198.0831	0.02	0	27.876167	26.804183	5.23742205	5.23742205	81.13905
198.1248	0.00833333	0	28.020393	26.793933	4.92582371	4.92582371	80.20785
198.1664	0.08333333	0	28.080863	26.849083	5.07655526	5.07655526	78.850217
198.2081	0.115	0	28.135503	26.876	5.05121729	5.05121729	78.4088
198.2498	-0.0066667	0	28.094913	26.863183	5.10707873	5.10707873	78.471217
198.2914	0.04	0	28.101153	26.867	5.03059332	5.03059332	79.789567
198.3331	0.15666667	0	28.107255	26.880283	4.79276976	4.79276976	80.128333
198.3748	23.821667	0	28.07554	26.9665	4.3668558	4.3668558	78.893217
198.4164	170.92167	0	28.023233	27.14925	5.29257638	5.29257638	78.6903
198.4581	380.00167	0	27.973388	27.215	5.15810829	5.15810829	78.182667
198.4998	570.81833	0	27.938628	27.167417	4.64851998	4.64851998	79.0056
198.5414	649.02667	0	27.918663	27.14155	4.1947931	4.1947931	79.533283
198.5831	844.29667	0	27.884505	27.087433	4.51617314	4.51617314	82.83745
198.6248	945.675	0	27.804238	27.060033	4.48117135	4.48117135	82.205217
198.6664	980.86167	0	27.830318	27.159233	4.64203814	4.64203814	81.477167
198.7081	871.95	0	27.955478	27.354517	4.75128614	4.75128614	80.278083
198.7498	749.46667	0	28.067567	27.4049	4.49554924	4.49554924	80.059367
198.7914	547.88333	0	28.103388	27.474567	4.32761138	4.32761138	79.344417
198.8331	297.25333	0	28.117112	27.57145	4.62648179	4.62648179	79.274433
198.8748	101.22667	0	28.118758	27.414617	4.59218712	4.59218712	81.182417
198.9164	2.57	0	25.82202	26.884683	4.42695988	4.42695988	82.176417
198.9581	-0.1616667	0	28.340775	26.087733	4.70791695	4.70791695	84.305833
199.0012	0.28833333	0	28.461905	26.110517	3.58703483	3.58703483	81.508517
199.0428	0.525	0	28.18499	26.950167	4.36202386	4.36202386	85.039117
199.0845	0.12833333	0.00016667	28.248867	27.292	5.26605988	5.26605988	81.057317
199.1262	-0.005	0	28.111472	27.20215	5.37990407	5.37990407	81.000933
199.1678	0.10833333	0	28.157782	27.152917	5.27584157	5.27584157	81.94315
199.2091	-0.0183333	0	28.174158	26.97725	4.95434366	4.95434366	82.0033
199.2505	-0.1	0	28.112712	26.89765	4.82211469	4.82211469	82.34365
199.2918	-0.0216667	0	28.109365	26.92045	4.53090458	4.53090458	82.504917
199.3331	0.06833333	0	28.081347	26.993183	4.77108513	4.77108513	81.420067
199.3748	4.78	0	28.083653	26.944233	4.75600021	4.75600021	82.20815
199.4164	44.486667	0	28.118003	27.06565	4.51570178	4.51570178	82.624017
199.4581	237.69167	0	28.1607	27.30025	4.54528239	4.54528239	80.52865

199.4998	435.38333	0	28.070015	27.77805	3.52150965	3.52150965	76.644283
199.5414	540.95833	0	28.16493	28.5791	2.67380642	2.67380642	73.829383
199.5831	902.035	0	28.243523	29.040833	3.27755781	3.27755781	68.156483
199.6248	949.18167	0	28.290525	29.2061	3.12128721	3.12128721	68.168417
199.6664	927.16	0	28.32299	29.579467	3.0583547	3.0583547	66.727617
199.7081	739.17333	0	28.342202	29.619583	3.02170295	3.02170295	67.77735
199.7498	620.95333	0	28.37344	29.658683	2.8854671	2.8854671	66.332733
199.7914	440.55	-0.0001667	28.405693	29.371117	2.95723843	2.95723843	67.544567
199.8331	353.15167	0	28.451037	28.985883	3.18068418	3.18068418	67.195367
199.8748	144.69167	0	28.48596	28.567633	2.55018061	2.55018061	69.989167
199.9164	11.333333	0	28.502093	27.80975	2.67251008	2.67251008	75.7681
199.9581	-0.3983333	0	28.505502	27.27705	2.26945921	2.26945921	77.893633
199.9998	0.05166667	0	28.504843	27.029567	1.8114897	1.8114897	80.691067
200.0414	0.03666667	0	28.499115	27.12425	1.91331308	1.91331308	79.318
200.0844	-0.2583333	0	28.480955	26.705467	1.25028266	1.25028266	79.919417
200.1293	-0.07	0	28.436455	26.2601	1.30649765	1.30649765	82.6878
200.171	0.46666667	0	28.318743	27.039667	4.16921946	4.16921946	81.388133
200.2126	0.4	0	28.26556	27.433067	5.74147138	5.74147138	81.26035
200.2543	0.42833333	0	28.197257	27.405183	5.60829956	5.60829956	83.201867
200.296	0.36	0	28.18996	27.38845	5.80228257	5.80228257	82.059983
200.3376	0.42833333	0	28.28922	27.422467	6.13556554	6.13556554	81.34075
200.3793	8.7433333	0	28.246942	27.43585	5.83622369	5.83622369	79.5732
200.421	124.785	0	28.235603	27.520667	6.09431767	6.09431767	77.799533
200.463	282.65167	0	28.09751	27.458967	5.18085351	5.18085351	78.844533
200.5048	576.71833	0	28.243088	27.680333	5.47312436	5.47312436	76.783233
200.5464	768.12	0	28.359837	27.726717	5.01668693	5.01668693	76.444533
200.5881	865.305	0	28.419302	27.680083	4.48623897	4.48623897	78.55895
200.6298	833.14	0	28.496235	27.558517	5.18120706	5.18120706	80.599633
200.6714	924.78833	0	28.547157	27.764533	5.42751597	5.42751597	77.177533
200.7131	820.86167	0	28.527862	27.772783	4.90826385	4.90826385	77.760383
200.7548	633.08	0	28.441518	27.723783	5.16176163	5.16176163	79.2737
200.8001	447.06833	0	28.363767	27.733933	4.46467222	4.46467222	79.0134
200.8501	203.33667	0	28.288807	27.690733	4.30840162	4.30840162	78.880767
200.8918	37.323333	0	28.271592	27.638617	4.21270652	4.21270652	78.669983
200.9335	0.215	0	28.251362	27.5894	4.22295957	4.22295957	80.182683
200.9751	0.285	0	28.244265	27.611133	4.44239835	4.44239835	80.778367

201.0168	0.36	0	28.450682	27.661433	4.90885315	4.90885315	80.904333
201.0585	0.29	0	28.422282	27.640483	4.60574002	4.60574002	82.0649
201.1001	0.22833333	0	28.456772	27.660833	4.97296412	4.97296412	81.3869
201.1418	0.17	0	28.440998	27.625767	5.53464265	5.53464265	80.344733
201.1835	-0.07	0	28.437237	27.450017	5.1020111	5.1020111	81.312667
201.2251	-0.005	0	28.456292	27.39095	4.94220497	4.94220497	81.04585
201.2668	0.065	0	28.359948	27.416533	3.60035205	3.60035205	80.73255
201.3085	0.01666667	0	28.277313	27.337367	3.88119125	3.88119125	81.576717
201.3501	0.09333333	0	28.26474	27.318367	4.13622112	4.13622112	79.8654
201.3918	36.756667	0	28.268847	27.395433	3.74460183	3.74460183	78.7916
201.4335	166.32833	0	28.296012	27.12105	3.5271665	3.5271665	83.4515
201.4751	258.44167	0	28.309008	26.808283	3.39564464	3.39564464	86.7507
201.5168	653.08833	0	28.343452	27.288117	3.25068775	3.25068775	82.6123
201.5585	766.735	0	28.431423	27.468167	3.94695218	3.94695218	81.936267
201.6001	873.30667	0	28.496265	27.4974	4.25206875	4.25206875	81.6388
201.6418	962.795	0	28.691137	27.6173	4.26915719	4.26915719	78.542467
201.6835	841.385	0	28.845183	27.98765	3.82768688	3.82768688	75.11465
201.7251	629.46333	0	28.786947	28.178233	3.68225856	3.68225856	72.8226
201.7668	423.145	0	28.883753	28.210583	3.8974547	3.8974547	69.680267
201.8085	192.21667	0	28.792698	28.172983	3.57866742	3.57866742	71.235533
201.8501	106.00167	0	28.66853	27.9113	3.7099536	3.7099536	77.656617
201.8918	28.373333	0.00483333	28.548182	27.34435	3.86162801	3.86162801	77.656233
201.9335	0.13666667	0	28.463577	27.726533	3.60424114	3.60424114	79.899133
201.9751	0.15	0	28.426838	27.759017	3.15086782	3.15086782	80.08565
202.0168	0.08	0	28.460115	27.7937	3.09524206	3.09524206	79.582733
202.0585	0.045	0	28.67274	27.700483	2.32449567	2.32449567	81.616083
202.1001	-0.02	0	28.67736	27.456767	1.99168412	1.99168412	83.344283
202.1418	-0.2166667	0	28.616127	26.847183	2.42160505	2.42160505	79.456567
202.1835	0.20666667	0	28.564188	26.925667	1.92356612	1.92356612	83.930983
202.2251	0.31666667	0	28.536597	26.9312	2.07064433	2.07064433	84.10745
202.2668	2.2633333	0	28.595422	26.89075	1.37249426	1.37249426	84.952167
202.3085	0.845	0	28.527022	27.00405	3.06495434	3.06495434	84.9816
202.3501	0.14	0	28.413108	26.776467	2.97138057	2.97138057	85.2712
202.3918	42.426667	0	28.384162	26.931983	2.82112038	2.82112038	83.388867
202.4335	236.03833	0	28.291335	27.404033	2.7974323	2.7974323	80.197617
202.4751	218.29	0	28.297068	27.044667	3.47531195	3.47531195	83.72375

202.5168	651.59	0	28.378412	27.029217	3.36736037	3.36736037	82.261
202.5585	843.98833	0	28.508915	27.25565	3.1723167	3.1723167	80.631767
202.6001	912.42333	0	28.543337	27.31485	2.82064895	2.82064895	80.2368
202.6418	980.05333	0	28.625033	27.348017	2.47157388	2.47157388	79.763483
202.6835	946.535	0	28.75409	27.472733	2.47239886	2.47239886	78.879183
202.7251	823.02333	0	28.845547	27.562583	3.16512783	3.16512783	79.2059
202.7668	636.76167	0	28.679268	27.586517	3.24762357	3.24762357	79.57005
202.8085	308.52333	0	28.881105	27.60135	3.2063757	3.2063757	81.025
202.8501	229.37	0	28.803038	27.633783	3.32139843	3.32139843	80.656983
202.8918	25.938333	0	28.812105	27.641717	3.39788376	3.39788376	79.618233
202.9335	0.01666667	0	28.776907	27.585683	3.83263663	3.83263663	82.0689
202.9751	0.21166667	0	28.743853	27.649533	4.03710829	4.03710829	80.939283
203.0168	0.24166667	0	28.6983	27.73	4.06291769	4.06291769	78.668817
203.0585	0.175	0	28.672068	27.755933	3.85302485	3.85302485	78.425767
203.1001	0.09833333	0	28.640308	27.659517	3.74153766	3.74153766	79.834217
203.1418	-0.0316667	0	28.607385	27.5969	3.17149179	3.17149179	79.41925
203.1835	0.1	0	28.576252	27.545183	2.86154327	2.86154327	81.287283
203.2251	0.03666667	0	28.599775	27.500183	3.37219224	3.37219224	80.75215
203.2668	-0.0866667	0	28.594352	27.430917	3.33306569	3.33306569	80.78895
203.3085	-0.0966667	0	28.59191	27.3166	3.03938062	3.03938062	82.740767
203.3501	0.105	0	28.556742	27.360417	3.16300651	3.16300651	82.244767
203.3918	23.691667	0	28.518517	27.398217	2.97149837	2.97149837	82.09235
203.4335	223.32167	0	28.516525	27.589967	3.10254888	3.10254888	81.525767
203.4751	473.49	0	28.557473	27.72195	3.31597725	3.31597725	79.952367
203.5168	646.235	0	28.534082	27.745967	2.64186881	2.64186881	80.22165
203.5585	850.985	0	28.508897	27.846083	2.25908829	2.25908829	79.707517
203.6001	878.36833	0	28.82759	27.995033	2.09739659	2.09739659	80.766583
203.6418	986.435	0	29.02503	27.931167	2.47310597	2.47310597	81.175633
203.6835	838.68667	0	29.00587	27.984167	2.76714451	2.76714451	79.852917
203.7251	834.19833	0	29.07659	28.017117	2.4583746	2.4583746	77.97955
203.7668	518.47833	0	28.893973	28.0482	2.12791998	2.12791998	77.813317
203.8085	350.56167	0	29.049758	28.074567	2.21548342	2.21548342	77.108317
203.8501	228.065	0	29.053963	28.21095	2.09562882	2.09562882	75.768717
203.8918	37.911667	0	29.124445	28.070733	2.6246625	2.6246625	76.782417
203.9335	-0.1433333	0	29.117885	27.935083	3.12128721	3.12128721	78.237467
203.9751	0.16	0	29.142217	27.941683	3.41886129	3.41886129	78.37095

204.0168	0.24666667	0	29.03607	27.887167	3.78042853	3.78042853	80.390933
204.0585	0.22	0	28.949535	27.814533	3.88472678	3.88472678	80.5773
204.1001	-0.035	0	28.843872	27.752283	3.68367278	3.68367278	80.0227
204.1418	0.08166667	0	28.889882	27.770483	3.35451457	3.35451457	79.284833
204.1835	0.32666667	0	28.854027	27.72395	3.47766902	3.47766902	80.248933
204.2251	0.14666667	0	28.745345	27.679417	3.35522168	3.35522168	80.6547
204.2668	0.09833333	0	28.731828	27.67065	3.02264581	3.02264581	81.4479
204.3085	0.215	0	28.708495	27.610417	3.63016834	3.63016834	82.61065
204.3501	0.27833333	0	28.643577	27.409817	4.05478596	4.05478596	84.839233
204.3918	39.825	-0.0001667	28.635585	26.61495	5.33735986	5.33735986	85.824833
204.4335	137.7	0	28.60474	27.01435	5.7481889	5.7481889	81.0194
204.4751	204.685	0	28.579068	27.24935	4.68835364	4.68835364	83.11835
204.5168	531.325	0	28.643885	26.9564	6.39507373	6.39507373	82.715717
204.5585	432.94	0	28.340997	27.225933	5.24390389	5.24390389	81.548517
204.6001	940.505	-0.0001667	28.377387	27.404983	4.40008982	4.40008982	81.83945
204.6418	962.19	0	28.493428	27.500067	3.15499258	3.15499258	82.58275
204.6835	981.09167	0	28.518558	27.600567	3.15911742	3.15911742	81.52665
204.7251	737.64167	0	28.574108	27.833717	3.22546758	3.22546758	80.219067
204.7668	517.38333	0	28.446805	27.969667	4.24004794	4.24004794	77.9427
204.8085	277.73667	0	28.544905	27.081933	5.31155046	5.31155046	81.59275
204.8501	220.11667	0	28.658078	27.09	4.75105046	4.75105046	84.824717
204.8918	27.621667	0	28.664688	27.27825	5.50965816	5.50965816	82.104517
204.9335	0.7	0	28.549427	27.237067	5.71094792	5.71094792	83.378483
205.3176	113.52333	0.00033333	28.760258	28.21245	4.43355952	4.43355952	76.457133
205.8741	137.77167	0	29.011612	28.5502	1.68621399	1.68621399	73.428233
205.9159	10.406667	0	29.044718	27.968233	1.70495232	1.70495232	77.951683
205.9575	-0.12	0	29.064615	27.476267	1.29388753	1.29388753	80.633617
205.9992	-0.2083333	0	29.105558	26.911983	1.24014742	1.24014742	84.97795
206.0409	0.055	0.001	29.10094	26.597017	1.61703533	1.61703533	84.539367
206.0825	0.82166667	0.07333333	29.102565	24.471367	0.81152291	0.81152291	93.6983
206.1242	2.3933333	0	29.11599	25.29075	0.97863579	0.97863579	91.733967
206.1659	1.2583333	0.00183333	29.102393	25.85025	1.16967249	1.16967249	91.2482
206.2075	1.12	0	29.025148	25.98775	1.2849309	1.2849309	89.808033
206.2492	1.0483333	0	29.005498	26.09705	2.37517168	2.37517168	87.8609
206.2909	0.08166667	0	29.007758	26.02255	2.57434011	2.57434011	87.72665
206.3325	0.415	0	28.985527	25.758917	2.56939036	2.56939036	88.52285

206.3742	4.1683333	0	28.960967	26.015083	2.15832557	2.15832557	87.981867
206.4159	119.205	-0.0001667	28.921693	26.571433	1.78226264	1.78226264	86.294167
206.4575	363.03	-0.0001667	28.90695	28.087867	2.50127236	2.50127236	79.15145
206.4992	450.005	0	28.905427	28.7487	2.90880162	2.90880162	74.832267
206.5409	688.965	0	28.890222	29.2817	3.14356107	3.14356107	73.118633
206.5825	512.25333	0.00683333	28.920817	28.96945	3.10313811	3.10313811	71.608
206.6242	523.525	0.00166667	28.91219	27.510817	2.45401408	2.45401408	76.20905
206.6659	701.19	0.0025	28.885845	28.499917	3.14733228	3.14733228	72.902883
206.7075	698.96167	0	28.885122	29.186283	2.95877045	2.95877045	73.285967
206.7492	705.545	0	28.889612	29.867283	3.30230654	3.30230654	65.415983
206.7909	522.20167	0	28.898153	29.6412	3.54649406	3.54649406	66.3425
206.8325	262.305	-0.0001667	28.919442	28.959917	3.13283659	3.13283659	70.91665
206.8742	140.10333	0	28.875593	28.22775	3.13165806	3.13165806	74.75965
206.9159	13.316667	0.00016667	28.852527	26.671533	5.08515842	5.08515842	82.81085
206.9575	0.84833333	0.0045	28.698027	27.377183	5.28055557	5.28055557	83.78475
206.9992	0.505	0	28.588448	27.383167	4.90119278	4.90119278	83.370817
207.0409	0.68	0.0005	28.584038	27.41725	5.48832716	5.48832716	81.662083
207.0825	0.44	0.00016667	28.518198	27.428933	5.59616094	5.59616094	83.745817
207.1242	0.52333333	-0.001	28.527525	27.851933	6.18848067	6.18848067	80.841933
207.1659	0.465	-0.0001667	28.626628	27.87805	6.33544108	6.33544108	79.6468
207.2075	0.44	0.00016667	28.73503	27.740483	6.19614104	6.19614104	81.465933
207.2492	0.515	-0.0001667	28.869532	27.6363	6.27451202	6.27451202	81.97745
207.2909	0.88666667	0.00616667	28.9075	27.101967	6.12543037	6.12543037	83.801083
207.3325	1.0233333	0.00616667	28.822872	26.965517	6.00687211	6.00687211	85.220717
207.3742	6.46	0.00016667	28.71447	26.363583	5.94535382	5.94535382	87.247433
207.4159	116.83167	-0.001	28.601952	27.179333	6.16656036	6.16656036	84.85025
207.4575	324.02167	-0.0001667	28.479742	27.305933	6.05507324	6.05507324	82.953917
207.4992	467.405	0.00366667	28.265522	27.130467	5.75396356	5.75396356	85.056867
207.5409	788.69333	-0.0005	28.277547	27.568983	5.31320035	5.31320035	81.263333
207.5825	890.19333	5.7824E-20	28.26745	27.608167	5.50187999	5.50187999	82.050067
207.6242	909.49	-0.0006667	28.617307	27.797933	5.34266316	5.34266316	81.238433
207.6659	966.145	0.00016667	28.77087	27.86645	5.25804602	5.25804602	79.719983
207.7075	866.04667	0	28.749028	27.8411	4.94008365	4.94008365	80.73955
207.7492	605.365	0	28.819152	27.817083	4.63425997	4.63425997	80.929333
207.7909	420.93	0.0205	28.742802	27.261217	4.07328861	4.07328861	82.80795
207.8325	224.905	0.00033333	28.65213	27.602817	4.05018977	4.05018977	82.021117

207.8742	52.441667	0	28.75451	27.803583	3.91006482	3.91006482	80.5655
207.9159	2.065	0.00016667	28.842383	27.708483	3.76357584	3.76357584	81.958833
207.9575	0.48666667	-0.0001667	28.871667	27.602917	4.11701136	4.11701136	83.525233
207.9992	0.4	-0.0001667	28.81161	27.524833	4.69813533	4.69813533	83.056883
208.0409	1.0716667	0.0245	28.755003	27.1908	4.83059998	4.83059998	87.261533
208.0825	0.725	0.00016667	28.749718	27.590433	5.38237894	5.38237894	84.5243
208.1242	0.995	0.01133333	28.820933	27.157033	4.67138308	4.67138308	87.011733
208.1659	0.78166667	0.0005	28.809007	26.8684	4.94338351	4.94338351	87.46685
208.2075	1.8316667	0.02066667	28.704317	26.584283	3.86893475	3.86893475	89.8263
208.2492	0.90833333	-0.0003333	28.72077	27.223017	5.09647213	5.09647213	85.502783
208.2909	0.76166667	0	28.702853	27.4635	5.80829298	5.80829298	83.6991
208.3325	0.47333333	0.00033333	28.684083	27.2133	5.61666704	5.61666704	85.620333
208.3742	16.768333	-0.0001667	28.697263	27.3616	6.14346159	6.14346159	83.471533
208.4159	142.105	0	28.659895	27.426683	6.06874395	6.06874395	83.101217
208.4575	356.93	-0.0003333	28.646632	27.592033	5.99284785	5.99284785	81.00325
208.4992	593.345	0.00016667	28.650422	27.653	5.8810071	5.8810071	80.733017
208.5409	772.88667	0	28.633472	27.730917	5.48832716	5.48832716	79.727283
208.5825	533.47667	0.00033333	28.626697	27.411417	5.06453445	5.06453445	83.529367
208.6242	483.53667	0.00066667	28.625492	26.72905	5.84034846	5.84034846	87.0451
208.6659	772.59	0.00033333	28.465065	27.519533	6.04753075	6.04753075	83.2425
208.7075	777.39667	-0.0001667	27.98634	27.598583	5.45521094	5.45521094	83.056633
208.7492	646.085	0	27.89199	27.497317	5.01869038	5.01869038	84.0149
208.7909	445.02667	-0.0001667	28.14627	27.560933	5.46817461	5.46817461	83.95545
208.8325	229.29833	-0.0005	28.128583	27.565533	5.55173102	5.55173102	83.571833
208.8742	52.168333	0.00016667	28.081628	27.489583	5.5555023	5.5555023	84.484017
208.9159	1.1383333	0.0005	28.006412	27.441383	6.44492476	6.44492476	84.9613
208.9575	0.765	0.0065	28.010778	26.4722	5.41490586	5.41490586	88.62085
208.9992	1.3133333	0	28.407545	26.42905	6.75958727	6.75958727	89.739433
209.0409	0.51833333	0	28.839253	26.58335	6.18223459	6.18223459	87.935167
209.0825	0.56	-0.0001667	28.831092	27.241217	6.03327074	6.03327074	81.898283
209.1242	0.36666667	-0.0006667	28.86133	27.271467	6.15677874	6.15677874	82.452383
209.1659	0.21833333	0.00016667	28.863537	27.232167	5.4114882	5.4114882	83.43515
209.2075	0.36833333	0	28.974248	27.308817	5.28845162	5.28845162	83.558967
209.2492	0.275	0	29.148148	27.34745	4.7265374	4.7265374	84.164467
209.2909	0.2	0.00183333	29.055492	27.292317	3.92373553	3.92373553	85.147367
209.3325	0.30833333	-0.0001667	29.094135	27.5726	4.30356975	4.30356975	82.19485

209.3742	18.953333	-0.0001667	29.207667	27.663467	4.1794725	4.1794725	81.623
209.4159	179.53833	0.00016667	29.217633	27.493033	4.15743432	4.15743432	82.74865
209.4575	258.08833	0.0005	29.208693	26.838483	5.05027451	5.05027451	85.42955
209.4992	190.21833	0.00683333	29.199755	26.613917	8.6807964	8.6807964	87.201517
209.5409	755.28	-0.0001667	29.211143	27.142233	3.24479514	3.24479514	86.459667
209.5825	849.92	-0.0003333	29.183068	27.666333	3.36111421	3.36111421	81.0542
209.6242	993.43167	0	29.202168	27.659283	3.00909291	3.00909291	81.716483
209.6659	959.74667	-0.0005	29.291852	27.70425	2.78988981	2.78988981	80.62055
209.7075	852.34	-0.0003333	29.390972	27.852883	2.79660732	2.79660732	79.676983
209.7492	641.935	0.00083333	29.299908	27.849767	2.9977792	2.9977792	81.145283
209.7909	445.59333	0	29.183373	34.310133	2.82807357	2.82807357	78.937533
209.8325	187.41833	0.00033333	29.166325	27.915933	2.31459617	2.31459617	80.50175
209.8742	55.946667	0.00066667	29.179568	27.574217	2.15502579	2.15502579	83.968617
209.9159	0.29	0.0005	29.1941	27.301433	3.89356562	3.89356562	84.553417
209.9575	0.24666667	0	29.099997	27.224917	3.40955102	3.40955102	85.018183
209.9992	0.46666667	-0.0003333	29.118263	27.310233	2.67580993	2.67580993	84.829467
210.0409	0.26833333	-0.0003333	29.15048	27.34415	1.44933322	1.44933322	82.044283
210.0825	0.155	0.00033333	29.258093	27.229167	0.97922502	0.97922502	84.849633
210.1242	0.72333333	0.0495	29.145337	26.2277	2.79271823	2.79271823	88.7036
210.1659	3.235	0.00016667	29.083267	27.471967	2.63090865	2.63090865	82.871133
210.2075	0.565	-0.0005	29.11486	27.712333	2.11424928	2.11424928	78.348617
210.2492	0.305	0	29.037097	27.656167	1.83234935	1.83234935	78.583033
210.2909	-0.0983333	0	28.931422	27.580933	1.10886131	1.10886131	81.923317
210.3325	0.47	0.00533333	28.922528	27.07875	2.34264477	2.34264477	83.950417
210.3742	23.616667	0.00033333	29.031863	27.0522	1.98119533	1.98119533	76.662567
210.4159	197.26	-0.0001667	28.987237	27.675683	1.01069127	1.01069127	80.145417
210.4575	462.02833	-0.0005	28.980317	27.933233	0.77604969	0.77604969	77.196483
210.4992	666.75333	-0.0001667	29.011867	28.180883	0.8214224	0.8214224	75.830933
210.5409	825.02833	-0.0001667	29.055468	28.281083	0.98688539	0.98688539	78.115617
210.5825	939.78167	0.00016667	29.127328	28.198767	1.07480231	1.07480231	78.910917
210.6242	937.47333	-0.0001667	29.142768	28.395233	1.1234748	1.1234748	77.298717
210.6659	916.64333	0.00016667	29.141777	28.33295	0.78618487	0.78618487	77.324783
210.7075	786.18	0.00033333	29.145802	28.325233	0.9983169	0.9983169	77.390783
210.7492	598.17	-0.0001667	29.091982	28.383717	1.1628371	1.1628371	77.048033
210.7909	380.80833	-0.0001667	29.062348	28.342617	1.93440847	1.93440847	78.10655
210.8325	143.56333	0	29.218958	28.3791	1.69057444	1.69057444	76.540217

210.8742	17.97	0	29.175238	28.69595	1.36789807	1.36789807	71.2855
210.9159	0.1	-0.0003333	29.428148	28.681817	1.56577009	1.56577009	74.82825
210.9575	0.16	0	29.517655	28.52265	1.41126726	1.41126726	77.031133
210.9992	0.26166667	-0.0001667	29.706055	28.66085	1.14669152	1.14669152	75.067667
211.0409	-0.0283333	0	29.683845	28.235783	1.09012298	1.09012298	78.092967
211.0825	0.07333333	0.00033333	29.44644	28.08715	0.83756798	0.83756798	77.782733
211.1242	4.6259E-19	0.00016667	29.540962	28.16835	1.0376792	1.0376792	76.639117
211.1659	0.14166667	0.00833333	29.60968	27.88655	1.69257796	1.69257796	78.0742
211.2075	2.295	0.0005	29.431168	27.683233	2.45743174	2.45743174	80.618667
211.2492	0.18666667	-0.0003333	29.518868	26.888733	4.38818681	4.38818681	80.378133
211.2909	0.405	0	29.42099	26.707117	3.15487478	3.15487478	77.406117
211.3325	0.30833333	-0.0001667	29.396425	27.394617	3.58998113	3.58998113	79.89895
211.3742	13.831667	-0.0001667	29.308543	27.11805	3.10502375	3.10502375	80.405883
211.4159	113.30667	-0.0003333	29.25407	27.125033	3.57536756	3.57536756	80.545033
211.4575	247.675	0	29.34837	27.222433	3.14308964	3.14308964	82.8961
211.4992	621.09667	-0.0001667	29.505857	27.684417	2.60698483	2.60698483	81.680717
211.5409	510.77	0.00033333	29.554053	28.004717	2.5571338	2.5571338	76.966
211.5825	509.44167	0.001	29.56626	28.087883	0.97557168	0.97557168	77.18655
211.6242	870.73333	0	29.590368	28.431833	2.31636394	2.31636394	75.37395
211.6659	610.03833	-0.0003333	29.582998	28.41785	2.80591758	2.80591758	75.95455
211.7075	10.775	0.52383333	29.487172	24.383317	4.39561143	4.39561143	93.41865
211.7492	30.583333	0.03383333	29.422048	24.707883	3.10089891	3.10089891	93.56
211.7909	127.245	0.00016667	29.392028	25.44705	2.11684202	2.11684202	88.355017
211.8325	26.11	0.0005	29.303227	25.3465	7.79208126	7.79208126	86.281733
211.8742	5.2983333	0.00466667	29.148547	25.147183	3.33059081	3.33059081	87.997683
211.9159	1.0316667	0	29.270512	25.703	3.31456304	3.31456304	86.590883
211.9575	0.515	-0.0001667	29.35813	26.236783	3.29888881	3.29888881	85.09865
211.9992	0.515	0	29.253815	26.825583	3.36087853	3.36087853	81.77535
212.0409	0.48833333	-0.0001667	29.134663	27.18285	3.24503089	3.24503089	82.691483
212.0825	0.77833333	0.00233333	29.030422	27.756367	3.13319015	3.13319015	80.176833
212.1242	0.54166667	-0.0001667	29.235613	28.220617	6.36396103	6.36396103	78.355833
212.1659	0.35666667	0	29.240062	28.0289	6.36396103	6.36396103	79.664667
212.2075	0.41166667	-0.0001667	29.147168	27.966617	6.36396103	6.36396103	79.91705
212.2492	0.44333333	0	29.122882	27.9115	6.36396103	6.36396103	80.6355
212.2909	0.45333333	0	29.005972	27.899233	6.36396103	6.36396103	80.744833
212.3325	0.62666667	-0.0001667	28.977885	27.857033	6.36396103	6.36396103	80.639633

212.3742	34.901667	-0.0006667	28.969517	27.835817	6.36396103	6.36396103	81.483083
212.4159	271.68167	0.00016667	28.97138	27.580733	6.36396103	6.36396103	80.616183
212.4575	331.57667	-0.0001667	28.985033	27.566233	6.36396103	6.36396103	82.175183
212.4992	385.23333	0.00016667	29.015782	27.698983	6.36396103	6.36396103	82.1017
212.5409	786.09667	0.00416667	29.05327	27.5308	1.4777353	1.4777353	79.716583
212.5826	945.73167	-0.0003333	29.122348	28.20345	4.5225371	4.5225371	80.494783
212.6243	977.395	0.00016667	29.091458	28.186533	4.05231109	4.05231109	80.259267
212.666	872.71833	0	29.153922	28.162183	3.63134687	3.63134687	80.788583
212.7076	715.95333	0	29.13119	28.174333	4.46714709	4.46714709	80.4385
212.7493	432.50167	-0.001	29.077617	28.182283	4.44463755	4.44463755	80.369717
212.791	351.67833	-0.0003333	29.163467	28.187817	4.89365035	4.89365035	80.1831
212.8326	91.413333	-0.0003333	29.17373	28.08565	4.81469007	4.81469007	80.847033
212.8743	3.2583333	0.00016667	29.14353	28.01065	4.78228104	4.78228104	80.627167
212.916	0.31833333	-0.0003333	29.152358	28.008233	4.65747669	4.65747669	80.598067
212.9576	0.345	-0.0001667	29.114192	27.9681	4.61281109	4.61281109	81.013017
212.9993	0.26833333	0	29.063887	27.8419	4.69483547	4.69483547	81.96205
213.041	0.33833333	0.00016667	28.885028	27.253817	4.21659561	4.21659561	80.318317
213.0826	0.29666667	-0.0001667	28.764072	27.592367	3.81719808	3.81719808	82.410483
213.1243	0.25666667	-0.0001667	28.656423	27.422267	3.71030716	3.71030716	81.841467
213.166	0.265	0.00016667	28.49498	27.247033	3.38798427	3.38798427	83.86145
213.2076	0.30833333	0.00016667	28.27253	27.124267	3.5265772	3.5265772	84.971833
213.2493	0.27666667	0.00016667	28.029183	27.0301	3.83039743	3.83039743	84.01795
213.291	0.30333333	0.00016667	27.946262	26.98985	3.59976275	3.59976275	84.728233
213.3326	1.1283333	0	27.991115	27.01305	3.95838376	3.95838376	83.96035
213.3743	82.425	0.00016667	27.969915	27.0992	3.66022038	3.66022038	83.24095
213.416	270.55833	0	27.963805	27.22935	3.52092034	3.52092034	82.54265
213.4576	477.69	-0.0001667	27.984095	27.278667	3.55250447	3.55250447	82.958833
213.4993	672.34333	-0.0005	28.03018	27.2018	4.13681035	4.13681035	83.01675
213.541	744.33	0.00033333	28.087247	27.12185	3.80812357	3.80812357	84.350783
213.5826	473.65	-0.0006667	28.13405	27.29405	3.57807819	3.57807819	83.099817
213.6243	200.36667	0.16633333	28.115645	26.47675	4.23663028	4.23663028	86.078017
213.666	161.70667	0.067	28.081087	24.484667	5.84836231	5.84836231	95.094167
213.7076	198.895	0.00666667	27.993332	24.60825	5.60570688	5.60570688	93.389067
213.7493	143.96833	0.01333333	27.953602	24.415517	4.91604202	4.91604202	91.164917
213.791	86.525	0.00983333	27.914402	23.98215	3.66988419	3.66988419	92.619683
213.8326	10.416667	0.08066667	27.874255	23.93695	3.65880616	3.65880616	94.223517

213.8743	1.4716667	0.0065	27.91827	23.71255	2.47758429	2.47758429	93.52875
213.916	1.4266667	-0.0001667	27.883398	23.922983	1.62009951	1.62009951	93.324117
213.9576	1.9216667	-0.0003333	27.915802	24.790783	1.56588797	1.56588797	88.39055
213.9993	1.7016667	0	27.899717	25.259717	1.12512476	1.12512476	86.0013
214.041	1.195	0	27.89408	25.489783	1.23555123	1.23555123	80.211167
214.0826	0.48833333	0	27.879918	25.510883	0.91098921	0.91098921	88.662383
214.1243	0.47	0	27.743658	25.736683	0.90167902	0.90167902	87.988817
214.166	0.33666667	0.00016667	27.680743	25.92955	2.60922402	2.60922402	87.238967
214.2076	0.39166667	-0.0001667	27.606818	25.673367	4.63131374	4.63131374	86.64915
214.2493	0.61166667	0	27.468558	25.73815	4.24287637	4.24287637	84.399617
214.291	0.565	-0.0001667	27.278473	26.513967	4.65618028	4.65618028	85.642967
214.3326	0.73833333	0	27.133877	26.553967	4.65005207	4.65005207	84.8368
214.3743	37.415	-0.0001667	27.106352	26.560533	3.75344067	3.75344067	85.869883
214.416	153.875	0	27.098095	26.641667	3.05752972	3.05752972	85.925617
214.4576	473.15833	-0.0001667	27.103095	26.821733	2.97856944	2.97856944	85.918483
214.4993	581.39167	0	27.134843	26.960767	2.28678333	2.28678333	85.294783
214.541	522.07667	-0.0003333	27.168612	26.9646	3.05434774	3.05434774	86.288783
214.5826	764.11833	0	27.228018	26.998833	4.371452	4.371452	85.438733
214.6243	758.27	0	27.259703	27.058	4.64863785	4.64863785	82.329467
214.666	724.24333	0.00016667	27.270695	26.962067	4.85617369	4.85617369	82.27865
214.7076	611.87667	-0.0001667	27.285155	26.92295	5.67571045	5.67571045	82.459267
214.7493	532.595	0.00016667	27.24494	26.96835	5.86863273	5.86863273	81.513033
214.791	376.78333	0	27.264337	26.983833	5.5426565	5.5426565	81.609183
214.8326	114.885	0	27.245212	26.964483	5.41054541	5.41054541	81.464817
214.8743	1.035	0	27.191463	26.88005	5.68667061	5.68667061	82.056733
214.916	0.34	0.00016667	27.161488	26.874683	6.49253659	6.49253659	81.85635
214.9576	0.38833333	0	27.41569	26.8894	6.79211419	6.79211419	81.344067
214.9993	0.39166667	0	27.581855	26.944567	6.62464775	6.62464775	82.45455
215.041	0.34166667	-0.0001667	27.654843	26.9934	6.6577639	6.6577639	82.555917
215.0826	0.31833333	0	27.488095	26.946167	6.52470995	6.52470995	81.578683
215.1243	0.24	0	27.351057	26.843733	6.53402021	6.53402021	78.802133
215.166	0.135	0	27.368898	26.78175	5.96774555	5.96774555	82.592867
215.2076	0.035	0.00016667	27.363353	26.738683	5.22327992	5.22327992	82.241017
215.2493	0.05833333	-0.0001667	27.35514	26.674183	5.47760268	5.47760268	83.126533
215.291	0.175	0	27.355985	26.68195	5.31909289	5.31909289	82.559533
215.3326	0.46666667	0	27.357555	26.711517	5.37589718	5.37589718	81.33

215.3743	70.146667	0	27.362995	26.780867	6.09031071	6.09031071	80.823967
215.416	263.36333	0	27.420187	26.983083	6.17480997	6.17480997	81.00805
215.4576	497.2	0	27.463205	27.021217	5.00938012	5.00938012	79.4193
215.4993	698.25	0	27.475112	27.029283	4.82989287	4.82989287	80.1453
215.541	805.47167	0	27.505055	27.024967	4.43049541	4.43049541	82.126767
215.5826	695.41333	0	27.55168	27.178033	4.41800317	4.41800317	81.55435
215.6243	904.04167	-0.0001667	27.593987	27.131833	3.64596044	3.64596044	82.20395
215.666	906.43167	-0.0001667	27.604158	27.3972	5.41938425	5.41938425	80.990083
215.7076	647.09167	-0.0001667	27.602093	27.546967	6.09290345	6.09290345	79.556733
215.7493	404.41333	0	27.793158	27.500167	6.54403758	6.54403758	79.08585
215.791	227.44	0	28.390762	27.4649	6.36820367	6.36820367	80.40555
215.8326	68.243333	0.00016667	28.797175	27.44615	6.05966944	6.05966944	80.549667
215.8743	3.5733333	0	28.923845	27.4324	5.55373453	5.55373453	79.433967
215.916	0.10666667	0	28.844	27.432483	5.85354781	5.85354781	78.907833
215.9576	0.37	0	28.859578	27.515383	5.6071211	5.6071211	78.04195
215.9993	0.435	0	29.01771	27.629583	5.45792157	5.45792157	78.37535
216.041	0.38833333	0	29.033147	27.6931	5.50506197	5.50506197	78.6503
216.0826	0.44166667	0	29.047137	27.7205	5.7011663	5.7011663	78.118467
216.1243	0.33166667	0	28.940385	27.640483	5.60276058	5.60276058	78.912117
216.166	0.20833333	0	28.890967	27.562383	6.01288251	6.01288251	78.876017
216.2076	0.335	0	28.94282	27.49225	6.35653641	6.35653641	78.478583
216.2493	0.21333333	0.00016667	28.92121	27.4282	5.93580787	5.93580787	78.0911
216.291	0.2	-0.0001667	28.754843	27.3638	5.70281619	5.70281619	77.501183
216.3326	0.27166667	0	28.765842	27.331333	5.39463551	5.39463551	77.5168
216.3743	24.733333	0	28.769843	27.325883	4.90649608	4.90649608	77.898467
216.416	155.695	0	28.720672	27.38975	5.02352225	5.02352225	74.872
216.4576	289.66333	0	28.684117	27.467867	4.90189989	4.90189989	76.590617
216.4993	455.11167	-0.0001667	28.695032	27.671217	5.12876336	5.12876336	74.767683
216.541	635.74	0	28.7279	27.784967	5.82927043	5.82927043	74.3686
216.5826	875.01333	0	28.729372	27.7806	6.28087598	6.28087598	75.4558
216.6243	939.71333	0	28.813935	27.772683	5.97693794	5.97693794	77.347817
216.666	870.17167	0	29.198677	27.875783	5.7953293	5.7953293	77.972867
216.7076	702.02167	0	29.131588	28.021033	5.93745777	5.93745777	77.37795
216.7493	521.54667	0	29.055467	28.179633	5.76339169	5.76339169	75.560017
216.791	395.89667	0	28.99978	28.247633	5.23188307	5.23188307	75.247483
216.8326	138.05167	0	29.07054	28.185817	5.3651727	5.3651727	74.659733

216.8743	12.526667	0	28.959552	28.068083	5.32498549	5.32498549	75.351917
216.916	0.34166667	0	28.974733	28.071117	5.06241313	5.06241313	76.13705
216.9576	0.17333333	0	29.066097	28.129483	5.11756745	5.11756745	76.211367
216.9993	0.04333333	0	28.964708	27.5783	4.56119229	4.56119229	80.859617
217.041	0.47	-0.0003333	28.897438	27.4889	5.05015663	5.05015663	79.814917
217.0826	0.43666667	0	28.901155	27.532717	3.90664709	3.90664709	78.779167
217.1243	0.17166667	0	28.851503	28.109467	4.57898784	4.57898784	78.193333
217.166	0.22166667	0	28.822893	28.063033	4.78946991	4.78946991	77.690517
217.2076	0.36833333	0	28.722597	27.985233	4.55742108	4.55742108	78.612317
217.2493	-0.5483333	0.00016667	28.870888	26.6958	5.26700273	5.26700273	84.4254
217.291	0.255	0.28	28.847217	24.466417	5.99909393	5.99909393	94.174083
217.3326	1.5083333	0.01566667	29.026477	24.425933	5.90092396	5.90092396	93.908033
217.3743	10.093333	0.0035	29.031898	25.6123	2.80568183	2.80568183	88.482617
217.416	87.308333	0	29.025258	26.335883	0.97498238	0.97498238	89.13865
217.4576	90.798333	-0.0003333	29.043275	26.6789	1.91790927	1.91790927	87.05525
217.4993	30.916667	0.24483333	29.033175	25.1146	3.26341567	3.26341567	89.946483
217.541	136.185	0.08133333	28.997407	25.302017	3.49440384	3.49440384	90.651817
217.5826	239.72167	0.08883333	28.983677	25.850467	3.2510413	3.2510413	85.236483
217.6243	231.665	0.02283333	28.995987	24.91825	5.05298506	5.05298506	91.596017
217.666	245.55167	0.00616667	28.84067	24.770767	4.62259271	4.62259271	89.8906
217.7076	250.26333	0.004	28.918463	24.340217	3.71949954	3.71949954	92.364733
217.7493	198.795	-0.0001667	28.689142	24.104467	2.51847868	2.51847868	93.056417
217.791	159.97167	-0.0003333	29.064862	25.074283	1.7386577	1.7386577	86.072583
217.8326	54.543333	-0.0003333	29.20174	25.591367	1.01634812	1.01634812	81.2953
217.8743	13.863333	-0.0001667	29.042303	26.273467	0.67952962	0.67952962	78.610533
217.916	0.29333333	-0.0001667	28.906353	26.55375	1.04498595	1.04498595	80.133333
217.9576	0.18666667	0	28.72854	26.678083	1.81101834	1.81101834	83.754267
217.9986	0.34666667	0	28.73881	26.835217	2.01631499	2.01631499	84.783567
218.0404	0.46166667	-0.0001667	28.772405	27.058717	2.32602776	2.32602776	85.107617
218.0822	0.65833333	0	28.826883	27.63975	3.62981479	3.62981479	79.61685
218.1238	0.395	0	28.891128	27.8749	4.6317851	4.6317851	75.447067
218.1655	0.31	-0.0001667	28.58935	27.61315	4.64498445	4.64498445	77.30595
218.2072	0.32	0	28.430983	27.37055	4.35153513	4.35153513	79.48895
218.2488	0.22166667	0	28.268237	27.219117	4.33656801	4.33656801	80.192633
218.2905	0.22	0.00033333	28.15758	27.128067	4.53573645	4.53573645	80.759733
218.3322	0.01333333	-0.0001667	28.224893	26.8151	3.89085506	3.89085506	83.478683

218.3738	10.316667	0	28.24247	27.203283	4.42542779	4.42542779	80.97175
218.4155	92.688333	0	28.26818	27.2648	4.51122339	4.51122339	80.457067
218.4572	222.45667	0.00016667	28.197517	27.188217	4.58971224	4.58971224	81.026717
218.4988	431.47167	0.00016667	28.154342	27.074267	3.51490993	3.51490993	79.375367
218.5405	587.68333	-0.0001667	28.19385	27.318667	3.97665066	3.97665066	80.637933
218.5822	747.375	0.00016667	28.293487	27.4398	3.72209222	3.72209222	83.616717
218.6238	789.09	0.00016667	28.319268	27.551183	4.0149523	4.0149523	82.889667
218.6655	861.11	-0.0003333	28.398743	27.899533	4.44015916	4.44015916	78.98215
218.7072	755.32167	0	28.493412	27.670583	4.58676601	4.58676601	81.869217
218.7488	604.13833	0	28.6094	27.414167	5.02800064	5.02800064	83.75905
218.7905	431.99833	-0.0001667	28.672712	27.422533	4.72441608	4.72441608	82.385
218.8322	222.79333	-0.0001667	28.71814	27.53725	4.36944848	4.36944848	81.297033
218.8738	28.51	0.00033333	28.677985	27.445867	4.52182999	4.52182999	81.464
218.9155	0.075	0.00016667	28.657622	27.547183	4.65087698	4.65087698	78.724483
218.9572	0.12166667	0	28.570677	27.59805	4.29084182	4.29084182	76.8684
218.9995	0.18	0.00016667	28.544567	27.614083	4.33468244	4.33468244	77.637867
219.0412	0.325	0	28.554625	27.66175	4.11170806	4.11170806	78.102083
219.0829	0.13	-0.0001667	28.545302	27.668983	4.39655429	4.39655429	79.274433
219.1245	0.27833333	0	28.481555	27.723067	4.12361107	4.12361107	75.533183
219.1662	0.32166667	0	28.471687	27.661917	3.69145095	3.69145095	78.039783
219.2079	0.22333333	0	28.426158	27.643267	3.41285088	3.41285088	79.871183
219.2495	0.21166667	0.00016667	28.416335	27.656467	3.25881948	3.25881948	79.77555
219.2912	0.065	0	28.396712	27.57315	2.77185858	2.77185858	81.232667
219.3329	0.065	0	28.362383	27.55035	3.24432379	3.24432379	80.691433
219.3745	17.9	0	28.381097	27.55645	3.33318349	3.33318349	80.012617
219.4162	174.43667	0	28.393593	27.8567	2.8984307	2.8984307	77.831517
219.4579	407.76833	0.00016667	28.39701	27.902517	2.95523492	2.95523492	75.345167
219.4995	644.67667	0	28.445955	27.971267	2.61641297	2.61641297	79.14115
219.5412	820.69167	0	28.542477	27.97435	2.78022599	2.78022599	79.86875
219.5829	912.65833	0.00016667	28.646175	28.2616	3.66128104	3.66128104	74.965567
219.6245	925.87	-0.0005	28.623603	28.2313	3.24184891	3.24184891	74.496333
219.6662	927.215	0	28.727455	28.165233	3.09842404	3.09842404	76.17275
219.7079	491.02	0.02333333	28.758262	27.774933	3.25375185	3.25375185	77.588167
219.7495	640.42	-0.0001667	28.823257	27.994333	3.62250804	3.62250804	79.410367
219.7912	458.76667	-0.0001667	28.830695	28.305467	3.94223818	3.94223818	77.269617
219.8329	201.105	0	28.95817	28.116467	3.27755781	3.27755781	76.599233

219.8745	60.096667	0.00033333	29.194247	28.009517	3.20036529	3.20036529	79.109167
219.9162	0.19666667	0.00016667	29.144287	28.1492	3.8550283	3.8550283	76.863767
219.9579	0.14166667	0.22866667	28.922247	27.653017	3.83357941	3.83357941	74.881333
219.9995	0.15333333	-0.0001667	28.76308	28.072783	3.18091986	3.18091986	75.514917
220.0412	0.26	0	28.420127	28.008833	2.86460745	2.86460745	77.271717
220.0829	-0.015	0.00016667	28.401705	27.97105	1.96740674	1.96740674	77.804833
220.1245	0.02	0	28.372583	27.864117	2.23610732	2.23610732	78.4342
220.1662	-0.1383333	0	28.28849	27.634367	1.63435945	1.63435945	80.019733
220.2079	-0.0133333	0	28.84586	27.537767	1.4654788	1.4654788	80.52735
220.2495	0.03333333	-0.0001667	29.190753	27.5522	1.41633488	1.41633488	78.828683
220.2912	0.03	0	29.438577	27.588267	1.39370747	1.39370747	78.0442
220.3329	0.085	0	29.289542	27.6912	1.56895207	1.56895207	76.229717
220.3745	15.03	0	29.343582	27.7334	1.41727767	1.41727767	77.618183
220.4162	172.12333	-0.0003333	29.51791	28.162667	1.397243	1.397243	76.902367
220.4579	399.61833	-0.0001667	29.551768	28.459017	0.87115555	0.87115555	75.838717
220.4995	615.00167	-0.0003333	29.484725	28.21785	0.65100965	0.65100965	76.9331
220.5412	737.745	0.00016667	29.564242	28.534283	0.55920361	0.55920361	76.950933
220.5829	765.75833	-0.0003333	29.966152	28.828967	0.71488496	0.71488496	75.806633
220.6245	976.67333	-0.0001667	29.9912	28.54965	0.80881228	0.80881228	74.387867
220.6662	951.10667	0	29.672498	28.5797	1.03166879	1.03166879	76.123783
220.7079	869.17167	0	29.582567	28.475683	1.01788021	1.01788021	77.3079
220.7495	682.3	0	29.56584	28.710517	0.87575175	0.87575175	76.262233
220.7912	504.52167	0.00016667	29.607943	28.923917	1.03426154	1.03426154	74.97815
220.8329	301.08167	0	29.342922	28.898833	0.80374473	0.80374473	75.401883
220.8745	57.261667	-0.0001667	29.333672	28.563983	1.55445638	1.55445638	75.022767
220.9162	0.20166667	0	29.450937	28.3655	1.76387787	1.76387787	75.959117
220.9579	0.17833333	0.00016667	29.508752	28.4766	1.61597467	1.61597467	77.429967
220.9995	0.29	0	29.550473	28.750617	2.01325088	2.01325088	75.211767
221.0412	0.13333333	0	29.55655	28.693717	2.70586197	2.70586197	76.45895
221.0829	2.6883333	0.00766667	29.704485	27.833883	1.93652979	1.93652979	76.75645
221.1245	0.66833333	-0.0003333	29.61686	27.845633	3.20696493	3.20696493	80.891517
221.1662	0.245	0	29.762925	27.69	3.82886535	3.82886535	79.503367
221.2079	0.10666667	-0.0001667	29.641012	27.786083	3.2404347	3.2404347	81.5246
221.2495	0.28	-0.0001667	29.486265	27.735733	3.69581147	3.69581147	83.116067
221.2912	0.08	0	29.293538	27.6468	3.84430389	3.84430389	83.946767
221.3329	0.14166667	-0.0001667	29.24034	27.676633	3.44184226	3.44184226	82.62805

221.3745	19.111667	0.23966667	29.312875	27.1817	3.23595631	3.23595631	81.74155
221.4162	105.615	0.00016667	29.198215	27.7736	3.02865622	3.02865622	82.936867
221.4579	368.27	0	29.181083	28.040383	2.7064512	2.7064512	81.0886
221.4995	612.925	0	29.286003	28.46855	2.54157745	2.54157745	79.669633
221.5412	737.53	0.00016667	29.42913	28.352367	2.08407936	2.08407936	79.9513
221.5829	928.47333	0	29.466905	28.20875	2.35466558	2.35466558	81.45345
221.6245	1041.0067	0	29.482415	27.67845	2.31530328	2.31530328	84.163083
221.6662	853.80167	0.00033333	29.566718	28.414867	1.51992603	1.51992603	81.0077
221.7079	779.15833	-0.0001667	29.721887	28.7619	1.17921843	1.17921843	78.787233
221.7495	396.81167	0	29.747882	28.338117	1.51686192	1.51686192	80.48105
221.7912	307.36	0	29.694642	27.773967	2.0823116	2.0823116	83.199167
221.8329	202.395	0	29.616233	28.409767	1.59075458	1.59075458	79.774283
221.8745	75.806667	0	29.60208	28.456833	1.2750314	1.2750314	79.1014
221.9162	0.20333333	0.00033333	29.553413	28.383217	0.92289222	0.92289222	78.338967
221.9579	-0.0783333	0.00016667	29.56848	28.533467	1.06089585	1.06089585	74.481983
221.9995	-0.07	0	29.60695	28.545867	0.78088157	0.78088157	76.087117
222.0412	-0.1033333	0	29.772298	28.572583	0.4323958	0.4323958	75.7008
222.0829	-0.0783333	0.00016667	29.775405	28.552367	0.65065609	0.65065609	75.6171
222.1245	-0.04	-0.0001667	29.642605	28.21235	1.40266418	1.40266418	80.834867
222.1662	-0.0416667	0	29.647523	28.066983	0.80339118	0.80339118	77.0911
222.2079	-0.085	-0.0001667	29.706935	28.066467	0.41625019	0.41625019	74.1951
222.2495	-0.0583333	-0.0001667	29.893038	28.124017	0.40010458	0.40010458	69.967217
222.2912	-0.0483333	0	29.685633	28.108417	0.28461048	0.28461048	75.727017
222.3329	-0.0333333	-0.0001667	29.524905	28.133167	0.48425029	0.48425029	75.547117
222.3745	6.9616667	0	29.498208	28.149567	0.58159533	0.58159533	75.183
222.4162	138.92833	-0.0005	29.490285	28.482333	1.02860469	1.02860469	74.30245
222.4579	365.205	0	29.543788	28.475533	1.02035509	1.02035509	76.60635
222.4995	465.09833	-0.0001667	29.532125	28.580367	1.07609865	1.07609865	78.05785
222.5412	345.40167	0.03483333	29.626135	27.157467	1.7908658	1.7908658	81.614633
222.5829	961.48167	0	29.693563	28.144217	0.56804245	0.56804245	80.704183
222.6245	1123.665	-0.0003333	29.758067	28.987667	0.57982756	0.57982756	77.017567
222.6662	878.74667	0.00016667	29.70586	28.660917	0.83580022	0.83580022	78.74365
222.7079	873.06333	0.00016667	29.693687	28.77815	0.78041021	0.78041021	76.5572
222.7495	764.87667	0	29.547233	29.096183	0.79844143	0.79844143	69.415083
222.7912	269.69	0	29.754897	28.8427	0.82660783	0.82660783	75.467033
222.8329	152.255	-0.0005	29.763472	28.7223	1.42870925	1.42870925	78.07805

222.8745	106.41833	-0.0003333	29.62265	28.901083	1.76269933	1.76269933	78.201867
222.9162	1.81	0	29.646935	28.875117	1.23425489	1.23425489	75.214833
222.9579	0.19833333	0	29.64311	29.039733	1.40702462	1.40702462	75.1421
222.9995	0.14666667	-0.0001667	29.652395	28.970033	2.27063775	2.27063775	76.0024
223.0412	0.875	0.00166667	29.612478	28.472033	3.46930155	3.46930155	79.699117
223.0829	0.45833333	0	29.748423	28.49245	3.41061168	3.41061168	79.7976
223.1245	0.08166667	0	29.86575	28.195783	3.83805773	3.83805773	82.549383
223.1662	0.24	0	29.86621	28.268117	4.04500434	4.04500434	81.793817
223.2079	0.21833333	0	29.747768	28.259117	4.919224	4.919224	81.529733
223.2495	0.265	0	29.601515	27.926883	4.63461352	4.63461352	80.5209
223.2912	0.1	0	29.746753	27.929367	4.10958674	4.10958674	80.793533
223.3329	0.27833333	0	29.545212	28.121583	3.97134736	3.97134736	79.01435
223.3745	6.3866667	-0.0003333	29.57041	27.7314	3.89922247	3.89922247	77.555533
223.4162	103.69333	0.00016667	29.30478	28.318517	3.57383555	3.57383555	78.639367
223.4579	301.725	0.00016667	29.363522	28.41365	3.56841437	3.56841437	79.143617
223.4995	542.20833	0	29.400283	28.523917	4.20410337	4.20410337	78.182333
223.5412	762.43833	0.00016667	29.752133	28.553117	4.0636248	4.0636248	78.051317
223.5829	905	0.00033333	29.812513	28.2686	4.611279	4.611279	79.968733
223.6245	1004.7733	-0.0001667	29.801372	28.1958	4.44935155	4.44935155	80.805467
223.6662	898.25667	0.00016667	29.874185	27.835033	6.17457429	6.17457429	81.706233
223.7079	841.07333	-0.0001667	29.940142	27.444717	5.84883374	5.84883374	83.92135
223.7495	507.54667	0.00133333	29.819753	27.335333	5.63858735	5.63858735	84.247767
223.7912	334.83167	0.0005	29.783605	27.698233	5.80169326	5.80169326	85.61405
223.8329	292.57333	0.0065	29.589318	27.45685	5.32074285	5.32074285	85.604467
223.8745	63.863333	0.0065	29.617948	27.58765	5.58496504	5.58496504	83.728933
223.9162	1.9116667	-0.0001667	29.651625	28.1897	5.82797409	5.82797409	82.366333
223.9579	0.49166667	-0.0001667	29.548563	28.36335	5.94665016	5.94665016	80.94435
223.9995	0.75166667	0.00233333	29.444857	28.233283	6.76830823	6.76830823	81.821383
224.0412	1.2066667	0.00183333	29.200703	27.9244	5.88796029	5.88796029	85.2335
224.0829	0.51	-0.0006667	29.012038	28.231983	6.30597827	6.30597827	83.671517
224.1245	0.44333333	0.00016667	28.895358	28.3244	7.0969953	7.0969953	81.15125
224.1662	0.415	0.00016667	28.959012	28.288867	6.83265495	6.83265495	80.743317
224.2079	0.365	-0.0003333	29.065677	28.041733	6.45847766	6.45847766	82.951
224.2495	0.395	-0.0001667	29.064102	28.2428	7.19846512	7.19846512	81.356883
224.2912	0.33833333	0.00033333	29.081255	28.128067	6.72199274	6.72199274	82.142883
224.3329	0.36	-0.0001667	28.980502	28.0959	6.60755932	6.60755932	79.631833

224.3745	12.938333	-0.001	28.791352	28.036967	6.32872357	6.32872357	80.02325
224.4162	109.09333	-0.0001667	28.789837	27.939783	5.67406049	5.67406049	81.957333
224.4579	244.945	0.00016667	28.784918	28.011583	6.55794397	6.55794397	80.334033
224.4995	519.81167	-0.0001667	28.797877	27.352733	5.64872252	5.64872252	79.271383
224.5412	780.2	-0.0003333	28.830302	27.812583	5.59580739	5.59580739	84.173383
224.5829	851.06167	-0.0001667	28.856672	28.159683	6.21747205	6.21747205	81.515783
224.6245	956.54667	-0.0001667	28.831227	28.204067	6.26260908	6.26260908	80.833833
224.6662	915.26333	-0.0003333	28.913903	28.268783	6.41593338	6.41593338	80.181783
224.7079	699.04833	-0.0001667	28.958023	28.311433	6.11941996	6.11941996	80.198333
224.7495	687.59333	0.00016667	28.95897	28.425633	5.73852508	5.73852508	78.242383
224.7912	393.19	0	28.8232	28.453417	5.80935364	5.80935364	78.8693
224.8329	97.518333	0	28.711665	27.677667	5.4826703	5.4826703	83.71025
224.8745	17.918333	0.00233333	28.6861	27.5019	6.1077527	6.1077527	85.252683
224.9162	1.015	-0.0001667	28.656347	28.019367	6.47721599	6.47721599	83.010467
224.9579	0.37	0	28.578695	28.162183	6.72199274	6.72199274	80.08725
224.9995	0.35833333	-0.0001667	28.701607	28.133467	7.24772642	7.24772642	79.781867
225.0412	0.29	0	28.599842	28.051383	7.30570918	7.30570918	79.4494
225.0829	0.25666667	-0.0001667	28.679645	27.87605	7.12068337	7.12068337	81.397517
225.1245	0.33833333	-0.0001667	28.934457	27.9369	7.16417044	7.16417044	79.847217
225.1662	0.35833333	0	29.126268	27.900617	7.10512702	7.10512702	79.84655
225.2079	0.34333333	0.00016667	29.182008	27.891017	6.36726089	6.36726089	77.7559
225.2495	0.255	-0.0005	29.100012	27.868617	6.47320903	6.47320903	78.096817
225.2912	0.255	-0.0001667	29.058608	27.716283	5.79686139	5.79686139	80.36045
225.3329	0.23333333	-0.0001667	29.018977	27.68355	5.36859036	5.36859036	79.998983
225.3745	8.6683333	0.00016667	29.005713	27.674933	5.49480892	5.49480892	80.435167
225.4162	92.551667	-0.0001667	29.024275	27.73065	5.52957503	5.52957503	79.862117
225.4579	163.77167	0.02733333	28.971412	27.669967	5.44212947	5.44212947	76.944333
225.4995	307.48667	0.03033333	28.96448	26.415267	4.56696702	4.56696702	79.069917
225.5412	566.85167	0	29.035902	27.237667	4.81963982	4.81963982	80.61535
225.5829	916.26167	0	29.113683	27.42725	4.80514413	4.80514413	81.8032
225.6245	846.22333	0.00016667	29.157767	26.910317	4.78192748	4.78192748	86.937633
225.6662	652.25	0.00016667	29.192443	26.8495	5.38485382	5.38485382	87.595533
225.7079	893.45	0	29.23629	26.883467	4.91568847	4.91568847	87.285067
225.7495	643.14	0.00033333	29.254207	27.1186	4.684111	4.684111	85.734717
225.7912	495.54833	0	29.272428	27.068233	5.01762972	5.01762972	86.75065
225.8329	325.60167	0.00016667	29.314365	27.011633	3.75780111	3.75780111	86.1769

225.8745	74.241667	-0.0006667	29.353332	27.28575	3.98336818	3.98336818	86.359883
225.9162	0.49	0.0005	29.310195	27.3484	4.04441511	4.04441511	86.104367
225.9579	0.32166667	-0.0001667	29.212433	27.429933	4.00599559	4.00599559	83.5451
225.9995	0.37833333	-0.0001667	29.011932	27.14755	4.00116372	4.00116372	81.380683
226.0412	0.32666667	-0.0001667	29.284062	27.728717	4.64663434	4.64663434	81.894533
226.0829	0.31833333	0.00016667	29.422457	27.770783	4.94079076	4.94079076	83.133533
226.1245	0.43666667	0	29.367157	27.958067	6.19048419	6.19048419	80.933683
226.1662	0.38166667	0	29.265592	28.111333	5.77682672	5.77682672	75.46645
226.2079	0.275	0	29.24932	28.150467	5.7064696	5.7064696	75.5186
226.2495	0.165	0.00016667	29.204427	27.85825	4.95434366	4.95434366	76.500783
226.2912	0.33333333	-0.0001667	29.0574	27.972333	5.83233461	5.83233461	76.509867
226.3329	0.39333333	-0.0001667	28.84636	28.060067	5.97387377	5.97387377	81.18055
226.3745	9.7466667	0	28.749782	28.195817	5.59451098	5.59451098	80.025083
226.4162	74.875	0.00016667	28.737718	28.241367	5.09588289	5.09588289	81.048633
226.4579	197.13667	0.08083333	28.735692	27.53895	5.6488404	5.6488404	84.788883
226.4995	584.19	-0.0005	28.755565	28.285883	5.46298912	5.46298912	80.607717
226.5412	839.97667	0	28.788343	28.577983	5.96656702	5.96656702	79.341983
226.5829	784.42	0	28.838995	28.603733	5.44319013	5.44319013	79.196067
226.6245	1014.705	0	28.897368	28.652533	4.95705421	4.95705421	76.8777
226.6662	950.53667	0	29.019102	28.740367	4.78357737	4.78357737	75.284017
226.7079	787.13167	0	29.249633	28.811333	4.31771188	4.31771188	76.69435
226.7495	555.11167	0	29.324635	28.873767	4.00953113	4.00953113	74.852033
226.7912	504.35	0	29.277485	28.896217	3.75709401	3.75709401	75.0442
226.8329	310.38167	0.00016667	29.20746	28.947033	3.63500028	3.63500028	75.873633
226.8745	54.395	0.00033333	29.140072	28.724767	2.94663183	2.94663183	77.920817
226.9162	0.24833333	0	29.135725	28.679667	2.30080759	2.30080759	76.740433
226.9579	-0.0016667	0	29.131412	28.639833	1.92498034	1.92498034	76.069817
226.9995	-0.0833333	0	29.122563	28.281933	2.6769884	2.6769884	78.548767
227.0412	0.09833333	-0.0001667	28.974702	27.864733	4.33986787	4.33986787	79.378983
227.0829	0.215	0	28.949982	27.797233	4.95351868	4.95351868	79.2611
227.1245	0.08	0	28.981145	27.78455	4.30851949	4.30851949	81.799567
227.1662	0.08	0	28.993352	27.745533	4.91839909	4.91839909	85.516967
227.2079	0.12166667	-0.0001667	29.022747	27.668283	5.43152286	5.43152286	86.7434
227.2495	0.21166667	0	29.014688	27.70355	4.72559462	4.72559462	85.548633
227.2912	0.13333333	-0.0001667	28.889297	27.7152	4.99229175	4.99229175	84.756567
227.3329	0.36333333	0	28.780398	27.78945	4.38936534	4.38936534	84.014017

227.3745	4.765	0	28.830637	27.497117	3.52457375	3.52457375	84.401233
227.4162	149.21667	0.00016667	28.813198	27.84855	3.79728129	3.79728129	84.4487
227.4579	381.73333	-0.0001667	28.796743	28.136267	3.76675782	3.76675782	81.62065
227.4995	610.33333	-0.0001667	28.796307	28.164867	3.65055663	3.65055663	78.46285
227.5412	805.265	0	28.825523	28.026667	2.95629558	2.95629558	83.391333
227.5829	909.05167	0	28.858407	28.018117	2.83655885	2.83655885	82.511117
227.6245	908.07667	-0.0003333	28.980932	42.202783	2.50563288	2.50563288	77.850117
227.6662	936.525	0	28.988022	27.98705	2.49361206	2.49361206	83.484633
227.7079	882.65	0	29.055963	28.024383	2.49007653	2.49007653	81.940767
227.7495	763.18833	0	29.092565	28.248867	2.62277693	2.62277693	80.711983
227.7912	494.205	0.00016667	29.219388	28.347567	3.19718331	3.19718331	79.613417
227.8329	250.34	0	29.246002	28.341033	3.26942608	3.26942608	79.891333
227.8745	76.058333	0	29.381042	28.413667	3.53730167	3.53730167	79.414733
227.9162	1.485	0	29.440258	27.923783	2.35277994	2.35277994	84.687133
227.9579	0.23833333	0.00016667	29.473783	27.78205	1.90506354	1.90506354	83.974367
227.9995	-0.1016667	-0.0001667	29.6317	27.673167	1.59688279	1.59688279	84.670117
228.0412	0.30833333	0	29.65284	27.713933	1.87241876	1.87241876	83.2871
228.0829	0.10833333	0.003	29.443678	27.4584	2.34818375	2.34818375	83.690883
228.1245	1.3716667	0	29.248953	27.261383	2.89194886	2.89194886	84.3153
228.1662	0.58	0	29.043385	27.5029	1.46276825	1.46276825	83.5005
228.2079	0.20666667	0	28.99502	27.376617	0.98346766	0.98346766	86.328533
228.2495	0.25	0	28.994293	27.194617	0.73751237	0.73751237	87.678267
228.2912	0.31833333	0.00066667	28.98945	27.258433	1.52676142	1.52676142	88.066333
228.3329	0.17666667	0.34683333	28.968868	25.883967	1.17544715	1.17544715	92.034617
228.3745	0.72666667	0.03816667	28.967332	24.941783	1.57307691	1.57307691	95.212
228.4162	3.9366667	0.01633333	28.981365	25.840233	2.11377785	2.11377785	94.377883
228.4579	13.545	0.08683333	29.12918	24.95795	1.57896944	1.57896944	95.212
228.4995	92.558333	0.05166667	29.3088	24.951233	2.92930772	2.92930772	94.838967
228.5409	179.39333	0.00016667	29.308727	27.090767	4.32160097	4.32160097	90.336467
228.5825	125.51333	0.00083333	29.218453	26.4352	4.41670683	4.41670683	90.226217
228.6242	88.628333	0.029	29.157198	26.346733	3.44620277	3.44620277	90.199717
228.6659	152.04833	0.01466667	29.14808	26.23215	4.67432938	4.67432938	88.952817
228.7075	86.33	0.00533333	29.135288	26.07725	3.75249781	3.75249781	90.522467
228.7492	90.53	0.00433333	29.129468	26.481717	3.39800164	3.39800164	90.11375
228.7909	102.09833	-0.0001667	29.156323	26.951233	4.03816895	4.03816895	85.70855
228.8325	90.04	-0.0001667	29.092335	27.296383	4.03168719	4.03168719	86.3082

228.8742	39.175	0	29.051347	27.55105	4.73148715	4.73148715	84.193983
228.9159	1.3183333	0	28.945717	27.594917	4.8645411	4.8645411	84.32145
228.9575	0.31166667	-0.0001667	28.878232	27.693667	4.35271367	4.35271367	84.3935
228.9992	0.17666667	-0.0001667	28.812855	27.686333	4.27387126	4.27387126	85.014283
229.0409	0.15333333	-0.0001667	28.920052	27.715417	4.2099959	4.2099959	85.023867
229.0825	0.165	0.0005	28.990665	27.788033	4.44546246	4.44546246	84.870217
229.1242	0.295	0	29.022257	27.823083	4.88917196	4.88917196	85.4703

Appendix G: Input profiles for PWP model runs

Table 1: Summer 2001 southeastern nonplume profile (Chapter 2)

Depth	Temp	Salinity	DIC	TA
0	27.4	36.04	2021.16	2365.75
0.3	27.4	36.04	2021.16	2365.75
20	27.4	36.05	2021.87	2368.36
50	27.2	36.1	2029.02	2373.26
75	27.1	36.14	2032.64	2373.11
100	25.1	36.25	2058.47	2382.66
149.5	16.8	35.69	2118.43	2349
200.2	13.3	35.23	2155.43	2330.3
300.3	10.7	34.9	2171.49	2305
499.9	8.2	34.68	2204.54	2298.92
749.6	5.7	34.49	2218.87	2294.95
1000	4.7	34.62	2215.7	2307.44
1500	4.3	34.95	2174	2313.29
2000	3.6	34.93	2162.77	2313.25
2500	3.1	34.92	2165.12	2317.94
3000	2.7	34.89	2171	2323.75
3497	2.5	34.88	2173.5	2325.43

Table 2: Summer 2001 R = 0% profile (Chapter 4)

Depth	Temp	Salinity	DIC	TA
0	27.3775	36	2024.5	2369.4
10	27.3775	36	2024.5	2369.4
15	27.3775	36.02388	2023.186	2368.878
20	27.3775	36.04775	2021.872	2368.355
50	27.2375	36.098	2029.021	2373.264
75	27.13	36.1365	2032.637	2373.114
100	25.1325	36.25363	2058.471	2382.662
149.5	16.765	35.689	2118.427	2348.996
200.1667	13.28667	35.23033	2155.433	2330.3
300.3333	10.71667	34.90067	2171.487	2304.998

Table 3: Summer 2001 R = 2.5 % profile (Chapter 4)

Depth	Temp	Salinity	DIC	TA
0	27.3775	35.1	1981.608	2316.498
10	27.3775	35.1	1981.608	2316.498
15	27.3775	35.57388	2001.74	2342.426
20	27.3775	36.04775	2021.872	2368.355
50	27.2375	36.098	2029.021	2373.264
75	27.13	36.1365	2032.637	2373.114
100	25.1325	36.25363	2058.471	2382.662

149.5	16.765	35.689	2118.427	2348.996
200.1667	13.28667	35.23033	2155.433	2330.3
300.3333	10.71667	34.90067	2171.487	2304.998

Table 4: Summer 2001 R = 5 % profile (Chapter 4)

Depth	Temp	Salinity	DIC	TA
0	27.3775	34.2	1938.715	2263.595
10	27.3775	34.2	1938.715	2263.595
15	27.3775	35.12388	1980.293	2315.975
20	27.3775	36.04775	2021.872	2368.355
50	27.2375	36.098	2029.021	2373.264
75	27.13	36.1365	2032.637	2373.114
100	25.1325	36.25363	2058.471	2382.662
149.5	16.765	35.689	2118.427	2348.996
200.1667	13.28667	35.23033	2155.433	2330.3
300.3333	10.71667	34.90067	2171.487	2304.998

Table 5: Summer 2001 R = 7.5 % profile (Chapter 4)

Depth	Temp	Salinity	DIC	TA
0	27.3775	33.3	1895.823	2210.693
10	27.3775	33.3	1895.823	2210.693
15	27.3775	34.67388	1958.847	2289.524
20	27.3775	36.04775	2021.872	2368.355
50	27.2375	36.098	2029.021	2373.264
75	27.13	36.1365	2032.637	2373.114
100	25.1325	36.25363	2058.471	2382.662
149.5	16.765	35.689	2118.427	2348.996
200.1667	13.28667	35.23033	2155.433	2330.3
300.3333	10.71667	34.90067	2171.487	2304.998

Table 6: Table 5: Summer 2001 R = 10 % profile (Chapter 4)

0	27.4	32.4	1852.9	2157.8
10	27.4	32.4	1852.9	2157.8
15	27.4	34.2	1937.4	2263.1
20	27.4	36	2021.9	2368.4
50	27.2	36.1	2029	2373.3
75	27.1	36.1	2032.6	2373.1
100	25.1	36.3	2058.5	2382.7
149.5	16.8	35.7	2118.4	2349
200.1667	13.3	35.2	2155.4	2330.3
300.3333	10.7	34.9	2171.5	2305

Appendix H, Table 1: Mean mixing-modeled TA at Macapa, with lower and upper confidence limits. Two observational samples are also listed (see Chapter 3).

		Solved Ar, mixing model		
Cruise	Dates	LCL	ALK	UCL
ET2	Sep9 -Oct11 95	173.3	277.3	381.3
MP8	April 18-May 22 2003	337.4	354.5	371.5
MP3	July 9 - August 19, 2001	275.9	294.8	313.7
ET1	12 April- 16 May 96	162.3	241.4	320.5
2002 hand sample	1-Apr		440.7	
Druffel	Nov-91		298.0	

Appendix H, Table 2: Modeled TA at Manacapuru, discharge (Qman) at Manacapuru, and dilution-modeled TA (using either Q_GPCP or Q_CMAP, precipitation-based total discharge) at Macapa. Average monthly values were calculated with errorprop.m.

	Month	JD	Monthly Qman	sdQman	ALKman	sdALKman	GPCPALK	sd_G_ALK	Q_GPCP	QGPCPerror	CMAPALK	sd_C_ALK	Q_CMAP	QCMAPerror
4/1/1979	4	91	108220	4811.6	683.05	100.15	264.48	43.93	280165	17118	302.13	43.93	247077	15970
5/1/1979	5	121	124315	3807.7	691.13	104.01	324.67	73.18	269120	42138	399.56	73.18	240104	71154
6/1/1979	6	152	132000	858.3	640.76	108.50	279.01	49.27	303884	14340	275.69	49.27	308577	9647.7
7/1/1979	7	182	125780	5101.0	530.60	98.05	258.72	51.89	258805	16121	245.48	51.89	273066	1859.9
8/1/1979	8	213	100656	8818.4	515.22	90.42	241.77	48.71	215221	2265.4	222.64	48.71	237300	24344
9/1/1979	9	244	74403	6647.2	511.13	85.33	227.73	44.43	167445	3406.4	202.45	44.43	191622	20771
10/1/1979	10	274	58399	2095.4	576.86	89.24	246.28	40.83	137068	5758.6	233.69	40.83	146911	15602
11/1/1979	11	305	59244	1624.2	562.90	107.72	220.04	55.62	154158	23811	210.94	55.62	174498	44151
12/1/1979	12	335	66637	3856.5	685.49	95.32	288.83	56.07	159493	19067	275.45	56.07	175446	35020
1/1/1980	1	1	75794	1230.5	623.45	87.42	251.95	44.58	188766	19955	240.70	44.58	205307	36496

2/1/1980	2	32	77367	474.3	620.46	88.45	228.21	47.84	213402	31431	228.11	47.84	219314	37343
3/1/1980	3	61	72680	2461.6	581.91	94.85	185.01	53.48	236605	48991	192.80	53.48	230461	42847
4/1/1980	4	92	89443	5415.8	678.18	92.47	232.40	149.65	292605	88930	245.01	149.65	274983	71308
5/1/1980	5	122	102341	3062.5	644.33	94.78	236.13	149.24	312308	94388	257.94	149.24	269089	51170
6/1/1980	6	153	109192	584.3	584.28	91.11	242.92	57.49	267899	44656	243.15	57.49	276661	53418
7/1/1980	7	183	104606	3749.6	559.42	89.82	241.82	51.39	244675	31966	238.61	51.39	255305	42596
8/1/1980	8	214	87596	6376.7	493.98	83.19	216.25	42.42	200687	12509	201.40	42.42	222541	34362
9/1/1980	9	245	65105	4882.1	479.48	79.32	185.14	38.61	169616	16716	174.22	38.61	188615	35715
10/1/1980	10	275	59601	466.1	598.66	113.75	252.44	55.10	142397	15019	243.51	55.10	152456	25078
11/1/1980	11	306	69090	4567.3	677.99	96.47	355.86	67.24	132421	13611	331.85	67.24	141880	4151.5
12/1/1980	12	336	74726	970.4	670.18	90.06	327.08	46.50	153359	6497.3	305.24	46.50	164886	5029.3
1/1/1981	1	1	75940	987.3	628.24	91.04	252.12	44.51	190314	18905	233.39	44.51	218369	46960
2/1/1981	2	32	81685	2783.3	652.72	99.19	238.48	60.33	229176	41864	239.66	60.33	236737	49424
3/1/1981	3	60	96030	4537.3	715.18	99.30	304.99	53.98	226375	22103	312.55	53.98	222609	18337
4/1/1981	4	91	107857	2509.5	696.95	100.12	293.63	50.84	257265	23966	307.67	50.84	246250	12952
5/1/1981	5	121	114734	1564.1	708.35	102.20	298.13	54.76	274625	30615	292.21	54.76	287583	43573
6/1/1981	6	152	118875	762.4	671.51	101.83	314.32	51.14	254569	14672	328.48	51.14	244034	4136
7/1/1981	7	182	116954	1854.8	633.63	100.14	309.65	51.56	239849	11327	287.29	51.56	265615	37093
8/1/1981	8	213	104552	6743.0	566.39	94.30	283.98	52.08	209062	4780.8	263.47	52.08	229316	25035
9/1/1981	9	244	74268	8468.3	505.21	85.03	208.23	44.60	180651	9199.8	190.15	44.60	205296	33845
10/1/1981	10	274	56896	1841.5	548.55	91.76	224.27	41.12	139588	9096.5	207.47	41.12	156622	26130
11/1/1981	11	305	55740	217.5	613.76	88.50	234.11	57.35	149738	27183	230.08	57.35	167649	45094
12/1/1981	12	335	62929	5126.8	700.65	100.94	304.10	52.67	145254	5602.8	286.14	52.67	157257	17605
1/1/1982	1	1	83831	5150.9	709.58	96.75	326.09	50.20	182780	3587.5	315.79	50.20	189944	10752
2/1/1982	2	32	93868	1948.0	664.86	94.22	278.89	42.49	224203	11151	273.87	42.49	230574	17522
3/1/1982	3	60	102242	2249.5	673.15	95.75	294.20	45.68	234433	13266	307.14	45.68	227366	20332
4/1/1982	4	91	113883	4799.4	699.18	100.40	250.04	43.70	319856	28457	288.35	43.70	278130	13269
5/1/1982	5	121	130686	4234.6	721.02	104.79	331.05	84.72	292366	55203	360.01	84.72	282604	64966
6/1/1982	6	152	140923	1739.3	680.80	108.61	318.87	68.55	304737	42281	336.40	68.55	297047	49971
7/1/1982	7	182	135950	4551.1	581.97	102.69	292.61	61.82	272461	29708	282.67	61.82	282989	19180
8/1/1982	8	213	116041	6390.4	552.44	93.58	302.45	63.90	213589	23625	276.58	63.90	232900	4313.8
9/1/1982	9	244	91515	8444.0	518.81	86.45	234.59	47.73	202981	12586	212.49	47.73	235482	45087
10/1/1982	10	274	66967	4480.3	596.76	90.96	269.00	46.27	148876	4206	243.36	46.27	166325	13243
11/1/1982	11	305	63800	2488.9	714.73	99.22	346.00	53.34	132037	6744.6	333.68	53.34	137156	1626.1
12/1/1982	12	335	77472	4595.1	755.76	97.97	366.13	53.51	160352	377.11	338.48	53.51	175421	15447
1/1/1983	1	1	88858	1973.8	762.71	100.01	419.59	73.17	162673	18137	400.96	73.17	170516	10294
2/1/1983	2	32	91433	166.6	733.35	99.35	370.38	53.68	181365	9209	346.59	53.68	194231	3656.6

3/1/1983	3	60	92087	1302.6	698.59	95.78	287.27	57.05	226693	31373	287.56	57.05	231837	36518
4/1/1983	4	91	100408	3290.1	705.23	97.64	309.14	49.83	229761	17184	312.88	49.83	228750	16173
5/1/1983	5	121	112090	3001.2	706.08	100.00	345.75	50.87	229382	4333.1	353.82	50.87	224408	640.24
6/1/1983	6	152	115530	1165.6	643.53	103.82	299.40	55.44	249547	22392	300.88	55.44	251172	24017
7/1/1983	7	182	104835	6006.3	511.32	94.44	219.67	58.70	249335	42672	216.08	58.70	267727	61064
8/1/1983	8	213	75350	8377.7	477.64	82.41	204.09	43.22	176921	2191.9	187.97	43.22	195170	20441
9/1/1983	9	244	61122	963.1	525.49	84.15	231.32	37.65	139311	391.88	210.96	37.65	154840	15137
10/1/1983	10	274	56088	1842.0	565.04	92.30	260.99	44.16	121859	94.34	255.49	44.16	124646	2693.2
11/1/1983	11	305	61439	3328.1	653.72	90.56	301.04	49.07	133732	8494	286.63	49.07	143690	18451
12/1/1983	12	335	70358	4303.1	694.93	95.73	385.86	83.24	128521	18961	365.67	83.24	135607	11876
1/1/1984	1	1	84218	2785.0	650.64	97.16	300.01	47.72	182998	6938.8	282.45	47.72	197911	21852
2/1/1984	2	32	92568	3378.7	677.49	101.69	332.73	53.35	188849	6840.4	347.55	53.35	182488	13202
3/1/1984	3	61	106037	3626.9	718.22	103.58	324.51	49.94	235112	8254.3	321.94	49.94	238275	11417
4/1/1984	4	92	113893	2032.2	710.98	104.78	339.60	63.74	240291	27216	361.97	63.74	231634	35873
5/1/1984	5	122	123784	2922.6	711.76	107.17	300.38	49.58	294055	18171	307.60	49.58	289912	22314
6/1/1984	6	153	130739	946.1	666.40	107.84	334.80	74.87	264118	39001	382.29	74.87	246297	56822
7/1/1984	7	183	127007	2630.9	609.70	104.35	256.42	51.37	303927	30608	265.15	51.37	295644	22325
8/1/1984	8	214	112391	6240.9	529.48	97.33	280.31	58.35	213173	16233	282.07	58.35	213596	15810
9/1/1984	9	245	90001	6027.9	536.71	90.43	289.92	66.51	168619	22754	266.41	66.51	182732	8641.5
10/1/1984	10	275	70814	4155.5	576.59	98.52	270.23	52.27	151563	9670.7	250.12	52.27	164024	2789.7
11/1/1984	11	306	68846	1008.7	600.85	97.80	280.78	46.78	147672	3646.7	270.21	46.78	153758	2438.8
12/1/1984	12	336	73460	4957.9	703.54	100.43	309.52	50.97	167277	5959.7	289.09	50.97	182707	21390
1/1/1985	1	1	91757	5797.6	649.03	104.43	302.70	54.98	197190	9335	293.83	54.98	205615	17760
2/1/1985	2	32	101973	1508.3	541.44	88.06	285.87	53.85	194164	18071	269.49	53.85	206016	6218.8
3/1/1985	3	60	99459	1039.6	595.14	90.48	267.83	41.88	221448	6641.5	281.80	41.88	210951	3855.8
4/1/1985	4	91	99124	1214.3	628.19	91.87	231.46	350.76	321954	103217	225.13	350.76	312660	93923
5/1/1985	5	121	108385	4782.9	632.57	92.80	268.32	46.53	256447	20416	292.98	46.53	234828	1203
6/1/1985	6	152	117201	1674.5	604.59	94.97	274.22	46.39	259070	15497	297.72	46.39	239071	4501.7
7/1/1985	7	182	115534	2652.9	577.64	91.25	282.00	46.44	237157	8234.8	293.95	46.44	227860	1062.2
8/1/1985	8	213	103391	4065.7	537.59	86.87	259.57	45.06	214607	9393.4	257.82	45.06	217501	12287
9/1/1985	9	244	88543	4748.5	524.23	83.03	283.50	59.67	165327	20537	260.97	59.67	179008	6856.8
10/1/1985	10	274	75810	2275.2	611.52	91.66	294.36	46.96	157800	6454.5	272.04	46.96	171554	7299.9
11/1/1985	11	305	74530	1280.8	603.99	99.70	301.82	52.48	149501	7318.2	281.03	52.48	161022	4202.6
12/1/1985	12	335	82256	5588.4	624.47	93.94	329.73	61.16	156376	12707	312.98	61.16	164933	4150.4
1/1/1986	1	1	91281	1664.1	552.48	94.30	272.60	47.34	185650	515.17	269.94	47.34	187579	1414.7
2/1/1986	2	32	93440	2128.0	612.44	94.42	279.09	44.89	205461	6996.4	283.56	44.89	202739	4274.5
3/1/1986	3	60	104645	4023.0	635.99	98.83	255.72	55.18	263603	36796	281.48	55.18	238217	11410

4/1/1986	4	91	117804	3756.6	688.46	104.75	320.24	53.94	253921	15915	337.60	53.94	244616	25220
5/1/1986	5	121	128925	2074.5	710.89	107.99	334.09	58.72	275535	23809	359.70	58.72	262432	36912
6/1/1986	6	152	135322	2677.6	675.19	110.99	318.38	54.32	287625	10284	330.98	54.32	279017	18891
7/1/1986	7	182	138557	1180.1	574.34	105.28	319.65	76.88	252836	37554	331.18	76.88	249774	40616
8/1/1986	8	213	125174	6877.2	514.91	100.22	294.85	72.12	221229	29244	282.06	72.12	231725	18748
9/1/1986	9	244	96872	8125.2	534.38	93.36	286.78	62.16	181476	16652	280.29	62.16	186569	11559
10/1/1986	10	274	81219	1153.5	628.92	97.46	327.02	60.96	157172	15982	311.64	60.96	165141	8012.6
11/1/1986	11	305	86464	1530.4	670.91	97.14	417.70	123.07	144458	31549	398.05	123.07	151379	24627
12/1/1986	12	335	92696	1693.8	647.24	97.57	381.85	83.07	159490	23784	348.13	83.07	173773	9500.9
1/1/1987	1	1	96326	673.4	691.64	96.64	322.20	50.06	207320	13963	318.66	50.06	212066	18709
2/1/1987	2	32	98635	2041.8	742.49	98.89	332.33	49.58	220864	13961	323.17	49.58	230640	23737
3/1/1987	3	60	108262	3474.2	750.88	100.91	360.98	52.73	225565	9874.9	382.68	52.73	215628	19811
4/1/1987	4	91	116671	3321.0	732.76	101.56	336.26	50.26	254692	11434	351.62	50.26	246234	19892
5/1/1987	5	121	126464	1854.5	697.03	101.97	369.06	92.30	245004	45252	371.31	92.30	247640	42616
6/1/1987	6	152	128691	1336.6	614.72	105.63	297.83	52.76	266251	9943.5	329.04	52.76	246190	30005
7/1/1987	7	182	120797	4829.9	547.62	94.23	254.38	49.09	261042	19608	249.93	49.09	269751	28317
8/1/1987	8	213	100530	6733.5	524.06	87.83	266.76	49.32	198072	2864	249.64	49.32	212950	12014
9/1/1987	9	244	77171	6867.7	509.93	81.99	229.37	43.40	172032	2754.2	224.06	43.40	176882	7604.8
10/1/1987	10	274	61442	2283.4	573.71	86.78	258.25	41.07	136817	2423.8	234.37	41.07	154302	19909
11/1/1987	11	305	61562	1824.3	682.43	90.33	331.00	45.76	127194	1616.9	307.42	45.76	138013	9201.7
12/1/1987	12	335	70777	4208.0	695.28	92.31	334.69	49.93	147370	1567.6	311.10	49.93	159789	10851
1/1/1988	1	1	82622	3312.7	653.27	101.55	299.25	49.55	180744	5688.6	289.26	49.55	188736	13680
2/1/1988	2	32	92217	3450.4	680.68	100.90	288.44	53.16	218932	22226	293.73	53.16	217092	20387
3/1/1988	3	61	105269	3094.9	668.02	103.79	302.29	48.79	233170	4836.5	325.48	48.79	217702	10632
4/1/1988	4	92	110468	1860.3	652.50	100.93	276.64	45.72	261155	14018	288.49	45.72	250892	3754.2
5/1/1988	5	122	123129	4462.1	675.94	104.71	268.83	51.74	311721	33240	279.13	51.74	301873	23392
6/1/1988	6	153	132560	2242.7	627.13	110.47	328.47	71.69	255690	31871	394.90	71.69	230706	56855
7/1/1988	7	183	130532	3682.1	526.84	102.61	252.19	50.55	273522	7086.3	249.33	50.55	277891	11456
8/1/1988	8	214	111959	7707.6	457.86	94.11	221.15	49.82	232578	11443	209.01	49.82	251207	30072
9/1/1988	9	245	81349	10063.4	435.96	85.19	203.92	48.70	174707	327.21	189.86	48.70	189255	14221
10/1/1988	10	275	60138	2173.0	565.74	96.78	242.43	45.91	140823	9887.6	222.61	45.91	160420	29485
11/1/1988	11	306	63816	2926.0	653.55	98.66	320.67	52.17	130327	3803.1	304.50	52.17	137645	3514.2
12/1/1988	12	336	80104	5736.4	612.44	112.79	346.93	88.50	143725	21896	311.52	88.50	158696	6924.9
1/1/1989	1	1	89243	1080.0	618.86	101.67	304.92	50.84	181638	2302.9	292.90	50.84	189609	5668
2/1/1989	2	32	100328	6261.8	685.00	91.78	283.41	59.13	245591	34762	275.23	59.13	264802	53973
3/1/1989	3	60	119635	5420.1	669.21	94.58	299.10	45.30	268470	508.01	309.79	45.30	259798	8163.9
4/1/1989	4	91	134327	3897.3	681.87	98.58	330.87	77.83	282647	48301	351.83	77.83	275631	55317

5/1/1989	5	121	146347	4268.2	684.31	101.83	420.48	502.48	279729	89008	426.26	502.48	278861	89876
6/1/1989	6	152	156751	2353.8	670.96	104.22	415.35	353.68	289588	90255	466.88	353.68	283118	96726
7/1/1989	7	182	154884	2662.8	650.40	103.95	455.72	718.24	254574	93778	1245.22	718.24	252353	96000
8/1/1989	8	213	137535	6730.9	553.78	96.32	336.42	103.09	235040	50229	329.22	103.09	242158	43110
9/1/1989	9	244	108611	9066.4	489.62	86.92	269.74	60.16	198430	20047	249.02	60.16	214637	3840.3
10/1/1989	10	274	83321	5164.3	559.17	97.76	332.28	100.71	145256	30359	310.01	100.71	154620	20994
11/1/1989	11	305	82419	3043.6	603.40	90.33	367.98	106.78	140200	29830	352.77	106.78	146384	23647
12/1/1989	12	335	82396	1373.4	528.02	87.40	310.19	80.14	143754	26066	291.48	80.14	152461	17359
1/1/1990	1	1	76355	1967.4	566.32	107.99	217.39	62.04	204597	38938	216.73	62.04	216449	50791
2/1/1990	2	32	86395	5391.3	716.12	98.46	296.91	54.44	209578	21348	303.25	54.44	207079	18848
3/1/1990	3	60	106861	4443.2	679.23	99.49	264.80	62.95	279820	47656	300.88	62.95	242886	10722
4/1/1990	4	91	116066	2889.7	688.32	100.85	304.04	45.84	263560	650.84	296.06	45.84	271143	6932.9
5/1/1990	5	121	126374	2677.9	665.31	102.02	290.35	45.54	290504	611.38	293.91	45.54	287149	2743.7
6/1/1990	6	152	132869	1796.8	614.33	101.41	316.69	64.00	259858	29601	313.03	64.00	264904	24556
7/1/1990	7	182	130910	2543.4	623.33	101.24	327.36	58.40	250077	17482	311.36	58.40	263239	4319.5
8/1/1990	8	213	116443	6193.3	539.81	94.09	307.83	66.95	205943	23769	294.50	66.95	215697	14015
9/1/1990	9	244	90896	7989.7	515.93	87.09	260.73	52.22	180329	9091.7	236.26	52.22	200248	10828
10/1/1990	10	274	64455	7938.6	521.97	93.35	215.61	53.27	157225	17134	209.08	53.27	167303	27212
11/1/1990	11	305	58612	2273.1	686.53	101.03	284.01	64.07	144119	22740	282.09	64.07	150360	28982
12/1/1990	12	335	74276	6016.6	729.01	99.32	353.35	57.66	153601	1728	343.68	57.66	158193	2864
1/1/1991	1	1	90689	4483.1	682.09	104.28	344.55	57.44	179895	6351.9	332.79	57.44	186519	271.98
2/1/1991	2	32	100618	870.1	607.12	97.47	296.26	48.24	206729	3130.1	297.04	48.24	206543	3316
3/1/1991	3	60	100269	2012.8	670.60	102.00	279.14	52.33	242519	25819	282.71	52.33	242345	25645
4/1/1991	4	91	113166	4826.3	683.48	104.07	288.50	48.11	268659	12885	305.99	48.11	253723	2050.4
5/1/1991	5	121	127729	4357.7	682.37	107.43	348.89	81.53	254316	40679	367.61	81.53	248942	46053
6/1/1991	6	152	137638	2277.1	647.33	110.45	322.82	64.73	277832	28529	347.64	64.73	265428	40933
7/1/1991	7	182	134043	3313.3	568.58	105.83	292.85	58.01	261090	15644	293.57	58.01	262036	14698
8/1/1991	8	213	120320	6137.3	484.44	100.92	279.61	70.94	210945	27465	265.07	70.94	222620	15790
9/1/1991	9	244	92979	9575.7	446.46	89.31	239.17	59.92	174801	17829	215.04	59.92	194014	1384.8
10/1/1991	10	274	64778	6239.0	525.95	87.55	235.89	46.86	144806	3464.8	216.70	46.86	161027	19687
11/1/1991	11	305	55111	2046.0	654.47	102.32	279.36	60.64	130803	18398	271.64	60.64	140608	28203
12/1/1991	12	335	62942	2590.1	658.90	104.64	272.54	60.90	154342	22449	266.68	60.90	164441	32548
1/1/1992	1	1	68266	2271.6	638.72	96.85	275.41	45.54	158676	8543.7	272.17	45.54	162060	11928
2/1/1992	2	32	72718	839.2	539.87	85.75	215.43	38.75	182999	15202	214.29	38.75	186401	18604
3/1/1992	3	61	80166	5713.5	669.97	98.75	292.04	49.06	184477	646.75	292.88	49.06	183998	167.61
4/1/1992	4	92	98431	3931.6	683.56	94.99	282.21	48.36	239504	21778	312.29	48.36	216180	1545.1
5/1/1992	5	122	105620	1338.3	651.51	96.69	253.36	61.25	277807	48930	271.03	61.25	259573	30695

6/1/1992	6	153	103540	1863.8	574.87	90.49	230.05	63.90	267200	53946	235.73	63.90	267952	54699
7/1/1992	7	183	94782	3027.2	557.00	88.42	235.54	53.57	227719	34666	239.62	53.57	228069	35016
8/1/1992	8	214	82865	4916.4	498.71	85.50	262.04	55.94	158900	17363	233.37	55.94	177841	1577.6
9/1/1992	9	245	69815	2673.9	591.71	88.38	282.41	47.96	146704	10155	261.01	47.96	158891	2031.3
10/1/1992	10	275	65075	1126.2	609.56	87.26	270.21	40.08	147073	4314.9	251.47	40.08	161036	18277
11/1/1992	11	306	61253	1386.7	641.44	88.07	273.55	49.80	144765	16737	262.83	49.80	156749	28721
12/1/1992	12	336	74013	6949.1	699.31	92.38	315.42	55.32	164416	9798.9	310.00	55.32	169283	14666
1/1/1993	1	1	89449	3085.7	704.83	98.98	385.71	72.60	164828	19494	380.72	72.60	168259	16064
2/1/1993	2	32	96662	2824.8	702.59	99.43	320.31	48.52	212399	8761.5	329.99	48.52	206595	2958
3/1/1993	3	60	110449	4414.7	702.36	101.74	321.28	49.18	242169	892.75	338.13	49.18	230994	10282
4/1/1993	4	91	123910	4194.9	724.56	106.03	384.16	106.02	241513	49300	392.27	106.02	242279	48533
5/1/1993	5	121	134171	2426.0	730.84	108.80	338.95	60.85	290923	28491	359.85	60.85	280467	38947
6/1/1993	6	152	138778	1433.4	684.67	109.71	387.83	117.29	254916	55681	390.26	117.29	258194	52403
7/1/1993	7	182	134182	3032.6	579.84	106.54	323.81	75.90	243455	33737	319.63	75.90	248766	28426
8/1/1993	8	213	115553	7274.0	542.01	95.43	335.93	94.64	191688	36466	322.17	94.64	200254	27900
9/1/1993	9	244	89961	6588.7	566.23	89.87	332.61	92.19	157572	30440	304.32	92.19	170469	17542
10/1/1993	10	274	73237	3343.3	604.67	95.16	314.02	64.41	142302	17130	286.87	64.41	155180	4251.3
11/1/1993	11	305	73145	3869.2	736.57	101.28	377.57	62.79	143126	10740	355.15	62.79	152242	1624
12/1/1993	12	335	89446	4361.8	730.20	100.49	422.88	88.85	156568	22710	391.48	88.85	168443	10836
1/1/1994	1	1	104500	3265.6	674.71	102.78	366.21	62.17	193076	12809	342.66	62.17	206480	594.61
2/1/1994	2	32	113278	2634.0	642.30	99.78	314.33	50.40	231995	5263.9	305.98	50.40	238659	1400.4
3/1/1994	3	60	124030	2585.8	668.65	103.71	350.82	83.05	241103	40151	378.18	83.05	233068	48187
4/1/1994	4	91	131045	2361.7	691.13	107.16	335.54	76.38	274573	43144	389.92	76.38	254693	63024
5/1/1994	5	121	139846	2783.5	718.60	110.68	373.92	113.49	279961	61883	393.16	113.49	276977	64868
6/1/1994	6	152	147373	2160.4	713.38	112.47	376.83	100.55	287133	55471	424.50	100.55	273308	69296
7/1/1994	7	182	147388	2956.1	667.14	112.81	406.81	150.71	256434	64623	394.55	150.71	265420	55638
8/1/1994	8	213	130006	6385.7	554.64	102.50	322.66	81.71	227418	35666	317.78	81.71	232974	30109
9/1/1994	9	244	104876	7342.7	505.04	91.80	269.93	56.62	196965	14131	253.65	56.62	209740	1356.8
10/1/1994	10	274	85126	4181.9	559.10	90.75	343.36	111.06	144969	33190	313.51	111.06	156339	21820
11/1/1994	11	305	73210	3216.8	614.28	95.38	318.10	58.30	141983	12087	299.84	58.30	150701	3368.7
12/1/1994	12	335	76289	3564.1	691.12	96.39	326.80	49.16	161705	2179.4	305.59	49.16	175028	15503
1/1/1995	1	1	87648	1308.1	623.08	98.16	284.09	47.85	192704	10772	275.07	47.85	201981	20049
2/1/1995	2	32	87537	792.7	640.09	99.47	255.22	56.97	223070	34016	253.56	56.97	232027	42973
3/1/1995	3	60	90199	1449.0	656.15	106.23	265.88	53.20	224436	25714	276.67	53.20	216869	18148
4/1/1995	4	91	101159	5788.8	693.46	101.00	305.84	49.29	229835	5490.8	322.43	49.29	218630	5714.2
5/1/1995	5	121	119193	4573.3	642.46	102.35	279.38	47.10	274702	8218.9	302.54	47.10	254953	11529
6/1/1995	6	152	129024	1441.6	610.39	106.14	287.03	50.52	275294	1804.5	298.38	50.52	265829	11269

7/1/1995	7	182	124190	4228.2	549.94	99.95	251.47	51.38	272911	23159	253.46	51.38	273492	23739
8/1/1995	8	213	104117	7777.8	470.23	95.94	207.77	53.68	238552	31720	209.53	53.68	241098	34267
9/1/1995	9	244	67850	11416.3	456.71	84.14	174.80	55.17	181126	31202	172.47	55.17	193621	43698
10/1/1995	10	274	48878	1817.6	532.18	89.56	191.26	326.21	150615	50971	217.55	326.21	162579	62935
11/1/1995	11	305	53046	4537.7	659.52	94.95	283.77	66.76	125309	19520	278.84	66.76	133297	27508
12/1/1995	12	335	72683	6136.4	652.06	98.11	327.01	59.61	145230	7027	299.45	59.61	159393	7136.7
1/1/1996	1	1	85557	3787.4	666.03	93.87	335.57	50.59	170339	0	319.50	50.59	178909	0
2/1/1996	2	32	95335	3804.0	658.52	95.87	262.52	40.38	239910	0	259.76	40.38	242463	0
3/1/1996	3	61	110922	4434.9	683.45	97.68	297.17	44.95	255912	0	304.05	44.95	250123	0
4/1/1996	4	92	123108	2619.6	678.36	100.06	293.34	44.32	285609	0	306.76	44.32	273110	0
5/1/1996	5	122	132968	3194.0	688.46	103.12	337.89	51.99	271816	0	341.98	51.99	268562	0
6/1/1996	6	153	141036	1155.4	656.59	108.78	321.57	53.86	289001	0	334.20	53.86	278081	0
7/1/1996	7	183	136738	3560.7	532.31	103.06	276.99	54.78	263902	0	281.51	54.78	259658	0
8/1/1996	8	214	116770	7596.3	508.33	91.83	257.72	50.58	231269	0	253.68	50.58	234946	0
9/1/1996	9	245	88423	10300.6	492.06	85.26	260.44	56.18	167742	0	247.18	56.18	176739	0
10/1/1996	10	275	67366	1239.9	613.16	94.44	280.09	44.00	147972	0	263.53	44.00	157268	0
11/1/1996	11	306	71794	1931.4	650.00	93.26	304.99	45.21	153487	0	287.15	45.21	163024	0
12/1/1996	12	336	80127	2716.6	622.81	95.91	333.68	53.49	150066	0	312.07	53.49	160459	0
1/1/1997	1	1	89685	1681.2	589.79	93.43	298.05	48.14	178085	0	284.58	48.14	186517	0
2/1/1997	2	32	94011	2297.7	602.32	100.82	246.50	42.25	230563	0	256.86	42.25	221255	0
3/1/1997	3	60	114300	8614.8	706.89	100.13	380.67	62.79	212930	0	384.13	62.79	211011	0
4/1/1997	4	91	136863	4592.2	690.25	104.47	330.42	52.08	286864	0	361.16	52.08	262443	0
5/1/1997	5	121	150817	3514.7	683.81	107.78	365.72	59.06	282964	0	374.56	59.06	276285	0
6/1/1997	6	152	155340	1185.2	675.43	109.01	331.03	54.00	318056	0	356.24	54.00	295550	0
7/1/1997	7	182	145080	5070.4	562.24	113.94	339.42	70.76	241401	0	348.33	70.76	235232	0
8/1/1997	8	213	117271	11152.0	495.35	92.18	279.84	60.13	208491	0	268.81	60.13	217045	0
9/1/1997	9	244	77009	11870.5	489.63	83.25	261.55	62.32	144756	0	240.04	62.32	157729	0
10/1/1997	10	274	54124	1859.5	530.68	85.80	224.30	37.67	128511	0	202.55	37.67	142314	0
11/1/1997	11	305	54312	4880.7	624.72	100.18	265.22	50.18	128404	0	251.55	50.18	135379	0
12/1/1997	12	335	68119	3999.5	710.62	94.85	364.68	54.51	133131	0	341.57	54.51	142138	0
1/1/1998	1	1	82060	3912.3	724.70	96.96	410.94	59.66	145142	0	410.13	59.66	145431	0
2/1/1998	2	32	89324	1188.0	701.38	96.42	344.94	48.22	182166	0	342.83	48.22	183290	0
3/1/1998	3	60	97662	3135.6	715.01	98.58	322.34	46.42	217290	0	320.85	46.42	218295	0
4/1/1998	4	91	110485	4625.4	730.05	102.02	372.44	55.42	217238	0	393.44	55.42	205642	0
5/1/1998	5	121	128537	5182.9	718.23	105.27	379.40	58.76	244114	0	391.32	58.76	236679	0
6/1/1998	6	152	140074	1667.1	638.79	113.02	385.15	68.99	233212	0	383.96	68.99	233933	0
7/1/1998	7	182	138404	3283.5	552.83	102.90	320.32	60.84	239846	0	307.95	60.84	249477	0

8/1/1998	8	213	116716	9219.5	479.69	94.04	277.31	60.02	202808	0	262.78	60.02	214024	0
9/1/1998	9	244	79416	10719.5	455.17	82.05	210.07	48.99	172824	0	190.33	48.99	190743	0
10/1/1998	10	274	56434	4815.9	483.53	95.45	190.71	42.05	143740	0	181.20	42.05	151281	0
11/1/1998	11	305	63065	7133.0	689.81	94.92	334.86	61.72	130323	0	310.82	61.72	140405	0
12/1/1998	12	335	77245	1524.6	598.78	94.56	338.38	54.54	137158	0	317.73	54.54	146073	0
1/1/1999	1	1	80963	4927.4	612.29	94.20	263.79	44.67	188575	0	240.47	44.67	206859	0
2/1/1999	2	32	104529	7260.9	707.21	97.93	328.36	52.25	225829	0	325.64	52.25	227718	0
3/1/1999	3	60	126042	4445.5	705.43	101.94	403.84	61.14	220874	0	407.28	61.14	219006	0
4/1/1999	4	91	137179	3710.8	698.02	104.02	322.42	49.57	297955	0	326.76	49.57	294002	0
5/1/1999	5	121	150954	4413.4	717.95	108.76	349.74	54.80	310906	0	351.62	54.80	309249	0
6/1/1999	6	152	160444	1289.8	716.66	111.97	421.67	66.63	273606	0	439.31	66.63	262621	0
7/1/1999	7	182	159653	2313.7	633.98	114.30	379.76	69.41	267573	0	371.92	69.41	273214	0
8/1/1999	8	213	144655	7085.3	536.96	102.02	340.60	68.01	229025	0	342.86	68.01	227517	0
9/1/1999	9	244	109036	13598.8	457.79	88.92	287.48	68.55	174443	0	265.17	68.55	189123	0
10/1/1999	10	274	74313	4614.3	517.45	83.30	267.70	47.26	144168	0	247.75	47.26	155774	0
11/1/1999	11	305	62978	2551.5	564.68	94.54	260.37	45.63	137089	0	241.86	45.63	147581	0
12/1/1999	12	335	66379	3219.9	644.30	101.40	247.78	41.63	173213	0	225.89	41.63	189999	0
1/1/2000	1	1	82790	2714.0	612.62	101.74	293.05	50.37	173707	0	290.18	50.37	175427	0
2/1/2000	2	32	89693	2414.4	608.54	90.58	260.75	40.04	210004	0	263.69	40.04	207666	0
3/1/2000	3	61	100422	4847.8	649.67	95.62	254.79	40.30	256898	0	265.18	40.30	246830	0
4/1/2000	4	92	117951	5936.5	676.83	99.98	283.07	45.12	282954	0	299.06	45.12	267826	0
5/1/2000	5	122	136646	5035.7	704.20	105.37	318.63	49.97	302996	0	349.28	49.97	276408	0
6/1/2000	6	153	148845	2136.4	681.35	108.20	329.59	53.15	308768	0	342.41	53.15	297209	0
7/1/2000	7	183	149636	1861.3	645.21	106.73	333.77	55.96	290299	0	337.52	55.96	287072	0
8/1/2000	8	214	137725	5153.0	577.13	102.38	326.07	60.05	244726	0	315.89	60.05	252611	0
9/1/2000	9	245	112374	10080.3	510.13	91.96	328.69	68.00	175134	0	303.84	68.00	189458	0
10/1/2000	10	275	86704	3940.6	547.87	86.79	283.87	47.69	167927	0	269.74	47.69	176728	0
11/1/2000	11	306	75399	2742.7	517.58	85.24	271.35	46.52	144342	0	252.73	46.52	154980	0
12/1/2000	12	336	70097	3689.4	588.80	94.18	235.11	40.42	176174	0	216.89	40.42	190979	0
1/1/2001	1	1	83179	5587.3	638.22	101.55	281.42	49.80	189318	0	274.22	49.80	194286	0
2/1/2001	2	32	103130	4589.7	694.05	100.65	337.24	52.19	212923	0	338.26	52.19	212286	0
3/1/2001	3	60	116950	3798.7	673.19	101.86	322.64	50.75	244826	0	346.06	50.75	228259	0
4/1/2001	4	91	131922	4491.6	681.71	106.20	298.49	48.39	302330	0	297.90	48.39	302930	0
5/1/2001	5	121	141608	1936.1	690.36	109.15	379.95	60.97	258185	0	397.79	60.97	246605	0
6/1/2001	6	152	147310	1112.6	656.10	110.89	348.39	59.50	278432	0	364.53	59.50	266107	0
7/1/2001	7	182	142900	3686.9	584.77	106.66	347.68	64.87	241312	0	353.93	64.87	237053	0
8/1/2001	8	213	123824	7524.6	520.08	101.70	293.38	61.27	220481	0	276.61	61.27	233850	0

9/1/2001	9	244	91557	9623.0	516.59	90.96	257.79	54.50	184230	0	243.25	54.50	195247	0
10/1/2001	10	274	67955	5974.2	529.51	87.36	234.37	45.06	154115	0	220.50	45.06	163809	0
11/1/2001	11	305	63940	1977.6	602.51	88.67	318.70	48.71	121269	0	299.78	48.71	128922	0
12/1/2001	12	335	72282	6072.3	670.37	96.78	303.05	52.12	160415	0	282.92	52.12	171832	0
1/1/2002	1	1	88455	4202.3	638.38	101.01	310.88	52.38	182280	0	302.28	52.38	187467	0
2/1/2002	2	32	90994	1703.0	670.71	98.11	289.25	43.21	211671	0	301.01	43.21	203399	0
3/1/2002	3	60	102302	3290.9	712.31	96.43	280.27	39.69	260775	0	279.67	39.69	261336	0
4/1/2002	4	91	114971	4662.4	727.22	99.41	313.96	45.66	267107	0	353.48	45.66	237242	0
5/1/2002	5	121	127483	3553.4	721.08	101.75	312.05	45.60	295498	0	323.38	45.60	285144	0
6/1/2002	6	152	139656	3616.1	681.40	105.27	354.46	56.33	269378	0	358.94	56.33	266019	0
7/1/2002	7	182	140867	2332.8	590.03	100.94	293.56	51.03	284188	0	282.59	51.03	295213	0
8/1/2002	8	213	126092	6327.7	585.77	99.50	312.38	56.41	237347	0	290.57	56.41	255162	0
9/1/2002	9	244	100433	7437.0	517.94	87.37	276.14	52.15	189099	0	248.82	52.15	209866	0
10/1/2002	10	274	74119	8770.4	523.65	91.85	249.38	54.52	156286	0	225.96	54.52	172483	0
11/1/2002	11	305	64529	3599.9	712.92	98.93	337.38	51.66	136778	0	313.47	51.66	147210	0
12/1/2002	12	335	77176	3696.0	727.09	94.03	385.22	54.33	146084	0	364.29	54.33	154475	0
1/1/2003	1	1	85206	589.9	726.47	97.77	337.27	45.93	184064	0	306.39	45.93	202616	0
2/1/2003	2	32	87980	1134.1	687.63	95.73	302.30	42.77	200728	0	286.26	42.77	211975	0
3/1/2003	3	60	93541	2227.5	724.03	97.49	257.42	35.74	263870	0	261.93	35.74	259320	0
4/1/2003	4	91	108728	6406.3	709.84	99.11	336.81	52.29	229862	0	365.87	52.29	211605	0
5/1/2003	5	121	124179	2806.9	706.72	102.16	309.42	45.92	284521	0	326.52	45.92	269616	0
6/1/2003	6	152	133129	3177.7	701.92	104.19	324.31	49.46	289073	0	340.89	49.46	275016	0
7/1/2003	7	182	132630	2658.7	658.03	106.92	337.34	55.92	259633	0	338.16	55.92	259004	0
8/1/2003	8	213	119793	5442.6	546.75	94.68	278.30	50.72	236256	0	266.21	50.72	246981	0
9/1/2003	9	244	97511	7751.1	507.88	87.86	258.49	50.49	192353	0	236.20	50.49	210506	0
10/1/2003	10	274	74686	5077.0	566.79	89.81	290.94	51.40	146022	0	270.35	51.40	157141	0
11/1/2003	11	305	68894	1088.4	631.52	91.41	300.47	44.29	145256	0	276.99	44.29	157570	0
12/1/2003	12	335	70347	888.7	684.02	98.89	300.62	44.13	160569	0	278.34	44.13	173422	0
1/1/2004	1	1	79006	5689.1	757.60	106.69	324.27	52.69	185169	0	299.13	52.69	200735	0
2/1/2004	2	32	89521	1553.9	576.71	94.64	251.26	41.95	206210	0	241.17	41.95	214837	0
3/1/2004	3	61	97064	3746.7	625.78	97.93	290.02	47.57	210160	0	290.29	47.57	209965	0

Appendix I: Short Matlab analytical scripts used during the analysis

Contents and Notes:

1) lanczos.m
    a) Purpose: treats any data stream with a lanczos filter
    b) Source: C. Tilburg, 2004
    c) Input: lanczos(data, time (sec), 100, $9.26x10^{-5}$)
    d) Output: variable in Matlab
2) fluxavg.m
    a) Purpose: averages data that have standard deviations using a Monte Carlo method, returns mean, standard deviation
    b) Source: S. Cooley
    c) Input: A = fluxavg(flux, s.d.)
    d) Output: A, a variable in Matlab

1. lanczos.m

```
function M=lanczos(data,t,end_M,omega_c)

% This function provides a Lanczos low-pass filter to the input
data.
%
% Usage M=lanczos(data,t,end_M,omega_c)
% where
%
%   data    = data to be filtered
%   t       = time series   (s)
%   end_M   = used to create number of weights (2*M+1)
%   omega_c = cut off frequency  (1/s)
%
%
% Charles Tilburg 07/12/01
%
mndata = mean(data);
data = data - mndata;
dt = t(2)-t(1);
omega_N = 1/(2*dt);                % Nyquist frequency
```

```
N = length(data);
y = zeros(size(data));
%
% Calculating weights (note the weights are symmetric)
%
for k = 1:end_M
  F(k) =
0.5*sin(pi*k*omega_c/omega_N)/(pi*k*omega_c/omega_N)*sin(pi*k/end
_M)/(pi*k/end_M);
end
%
% Filtering data
%
for n = end_M+1:N-end_M-1
  Fsum = 0;
  for k = 1:end_M;
    Fsum = F(k)*(data(n-k) + data(n+k)) + Fsum;
  end
  y(n) = 2*omega_c/omega_N*(0.5*data(n)+Fsum);
end
M=y+mndata;
```

2. fluxavg.m

```
function [outpt] = fluxavg(flux, sd)% averaging fluxes including
error with monte carlo method

for i = 1:2000;
    fluxpert(:,i) = flux + sd.*randn;
end

[j,k]= size (fluxpert);
f = sum(sum(fluxpert,1),2);
f = f./(j.*k);

for m = 1:j;
    for n = 1:k;
        xi_xbar = fluxpert(m,n) - f;
        resid_xixbar(m,n) = xi_xbar;
    end
end
st = (1/(j.*k-1).*sum(sum((resid_xixbar.^2),1),2)).^0.5;

outpt = [f st];
```

Appendix J: Directory of online data sources used

Atmospheric pCO_2

Source: NOAA CMDL (www.cmdl.noaa.gov/infodata/)

Data: Ragged Point, Barbados pCO_{2atm} from September 1995 - May 2003

NOAA NCEP NCAR heat, freshwater, and momentum fluxes

Source: IRI-LDEO Climate Data Library (http://ingrid.ldeo.columbia.edu)

Data: Reanalysis CDAS-1 Monthly Diagnostic surface net solar flux, surface precipitation rate, above ground temperature, above ground zonal wind, above ground meridional wind, and surface temperature.

CO2SYS

Sources: CDIAC ORNL (http://cdiac.ornl.gov/oceans/co2rprt.html) (DOS version) and Washington State Department of Ecology (http://www.ecy.wa.gov/programs/eap/models/) (Visual Basic version)

PWP code

Source: P. Lazarevich and S. Stoermer, URI, (http://www.po.gso.uri.edu/rafos/research/pwp/) (version 1.4)

Hidroweb data

Source: Brazilian National Water Agency (ANA), http://hidroweb.ana.gov.br

Data: Discharge records for 1968-2004 for Sao Paulo de Olivenca, Manacapuru, Obidos.

Spring 2003 Underway pCO_2 data

Source: Self collected, available at CDIAC (http://cdiac.ornl.gov/)

SSM/I gridded winds

Source: http://podaac.jpl.nasa.gov/products/product079.html

Data: January 1, 1995 – July 20, 1999, Level 3.0 SSM/I global ocean surface winds

QuikSCAT gridded winds

Source: JPL SeaWinds Project, http://podaac.jpl.nasa.gov/products/product109.html

Data: July 21, 1999 – December 31, 2005 QuikSCAT level 3 daily gridded ocean winds

SOC climatology

Source: IRI-LDEO Climate Data Library (http://ingrid.ldeo.columbia.edu)

(SOCGASC97 version)

GPCP precipitation

Source: NASA; http://precip.gsfc.nasa.gov/gpcp_v2_comb.html

Data: NASA GPCP V2 Combined Precipitation Data Set

CMAP precipitation

Source: National Weather Service, http://www.cpc.noaa.gov/products/

Data: CPC Merged Analysis of Precipitation